Interval observers-based Fault-Tolerant Control of LPV Switched Systems

Duc To Nguyen

université PARIS-SACLAY

Interval Observers-Based Fault-Tolerant Control Of LPV Switched Systems

Contrôle Tolérant Aux Défauts Basé Observateurs Par Intervalle Pour Systèmes LPV Commutés

Thèse de doctorat de l'université Paris-Saclay

École doctorale n° 580, Sciences et Technologies de l'Information et de la Communication (STIC)
Spécialité de doctorat: Automatique
Graduate School : Sciences de l'ingénerie et des systèmes. Référent : Université d'Évry Val d'Essonne

Thèse préparée dans le laboratoire IBISC (Université Paris-Saclay, Univ Evry) sous la direction de **Saïd MAMMAR**, Professeur des Universités, l'encadrement de **Dalil ICHALAL**, Professeur des Universités et de **Mohand SMAILI**, Chercheur.

Thèse Soutenue à Paris-Saclay, le 25 June 2025, par

Duc To NGUYEN

Composition du jury

Membres du jury avec voix délibérative

Guillaume SANDOU Professeur, CentraleSupélec Université Paris-Saclay	Présidente
Ahmed EL HAJJAJI Professeur, Université de Picardie Jules-Verne	Rapporteur & Examinateur
Kevin GUELTON Professeur,Université de Reims	Rapporteur & Examinateur
Sihem TEBBANI Professeur, CentraleSupélec Université Paris-Saclay	Examinatrice
Ali ZEMOUCHE Maître de conférences-HDR, Université de Lorraine	Examinateur

THESE DE DOCTORAT
NNT : 2025UPAST039

To my whole family I wasn't to achieve this work without your faith.

Acknowledgements

First of all, I would like to express my sincerest gratitude to my supervisor, Prof. Said MAMMAR, Prof. Dalil ICHALAL and Associate Researcher Mohand SMAILI for invaluable guidance, patience, continuous encouragement, and support throughout my studies. Without his valuable suggestions and supervision, this thesis could never be completed.

My deepest thanks go to the dissertation committee members. I would like to thank Ahmed EL HAJJAJI, Professor at University of Picardie Jules Verne and Kevin GUELTON, Professor at University of Reims, for the honor they have given me by accepting to be reporters of this thesis. I would also express my gratitude to Guillaume SANDOU, Professor at CentraleSupelec University of Paris-Saclay and Ali Zemouche, Associate Professor at University of Paris-Saclay, who kindly accepted to be examiners.

Besides, I would like to thank Ali Zemouche, Associate Professor at University of Lorraine and Mrs. Aurélia Fraysse, Associate Professor at University of Paris-Saclay who served as members of my CSI jury. Thank you so much for the time and advice to me during three year of doctoral research.

I extend my sincere thanks to Dr. Eslam ABOUSELIMA for sharing his knowledge and discussing with me many technical details of various topics, which significantly increased the quality of the result.

I would like to thank all my labmates and friends in the IBISC (Informatique, Bioinformatique, Systèmes Complexes) Lab, for creating a great study and research environment. All the fun we have had made my stay at the University of Évry much more enjoyable.

Last but not least, I would like to thank my parents for their support throughout my life. There are no words to express how grateful I am to my parents for all of their sacrifices and encouragement. They have been my pillars of strength, offering me immense emotional and psychological support during every challenge. Their love and values will forever be a source of foundation and inspiration for my life, and for that, I am eternally grateful.

Contents

List of Notations and Acronyms **vii**

List of Figures **xi**

1 General Introduction **1**

1.1 Context . . . 1

1.2 Thesis objectives . . . 7

1.3 Thesis structure and contributions . . . 7

1.4 List of publications . . . 9

1.4.1 Journal articles . . . 9

1.4.2 Conference articles . . . 9

2 Theoretical Background **11**

2.1 Switched systems . . . 11

2.1.1 Introduction to switched systems . . . 11

2.1.2 Representation of switched LPV system . . . 13

2.1.3 Stability of switched system . . . 17

2.2 Interval observer . . . 25

2.2.1 Nonnegative and Metzler matrices . . . 27

2.2.2 Positive switched systems . . . 27

2.2.3 Interval relation . . . 27

2.2.4 Interval observers design for switched systems . . . 28

2.2.5 Useful lemmas . . . 32

2.3 Fault-Tolerant Control . . . 33

2.3.1 Types of fault-tolerant control . . . 33

2.3.2 Classification of fault . . . 36
2.3.3 Co-design of observers and controllers . . . 37
2.4 Conclusions . . . 41

3 Switched Unknown Input Interval Observers-based Fault-Tolerant Control For Uncertain Switched Systems 43

3.1 Introduction . . . 44
3.1.1 Related works . . . 44
3.1.2 Chapter contributions . . . 46
3.2 Problem formulation . . . 47
3.2.1 General case . . . 47
3.2.2 Case study: switched vehicle lateral dynamics model . . . 48
3.3 Main results . . . 50
3.3.1 Switched Unknown Input Interval Observer . . . 51
3.3.2 Dynamic Proportional Integral Observer . . . 54
3.3.3 Fault-tolerant controller . . . 56
3.4 Simulation . . . 65
3.4.1 General profile . . . 67
3.4.2 Double Lane Change Maneuver . . . 74
3.5 Conclusions . . . 80

4 Simultaneous Interval State and Unknown Input Estimation and Fault-Tolerant Tracking Control For Uncertain Switched LPV Systems 83

4.1 Introduction . . . 84
4.1.1 State of the art . . . 84
4.1.2 Chapter contributions . . . 85
4.2 Problem formulation . . . 86
4.2.1 General case . . . 86
4.2.2 Case study: Switched LPV vehicle lateral dynamics model . . . 87
4.3 Main results . . . 89
4.3.1 Switched unknown input interval observer . . . 90
4.3.2 Unknown input interval reconstruction . . . 93
4.3.3 Observer-based fault tolerant control . . . 95
4.4 Simulation results . . . 102
4.4.1 Yaw rate profile tracking . . . 103

4.4.2 Double Lane Change Maneuver . . . 113
4.5 Conclusions . . . 120

5 Interval Observer-based Active Fault-Tolerant Control For Discrete-Time Uncertain Switched LPV Systems 121

5.1 Introduction . . . 122
5.1.1 State of the art . . . 122
5.1.2 Chapter contribution . . . 123
5.2 Problem formulation . . . 124
5.3 TNL Interval Observer-Based Fault Tolerant Control . . . 125
5.3.1 Observer matrices determination . . . 128
5.3.2 Integrated observer and FTC synthesis . . . 129
5.4 Application to lateral vehicle dynamics . . . 137
5.5 Conclusions . . . 145

6 General Conclusion and Perspectives 149

6.1 Conclusions . . . 149
6.2 Perspectives . . . 150

Appendices 153

A Vehicle Lateral Dynamics Models 155

A.1 Bicycle model . . . 155
A.2 Impact of lateral wind gust . . . 157
A.3 Direct yaw moment control . . . 157
A.4 Vision system dynamics . . . 158
A.5 Derivation using slip angle as a state variable . . . 158

Bibliography 161

List of Notations and Acronyms

Notations

$\succ \prec$	Positive negative definite matrix.
$\succeq \preceq$	Positive negative semi-definite matrix.
$\|.\|$	Absolute value.
$\|.\|_2$	Euclidean norm or L_2 norm
$\|.\|_\infty$	Infinity norm.
I_n	Identity matrix.
x^T	Transpose of vector x
M^T	Transpose of matrix M
$M^\dagger$	Pseudo inverse of matrix M
M^{-1}	Inverse of matrix M
$rank(M)$	Rank of matrix M
$M^+ = \max\{M, 0\}$	The matrix with all positive elements of the matrix M
$M^- = M^+ - M$	The matrix with all negative elements in absolute value of the matrix M

Acronyms

LTI	Linear Time Invariant
LPV	Linear Parameter Varying
ISS	Input-to-State-Stable
LMI	Linear Matrix Inequality
FE	Fault Estimation
FTC	Fault-Tolerant Control
AFTC	Active Fault-Tolerant Control
PFTC	Passive Fault-Tolerant Control
CG	Center of Gravity
FDI	Fault Detection and Isolation
SMC	Sliding Mode Control
DOF	Degrees Of Freedom
ADT	Average Dwell Time

Nomenclature

v_x	Vehicle longitudinal velocity (m/s).
v_y	Vehicle lateral velocity (m/s).
$\dot{\psi}$	Yaw rate (rad/s).
β	Sideslip angle at center of gravity (rad).
δ_f	Front steering angle (rad).
ψ_L	Lateral angular displacement (rad).
y_L	Lateral offset displacement (m).
F_y	Lateral tire force (N).
F_{yf}	Front lateral tire force (N).
F_{yr}	Rear lateral tire force (N).
c_f	Cornering stiffness of the front tire (N/rad).
c_r	Cornering stiffness of the rear tire (N/rad).
I_z	Moment of inertia along the vertical axis $(kg.m^2)$.
l_f	Distance from the center of gravity to the front axis (m).
l_r	Distance from the center of gravity to the rear axis (m).
m	Vehicle total mass (kg).
M_z	Yaw moment $(N.m)$.

List of Figures

2.1 The polytopic implementation 17

2.2 For each subsystem, the value of its Lyapunov function at the beginning of each activation interval is greater than its value at the beginning of the next interval in which the same i^{th} subsystem is active, then the switched system is asymptotically stable. 19

2.3 General structure of an observer 25

2.4 Conventional and interval observer 26

2.5 Architecture of passive FTC 34

2.6 Architecture of active FTC 35

2.7 Additive and Multiplicative Faults 38

2.8 Structure of co-design of FE and FTC 39

2.9 Bi-directional interaction between observer and controller 41

3.1 Robust co-design of the interval observers and controllers. 57

3.2 Switching signal $\sigma(t)$. 67

3.3 Front steering angle $\delta_f(t)$ profile. 68

3.4 Longitudinal velocity $v_x(t)$ profile. 69

3.5 Actuator fault estimation $\hat{f}(t)$. 69

3.6 Yaw moment control input $u(t)$. 70

3.7 Sideslip angle $\beta(t)$ interval estimation. 70

3.8 Yaw rate $r(t)$ interval estimation. 71

3.9 Comparison of sideslip angle $\beta(t)$ interval estimations between the proposed approach and compared method in [1]. 71

3.10 Comparison of yaw rate $r(t)$ interval estimations between the proposed approach and compared method in [1]. 72

3.11 Comparison of sideslip angle $\beta(t)$ between with and without FTC. 72
3.12 Comparison of yaw rate $r(t)$ between with and without FTC. 73
3.13 Sideslip angle tracking errors $e_\beta(t)$ 73
3.14 Yaw rate tracking errors $e_r(t)$ 74
3.15 Front steering angle $\delta_f(t)$ profile. 75
3.16 Longitudinal velocity $v_x(t)$ profile. 76
3.17 Actuator fault estimation $\hat{f}(t)$. 76
3.18 Sideslip angle $\beta(t)$ interval estimation. 77
3.19 Yaw rate $r(t)$ interval estimation. 77
3.20 Comparison of sideslip angle $\beta(t)$ between with and without FTC. 78
3.21 Comparison of yaw rate $r(t)$ between with and without FTC. 78
3.22 Sideslip angle tracking error $e_\beta(t)$. 79
3.23 Yaw rate tracking error $e_r(t)$. 79
3.24 Comparison of actuator fault estimation $\hat{f}(t)$ between the proposed approach and method presented in [2]. 80
3.25 Sideslip angle $\beta(t)$ performance between the proposed co-design approach and separation principle design method discussed in [2]. 81
3.26 Yaw rate $r(t)$ performance between the proposed co-design approach and separation principle design method discussed in [2]. 81

4.1 Front steering angle and longitudinal velocity profile. 103
4.2 Front steering angle $\delta_f(t)$ profile. 105
4.3 Longitudinal velocity $v_x(t)$ profile. 105
4.4 The actuator fault profile $f(t)$ and its lower and upper bounds. 106
4.5 Yaw rate control input $u(t)$. 106
4.6 Lateral velocity interval estimation $v_y(t)$. 107
4.7 Yaw rate interval estimation $r(t)$. 107
4.8 State tracking lateral velocity $v_y(t)$ with and without FTC. 108
4.9 State tracking yaw rate $r(t)$ with and without FTC. 108
4.10 Lateral velocity tracking errors e_{v_y}. 109
4.11 Yaw rate tracking errors e_r. 109
4.12 Comparison of lateral velocity $v_y(t)$ between the proposed approach with the method in [3] 110
4.13 Comparison of lateral velocity interval width between the proposed approach with the method in [3] . . 110
4.14 Comparison of yaw rate interval width between the proposed approach with the method in [3] 111

4.15 Comparison of unknown input interval reconstruction between the proposed approach with the method in [3]. . . . 111
4.16 Comparison of lateral velocity $v_y(t)$ performance between the co-design approach with the separated method. . . . 112
4.17 Comparison of yaw rate $r(t)$ performance between the co-design approach with the separated method. 112
4.18 Front steering angle profile $\delta_f(t)$. . . . 113
4.19 Front steering angle profile $\delta_f(t)$. . . . 114
4.20 Longitudinal velocity profile $v_x(t)$. . . . 114
4.21 Yaw moment control input $u(t)$. . . . 116
4.22 Comparison of lateral velocity $v_y(t)$ performance with and without FTC. . . . 116
4.23 Comparison of yaw rate $r(t)$ performance with and without FTC. . . . 117
4.24 Lateral velocity tracking error $e_{v_y}(t)$. . . . 117
4.25 Yaw rate tracking error $e_r(t)$. . . . 118
4.26 Actuator fault interval estimation. . . . 118
4.27 Lower and upper bounds of lateral velocity $v_y(t)$. . . . 119
4.28 Lower and upper bounds of yaw rate $r(t)$. . . . 119

5.1 Front steering angle $\delta_f(k)$ profiles. . . . 138
5.2 Longitudinal velocity $v_x(k)$ profiles. . . . 138
5.3 Switching signal $\sigma(k)$ profiles. . . . 140
5.4 Disturbance wind gust $w(k)$. . . . 141
5.5 Measurement noise $v(k)$. . . . 141
5.6 Lateral vehicle velocity $v_y(k)$ interval estimation. . . . 142
5.7 Yaw rate $r(k)$ interval estimation. . . . 143
5.8 Actuator fault $f(k)$ interval estimation. . . . 143
5.9 Yaw moment control input $u(k)$. . . . 144
5.10 Comparison of lateral velocity $v_y(k)$ performance between with and without FTC. . . . 144
5.11 Comparison of yaw rate $r(k)$ performance between with and without FTC. . . . 145
5.12 Comparison of lateral velocity $v_y(k)$ interval estimation between the proposed and compared method. 145
5.13 Comparison of actuator fault $r(k)$ interval estimation between the proposed and compared method. . 146
5.14 The lateral velocity $v_x(k)$ performance between the co-design and separated approach. . . . 146
5.15 The yaw rate $r(k)$ performance between the co-design and separated approach. . . . 147

A.1 Classical bicycle model. . . . 156
A.2 Vision system dynamics. . . . 159

Chapter 1

General Introduction

Chapter abstract

Switched systems have drawn considerable attention from researchers due to their ability to represent a wide range of practical systems. However, such systems are frequently exposed to unknown inputs and faults caused by unpredictable external disturbances, measurement noise, and potential faults. It is, therefore, crucial to enhance the safety and reliability through well-designed algorithms capable of detecting and compensating for faults that impact the system performance. This chapter provide an introduction to the thesis topic and its motivation on switched systems. Furthermore, Fault-Tolerant Control (FTC) and vehicle lateral dynamics concepts are presented. Finally, the chapter concludes by outlining the thesis structure and summarizing its contributions.

1.1 Context

Switched systems recently drew considerable attention due to their ability to model complex and nonlinear behavior and their extensive application in real-world scenarios [4]. Switched systems represent a special class of hybrid systems involving a finite number of subsystems and a switching law specifying the active subsystem at each time instant [5]. Switched systems have been widely studied for decades because of their importance both in theoretical development and engineering applications. Some typical examples of switched systems with greater theoretical challenges and high practical interest can be found, for instance, in aircraft [6], power systems [7], DC-DC converter [8], hydro-Turbine Governing System [9].

The main design challenge of switched systems is ensuring stability when switching between subsystems with a specified switching rule. Research in [10] demonstrates that the stability of a switched system is affected not only by the dynamics of each subsystem but also by the characteristics of switching signals. Therefore, the stability of switched systems is studied from two perspectives: analyzing the stability of switched systems with given switching

signals (maybe arbitrary, slow switching) and identifying the switching signals guaranteeing the stability of a given collection of dynamical systems [11]. In general, a switched system does not inherit the properties of the individual subsystems. For example, the switched system might not be stable even if all the subsystems are exponentially stable. Another remarkable fact is that one may carefully switch between unstable subsystems to make the switched system exponentially stable [12].

There are various methods that can be considered when attempting to analyze the stability and design controllers of switched systems. The basic definition of dwell-time has been introduced in [13] in order to formulate stability conditions for general switched systems. The related studies for switched systems under dwell-time constraints are available in the literature. Dwell time analysis for continuous-time switched linear positive systems is studied in [14]. In [15], piecewise quadratic functions utilized to characterize the Lyapunov function for obtaining a sequence upper bounds of the minimum dwell time were deployed to analyze the stability of switched systems. A model predictive control (MPC) was proposed in [16] to co-optimize the switching sequences and control input for switched linear systems subject to persistent dwell time.

More recently, tremendous efforts from researchers and engineers have been devoted to the study of average dwell time (ADT) switching since it is effective and flexible in various applications including stability analysis, stabilization, and control synthesis. The ADT switching strategy enforces the slow-switching properties of the switching signal so that the systems achieve global stability under the switching sequence. By ADT switching strategy, only a limited number of switches are allowed within a finite time interval. The concept of average dwell time has been proposed in [17] in order to obtain less restrictive conditions compared to dwell-time conditions. Since then, numerous achievements in the literature have been focusing on ADT concepts as a way to efficiently characterize the stability of switched systems or, more generally, the stability of hybrid systems. The works in [18] investigated the stability problems of switched systems with stable and unstable subsystems using average dwell time. In [19], an ADT approach for FTC is developed for a class of uncertain switched linear delay systems. The authors in [20] deal with the problems of H_∞ state tracking model reference adaptive control for a class of switched systems by converting into the stability analysis of the error switched system guaranteed under a class of switching signals characterized by an average dwell time.

Note that the design of state feedback controllers requires the knowledge of full-state variables. In many practical applications, however, the full-state vector cannot be completely measured or accessed. This is due to economic and technical reasons, such as the high cost and insufficient precision of the sensors. To address this issue, observer design techniques have been introduced to estimate the state vectors from inputs and output measurements of the system. It is worth mentioning that state estimation plays a crucial role in a variety of fields, such as aerospace engineering [21], automotive systems [22], and electrical power grid [23].

The state estimation problem for switched systems has been intensively investigated in the literature. For example, in [24], a Luenberger-like observer is investigated for a class of switched discrete-time linear systems. The

works in [25] have been extended to high-order sliding-mode observer proposed for continuous and discrete state estimation of linear switched systems with unstable internal dynamics. In [26, 27], an alternative approach based on adaptive fuzzy observer is designed for switched systems to estimate state and faults simultaneously.

However, the aforementioned observers are designed with the perfect knowledge of structural models and parameters. Therefore, the traditional observers, such as the Luenberger observer or Kalman filter, may be ineffective in dealing with the state estimation issues in the presence of uncertainties coming either from external disturbances and measurement noise or from the mismatch between the model and the real system.

To deal with this challenge, recently, a robust alternative approach, the so-called interval observer, has been proposed in [28, 29]. The interval observer provides lower and upper bounds that encompass all possible state trajectories of the uncertain dynamical system [30]. The problem of interval observer design is based on the assumption that the uncertainties are unknown but bounded by prior known bounds. In addition to stability conditions, it is worth mentioning that a specific feature of an interval observer is that the cooperativity of the estimation errors should be guaranteed, which is based on the monotone system theory.

However, the additional cooperative condition is the main challenge of the problem of interval observer design since searching for a single gain matrix simultaneously ensuring both the stability and positivity properties of the estimation errors in the original state coordinate is not a straightforward task in some cases. To overcome this challenge, interval observer design techniques based on coordinate transformations have been developed. These advanced approaches aim to relax the restrictive design conditions imposed by the traditional design methods, offering a more flexible and efficient framework for interval observer design. For example, studies in [31] and [32, 33] considered a time-invariant change of coordinate for a class of continuous-time systems and discrete-time systems. An extension to the time-varying change of coordinate to the LTI system is proposed in [34]. Another possibility is presented in [35] to decompose the system into two coupled positive systems.

The concept of interval observer was initially introduced in [36] for estimating the state of biological systems affected by unknown uncertainties. Since then, there have been numerous contributions and significant results proposed to deal with the interval observer design problem for various types of systems, such as delay systems [37], discrete-time LPV systems [32, 38], and time-varying systems [39, 40]. Although the abundant achievements in the design of interval state observers are investigated in the literature, the field of interval observers design remains an open question and requires further research.

Researchers have recently paid a great attention to the problem of interval observer design for switched systems. For example, in [41], the authors deal with the issue of interval observer design to estimate the states and unknown input for switched linear systems with known switching signals in an unknown but bounded error framework. The works in [42] introduced a solution to design H_∞ interval observers for discrete-time switched systems in the presence of unknown but bounded disturbances, aiming to obtain the optimal observer gain matrices. The design of interval observers for switched uncertain systems with bounded uncertainties in both the state and out-

put equations is structured in [43]. In [44], the researchers addressed the problem of the interval observer-based event-triggered controller design for switched systems subject to additive disturbance and measurement noise. Another application of the interval observer presented in the reference [45] is to tackle the problem of L_∞ interval fault detection observer for a class of discrete-time switched systems with sensor faults. The extended results on the interval observer-based switching control systems are investigated in [46] for nonlinear switched systems under ADT constraints and non-linear vector function assumed to satisfy Lipschitz conditions.

In engineering applications, there are strict requirements for stability and performance criteria since faults/failures are inevitable to occur. In this context, it is obvious that conventional feedback control design may result in unsatisfactory performance in the event of malfunctions in the actuators, sensors, or other components of the system. In extreme cases, this may even lead the system to instability. In order to maintain the current performance close to the desired one and preserve the stability of the system in the presence of faults, fault-tolerant control techniques are necessary to design for such scenarios. In recent years, FTC has become increasingly popular among industrial and academic fields. Several survey papers and books have been published [47, 48].

In general, fault-tolerant control may be grouped into two main categories: passive fault-tolerant control and active fault-tolerant control. A hybrid of these methods called Hybrid FTC is also constructed by combining both parts [49, 50].

In the passive FTC scheme, the controller is synthesized offline with fixed structure and parameters during the system operation [51]. This controller is capable of handling all anticipated faults without the need for fault detection and identification (FDD). This control technique does not react to fault occurrence and fault-tolerance is often achieved by considering faults as uncertainties. From the classical control theory point of view, passive FTC is closely related to robust control. In practice, approaches like H_∞ control and Sliding Model Control (SMC) are often used since they can maintain stability and system performance despite the presence of faults. The H_∞ methodology is a well-known technique in the field of robust control and can take into account the performance and stability requirements [52]. The fundamental idea behind the H_∞ control technique is to design a controller that can ensure stabilizing properties while minimizing the effect of uncertainties or disturbances on certain outputs of interest. Another robust control approach is SMC proposed in [53]. The key feature of SMC is its ability to provide robustness against parameter variation and external disturbances by altering the dynamics of the system through discontinuous control actions.

Researchers have explored various approaches to enhance the robustness and reliability of passive FTC systems without requiring real-time fault diagnosis or control reconfiguration. For example, the authors in [54] designed a robust H_∞ passive FTC for uncertain singular systems. In [55], a passive FTC system based on a regular and cascaded sliding mode controller (SMC) is studied for quadrotor application. Additionally, the works in [56] proposed a solution to design an interval observer-based passive fault tolerant control for discrete-time LPV systems subject to

component faults considered unknown but bounded. A passive FTC system design based on Feed-forward Neural Networks is structured in [57] against partial actuator faults.

In comparison with passive FTC, the active fault-tolerant control strategy is designed to meet the control objectives with minimum system performance degradation by using the reconfiguration mechanism. Specifically, this approach actively responds to faults/failures by adjusting the control actions to maintain stability and preserve acceptable system performance. It should be noted that in the framework of active FTC, the design process typically begins with the construction of a module for fault detection and estimation, which monitors the systems and estimates faults as occurring. A supervisory controller is then developed to automatically update the control scheme or reconfigure the control setting in response to the information of fault estimation.

The main drawback of active FTC is that the fault is not tolerated during the time needed for the detection process, possibly making the system unstable if the detection process takes too long. In other words, when a fault occurs, it takes some time for the FDD module to detect, isolate, and identify the fault. Additionally, there may also be some delay from the controller reconfiguration. During this phase, the system operates with the nominal controller, and the performance of the system mainly depends on the severity of the fault and the robustness of the nominal controller. It is evident that the controlled system may become unstable in this phase. In several contexts, passive FTC is preferable as it does not require the fault detection and estimation framework. However, the active FTC approaches have still received much more attention in the literature than the passive ones due to their superior performance and ability to deal with various types of faults.

Over the past few decades, researchers have shown an increasing interest in the active FTC approaches, which play a crucial role in the area of reliability and safety of dynamic systems. The active FTC method is applied across various fields such as robotic manipulator [58], wind turbines [59], fixed wing UAV [60]. In the last three decades, a lot of research has been carried out in the area of FDD and FTC for a class of switched systems. The authors in [61] proposed an FTC approach for discrete-time switched linear systems using linear output feedback against multiple actuator failures. The online controller re-design is performed such that the stability of the closed-loop system is guaranteed with LMI pole-placement technique. The studies in [62] addressed the FTC problem of switched systems by using a new concept, namely the generalized separation principle, which allows the design of the observers, controllers, and switching law separately. This method facilitates the design in engineering. In [63], an integrated design scheme of active FTC is investigated for switched LPV systems under dwell-time constraints against actuator faults in the discrete-time domain. The establishment of sufficient conditions for the stability of the switched systems is formulated in terms of LMIs with ISS properties under dwell-time switching signal. Similarly, an integrated design methodology is proposed in [64] to deal with the issue of switched fuzzy observer and FTC to stabilize the closed-loop systems and compensate for the effects of different faults for switched Takagi-Sugeno (T-S) fuzzy systems subject to actuator and sensor faults and external disturbances. In [65], an interval observer is deployed to estimate simultaneously the system state and faults for polytopic LPV systems subject to uncertainties and actuator faults.

Based on the estimated variables, an active FTC scheme is then proposed to stabilize the closed-loop systems in the presence of faults. Besides, the works in [66] investigated an interval observer-based fault tolerant control system for Heat Exchanger/Reactor affected by faults.

Recently, automotive manufacturers and researchers have increased their attention to techniques to assist drivers, improve performance, and maintain vehicle stability by introducing and implementing numerous passive and active safety systems. These safety systems include the Adaptive Cruise Control (ACC), which maintains the preset desired distance [67]; the Anti-lock Braking System (ABS), which prevents wheel lock during braking [68]; Dynamic Stability Control (DSC); and the Electronic Stability Program (ESP), both of which are essential for controlling the vehicle's trajectory. Thanks to advanced modern technologies in embedded electronic systems, these solutions have become more sophisticated, reliable, compact, and lightweight.

Despite being thought of as life-saving technologies, the design and implementation of these systems are constrained by accurate information on the available vehicle state and its environments. In fact, the safety systems mainly depend on inexpensive measurement equipment such as optical sensors, radar sensors and inertial central, etc. Additionally, some other important parameters of the vehicle, such as its lateral velocity, side-slip angle, and yaw rate are challenging to measure directly due to constraints related to technical requirements and economical reasons (high-cost sensor required and implementation of measuring instruments) and the design of feedback control that guarantees closed-loop stability also could not be satisfied due to the uncertainties of such a model and some lacking measurements. These challenges have been addressed in previous works based on the estimation/observation techniques using only the accessible and available measurements [69, 70].

One of the fundamental requirements for autonomous vehicle systems function effectively in unstructured environments is the capable of accurately estimating the state in the presence of parameter uncertainties and disturbance inputs. The majority of existing approaches for estimating the state of the vehicle lateral dynamics model are based on the perfect knowledge of structure model and dynamics parameters of the vehicle [69, 70].

Nevertheless, in real-world scenarios, vehicle parameters such as cornering stiffness, the position of the center of gravity, and the mass can be subject to substantial uncertainties arising from many factors like vehicle dynamics, varying load conditions, and road surface friction. Notably, these critical parameters are difficult or even impossible to measure accurately and fluctuate due to various factors, including vehicle motion and environmental conditions. Consequently, it is essential to take the impact of these parameter uncertainties on estimation errors into consideration to achieve a desirable level of robust performance.

Another important aspect of automotive engineering is vehicle safety performance. Modern automobiles consist of numerous interrelated subsystems, increasingly equipped with various actuators, sensors, and control units that collectively enhance passenger comfort and safety, making them more safety-critical. Thus, the analysis, modeling, and control of overall vehicle dynamics have become increasingly challenging due to stringent performance and

safety requirements. Additionally, the need for robustness against external disturbances, modeling uncertainty, and potential faults in sensors and actuators further complicates these tasks.

When a vehicle operates based on sensor signals and actuators, any faults/ failures can pose a significant threat to the driver and the surrounding environment. Consequently, fault-tolerant control is designed to ensure stability and maintain an acceptable performance level of vehicle dynamics in the presence of faults. These efforts are vital for enhancing the performance and reliability of active safety systems. Many works dealing with FTC design for vehicle lateral dynamics have been developed in the literature. For example, in [71], the FTC approach is proposed to reform the yaw rate and the roll sensor failures of the vehicle lateral control system. The authors in [72] present an output feedback observer-based FTC architecture for vehicle lateral dynamics with parametric uncertainties and sensor faults. However, only sensor faults are considered in the aforementioned works. An extended approach to actuator faults has been presented in [73], based on Proportional-Integral Observer, a fault-tolerant control is proposed to preserve the stability of the vehicle lateral dynamics with roll effect even in the presence of sensor and actuator faults.

1.2 Thesis objectives

With regard to the aforementioned challenging statement, specific thesis objectives are summarized as follows:

- Develop robust interval state observer approaches for uncertain switched systems. The first objective is to design a interval observer which can deal with the uncertainties in switched systems. Based on the cooperative theory, the interval observer guarantees that the actual system states are bounded within the lower and upper estimation.
- Develop a co-design approach to handle bi-directional interaction: This goal is to incorporate the complex bi-directional interactions between observers and controllers into the design process. This method ensures that observer and control design is well integrated to achieve mutual optimization.
- Synthesize a fault-tolerant control strategy: a fault-tolerant control is designed to guarantee the stability of the closed-loop systems and preserve the system performance level in the existence of faults.
- Apply approach to vehicle lateral dynamics model: Finally, the proposed approach is applied to the vehicle lateral dynamics estimation and control. This application is to evaluate the effectiveness and performance of the proposed methodology in the practical scenarios.

1.3 Thesis structure and contributions

***Chapter* 2** This chapter recalls the theoretical background of switched systems, interval observers, and fault-

tolerant control systems. For this purpose, some fundamental definitions, key lemmas associated to the interval observers are recalled and the stability of switched systems is analysed. Furthermore, the fundamental principles of fault-tolerant control systems are presented, emphasising the role in maintaining system reliability and performance level under fault conditions. In addition, sufficient conditions for the positivity and stability properties of switched interval observer are formulated, along with an investigation of co-design approach which are foundational to the techniques and applications deployed in the following chapters.

***Chapter* 3** The primary focus of this chapter is to design an unknown input observer-based FTC for a class of uncertain switched LTI systems subject to unknown but bounded uncertainties. A switched unknown input interval observer (SUIIO) is designed to estimate the lower and upper bounds of system states without being sensitive to the negative effects of the unknown inputs. In real-world applications, the presence of unknown faults is unavoidable, which necessitates effective handling within the control theory. In this chapter, a Dynamics Proportional Integral Observer (DPIO) is also developed to deal with the fast time-varying fault signals. A co-design approach is adopted to take the bi-directional interactions of observers and controllers into consideration during the design phase. The sufficient and necessary conditional for the existence of the proposed methodology are provided through a single-step LMI formulation. Finally, in order to illustrate the applicability and effectiveness of the proposed algorithm, the vehicle lateral dynamics model is simulated under various scenarios, showcasing the the ability of the proposed approach to maintain robust performance in the existence of faults.

***Chapter* 4** This chapter is dedicated to the development of robust state estimation, unknown input reconstruction and a fault-tolerant control method for a class of continuous-time switched LPV systems with both measurable and unmeasurable parameters. Notably, the observer design of switched LPV systems becomes more complex when dealing with unmeasurable parameters. To overcome this challenge, this topic is addressed in this chapter by assuming that the unmeasurable parameters are unknown but bounded by prior known bounds. An algebraic unknown input interval reconstruction is established to construct the lower and upper bounds of fault signals. A fault-tolerant control technique is then developed to guarantee that the system tracks the reference system and maintains the stability of the closed-loop system, even in the presence of actuator faults. The sufficient conditions for the existence of such observers and controllers are formed in terms of LMIs using multiple ISS Lyapunov functions associated with ADT-constrained switching signals. An application to vehicle lateral dynamics estimation and control demonstrates the effectiveness of the proposed approach.

***Chapter* 5** This chapter deals with the system state and fault estimation along with fault-tolerant control for a class of discrete-time switched LPV systems subject to actuator faults as well as unknown but bounded external disturbances and measurement noise. Traditionally, interval observer design approaches are usually based on the

positive system theory, which ensures that the estimation errors remain nonnegative. However, the requirement of nonnegativity can introduce conservatism. To deal with this problem, a coordinate transformation is proposed in some existing works to relax the nonnegativity constraints. The transformation technique could be challenging to integrate the coordinate transformation with additional control design constraints such as disturbance attenuation. In the view of drawbacks, the main purpose of this approach is to propose a novel TNL interval structure. The key idea is to provide more degree of freedom design of interval observer by introducing the weighting matrices in addition to the gain matrices. First, the interval observer is designed using an augmented technique to simultaneously estimate the lower and upper bounds of state and fault vectors. Based on the estimated variable provided by the interval observer, the chapter proposes a fault-tolerant control strategy synthesized to stabilize the closed-loop system and compensate for the effects of the actuator fault. The simulation results on the vehicle lateral dynamics are proposed to highlight the effectiveness of the proposed approach.

***Chapter* 6** This chapter provides a general summary and conclusion of the thesis. Furthermore, some discussion on potential future works are outlined for this research that can complete and enhance the presented techniques in a way that guarantees a wide use in real-time application.

1.4 List of publications

1.4.1 Journal articles

1. Duc To Nguyen, Saïd Mammar, Dalil Ichalal and Mohand Smaili, ”Interval Observers based Vehicle Lateral Dynamics Estimation and Fault Tolerant Control”, Vehicle System Dynamics, under review.

2. Duc To Nguyen, Saïd Mammar, Dalil Ichalal, ”Interval Observers for Discrete-Time Uncertain Switched LPV Systems Active Fault Tolerant Control”, International Journal of Control, under review.

1.4.2 Conference articles

1. D. T. Nguyen, S. Mammar, D. Ichalal and M. Smaili, ”An integrated design of PI interval observer-based FTC for LTI systems,” 2022 30th Mediterranean Conference on Control and Automation (MED), Vouliagmeni, Greece, 2022, pp. 878-883.

2. S. Mammar, D. -T. Nguyen, D. Ichalal and M. Smaili, ”Control and Dynamic Proportional Integral Observer co-Design for Uncertain Linear Systems,” 2022 IEEE International Conference on Systems, Man, and Cybernetics (SMC), Prague, Czech Republic, 2022, pp. 2209-2214.

3. D. T. Nguyen, S. Mammar, D. Ichalal and M. Smaili, ”Interval Observers based Vehicle Lateral Dynamics Estimation and Fault Tolerant Control”, 2023 7th International Symposium on Future Active Safety Technology toward zero traffic accidents (FAST-zero’23), Kanazawa, Japan, 2023.

4. D. T. Nguyen, S. Mammar, D. Ichalal and M. Smaili, ”Functional Unknown Input Interval Observer and Fault Tolerant Control with Application to Vehicle Lateral Dynamics,” 2023 IEEE 11th International Conference on Systems and Control (ICSC), Sousse, Tunisia, 2023, pp. 183-188.

5. D. T. Nguyen, S. Mammar, D. Ichalal and M. Samili, ”Parameter-Dependent Lyapunov Function Based Interval Observer Design For Switched LPV Systems,” 2024 36th Chinese Control and Decision Conference (CCDC), Xi’an, China, 2024, pp. 3587-3592.

6. D. T. Nguyen, S. Mammar, D. Ichalal and M. Smaili, ”Switched Unknown Input Interval Observer-based Fault-Tolerant Tracking Control: Application to Vehicle Lateral Dynamics,” 2024 10th International Conference on Control, Decision and Information Technologies (CoDIT), Vallette, Malta, 2024, pp. 598-603.

7. D. T. Nguyen, S. Mammar, D. Ichalal and M. Smaili, ”Switched Unknown Input Interval Observers for Vehicle Lateral Dynamics Fault-Tolerant Tracking Control”, 2024 27th IEEE International Conference on Intelligent Transportation Systems (ITSC), Edmonton, Canada, 2024.

8. D. T. Nguyen, S. Mammar, D. Ichalal, ”Interval observer-based active fault tolerant control for discrete-time uncertain switched LPV systems”, 2024 63rd IEEE Conference on Decision and Control (CDC), Allianz MiCo, Milan Convention Centre, Italy, 2024.(in proceeding)

9. D. T. Nguyen, S. Mammar, D. Ichalal and N. Ait-Oufroukh, ”Dynamic Proportional Integral Interval Observer-Based Fault Tolerant Control for Switched Systems: Application to Vehicle Lateral Dynamics,” 2024 18th International Conference on Control, Automation, Robotics and Vision (ICARCV), Dubai, United Arab Emirates, 2024, pp. 1041-1046.

Chapter 2

Theoretical Background

Chapter abstract

This chapter provides theoretical background on control theory and optimization needed for the following chapters. Some basic concepts including mathematical frameworks and stability analysis techniques for switched systems are recalled. Key results from the literature on the estimation tools are introduced within a concentration on interval observer theory. As the thesis primarily focuses on observer-based fault-tolerant control for switched systems, the final section presents a state-of-the-art of fault-tolerant control methods in this chapter.

2.1 Switched systems

2.1.1 Introduction to switched systems

Switched systems, as an important class of hybrid systems, consist of a family of subsystems with a switching signal that determines which subsystem is active at a certain time interval. It is obvious that only one subsystem is active at a given instant of time, and the selection of the active subsystem can be based on the time criteria, on the state space regions, or on the evolution of certain physical parameters. Once a subsystem is selected, the switching signal remains constant for every time interval.

Formally, a continuous-time switched nonlinear system is defined by the relation:

$$\begin{cases} \dot{x}(t) = f_{\sigma(t)}\big(x(t), u(t)\big) \\ y(t) = h_{\sigma(t)}\big(x(t), u(t)\big) \end{cases} \tag{2.1}$$

where $x(t) \in \mathbf{R}^{n_x}$ is the state vector, $u(t) \in \mathbf{R}^{n_u}$ is the control input vector and $y(t) \in \mathbf{R}^{n_y}$ is the measurement output vector. Functions $f : \mathbf{R}^{n_x} \times \mathbf{R}^{n_u} \to \mathbf{R}^{n_x}$ and $h : \mathbf{R}^{n_y} \times \mathbf{R}^{n_u} \to \mathbf{R}^{n_y}$ are vector fields describing the different

subsystems. Switching signal $\sigma(t) \in \mathcal{N} = \{1, \cdots, N\}$ with N is the number of subsystems.

The representation (2.1) is very convenient since it is derived from the system knowledge and the physics equations, so it can fit most physical systems. However, there exist no systematic mathematical tools for identification, observation, control synthesis, or analysis of these systems.

If the switched system (2.1) is described by linear vector fields, the following continuous-time switched system is obtained:

$$\begin{cases} \dot{x}(t) = A_{\sigma(t)}x(t) + B_{\sigma(t)}u(t) \\ y(t) = C_{\sigma(t)}x(t) + D_{\sigma(t)}u(t) \end{cases} \tag{2.2}$$

where $A_{\sigma(t)} \in \mathbf{R}^{n_x \times n_x}$, $B_{\sigma(t)} \in \mathbf{R}^{n_x \times n_u}$, $C_{\sigma(t)} \in \mathbf{R}^{n_y \times n_x}$ and $D_{\sigma(t)} \in \mathbf{R}^{n_y \times n_u}$, $\forall \sigma(t) \in \mathcal{N}$ are distribution matrices.

The discrete-time representation of a switched system (2.2) can be expressed as:

$$\begin{cases} x(k+1) = A_{\sigma(k)}x(k) + B_{\sigma(k)}u(k) \\ \quad y(k) = C_{\sigma(k)}x(k) + D_{\sigma(k)}u(k) \end{cases} \tag{2.3}$$

where $A_{\sigma(k)} \in \mathbf{R}^{n_x \times n_x}$, $B_{\sigma(k)} \in \mathbf{R}^{n_x \times n_u}$, $C_{\sigma(k)} \in \mathbf{R}^{n_y \times n_x}$, $D_{\sigma(k)} \in \mathbf{R}^{n_y \times n_u}$, $\forall \sigma(k) \in \mathcal{N}$ are distribution matrices.

In general, switching signals can be categorized into two types of switching laws. The first type involves a switching signal $\sigma(t)$ is not a priori fixed, but its value is available instantly at each time t. This switching signal may depend on various factors including the previous active mode, the state, and/or external signal. The second type of switching signal $\sigma(t)$ is designed to achieve specific control objectives such as stability or stabilizability. In both cases, the design of the switching law plays a crucial role in the overall performance and robustness of switched systems.

In practical scenarios, it is well known that uncertainties are inevitable in the dynamics systems due to factors such as mismatching modeling between the actual system and its mathematical model, external disturbances, and measurement errors. These uncertainties can significantly affect the system's performance, potentially leading to instability and degraded control accuracy. Consequently, designing controllers handling these uncertainties robustly is essential to maintain the stability and the performance level under across a range of operating conditions. Robust control theory deals with these challenges by taking uncertainties into account during the design process. Among a variety of approaches in robust control, the norm-bounded uncertainty framework is a common and effective way to represent uncertainties. In the context of norm-bounded uncertainties, the model's parameters are assumed to lie within a predefined convex set. This can be mathematically expressed using the concept of norm-bounded uncertainties.

$$\begin{cases} \dot{x}(t) = \Big(A_{\sigma(t)} + \Delta A_{\sigma(t)}\Big)x(t) + \Big(B_{\sigma(t)} + \Delta B_{\sigma(t)}\Big)u(t) \\ y(t) = \Big(C_{\sigma(t)} + \Delta C_{\sigma(t)}\Big)x(t) + \Big(D_{\sigma(t)} + \Delta D_{\sigma(t)}\Big)u(t) \end{cases} \tag{2.4}$$

where $\Delta A_{\sigma(t)} \in \mathbb{R}^{n_x \times n_x}$, $\Delta B_{\sigma(t)} \in \mathbb{R}^{n_x \times n_u}$, $\Delta C_{\sigma(t)} \in \mathbb{R}^{n_y \times n_x}$, $\Delta D_{\sigma(t)} \in \mathbb{R}^{n_y \times n_u}$ are uncertainties in system matrices of appropriate dimensions which has the following form

$$\begin{cases} \Delta A_{\sigma(t)} = M_{a,\sigma(t)} \Delta_{a,\sigma(t)}(t) N_{a,\sigma(t)} \\ \Delta B_{\sigma(t)} = M_{b,\sigma(t)} \Delta_{b,\sigma(t)}(t) N_{b,\sigma(t)} \\ \Delta C_{\sigma(t)} = M_{c,\sigma(t)} \Delta_{c,\sigma(t)}(t) N_{c,\sigma(t)} \\ \Delta D_{\sigma(t)} = M_{d,\sigma(t)} \Delta_{d,\sigma(t)}(t) N_{d,\sigma(t)} \end{cases} \tag{2.5}$$

where $M_{a,\sigma(t)}, N_{a,\sigma(t)}$, $M_{b,\sigma(t)}, N_{b,\sigma(t)}$, $M_{c,\sigma(t)}, N_{c,\sigma(t)}$, $M_{d,\sigma(t)}, N_{d,\sigma(t)}$ are known constant matrices of appropriate dimensions that characterize the structure of uncertainties while $\Delta(t)$ is an unknown time-varying matrix function satisfying

$$\begin{cases} \Delta_{a,\sigma(t)}^T(t) \Delta_{a,\sigma(t)}(t) \leq I \\ \Delta_{b,\sigma(t)}^T(t) \Delta_{b,\sigma(t)}(t) \leq I \\ \Delta_{c,\sigma(t)}^T(t) \Delta_{c,\sigma(t)}(t) \leq I \\ \Delta_{d,\sigma(t)}^T(t) \Delta_{d,\sigma(t)}(t) \leq I \end{cases} \tag{2.6}$$

2.1.2 Representation of switched LPV system

In general, LPV systems are a type of dynamics system characterized by linear dynamics that depend on time-varying parameters referred to as scheduling variables or premise variables. LPV control techniques are designed to provide stability and performance guarantee over a wide range of parameter variations. Due to the complicated behavior of switched LPV system resulting from the combination of the ***hard switching*** between the subsystems, which are LPV systems and the ***soft switching*** among the linear models within a subsystem, very few results on such system appears in the literature.

Especially when each subsystem of a switched system (2.2) is a polytopic LPV system, resulting in the switched system being a switched LPV system [74]. The switched LPV representation of (2.2) is expressed as:

$$\begin{cases} \dot{x}(t) = A_{\sigma(t)}\big(\rho\big) x(t) + B_{\sigma(t)}\big(\rho\big) u(t) \\ y(t) = C_{\sigma(t)}\big(\rho\big) x(t) + D_{\sigma(t)}\big(\rho\big) u(t) \end{cases} \tag{2.7}$$

where $x(t)$ is the state, $u(t)$ is control input, $y(t)$ output vector. Matrices $A_{\sigma(t)}\big(\rho\big) \in \mathbf{R}^{n_x \times n_x}$, $B_{\sigma(t)}\big(\rho\big) \in \mathbf{R}^{n_x \times n_u}$, $C_{\sigma(t)}\big(\rho\big) \in \mathbf{R}^{n_y \times n_x}$, $D_{\sigma(t)}\big(\rho\big) \in \mathbf{R}^{n_y \times n_u}$, $\sigma(t) \in \mathcal{N}$ are state-space matrices depending on the measurable or unmeasurable schedule variables ρ.

It can be demonstrated that according to the following cases of ρ, various types of system (2.7) can be obtained:

- $\dot{\rho} = 0$, this implies that the parameter vector ρ is constant value, the representation (2.7) is referred to as

switched LTI system.

- $\dot{\rho} \neq 0$, this implies that the parameter vector $\rho(t)$ is time-varying parameter.
  - $\rho = \rho(t)$ where the variation of parameter vectors with respect to time is known explicitly, the system (2.7) is a switched Linear Time-Varying (LTV) system.
  - ρ = $\rho(t)$ is an externally measurable or estimated parameter vector, the representation (2.7) is referred to as a switched LPV system.
  - ρ = $\rho(x(t))$, the representation (2.7) is referred as a switched quasi-Linear Parameter Varying $(qLTV)$ system.

Thereby, a switched LPV system can be considered as a switched nonlinear system linearized along the trajectories of varying parameters, denoted by $\rho \in \mathcal{P}_\rho$. This approach enables to describe the representation of the dynamics of a nonlinear system while preserving the linear structure, making the system more tractable for analysis and control design. In other words, by linearizing the nonlinear models along the trajectory of ρ, the switched LPV system can capture nonlinear plant behaviors. Consequently, tools of linear control theory, with some modification, can be effectively applied to such systems.

Based on the dependence of the state-space matrices on the scheduling parameters ρ, the switched LPV systems are categorized into two types, namely affine and polytopic switched systems.

Affine switched LPV system

An affine-switched LPV system is a switched linear parameter-varying system whose state-space matrices are affine functions of the scheduling parameters ρ. In this case, let's assume that all distribution matrices depend affinely on the parameter vector $\rho = \{\rho_1, \quad \cdots, \quad \rho_{n_\rho}\}$ presented under the general expression:

$$\begin{cases} A_{\sigma(t)}(\rho) = A_{\sigma(t),0} + \sum_{j=1}^{n_\rho} A^j_{\sigma(t)} \rho^j \\ B_{\sigma(t)}(\rho) = B_{\sigma(t),0} + \sum_{j=1}^{n_\rho} B^j_{\sigma(t)} \rho^j \\ C_{\sigma(t)}(\rho) = C_{\sigma(t),0} + \sum_{j=1}^{n_\rho} C^j_{\sigma(t)} \rho^j \\ D_{\sigma(t)}(\rho) = D_{\sigma(t),0} + \sum_{j=1}^{n_\rho} D^j_{\sigma(t)} \rho^j \end{cases} \tag{2.8}$$

where:

- ρ^j is the j^{th} of ρ and $A^j_{\sigma(t)}, B^j_{\sigma(t)}, C^j_{\sigma(t)}, D^j_{\sigma(t)}$ are constant matrices of appropriate dimensions representing the linear dependence of the system dynamics on the scheduling variables.

- $A_{\sigma(t),0}, B_{\sigma(t),0}, C_{\sigma(t),0}, D_{\sigma(t),0}$ are switching constant matrices representing the constant terms.
- n_ρ represents the number of scheduling parameters.

The affine representation of switched LPV system (2.7) can be expressed as:

$$\begin{cases} \dot{x}(t) = A_{\sigma(t),0}x(t) + B_{\sigma(t),0}u(t) + \sum_{j=1}^{n_\rho} \rho^j \left(A^j_{\sigma(t)}x(t) + B^j_{\sigma(t)}u(t) \right) \\ y(t) = C_{\sigma(t),0}x(t) + D_{\sigma(t),0}u(t) + \sum_{j=1}^{n_\rho} \rho^j \left(C^j_{\sigma(t)}x(t) + D^j_{\sigma(t)}u(t) \right) \end{cases} \tag{2.9}$$

This is one of the most common switched LPV system formulations encountered in control synthesis, where the affine-dependent system leads to a low degree of conservatism of stability conditions.

Polytopic switched LPV systems

In the LPV modeling framework, the dynamics of the switched LPV system can be represented by an equivalent polytopic form. This representation allows each subsystem of the switched system to be described as a convex combination of sub-models defined by the vertices of a convex polytope. The time-varying parameter ρ takes values in the parameter space $\mathcal{P}_\rho$ (a convex set) such that,

$$\rho = \{\rho_1, \quad \cdots, \quad \rho_{n_\rho}\} \in \mathcal{P}_\rho \tag{2.10}$$

representing n_ρ time-varying parameter vectors, and it is assumed that each parameter is bounded as

$$\rho_i(t) \in \left[\underline{\rho}_i \quad \overline{\rho}_i \right], \quad \forall i = 1, \cdots, n_\rho \tag{2.11}$$

with $\underline{\rho}_i$ and $\overline{\rho}_i$ are the minimum and maximum values of varying parameter ρ_i then the time-varying parameters ρ evolve inside a polytope represented by 2^{n_ρ} vertices.

The switched weighting function $\mu^j_{\sigma(t)}(\rho)$ for j^{th} sub-model depending on the time-varying parameter ρ satisfies the following convex sum properties:

$$\begin{cases} 0 \leq \mu^j_{\sigma(t)}(\rho) \leq 1 \\ \sum_{j=1}^{2^{n_\rho}} \mu^j_{\sigma(t)}(\rho) = 1 \end{cases}, \quad \forall j = 1, \cdots, 2^{n_\rho} \tag{2.12}$$

The switched weighting functions $\mu^j_{\sigma(t)}(\rho)$ are generally non-linear and depend on the scheduling parameter ρ, which is assumed to be available online, but not in advance.

It should be noted that when all scheduling parameters $\rho_i(t)$ are independent and bounded in $[\underline{\rho}_i, \overline{\rho}_i]$, i.e. the set $\mathcal{S}$

is a hypercube of 2^{n_ρ} vertices w_i, as

$$\rho \in \mathcal{S}\left\{w_1, w_2, \cdots, w_{2^{n_\rho}}\right\} \tag{2.13}$$

the state-space matrices of system (2.7) can be equivalently expressed as a convex combination of matrices at vertices of a polytope:

$$\begin{cases} A_{\sigma(t)}(\rho) = \sum_{j=1}^{2^{n_\rho}} \mu^j_{\sigma(t)}(\rho) A^j_{\sigma(t)} \\ B_{\sigma(t)}(\rho) = \sum_{j=1}^{2^{n_\rho}} \mu^j_{\sigma(t)}(\rho) B^j_{\sigma(t)} \\ C_{\sigma(t)}(\rho) = \sum_{j=1}^{2^{n_\rho}} \mu^j_{\sigma(t)}(\rho) C^j_{\sigma(t)} \\ D_{\sigma(t)}(\rho) = \sum_{j=1}^{2^{n_\rho}} \mu^j_{\sigma(t)}(\rho) D^j_{\sigma(t)} \end{cases} \tag{2.14}$$

where

$$\mu^j_\sigma(\rho) = \frac{\Pi_{j=1}^{n_\rho} |\rho_j - \mathcal{S}(w_j)|}{\Pi_{j=1}^{n_\rho} (\overline{\rho}_j - \underline{\rho}_j)} \tag{2.15}$$

and $\mathcal{S}(w_j)_k$ is the k^{th} component of the vector $\mathcal{S}(w_j)$ defined as

$$\mathcal{S}(w_j)_k := \left\{\rho_k : \rho_k = \overline{\rho}_k \quad \text{if} \quad (w_j)_k = \underline{\rho}_k \quad \text{or} \quad \rho_k = \underline{\rho}_k\right\} \tag{2.16}$$

Now, the polytopic representation of the switched LPV system is computed at each vertex of the polytopic system. It means that a set of 2^{n_ρ} sub-models is derived:

$$\begin{cases} \dot{x}(t) = \sum_{j=1}^{2^{n_\rho}} \mu^j_{\sigma(t)}(\rho) \left(A^j_{\sigma(t)} x(t) + B^j_{\sigma(t)} u(t) \right) \\ y(t) = \sum_{j=1}^{2^{n_\rho}} \mu^j_{\sigma(t)}(\rho) \left(C^j_{\sigma(t)} x(t) + D^j_{\sigma(t)} u(t) \right) \end{cases} \tag{2.17}$$

where $A^j_{\sigma(t)}, B^j_{\sigma(t)}, C^j_{\sigma(t)}, D^j_{\sigma(t)}$ are constant switching matrices of appropriate dimensions defined at j^{th} vertex representing the set of 2^{n_ρ} local linear sub-models and 2^{n_ρ} is the number of the sub-models. The switched weighting function $\mu^j_{\sigma(t)}(\rho)$ is determined as:

$$\mu^j_{\sigma(t)}(\rho) = \frac{\Pi_{k=1}^{n_\rho} |\rho_k - \mathcal{S}(w_j)_k|}{\Pi_{k=1}^{n_\rho} (\overline{\rho}_k - \underline{\rho}_k)}, \quad j = 1, \cdots, 2^{n_\rho} \tag{2.18}$$

As illustrated in Figure 2.1 (in the case of 2 scheduling parameters), the system evolves in a set according to the parameter variation. This representation provides significant convenience in control design and implementation by allowing each subsystem of the switched system to be described as a convex combination of a finite number of

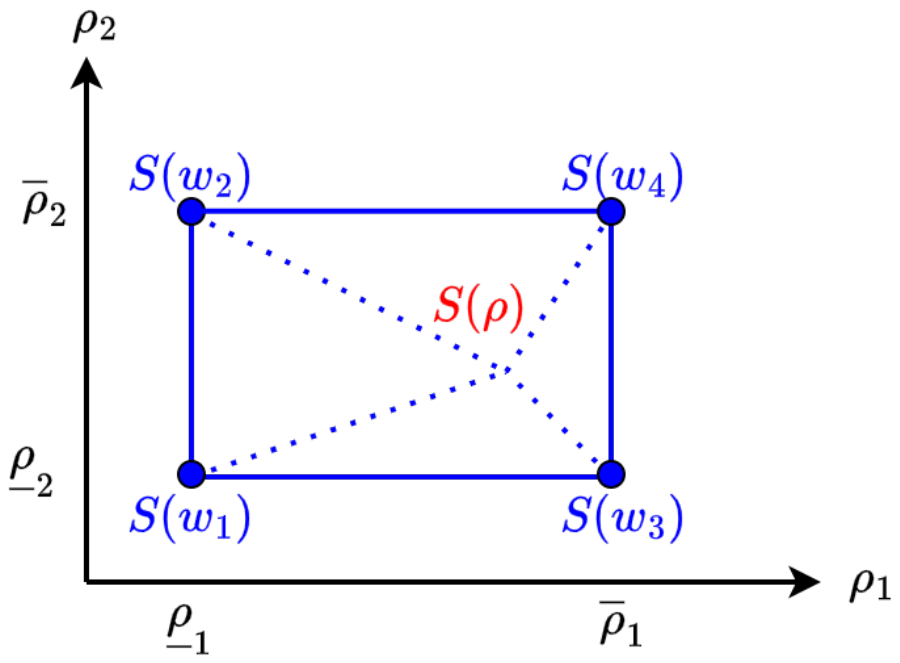

Figure 2.1: The polytopic implementation

LTI systems, which correspond to sub-models defined by the vertices of a convex polytope.

2.1.3 Stability of switched system

The stability of switched systems depends not only on the dynamics of each subsystem but also on the properties of the switching signal [10]. Therefore, stability analysis of switched systems typically involves investigating the stability properties of each subsystem and evaluating how the switching mechanism influences the overall system behavior. It is important to note that the stability of all subsystems does not guarantee the stability of switched systems under arbitrary switching and switched systems with unstable subsystems can still achieve stability under certain desirable switching rules. In general, the stability studies of switched systems mainly focus on two kinds of problems: analyzing the stability of switched systems under a given switching signal (may be arbitrary, slow switching) and designing a stabilizing switching signal for a set of dynamics systems.

The concept of stability leads to the Lyapunov stability theory, a fundamental approach in the analysis and control of dynamical systems. In the context of switched systems, techniques from hybrid system theory, such as common Lyapunov functions or multiple Lyapunov functions, are frequently employed to analyze system stability. A Lyapunov function is a scalar function that, by its construction, is positive definite, meaning it takes positive values everywhere except at an equilibrium point where it equals zero. Its most important property is that it decreases along every trajectory of dynamical systems, signifying that the system is evolving toward stable equilibrium. Hence, the method

of Lyapunov functions plays a crucial role in stability analysis and control theory of dynamical systems. In fact, it is the only universal framework for the investigation of the stability of nonlinear dynamical systems with general configuration. For many classes of systems, the existence of Lyapunov functions is a necessary and sufficient condition for establishing stability.

Stability of switched LTI systems

In this section, we will analyze the stability issues for autonomous switched linear systems without control input $u(t)$, the subsystems of which are continuous-time LTI systems

$$\dot{x}(t) = A_{\sigma(t)}x(t) \tag{2.19}$$

or a collection of discrete-time LTI systems

$$x_{k+1} = A_{\sigma(k)}x_k \tag{2.20}$$

It is possible to analyze the stability of switched systems through the Lyapunov theory. First, if a constant Lyapunov function is used, it leads to the following definition.

Definition 2.1 *The system* (2.19) *is said to be asymptotically stable if there exists a Lyapunov function* $V(x(t)) = x^T(t)Px(t) > 0$ *with a positive definite symmetric matrix* $P = P^T$ *satisfying:*

$$A_{\sigma(t)}^T P + P A_{\sigma(t)}^T \prec 0, \quad \forall \sigma(t) \in \mathcal{N} \tag{2.21}$$

for the continuous-time case, or

$$A_{\sigma(k)}^T P A_{\sigma(k)} - P < 0, \quad \forall \sigma(k) \in \mathcal{N} \tag{2.22}$$

for the discrete-time case.

In general, the existence of a single Lyapunov function is only sufficient for the asymptotic stability of switched systems under arbitrary switching signals and the results could be rather conservative. Due to the conservative of the common Lyapunov function, one reasonable approach to avoid this conservativeness is to use multiple Lyapunov functions. The fundamental idea is to construct a non-conventional Lyapunov function by concatenating together multiple Lyapunov functions, each associated to a single subsystem or region of the state space. Unlike conventional Lyapunov functions, this multi-Lyapunov function may exhibit non-monotonic decreasing along state trajectories, include discontinuities, and be only piecewise differentiable.

There are several versions of multiple Lyapunov function results in the literature. For example, the switching signals may be constrained such that, at every time when a certain subsystem switches, the value of its corresponding

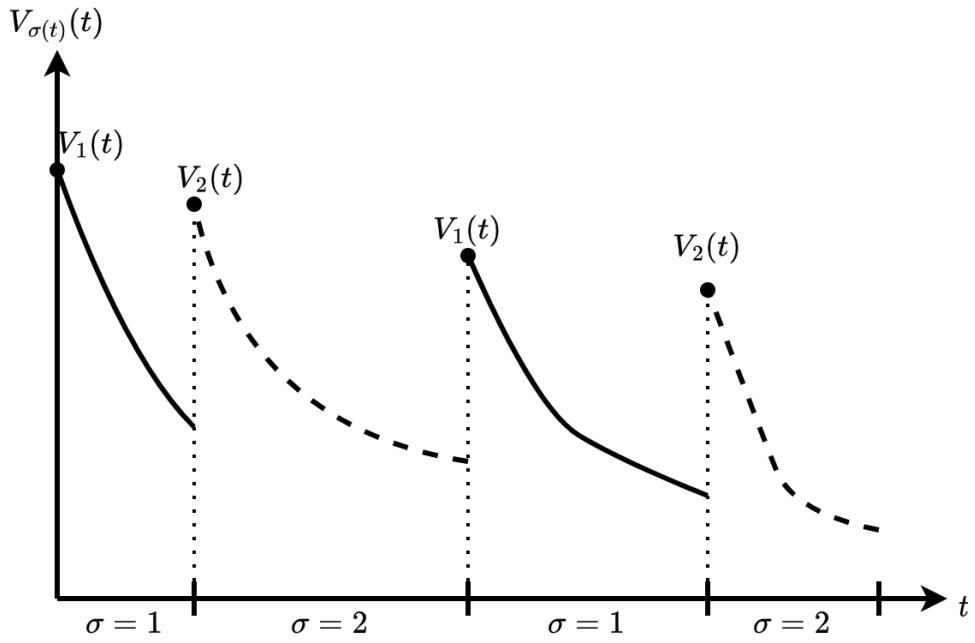

Figure 2.2: For each subsystem, the value of its Lyapunov function at the beginning of each activation interval is greater than its value at the beginning of the next interval in which the same i^{th} subsystem is active, then the switched system is asymptotically stable.

Lyapunov function is strictly less than its value at the previous switching time. Under this condition, the switched system is asymptotically stable [75]. In other words, for each subsystem, the sequence of its Lyapunov function values at every switching instants is monotonically decreasing. Alternatively, the decreasing trend can be characterized by the value of the Lyapunov function at the time a subsystem becomes active. This case is demonstrated in Figure 2.2. Moreover, the Lyapunov function may exhibit temporary increases in value, provided that such increases are bounded by appropriately defined continuous functions [10].

Stability of switched LPV systems

In the case, that each subsystem of the switched system (2.19) is an LPV system, the autonomous switched system is expressed as:

$$\dot{x}(t) = A_{\sigma(t)}(\rho)x(t) \tag{2.23}$$

Switched LPV systems combine aspects of both ***LPV systems***, which depend on parameters that vary continuously over time, and ***switched systems***, which transition between different subsystems based on discrete switching signals. The stability analysis of switched LPV systems involves studying the behavior of a dynamical system whose parameters vary in a continuous manner based on a switching signal.

The LMI (2.21) is then given as:

$$A^T_{\sigma(t)}(\rho)P + PA^T_{\sigma(t)}(\rho) \prec 0 \tag{2.24}$$

The problem with the formulation (2.24) is that it results in an infinite-dimensional problem due to infinite values of ρ. Thus, one of the challenges in the LPV framework is how to relax this infinite-dimensional constraint into a finite one. A popular and simple approach is to use the polytopic formulation. It can be turned into the following polytopic switched LPV system:

$$\dot{x}(t) = \sum_{j=1}^{2^{n_\rho}} \mu_{\sigma(t)}(\rho) A^j_{\sigma(t)} x(t) \tag{2.25}$$

Definition 2.2 *The polytopic switched LPV system* (2.25) *is quadratically stable if and only if there exists matrix* $P = P^T \succ 0$ *such that:*

$$A_i^{jT} P + P A_i^j \prec 0 \tag{2.26}$$

hold for all $i \in \mathcal{N}$ *and* $j = 1, \cdots 2^{n_\rho}$.

One of the drawbacks of quadratic stability is its high conservatism, which can result in an infeasible solution in some cases. To mitigate the conservatism, a more flexible approach involves using multiple parameter-dependent Lyapunov functions, which is investigated in [76].

Definition 2.3 *The system* (2.23) *is said to be robustly stable if there exists a parameter-dependent Lyapunov function* $V_{\sigma(t)}(x(t), \rho(t)) = x^T P_{\sigma(t)}(\rho) x > 0$, $P_{\sigma(t)}(\rho) = P^T_{\sigma(t)}(\rho) \succ 0$ *satisfying:*

$$A^T_{\sigma(t)}(\rho(t)) P_{\sigma(t)}(\rho(t)) + P_{\sigma(t)}(\rho(t)) A_{\sigma(t)}(\rho(t)) + \dot{\rho} \frac{\partial P_{\sigma(t)}}{\partial \rho} \prec 0 \tag{2.27}$$

Remark 2.1 *Since* $P_{\sigma(t)}(\rho(t))$ *depends on the time-varying parameter* $\rho(t)$*, its derivative is also taken into for system stability. If* $P_{\sigma(t)}(\rho(t)) = P_{\sigma(t)}$*, the multiple Lyapunov function is a special case of multiple parameter-dependent Lyapunov function.*

In the following, the additional conditions that must be imposed on the switched system (2.28) to ensure stability under possible switching signals are presented. To this end, we present the method based on multiple quadratic ISS Lyapunov functions to guarantee stability for the switched systems.

Input-to-State-Stability

First, the systems we deal with in this subsection are switched linear systems subject to additive bounded disturbances, without control input, described as follows:

$$\dot{x}(t) = A_{\sigma(t)} x(t) + \delta_{\sigma(t)}(t) \tag{2.28}$$

The concept of Input-to-State-Stability (ISS) was first introduced in [77] to provide theoretical concepts for describing how the system stability is affected by bounded external disturbance regarded as inputs. An insightful discussion on

ISS can be found in [78] where the concept is further elaborated, providing deeper theoretical insights and practical applications. Further researches on ISS are given in [79], [80], [81], [82]. The following definitions and lemmas are needed when ISS is introduced.

Definition 2.4 *A function* α*:* $[0,\infty) \to [0,\infty)$ *is said to be of class* $\mathcal{K}$ *if it is continuous, strictly increasing, and* $\alpha(0) = 0$*. If* α *is also unbounded, then it is said to be of class* $\mathcal{K}_\infty$

Definition 2.5 *A function* β*:* $[0,\infty) \times [0,\infty) \to [0,\infty)$ *is said to be of class* $\mathcal{KL}$ *if* $\beta(.,t)$ *is of class* $\mathcal{K}$ *for each fixed* $t \geq 0$ *and* $\beta(r,t)$ *is decreasing to zeros at* $t \to \infty$ *for each fixed* $r \geq 0$*.*

We will write $\alpha \in \mathcal{K}_\infty$, $\beta \in \mathcal{KL}$ to indicate that α s a class $\mathcal{K}_\infty$ function and β is a class $\mathcal{KL}$ function, respectively.

Definition 2.6 *The system* (2.28) *is called input-to-state-stable(ISS) with respect to* $\delta_{\sigma(t)}(t)$ *if there exist functions* $\beta \in \mathcal{KL}$ *and* $\gamma \in \mathcal{K}_\infty$*, for all initial state conditions* $x(0)$ *and all input* $\delta_{\sigma(t)}(t)$*, with* $\forall t \geq 0$ *such that*

$$\|x(t)\| \leq \beta\big(\|x(0)\|, t\big) + \gamma\big(\|\delta_{\sigma(t)}(t)\|_\infty\big) \tag{2.29}$$

Stability analysis under arbitrary switching

Common quadratic Lyapunov functions offer a powerful framework for the study of the stability of dynamical systems. In the literature, numerous achievements for analyzing the stability of switched systems using common quadratic Lyapunov function have been researched in [83, 84].

Thus, if there exists a positive definite radically unbounded smooth function

$$V(x(t)) = x^T(t)Px(t) \tag{2.30}$$

with a symmetric positive definite matrix $P \succ 0$ for the family of uncertain switched systems

$$\dot{x}(t) = A_{\sigma(t)}x(t) + \delta_{\sigma(t)}(t), \quad \forall \sigma(t) \in \mathcal{N} \tag{2.31}$$

such that for any given scalar $\varepsilon > 0$ and $\gamma > 0$

$$\dot{V}(x(t)) < -\varepsilon V(x(t)) + \gamma\|\delta_{\sigma(t)}(t)\| \tag{2.32}$$

for all $x(t) \neq 0$ and bounded disturbance $\delta_{\sigma(t)}(t)$ with $\forall \sigma(t) \in \mathcal{N}$, then the switched system (2.31) is ISS stable for any switching signal $\sigma(t)$.

This case refers to the fundamental concept known as uniform input-to-state-stability. This concept is usually applied when there are no constraints imposed on the switching signal and requires that all subsystems possess the property of input-to-state-stability.

It is worth pointing out that stability assumption of each subsystem is not sufficient to assure stability for the switched systems under arbitrary switching. It is well established in [5], [10] that if there exists a common Lyapunov function for all the subsystems, then the stability of the switched system is guaranteed under arbitrary switching. In general, the existence of a common quadratic ISS-Lyapunov function is only sufficient for the asymptotic stability of switched linear systems under arbitrary switching signals. Moreover, finding such a function is not always feasible and it could be rather conservative, limiting its practical application. Further research of the existence of common Lyapunov functions for the switched system has been developed in [85, 86, 87], which provide related results not discussed in this thesis.

Stability analysis under constrained switching

In general, it is not straightforward to find a single ISS-Lyapunov function for all subsystems to ensure the overall stability of switched systems. This is because it is challenging to identify a single matrix that satisfies the stability conditions for all subsystems, especially when each subsystem may have distinct stability requirements. Using a common matrix may result in a conservative stability analysis. Moreover, when dealing with a large number of subsystems (N), the task of searching for such a single Lyapunov function may be a considerable challenge.

Due to the conservatism associated with a common quadratic ISS-Lyapunov function, significant efforts have been devoted to the development of a less conservative class of Lyapunov functions, known as multiple input-to-state-stability Lyapunov function considered as a powerful and effective tool for both stability analysis and controllers design in switched systems [88]. An overview of fruitful results in analyzing the stability of switched linear systems based on multiple Lyapunov functions is presented in [11, 89, 30].

The key idea behind this methodology is that if multiple ISS-Lyapunov function exists for each subsystem, stability can be guaranteed by putting appropriate restrictions on the switching signal. It has been proven in the literature that the stability of switched systems when all subsystems are stable and the switching between them occurs slowly enough [90]. To formulate this, the notion of average dwell time (ADT) is proposed in [17], which imposes minimum time between switches. This concept ensures the system has enough time in each subsystem to maintain stability. By combining multiple ISS-Lyapunov functions with ADT, this approach provides a robust framework for analyzing the stability of switched systems (2.31).

The following lemmas are needed when the multiple ISS-Lyapunov function is introduced.

Lemma 2.1 *[5] If there exist two positive numbers $\mathbf{N}_0 \geq 0$, and $\tau_a > 0$ such that the following condition*

$$\mathbf{N}_\sigma(t_0, t) \leq \mathbf{N}_0 + \frac{t - t_0}{\tau_a} \tag{2.33}$$

holds for any $t > t_0$, switching signal $\sigma(t)$ has an average dwell time τ_a. $\mathbf{N}_\sigma(t_0, t)$ is the number of discontinuities of a switching signal on an interval $[t_0, t)$ and constant $\mathbf{N}_0$ is called the chatter bound giving the tolerance number of

fast switching.

Lemma 2.2 *[17] Switched system* (2.28) *is called Input-to-State-Stable with respect to disturbance* $\delta_i(t)$ *if there exists a smooth function* $V_{\sigma(t)}(x(t))$ *such that the following inequalities*

$$\alpha\|x(t)\|^2 \leq V_i(x(t)) \leq \beta\|x(t)\|^2 \tag{2.34}$$

$$\dot{V}_i(x(t)) < -\varepsilon V_i(x(t)) + \gamma_i\|\delta_i(t)\| \tag{2.35}$$

hold for any $\sigma(t) = i \in \mathcal{N}$ *with* $\varepsilon > 0$, $\gamma_i > 0$, $\beta > \alpha > 0$ *and* $\sigma(t)$ *is switching signal with average dwell time*

$$\tau_a \geq \tau_a^* = \frac{\ln(\eta)}{\varepsilon} \tag{2.36}$$

where $\eta = \frac{\beta}{\alpha}$ *with* $\alpha = \min_{i\in\mathcal{N}} \lambda_m(P_i)$ *and* $\beta = \max_{i\in\mathcal{N}} \lambda_M(P_i)$.

Here, we will briefly discuss the conditions outlined in Lemma 2.2. First, it's important to note that the inequalities in (2.34)-(2.36) are well-established in the literature, particularly in contexts involving average dwell-time switching signals. As noted by [79], the existence of a function $V_i(x(t))$ that satisfies (2.34)-(2.35) is both a necessary and sufficient condition for the i^{th} subsystem to exhibit input-to-state stability (ISS).

Remark 2.2 *The lemma 2.1 means that if there exists a positive number* τ_a *such that a switching signal has the ADT property, the ADT between any two consecutive switching is no smaller than a common constant* τ_a *for all subsystems.*

Remark 2.3 *If* (2.36) *holds for* $\eta = 1$*, then the condition* (2.33) *which the average dwell-time has to satisfy in order that the system is ISS reduces to* $\tau_a > 0$*, which means that the system is ISS for arbitrarily small average dwell time. Actually,* $\eta = 1$ *in condition* (2.36) *implies the existence of a common ISS-Lyapunov function for the switched system* (2.31)*, and thus it is, in fact, ISS for arbitrary switching*

Multiple polytopic ISS-Lyapunov function

If each subsystem of the switched system is an LPV system, then the switched system (2.31) becomes a switched LPV system as:

$$\dot{x}(t) = A_{\sigma(t)}(\rho)x(t) + \delta_{\sigma(t)}(t), \quad \forall\sigma(t) \in \mathcal{N} \tag{2.37}$$

using a unique matrix $P_{\sigma(t)}$ of multiple ISS-lyaunov functions in lemma (2.2) to ensure the stability of all the local models $A^j_{\sigma(t)}$ for all $\sigma(t) \in \mathcal{N}, j \in \mathcal{P}$ that present the parameter-dependent switching matrix $A_{\sigma(t)}(\rho)$ is considered conservative. To avoid this issue, the concept of multiple polytopic ISS-Lyapunov functions is introduced in this subsection.

Polytopic Lyapunov functions exhibit linear dependence on the weighting functions $\mu_{\sigma(t)}(\rho)$. That is, the modeling consists of designing quadratic functions for each sub-model of subsystems, and the global Lyapunov function is then obtained by forming a convex combination of these functions. This kind of function is interesting as it takes into consideration the information of weighting functions in the system analysis. The researchers have paid great attention to the polytopic Lyapunov function for analyzing the stability of the LPV systems [91, 92, 93, 94].

Now, consider the multiple polytopic ISS-Lyapunov function $V(x(t),\rho) = V_{\sigma(t)}(x(t),\rho)$, where $V_{\sigma(t)}(x(t),\rho)$ is given by

$$V_{\sigma(t)}(x(t),\rho) = \sum_{j=1}^{2^{n_\rho}} \mu^j_{\sigma(t)}(\rho) x^T(t) P^j_{\sigma(t)} x(t) \tag{2.38}$$

switches among $V_i(x(t),\rho) = \sum\limits_{j=1}^{2^{n_\rho}} \mu^j_i(\rho) x^T(t) P^j_i x(t)$ for all $i \in \mathcal{N}$ in accordance with the piecewise constant switching signal $\sigma(t)$ with $P_i(\rho) = \sum\limits_{j=1}^{2^{n_\rho}} \mu^j_i(\rho) P^j_i$.

It is worth mentioning that the stability criteria of the polytopic Lyapunov function require an investigation into the derivative of the weighting functions, typically resulting in nonconvex conditions. This is a key point to use multiple polytopic Lyapunov functions in switched LPV systems.

The main statement of ISS under ADT switching signal of system (2.37) is stated in the following lemma.

Lemma 2.3 *[95] Switched system* (2.37) *is called Input-to-State-Stable with respect to disturbance* $\delta_i(t)$ *if there exists a smooth function* $V_{\sigma(t)}(x(t))$ *such that the following inequalities*

$$\alpha\|x(t)\|^2 \leq V_i(x(t)) \leq \beta\|x(t)\|^2 \tag{2.39}$$

$$\dot{V}_i(x(t)) < -\varepsilon V_i(x(t)) + \gamma_i\|\delta_i(t)\| \tag{2.40}$$

hold for any $\sigma(t) = i \in \mathcal{N}$ *with* $\varepsilon > 0$, $\gamma_i > 0$, $\beta > \alpha > 0$ *and* $\sigma(t)$ *is switching signal with average dwell time*

$$\tau_a \geq \tau^*_a = \frac{\ln(\eta)}{\varepsilon} \tag{2.41}$$

where $\eta = \frac{\beta}{\alpha}$ *with* $\alpha = \min\limits_{i\in\mathcal{N}, j\in\mathcal{P}} \lambda_m(P^j_i)$ *and* $\beta = \max\limits_{i\in\mathcal{N}, j\in\mathcal{P}} \lambda_M(P^j_i)$.

It is notable to emphasize that the use of the multiple polytopic ISS-Lyapunov function presented in lemma 2.3 for both polytopic subsystems and the switching modes allows a general approach which provides more degree of freedom for analyzing the stability and designing observers for the switched LPV systems than the one obtained with common Lyapunov function [96]. It is worth noting that, few research results on switched LPV systems with average dwell time switching signals have been studied in the literature with the multiple polytopic ISS-Lyapunov function.

In the following section, basic notions of fault diagnosis and terminology, classification of faults, and fault-tolerant

control methods are presented in detail.

2.2 Interval observer

State estimation has been extensively discussed and reported in numerous engineering fields. The concept of state observer was introduced by [97]. In control theory, an observer is a dynamic system that, using inputs and measurement output information of the real system, constructs the evolution of the state of a given system. The general structure of an estimator is illustrated in Figure 2.3.

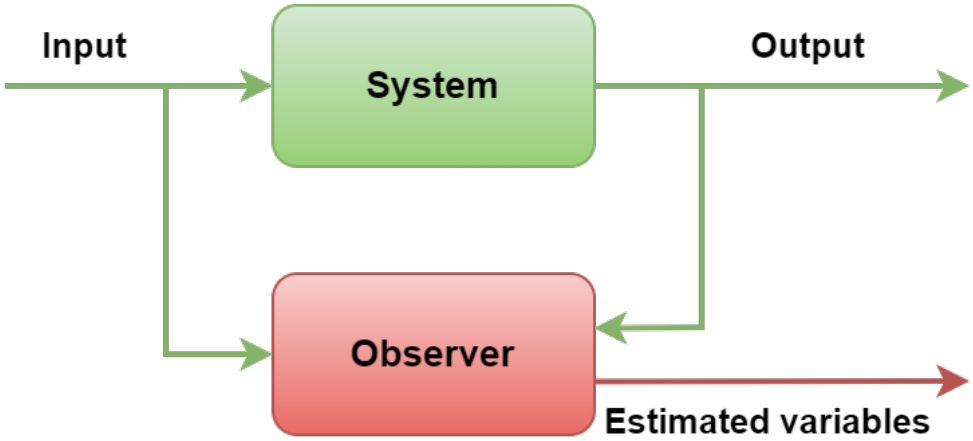

Figure 2.3: General structure of an observer

However, in real-world applications where uncertainties are inevitable, traditional observers may face the challenge of providing accurate estimates of the system states in the existence of uncertainties coming either from external disturbances or from the mismatch between the model and the real system. Since the conventional observer's convergence depends mainly on the accuracy of the mathematical model. The incorporation of uncertainty into the observer design procedure in order to enhance estimation precision and improve the performance of the system is of particular interest. In other words, the estimation error of a conventional observer generally does not go to zeros in the presence of uncertainties as time to infinity.

To overcome the limitations of the conventional observers and effectively estimate the system states in the presence of large and fluctuating disturbances (parameter and/or model uncertainties), a novel class of estimators has been developed recently known as interval observer based on **set-membership** and **bounded error estimation approaches**. In contrast to the conventional state estimation approach, the interval observers are a pair of estimators whose dynamic equation and initial conditions are defined such that their trajectories $\underline{x}(t)$ and $\overline{x}(t)$ represent the lower and upper bounds of the system's state $x(t)$ at any time as depicted in Figure 2.4. This new methodology is designed under the assumption that the uncertainties are unknown but bounded with a priori known bounds. There are several approaches to designing the interval/set membership estimator [98, 99, 100, 101, 102, 103, 42]. This

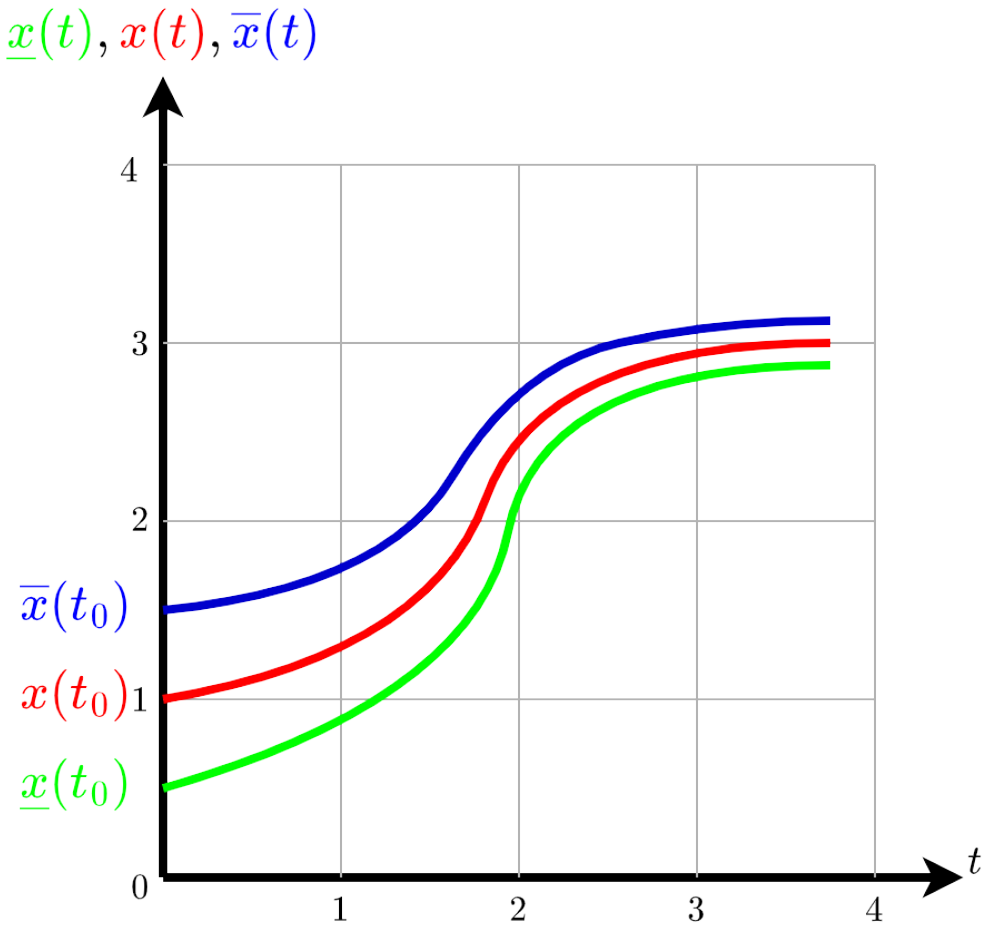

Figure 2.4: Conventional and interval observer

thesis is devoted to interval observer, which form a subclass of bounded error estimator and whose design is based on the monotone systems theory [104].

The width of the interval $e(t) = \overline{x}(t) - \underline{x}(t)$ is proportional to the size of model uncertainty and can be minimized by tuning the observer parameters.

It is worth noticed that ensuring the positivity and stability properties of the estimation errors is a crucial aspect in the design of interval observer. It is one of the most major challenges for the design of interval observers corresponding to the cooperativity of the estimation error dynamics. It is obvious that finding the observer gain matrices satisfying Hurwitz and Metzler conditions is not a straightforward task. Therefore, to address this challenge and relax the design conditions of interval observers, recent research has demonstrated that, under some mild conditions, a Hurwitz matrix can be transformed into a Hurwitz and Metzler (cooperative) form through a similarity transformation of coordinates [39]. This coordinate transformation can take the form of either time-invariant as proposed in [105] or time-varying as proposed in [32].

In the following section, we present the basics preliminaries and the design of interval observers.

2.2.1 Nonnegative and Metzler matrices

In this subsection , some definitions and lemmas on interval observer will be given.

Definition 2.7 *A matrix $A_{\sigma(t)}$ is said to be non-negative if all its elements are non-negative for all $\sigma(t) \in \mathcal{N}$, i.e. $A_{\sigma(t)} \geq 0$.*

Lemma 2.4 *A matrix $A_{\sigma(t)}$ is a Metzler matrix if all its off-diagonal elements are non-negative for all $\sigma(t) \in \mathcal{N}$.*

Lemma 2.5 *A matrix $A_{\sigma(t)}$ is a Metzler matrix if and only if there exists a constant $\beta_{\sigma(t)} \in \mathbb{R}^+$ such that $A_{\sigma(t)} + \beta_{\sigma(t)} I_{n_x} \geq 0$ for all $\sigma(t) \in \mathcal{N}$.*

2.2.2 Positive switched systems

Definition 2.8 *Positive system is a class of systems with states and output that remain non-negative, provided the initial state and input are non-negative.*

Lemma 2.6 *[106] If $A_{\sigma(t)}$ is a Metzler matrix, $x(t_0) \geq 0$ and $\delta_{\sigma(t)}(t) \geq 0$, $\forall \sigma(t)$ and $\forall t \geq t_0 \geq 0$ then the following continuous-time system is a positive switched system.*

$$\dot{x}(t) = A_{\sigma(t)} x(t) + \delta_{\sigma(t)}(t) \tag{2.42}$$

We have presented the positivity conditions of continuous-time systems which governed by differential equations. However, theses conditions do not apply to discrete-time systems which are described by difference equation forms. Next, we will introduce the equivalent positivity condition for discrete-time systems.

Lemma 2.7 *[107] If $A_{\sigma(k)}$ is a nonnegative matrix, $x(k_0) \geq 0$ and $\delta_{\sigma(k)}(k) \geq 0$, $\forall \sigma(k)$ and $\forall k \geq k_0 \geq 0$ then the following discrete-time system is a positive switched system.*

$$\dot{x}(k) = A_{\sigma(k)} x(k) + \delta_{\sigma(k)}(k) \tag{2.43}$$

At this stage, it is straightforward to verify whether the system is positive or not. In the following sections, we will illustrate how this positivity property can be utilized to design interval observers for switched LTI systems.

2.2.3 Interval relation

An interval vector $x(t) \in \mathbb{R}^{n_x}$ can be defined as $\underline{x}(t) \leq x(t) \leq \overline{x}(t)$ where $\underline{x}(t)$ and $\overline{x}(t)$ are the endpoints and the inequalities are understood element-wise. The relationship $x_1(t) \leq x_2(t)$ and $A_1 \leq A_2$ is understood element-wise for two vectors $x_1(t), x_2(t) \in \mathbb{R}^{n_x}$ or matrices $A_1, A_2 \in \mathbb{R}^{n_x \times n_x}$, respectively.

Definition 2.9 *For a matrix $A \in \mathbb{R}^{n_m \times n_x}$, we define*

$$A^+ = \max\{A, 0\}, A^- = A^+ - A \tag{2.44}$$

For a vector $x \in \mathbb{R}^{n_x}$, we define

$$x^+ = \max\{x, 0\}, x^- = x^+ - x \tag{2.45}$$

Lemma 2.8 *[106] Let $x \in \mathbb{R}^{n_x}$ be a vector such that $\underline{x} \leq x \leq \overline{x}$ with $\underline{x}(t), \overline{x} \in \mathbb{R}^{n_x}$. If $\mathcal{M} \in \mathbb{R}^{n_m \times n_x}$ is a constant matrix, then:*

$$\mathcal{M}^+\underline{x} - \mathcal{M}^-\overline{x} \leq \mathcal{M}x \leq \mathcal{M}^+\overline{x} - \mathcal{M}^-\underline{x} \tag{2.46}$$

If $\mathcal{M} \in \mathbb{R}^{n_m \times n_x}$ is a variable matrix satisfying $\underline{\mathcal{M}} \leq \mathcal{M} \leq \overline{\mathcal{M}}$ for some $\underline{\mathcal{M}}, \overline{\mathcal{M}} \in \mathbb{R}^{n_m \times n_x}$, then:

$$\begin{aligned} &\underline{\mathcal{M}}^+\underline{x}^+ - \overline{\mathcal{M}}^+\underline{x}^- - \underline{\mathcal{M}}^-\overline{x}^+ + \overline{\mathcal{M}}^-\overline{x}^- \leq \mathcal{M}x \leq \\ &\overline{\mathcal{M}}^+\overline{x}^+ - \underline{\mathcal{M}}^+\overline{x}^- - \overline{\mathcal{M}}^-\underline{x}^+ + \underline{\mathcal{M}}^-\underline{x}^- \end{aligned} \tag{2.47}$$

In the following, a comprehensive study on the interval observers is presented for a specific class of switched systems.

2.2.4 Interval observers design for switched systems

Throughout this subsection, we particularly focus on the design process and robust analysis of an interval observer for a switched linear system affected by unknown but bounded disturbances. As discussed in [108], researchers have developed a wide range of methodologies for defining the structure of an interval observer. In the subsequent discussion, we present a novel interval observer design, drawing inspiration from the ISS paradigm detailed in Section 2.1.3. This framework allows for a straightforward analysis of the impact of perturbation on the interval estimation errors.

Let's consider the following switched system:

$$\begin{cases} \dot{x}(t) = A_{\sigma(t)}x(t) + B_{\sigma(t)}u(t) + w_{\sigma(t)}(t) \\ y(t) = Cx(t) \end{cases} \tag{2.48}$$

where $x(t) \in \mathbb{R}^{n_x}$ is state vector, $u(t) \in \mathbb{R}^{n_u}$ is control input, $y(t) \in \mathbb{R}^{n_y}$ is measurement output, $w_{\sigma(t)}(t) \in \mathbb{R}^{n_x}$ is disturbance input and switching signal $\sigma(t) \in \mathcal{N} = \{1, \cdots, N\}$ is assumed to be available in real time with N is the number of subsystems. The matrices $A_{\sigma(t)} \in \mathbb{R}^{n_x \times n_x}$ and $B_{\sigma(t)} \in \mathbb{R}^{n_x \times n_u}$ are known constant switching matrices. Without loss of generality, the output matrix $C \in \mathbb{R}^{n_y \times n_x}$ is considered constant for all $\sigma(t) \in \mathcal{N}$.

The pair $\left(A_{\sigma(t)}, C\right)$ is at least detectable with $\forall \sigma(t) \in \mathcal{N}$ and the disturbance $w_{\sigma(t)}(t)$ is assumed to be unknown

but bounded by two priori known bounds.

$$\underline{w}_{\sigma(t)}(t) \leq w_{\sigma(t)}(t) \leq \overline{w}_{\sigma(t)}(t) \tag{2.49}$$

Additionally, the initial state conditions $x(t_0)$ is bounded by two prior known bounds $\underline{x}(t_0)$ and $\overline{x}(t_0)$

$$\underline{x}(t_0) \leq x(t_0) \leq \overline{x}(t_0) \tag{2.50}$$

The main goal is to estimate the lower bound $\underline{x}(t) \in \mathbb{R}^{n_x}$ and the upper bound $\overline{x}(t) \in \mathbb{R}^{n_x}$ of the state $x(t)$ with ability to guarantee the robustness in the presence of unknown perturbation $w_{\sigma(t)}(t)$ for switched system (2.48). The following structure of switched interval observer, similar to the structure of Luenberger observer is proposed for system (2.48):

$$\begin{cases} \dot{\overline{x}}(t) = \big(A_{\sigma(t)} - L_{\sigma(t)}C\big)\overline{x}(t) + B_{\sigma(t)}u(t) + L_{\sigma(t)}y + \overline{w}_{\sigma(t)}(t) \\ \dot{\underline{x}}(t) = \big(A_{\sigma(t)} - L_{\sigma(t)}C\big)\underline{x}(t) + B_{\sigma(t)}u(t) + L_{\sigma(t)}y + \underline{w}_{\sigma(t)}(t) \end{cases} \tag{2.51}$$

where $L_{\sigma(t)}$ is the interval observer gain matrices to be designed in order to ensure the stability and inclusion properties of the interval observer.

- **The inclusion property $\underline{x}(t) \leq x(t) \leq \overline{x}(t)$.**

By introducing the upper and lower estimation errors as follows:

$$\begin{cases} \overline{e}(t) = \overline{x}(t) - x(t) \\ \underline{e}(t) = x(t) - \underline{x}(t) \end{cases} \tag{2.52}$$

From equations (2.48) and (2.51), the upper and lower dynamics of estimation errors are given as:

$$\begin{cases} \dot{\overline{e}}(t) = \big(A_{\sigma(t)} - L_{\sigma(t)}C\big)\overline{e}(t) + \overline{w}_{\sigma(t)}(t) - w_{\sigma(t)}(t) \\ \dot{\underline{e}}(t) = \big(A_{\sigma(t)} - L_{\sigma(t)}C\big)\underline{e}(t) + w_{\sigma(t)}(t) - \underline{w}_{\sigma(t)}(t) \end{cases} \tag{2.53}$$

According to the condition (2.49), the following terms are non-negative:

$$\begin{cases} \overline{w}_{\sigma(t)}(t) - w_{\sigma(t)}(t) \geq 0 \\ w_{\sigma(t)}(t) - \underline{w}_{\sigma(t)}(t) \geq 0 \end{cases} \tag{2.54}$$

Since the initial error conditions $\underline{e}(t_0) = x(t_0) - \underline{x}(t_0)$ and $\overline{e}(t_0) = \overline{x}(t_0) - x(t_0)$ are non-negative by the construction (2.50), then according to lemma 2.6, the lower and upper estimation errors are non-negative, i.e. $\underline{e}(t) \geq 0$ and $\overline{e}(t) \geq 0$, for all $t \geq t_0$ provided that $A_{\sigma(t)} - L_{\sigma(t)}C$ are Metzler matrices $\forall \sigma(t) \in \mathcal{N}$. This implies that the system

state $x(t)$ is bounded.

$$\underline{x}(t) \leq x(t) \leq \overline{x}(t) \tag{2.55}$$

In order to guarantee that the system (2.51) is an interval observer of system (2.48), in addition to positivity conditions, the stability conditions of the estimation error need to be satisfied.

- **Stability property** $\underline{x}(t) \rightarrow x(t) \leftarrow \overline{x}(t)$

In order to analyze the stability of the proposed switched interval observer, the interval error is introduced as follows:

$$e(t) = \overline{x}(t) - \underline{x}(t) = \overline{e}(t) + \underline{e}(t) \tag{2.56}$$

Based on equation (2.53), the dynamics of interval error is given as:

$$\dot{e}(t) = \big(A_{\sigma(t)} - L_{\sigma(t)}C\big)e(t) + \nabla_{\sigma(t)}(t) \tag{2.57}$$

with $\nabla_{\sigma(t)}(t) = \overline{w}_{\sigma(t)}(t) - \underline{w}_{\sigma(t)}(t)$.

In the presence of the bounded disturbance $\nabla_{\sigma(t)}(t)$, the main goal is to demonstrate that the interval error $e(t)$ remains within a certain bound. Moreover, the objective is to establish the relationship between the bound of the interval error and the upper bound of perturbations denoted as Δ_{max}, where $\max \|\nabla_{\sigma(t)}(t)\| \leq \Delta_{\max}$ for all $\sigma(t) \in \mathcal{N}$. The sufficient condition for the existence of the switched interval observer (2.51) is performed by using multiple ISS-Lyapunov functions under ADT. The main result is given by the following theorem.

Theorem 2.1 *Under conditions 2.50, if there exists positive diagonal matrices P_i, a multiple ISS-Lyapunov function $V_{\sigma(t)}(e(t))$ switching among $V_i(e(t)) = e^T(t)P_ie(t)$, given matrices W_i and scalars $\varepsilon > 0$, $\eta_i > 0$, $\beta \geq \alpha \geq 0$ and positive scalar γ_i, such that the following LMIs hold for all $i \in \mathcal{N}$*

$$\min_{P_i, W_i} \gamma \tag{2.58}$$

$$\gamma_i \leq \gamma \tag{2.59}$$

$$\alpha I_{n_x} \leq P_i \leq \beta I_{n_x} \tag{2.60}$$

$$\begin{bmatrix} P_iA_i - W_iC + A_i^TP_i - C^TW_i^T + \varepsilon P_i & P_i \\ P_i & -\gamma_i I_{n_x} \end{bmatrix} \prec 0 \tag{2.61}$$

$$P_iA_i - W_iC + \eta_iP_i \geq 0 \tag{2.62}$$

then the interval observer (2.51) *can estimate the lower and upper bounds of the state of the system* (2.48) *with* $L_i = P_i^{-1}W_i$.

In addition, the system (2.53) *is ISS with respect to the disturbance* $\nabla_i(t)$ *under any switching signal* $\sigma(t)$ *with ADT satisfying the condition* (2.36)*, and*

$$\lim_{t\to\infty} \|e(t)\|_2 \leq \sqrt{\frac{\gamma}{\alpha\varepsilon}} \max \|\nabla_i(t)\|_\infty \quad \forall i \in \mathcal{N} \tag{2.63}$$

Proof 2.1 *Let's consider the following multiple ISS-Lyapunov function*

$$V_i(e(t)) = e^T(t) P_i e(t) \tag{2.64}$$

where $P_i \in \mathbb{R}^{n_x \times n_x}$ *are positive diagonal matrices.*

Then the first-time derivative of Lyapunov function along its trajectory is given as:

$$\begin{aligned} \dot{V}_i(e(t)) &= \dot{e}^T(t) P_i e(t) + e^T(t) P_i \dot{e}(t) \\ &= e^T(t)\Big(\big(A_i - L_i C\big)^T P_i + P_i\big(A_i - L_i C\big)\Big) e(t) + \nabla_i^T P_i e(t) + e^T(t) P_i \nabla_i(t) \end{aligned} \tag{2.65}$$

For any $\varepsilon > 0$ *and* $\gamma_i > 0$*, adding and subtracting* $\varepsilon V_i(e(t))$ *and* $\gamma_i \nabla^T(t)\nabla(t)$*, one can obtain:*

$$\dot{V}_i(e(t)) = \begin{bmatrix} e(t) & \nabla_i(t) \end{bmatrix} \Xi_i \begin{bmatrix} e(t) \\ \nabla_i(t) \end{bmatrix} - \varepsilon V(e(t)) + \gamma_i \nabla_i^T(t)\nabla_i(t) \tag{2.66}$$

where

$$\Xi_i = \begin{bmatrix} P_i A_i - W_i C + A_i^T P_i - C^T W_i^T + \varepsilon P_i & P_i \\ P_i & -\gamma_i I_{n_x} \end{bmatrix} \tag{2.67}$$

with the change of variables $W_i = P_i L_i$*.*

The following sufficient conditions for system (2.57) *is ISS with respect to the disturbance* $\nabla_i(t)$ *is that*

$$\Xi_i \prec 0 \tag{2.68}$$

This condition implies that

$$\dot{V}_i(e(t)) \prec -\varepsilon V_i(e(t)) + \gamma_i \nabla_i^T(t)\nabla_i(t) \tag{2.69}$$

Then one obtain that

$$V_i(e(t)) \leq V_i(0) e^{-\varepsilon t} + \gamma_i \int_0^t e^{-\varepsilon(t-\tau)} \|\nabla_i(t)\|_2^2 d\tau \tag{2.70}$$

Recall that, from the condition (2.60)*, it follows that*

$$\alpha \|e(t)\|_2^2 \leq V_i(e(t)) \leq \beta \|e(t)\|_2^2 \tag{2.71}$$

Then the inequality (2.70) *becomes*

$$\alpha\|e(t)\|_2^2 \leq \beta\|e(0)\|_2^2 e^{-\varepsilon t} + \gamma_i \int_0^t e^{-\varepsilon(t-\tau)}\|\nabla_i(t)\|_2^2 d\tau \tag{2.72}$$

which leads to

$$\|e(t)\|_2^2 \leq \sqrt{\frac{\beta\varepsilon\|e(0)\|_2^2 e^{-\varepsilon t} + \gamma_i \nabla_{max}}{\alpha\varepsilon}} \tag{2.73}$$

Therefore, when $t \to 0$*, the exponential term forwards to zero and with* $\gamma_i \leq \gamma$*, the inequality* (2.73) *becomes LMI* (2.63).

$$\lim_{t\to\infty} \|e(t)\|_2 \leq \sqrt{\frac{\gamma}{\alpha\varepsilon}}\nabla_{\max} \quad \forall i \in \mathcal{N} \tag{2.74}$$

Remark 2.4 *The inequality* (2.73) *leads to the following conclusions:*

- *If there are no disturbances, i.e.* $\|\nabla_i(t)\|_\infty = 0$*, then* $\|e(t)\| \to 0$ *when* $t \to \infty$*.*
- *Moreover, when the system subject to the additive perturbations* $\nabla_i(t)$*, the interval estimation error* $\|e(t)\|$ *is bounded by* $\sqrt{\frac{\gamma}{\alpha\varepsilon}}\Delta_{max}$*. Consequently, the Input-to-State-Stability is established through the inequality* (2.73)*.*

In the next step, we need to ensure the Metzler property. According to lemma 2.5, $A_i - L_i C$ *are Metzler matrices for all* $i \in \mathcal{N}$ *and positive scalar* η_i *if*

$$A_i - L_i C + \eta_i I_{n_x} \geq 0 \tag{2.75}$$

By multiplying the positive diagonal matrices P_i *on the left side of* (2.62) *and performing the change of variables* $W_i = P_i L_i$*, one can obtain:*

$$P_i A_i - W_i C + \eta_i P_i \geq 0 \tag{2.76}$$

which prove the positivity of the lower and upper estimation errors $\underline{e}(t)$ *and* $\overline{e}(t)$ *in the LMI of* (2.62)*.*

2.2.5 Useful lemmas

The following lemmas, which are applied later in the Theorems' proofs, are recalled.

Lemma 2.9 *[109] Suppose* Q *and* S *are symmetric matrices, the following statements are equivalent:*

$$\begin{bmatrix} Q & R \\ R^T & S \end{bmatrix} \prec 0 \tag{2.77a}$$

$$S < 0, Q - RS^{-1}R^T \prec 0 \tag{2.77b}$$

$$Q < 0, S - R^T Q^{-1} R \prec 0 \tag{2.77c}$$

Lemma 2.10 *[110] For given matrices X and Y with appropriate dimensions, if there exists matrix F verifying $F^TF \leq I$, the following inequality is always true with an arbitrary scalar $\eta > 0$:*

$$XFY + Y^TF^TX^T \leq \eta XX^T + \eta^{-1}Y^TY \tag{2.78}$$

Lemma 2.11 *[111] Given matrices X and Y with appropriate dimensions, for any invertible matrix F and scalar $\mu > 0$, we have:*

$$X^TY + Y^TX \leq \mu X^TFX + \mu^{-1}Y^TF^{-1}Y \tag{2.79}$$

Lemma 2.12 *[112] Given matrices $\mathcal{X} \in \mathbf{R}^{n\times m}$, $\mathcal{Y} \in \mathbf{R}^{m\times p}$ and $\mathcal{Z} \in \mathbf{R}^{n\times p}$ with $rank(\mathcal{Y}) = p$, the general solution $\mathcal{X}$ of the equation $\mathcal{X}\mathcal{Y} = \mathcal{Z}$ is:*

$$\mathcal{X} = \mathcal{Z}\mathcal{Y}^\dagger + \Xi(I_m - \mathcal{Y}\mathcal{Y}^\dagger) \tag{2.80}$$

where $\Xi \in \mathbf{R}^{n\times m}$ is an arbitrary matrix

2.3 Fault-Tolerant Control

As modern technological systems become more complex, the corresponding control systems must also evolve to handle faults effectively. A control that has the capability of accommodating faults among system components while maintaining the system stability and the acceptable performance despite the occurrence of faults is called Fault-Tolerant Control (FTC).

The field of FTC has gained significant importance across various fields, including aerospace engineering [113], automotive engineering [114], robotics [115].

2.3.1 Types of fault-tolerant control

The Fault-Tolerant Control (FTC) approaches are designed to enhance the safety and reliability of control systems by automatically compensating for faults, in some cases, failures in the system components while preserve the system stability and desired performance level in the presence of faults [116]. Therefore, the main objective in a FTC system is to design a controller with an appropriate structure to maintain stability and achieve the desired performance, not only in the normal operation conditions, but also in the situations involving malfunctions in sensors, actuators, or other system components (e.g. the system itself, control computer hardware or software).

Generally, the FTC system can be classified into two categories, namely, active FTC and and passive FTC [117, 118]. Passive FTC refers to a type of control system designed to tolerate system component faults without relying on the online faulty information to control the system. It is closely related to robust control where a fixed controller is designed to be robust against a predefined fault in the system [119].

In contrast with passive FTC systems, active FTC systems dynamically respond to occurrence of faults by re-configuring the controller based on real-time information from a FDD scheme. The term ”active” signifies the proactive nature of corrective actions taken actively by the reconfiguration mechanism to modify the control structure and parameters to compensate for the fault effects.

Both passive and active FTC have advantages and disadvantages, and choice between passive and active FTC depends on factors such as system complexity, performance specification and implementation feasibility.

In the following subsection, a brief illustration of the passive and active FTC are presented.

Passive and Active FTC

In this subsection, the objective is to investigate the recent studies in the field of passive and active FTC theory and highlights their advantages and disadvantages.

Passive FTC In a passive FTC approach, the design of the control system is incorporated a predetermined list of potential faults and failures which are assumed to be known a priori with normal operating conditions of the system during the design stage. The main objective of passive FTC is to design a controller with constant structure or parameters that makes the closed-loop system as insensitive as possible to certain faults. The structure of passive FTC is illustrated in Figure 2.5.

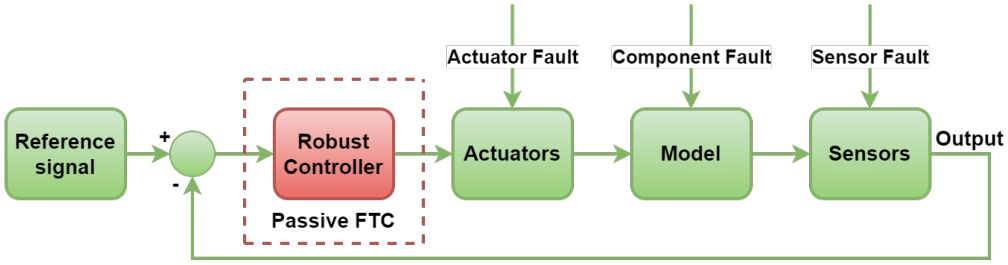

Figure 2.5: Architecture of passive FTC

The passive FTC systems maintain the robustness and reliability of the system without requiring the on-line fault information from FDD and reconfiguration mechanism. Therefore, there is no additional actions need to be taken by the controller in response to the faults with both normal and fault conditions and the control system deals with all expected faults passively.

In the literature, several approaches have been used in designing passive FTC varies from sliding mode control approach [120, 121] to robust H_∞ control [54], adaptive control [122], control allocation [123, 124]. These control techniques are generally less complicated due to their simplicity in design and low computational complexity [48].

The main advantages of passive FTC techniques can be described as follows: Neither FDD nor controller reconfiguration process is implemented and the control system operates with the same predefined parameters in all

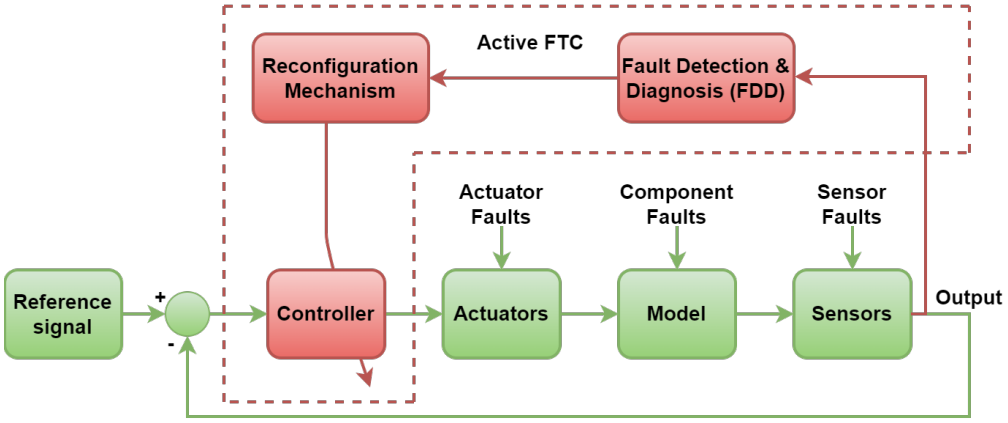

Figure 2.6: Architecture of active FTC

conditions [125].

Since both the FDI and controller reconfiguration are not taken into account during the control design, the time response of the system becomes very fast. Therefore, there is no delay between the fault occurrence and the corresponding control actions. The control system always take the control actions to the fault occurrence immediately. However, the detection of various types of faults may impose a considerable challenge for a passive FTC system since it is designed to work in the off-line mode. Hence, its functionality would be limited and less effective with complex and various kinds of simultaneous faults [126].

For these reasons, the active FTC system receives great attention among the researchers.

Active FTC In contrast to passive FTC technique, the active FTC system responses to each fault differently to maintain the performance and stability of the system through the designed control technique and real-time information provided by FDD system.

Generally, an active FTC system typically consists of three main subsystems as shown in Figure 2.6: FDD scheme, reconfigurable controller and controller reconfiguration mechanism [127, 128, 129].

Based on this structure, the main goal in active FTC is how to develop an effective FDD scheme which offers high sensitivity to fault information (time, type, magnitude) while minimizing uncertainties and external disturbances; a control scheme which is effectively reconfigured to compensate for the fault-induced effects so that the stability and acceptable closed-loop system performance are preserved; and a reconfiguration mechanism which aims at recovering the pre-fault system performance in the face of faults. It is essential for these three units working together to accomplish the control tasks.

The inclusion of both FDD and recongfigurable controller within the overall system structure is the main distinguishing active FTC from passive FTC.

In active FTC approach, the FDD scheme plays a vital role in enhancing the reliability, safety and performance of the system. It provides as precisely as possible, the real-time information typically including details about the

types, location and magnitude of faults to the controller. Based on the information provided by FDD, the active FTC effectively reconfigure the controller to guarantee the stability and acceptable closed-loop system performance.

Therefore, the active FTC system can attain optimal performance provided that the diagnostic information from the FDD scheme is accurate. Any uncertainties in FDD can result in loss of effectiveness in the designed controller.

The critical issues in any active FTC system are the limited amount of time available for the FDD to detect and identify the error and the time taken to synthesize and deploy the new control schemes [130]. There is no action performed until the new control system is synthesized. Therefore, the interval between the fault occurrence and the initiation of the reconfigured controller plays an important role in maintaining the safe operation of the system. If the FDD process takes unexpectedly long time, the integrity of the system may be in danger. In other words, the time need to get the fault information and the time taken to reconfigure the control should be fast enough to ensure the stability and performance of the system.

2.3.2 Classification of fault

Each type of fault present a unique challenges for strategy of FDD in the control system. Therefore, identifying faults from different perspectives can result in comprehensive approaches for detecting, isolating, and mitigating faults in order to address a specific type of faults and maintain the stability and performance of control systems in a variety of operating conditions. From a different point of view, faults can be categorized into various types.

Fault classification based on components

As can be seen in Figure 2.5, faults based on their component type can be classified into three categories namely component faults, sensor faults and actuator faults.

- **Component faults**: this category of fault refers to the malfunction or defect in individual component of the system which can affect the system's dynamics.
- **Sensor faults**: sensors are essentially the output interfaces of a system with the external environment. It provides the feedback to the control system. In the closed-loop systems, the measurement obtained by sensor are used to generate the control inputs. Hence, the accuracy and effectiveness of control signals can be compromised if a sensor fault occurs. Sensor faults may include:
  - Sensor Saturation: when a sensor reaches its maximum or minimum measurement range and the sensor's out remains constant at its the highest or lowest values despite further increase of decrease in the signal being measured.
  - Sensor Bias: Systematic errors in sensor readings, resulting in consistent deviations from the true value.

  - Sensor Failure: refers to a critical malfunction in which the sensor completely loss its functionality in the sensor, resulting in the absence of feedback signals.
  - Sensor Noise: refers to the random fluctuations in measurement output, making it challenging to discern true system behavior.
  - Sensor Drift: Gradual changes in sensor readings over time, leading to inaccuracies in feedback signals.

- **Actuator faults**: Actuators represent the functional components that are responsible for implementing the control actions based on the control system's commands. Hence, actuator faults can disrupt or modify the system's input signal, it may lead to the increased energy consumption and, in severe cases, complete loss of control. The most common scenarios of actuator faults can be listed as.
  - Actuator saturation: when an actuator reaches its maximum or minimum output, limiting the ability to respond to the control signal effectively.
  - Actuator Bias: systematic error in the actuator response leading to a consistent offset from the desired control action.
  - Actuator failure: complete loss of functionality in the actuator, preventing it from executing the control command altogether.
  - Actuator Deadband: this occur when the actuator dose not respond to the small control signal, leading to less precision in control action.

Faults classification based on representation

Faults can be also categorized into two groups, depending on how they are represented in model: additive or multiplicative [131]. This can be seen from Figure 2.7

- Additive Fault: a category of faults, impacts either on the input or output signal of the system. These fault are commonly represented by an additional term. Additive faults are often associated with issues in sensors and actuators.
- Multiplicative Fault: this category of fault is characterized by a multiplicative term which can modify the system's structure by affecting the model parameters.

2.3.3 Co-design of observers and controllers

Unlike the traditional FDI approach, fault estimation (FE) is considered a powerful alternative methodology in FTC systems, and considering a direct estimation of the fault signal via FE can offer significant advantages. FE functions take over both the fault detection and isolation roles and the more complex FDI role is thus eliminated. In this

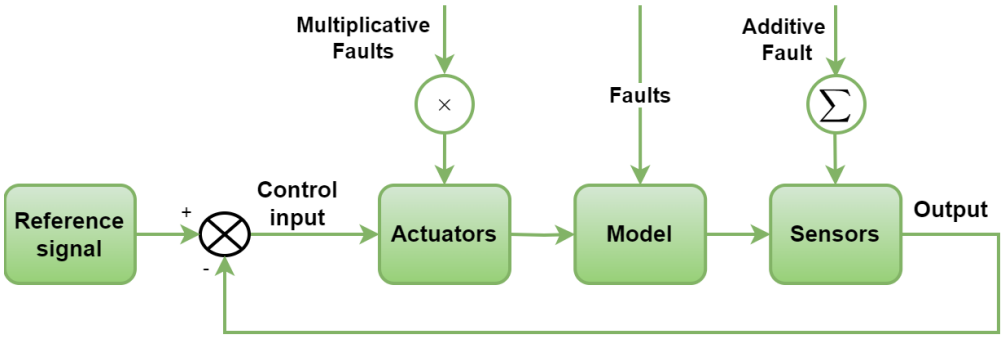

Figure 2.7: Additive and Multiplicative Faults

approach, the control system directly utilizes the reconstructed or estimated variables from the FE to compensate for the fault effects. Many techniques in FE design for FTC have been reported in the literature, e.g., based on sliding mode observer [132], unknown input observer [133], adaptive observer [134]. The observer-based controller approaches have been drawn considerable attention of researchers [135, 136]. However, most works are designed based on the Separation Principle, which states that the design of the observer and controller can be performed independently and then combined to ensure stability and performance. It may lead to the loss of the closed-loop stability in the presence of uncertainties and disturbances. This motivates researchers to develop an integrated control system by jointly designing the fault estimation (FE) and FTC system that consider the bi-directional interaction between the FE and FTC system during the control design process [137, 138, 139, 140, 141]. As a result, the concept of the co-design problem is presented to indicate the simultaneous design methodology of FE and active FTC using an integrated framework. In other words, the main objective of the proposed approach is to determine the observer and controller gain matrices in a joint way through a single-step LMI formulation. The structure of co-design is demonstrated in Figure 2.8.

Notably, the direct application of FE without requiring the reconfigurable mechanism provides tremendous convenience and potential in the field of FTC system design. This method can pave the way for the development of robust approaches to co-design FE and FTC by taking the bi-directional interaction into consideration. Nevertheless, few results on the integrated design of FE and FTC have been proposed. The authors in [142] deal with the integrated design problem with fault compensation as a UIO-based FTC loved through H_∞ optimization. In [143], the problem of integrated fault reconstruction and FTC in linear systems subject to actuator fault via learning observer is investigated. The works in [144] developed an integrated design of EF and FTC schemes for nonlinear Lipschitz systems in the presence of disturbances and actuator failures.

There is a bi-directional interactions between FE and FTC designs:

- The FE performance is influenced by the control system since the observer is constructed by using the system model in which the existence of the system mismatch is inevitable.

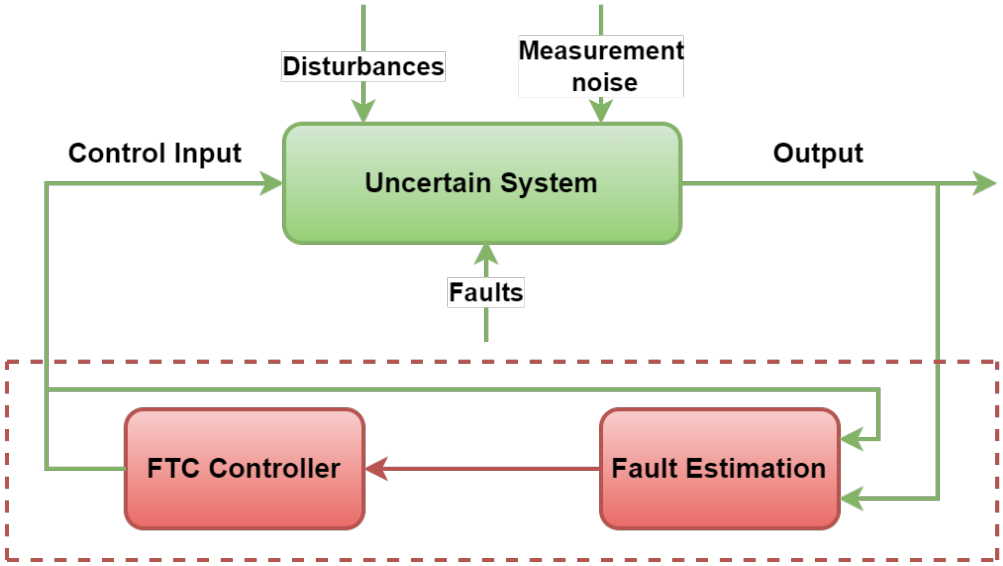

Figure 2.8: Structure of co-design of FE and FTC

- The FTC performance is affected by the estimation sine FTC system is synthesized based on the estimated variable from the estimators.

Let's consider the uncertain switched LPV system subject to faults which is assumed to be constant or slow-varying signal, i.e. $\dot{f}(t) \approx 0$.

$$\begin{cases} \dot{x}(t) = \Big(\mathcal{A}_{\sigma(t)}(\rho(t)) + \Delta\mathcal{A}_{\sigma(t)}(\rho(t))\Big)x(t) + \mathcal{B}_{\sigma(t)}(\rho(t))\Big(u(t) + f(t)\Big) \\ y(t) = \mathcal{C}x(t) \end{cases} \tag{2.81}$$

It is assumed that there is no uncertainty in distribution input matrices $\Delta\mathcal{B}_{\sigma(t)(\rho(t))} = 0$.

By considering fault as an auxiliary state variable. Define the augmented state $x_a(t) = \begin{bmatrix} x(t) \\ f(t) \end{bmatrix}$, then it follow from (2.81) that

$$\begin{cases} \dot{x}_a(t) = \Big(A_{\sigma(t)}(\rho(t)) + \Delta A_{\sigma(t)}(\rho(t))\Big)x_a(t) + B_{\sigma(t)}(\rho(t))u(t) \\ y(t) = Cx_a(t) \end{cases} \tag{2.82}$$

where $A_{\sigma(t)}(\rho(t)) = \begin{bmatrix} \mathcal{A}_{\sigma(t)}(\rho(t)) & \mathcal{B}_{\sigma(t)}(\rho(t)) \\ 0 & 0 \end{bmatrix}$, $B_{\sigma(t)}(\rho(t)) = \begin{bmatrix} \mathcal{B}_{\sigma(t)}(\rho(t)) \\ 0 \end{bmatrix}$, $\Delta A_{\sigma(t)}(\rho(t)) = \begin{bmatrix} \Delta\mathcal{A}_{\sigma(t)}(\rho(t)) \\ 0 \end{bmatrix}$, $C = \begin{bmatrix} \mathcal{C} & 0 \end{bmatrix}$.

Then the state $x_a(t)$ can be estimated by the following traditional observer:

$$\begin{cases} \dot{\hat{x}}_a(t) = A_{\sigma(t)}(\rho(t))\hat{x}_a(t) + B_{\sigma(t)}(\rho(t))u(t) + L_{\sigma(t)}(\rho(t))\Big(y(t) - \hat{y}(t)\Big) \\ \hat{y}(t) = C\hat{x}_a(t) \end{cases} \tag{2.83}$$

where $L_{\sigma(t)}(\rho(t)) = \sum_{j=1}^{2^{n_\rho}} \mu^j_{\sigma(t)}(\rho(t)) L^j_{\sigma(t)}$ is time-varying observer gain matrices.

Once $\hat{x}_a(t)$ is obtained, the state and fault are determined as:

$$\begin{cases} \hat{x}(t) = \begin{bmatrix} I_{n_x} & 0 \end{bmatrix} \hat{x}_a(t) \\ \hat{f}(t) = \begin{bmatrix} 0 & I_{n_f} \end{bmatrix} \hat{x}_a(t) \end{cases} \tag{2.84}$$

Let's $e(t) = x_a(t) - \hat{x}_a(t)$ be the estimation error. Subtracting (2.83) from (2.81) yields the estimation error system:

$$\dot{e}(t) = \Big(A_{\sigma(t)}(\rho(t)) - L_{\sigma(t)}(\rho(t))C\Big)e(t) + \Delta A_{\sigma(t)} x(t) \tag{2.85}$$

Consider the state feedback control law $u(t)$:

$$u(t) = -K_{\sigma(t)}(\rho(t))\hat{x}(t) - K_{\sigma(t),f}(\rho(t))\hat{f}(t) \tag{2.86}$$

where $K_{\sigma(t),f}(\rho(t))$ is accommodation gain and its value is $K_{\sigma(t),f}(\rho(t)) = \mathcal{B}^{\dagger}_{\sigma(t)}(\rho(t))\mathcal{B}_{\sigma(t)}(\rho(t))$ and $K_{\sigma(t)}(\rho(t))$ is the state feedback gain to be designed in order to ensure the stability of the closed-loop system.
By substituting the control law (2.86) into the system (2.81), one can get the following closed-loop system:

$$\dot{x}(t) = \Big(\mathcal{A}_{\sigma(t)}(\rho(t)) - \mathcal{B}_{\sigma(t)}(\rho(t))K_{\sigma(t)}(\rho(t))\Big)x(t) + \mathcal{B}_{\sigma(t)}(\rho(t))H_{\sigma(t)}(\rho(t))e(t) + \Delta\mathcal{A}_{\sigma(t)}(\rho(t))x(t) \tag{2.87}$$

where $H_{\sigma(t)}(\rho(t)) = \Big[K_{\sigma(t)}(\rho(t)) \quad K_{\sigma(t),f}(\rho(t))\Big]$.

From (2.85) and (2.87), the FE-based FTC system is given as follows:

$$\begin{bmatrix} \dot{x}(t) \\ \dot{e}(t) \end{bmatrix} = \begin{bmatrix} \mathcal{A}_{\sigma(t)}(\rho(t)) - \mathcal{B}_{\sigma(t)}(\rho(t))K_{\sigma(t)}(\rho(t)) + \Delta\mathcal{A}_{\sigma(t)}(\rho(t)) & B_{\sigma(t)}(\rho(t))H_{\sigma(t)}(\rho(t)) \\ \Delta A_{\sigma(t)} & A_{\sigma(t)}(\rho(t)) - L_{\sigma(t)}(\rho(t))C \end{bmatrix} \begin{bmatrix} x(t) \\ e(t) \end{bmatrix} \tag{2.88}$$

It is obvious that the coupling effects are represented by the off-diagonal elements $B_{\sigma(t)}(\rho(t))H_{\sigma(t)}(\rho(t))$ and $\Delta A_{\sigma(t)}(\rho(t))$ in the system distribution matrix of system (2.88). It is clear evidence for the existence of bi-directional interactions between the FE and FTC systems. Therefore, by designing the gains $K_{\sigma(t)}(\rho(t))$ and $L_{\sigma(t)}(\rho(t))$ while taking the coupling effects in to consideration, the stability of system (2.88) can be guaranteed to against the bi-directional interactions between observer and controller.

The presence of bi-directional interaction breaks down the Separation Principle, thus the stability of the closed-loop system cannot be ensured by separately designing gain matrices for the controller and observer $K_{\sigma(t)}(\rho(t))$ and $L_{\sigma(t)}(\rho(t))$ where the coupling effects are ignored.

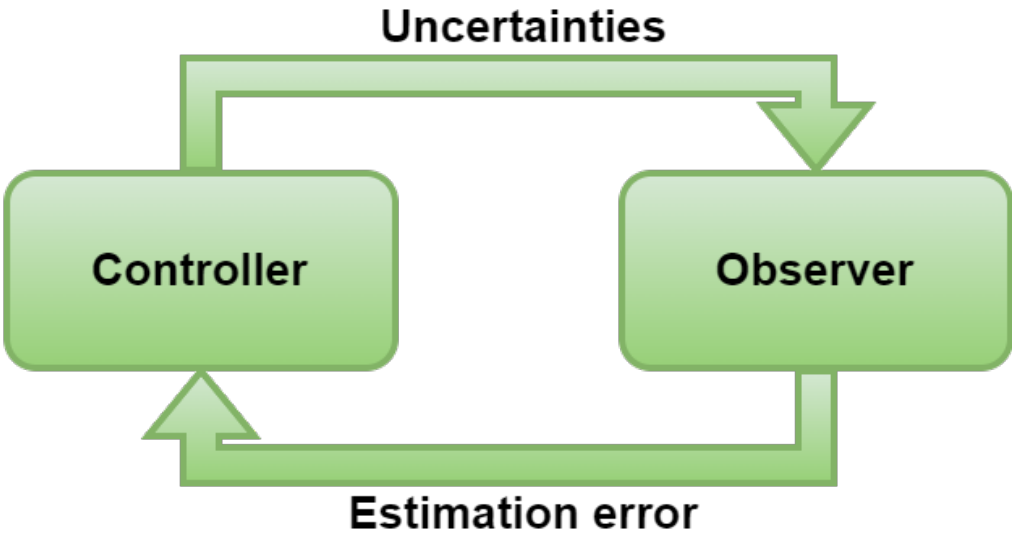

Figure 2.9: Bi-directional interaction between observer and controller

2.4 Conclusions

In this chapter, the theoretical background on stability of switched systems subject to unknown but bounded disturbances are recalled. Additionally, relevant lemmas and definition are mentioned for facilitating the exploration of the thesis. The interval observer and co-design methodologies are investigated for switched systems.

Chapter 3

Switched Unknown Input Interval Observers-based Fault-Tolerant Control For Uncertain Switched Systems

Chapter abstract

This chapter delves into the challenge of co-designing a switched unknown input interval observer (SUIIO) and a fault-tolerant control system for the lateral dynamics of a vehicle. The lateral dynamics are modeled as an uncertain switched linear system, characterized by unknown but bounded uncertainties. In the proposed methodology, a switched unknown input interval observer (SUIIO) and a dynamic proportional integral observer (DPIO) are introduced. These observers serve the purpose of estimating the lower and upper bounds of key parameters, including the sideslip angle, yaw rate, and the unknown input. Utilizing the estimates obtained from the observers, a Fault-Tolerant Controller (FTC) is developed. This controller aims to stabilize the closed-loop system and achieve reference model tracking, even in the presence of faults. The synthesis of such interval observers and controllers is based on sufficient Linear Matrix Inequalities (LMIs) conditions, expressed through Multiple Input-to-State-Stability (ISS) Lyapunov functions under average dwell time (ADT) conditions. The proposed approach demonstrates its effectiveness through evaluation in Matlab-Simulink, particularly under various vehicle handling maneuvers.

3.1 Introduction

3.1.1 Related works

Since modern vehicles are highly complex systems consisting of many interrelated subsystems, achieving more precise control designs and increasing the effectiveness of a vehicle dynamic control system become an enormous technical challenge. This necessitates an accurate knowledge of vehicle parameters, in particular, sideslip and yaw rate. Indeed, the value of these parameters plays crucial roles in vehicle handling, lateral stability, and performance enhancement. Nevertheless, onboard vehicle sensors are not always available in commercial vehicles due to economical and/or technical reasons [145]. The commercial physical sensors for the measurement of lateral speed or yaw rate are extremely expensive devices that cannot be directly applied in real-world applications [146]. Therefore, it is necessary to develop virtual sensors or estimation algorithms to reconstruct unmeasured vehicle dynamics state vectors using the available measurements from low-cost sensors.

The accurate estimation of states is pivotal in contemporary control theory, especially, within the intricate realm of vehicle dynamics. In practical applications, vehicles contend with an array of challenges, including unknown inputs, exogenous disturbances, measurement noise and potential faulty components. Addressing these complexities necessitates the development of robust and effective unknown input observers (UIO) capable of reliably estimating the vehicle's state vectors, especially without being sensitive to these unknown inputs [3]. Within the domain of vehicle dynamics, various UIO approaches have been explored, yielding promising outcomes as documented in the existing literature [147]. The authors in [69] present a robust state and fault estimation of vehicle lateral dynamics in the presence of road bank and sensor noise by means of unknown input proportional multiple integral observers (UIPMIO). An UIO is proposed in [148] to accurately estimate the lateral speed and yaw rate of the lateral dynamics described by the quasi-exact Takagi-Sugeno (T-S) structure with unmeasurable premise variables. A polytopic linear parameter varying (LPV) UIO is proposed to simultaneously estimate the lateral velocity, steering angle and the effective engine torque [112]; sideslip angle and driver torque [149] for nonlinear vehicle dynamics. A noteworthy approach is proposed in [150] where two cascaded unknown input observers are investigated to deal with the problem of lateral dynamics estimations of a vehicle.

However, the aforementioned works on UIO have designed the observers with the perfect knowledge of structure models and parameter information. In real-world scenarios, the vehicle dynamics model is inevitably encountered with uncertainties arising from the mismatching model, exogenous disturbances, and measurement noise. Therefore, it could be a non-trivial task for classical UIOs to deal with the problems of accurate estimation of the system state in the presence of uncertainties. To fill this gap of traditional observers, this motivates to the robust estimation methodology, the so-called interval observer. Unlike conventional observers, interval observers guarantee that un-

measured variables always belong to a given interval all the time in dynamical systems. The interval observer was first introduced in [36] to estimate states of uncertain biological systems. Since then, tremendous achievements have been reported in the literature, particularly regarding the development of unknown input interval observer (UIIO). In [151], an UIIO is designed using a coordinate transformation in order to ensure the positivity of the estimation errors. The stability of the observer is achieved through the ISS property, facilitated by the utilization of multiple Lyapunov functions under ADT conditions. Other researchers have explored novel structures of UIIO for LPV systems, ensuring L_2-gain and L_∞-gain performance in [152]. The work in [43] introduced a novel interval algebraic technique to guarantee and robust the estimation of vehicle lateral tire forces with respect to the corner stiffness variations. A switched unknown input interval observer (SUIIO) is trained in [153] to estimate the states of the vision system and vehicle lateral dynamics subject to unknown but bounded cornering stiffness.

Although the above-mentioned studies can effectively handle the problem of vehicle dynamics estimation and unknown input decoupling, none of the above literature takes the unknown input estimation or reconstruction into consideration. To address this issue, the problem of constant unknown input reconstruction is converted into an augmented state estimation with an augmentation technique [154]. In another approach, an algebraic relationship between system states and unknown input is established in [63]; this solution developed an UIO to simultaneously estimate the system states and the slow time-varying unknown input. A similar approach is proposed in [3] where an interval observer is developed to estimate vehicle states and unknown input interval reconstruction is then constructed to estimate the interval lateral wind gusts throughout the algebraic relationship between the estimated vehicle states and unknown input. It is worth mentioning that the fault estimation findings discussed above demonstrate satisfactory performance for slowly varying fault signals. However, if the faults change rapidly, the estimation algorithm may become ineffective in constructing fast time-varying fault signals [155]. To fill this gap, this chapter introduces a dynamics proportional integral observer (DPIO) with H_∞ performance index designed to deal with fast time-varying unknown input signals and efficiently attenuate the effects of uncertainties on the estimation error. Generally speaking, the estimated fault information can be utilized to synthesize fault-tolerant control.

Moreover, an important aspect of automotive engineering is vehicle safety performance. Over the last few decades, various advanced technical solutions have been fully equipped in modern vehicles. These safety systems include adaptive cruise control (ACC), antilock braking system (ABS), dynamic stability control (DSC), and electronic stability program (ESP). In general, the controller of the safety systems heavily depend on sensor signals and actuators, any faults/ failures can pose a significant threat to the driver and the surrounding environment. It is worth pointing out that the conventional feedback control approaches are incapable of adaptation in the case of system failures. To overcome this challenge, some researchers have paid considerable attention to developing a control strategy that has the ability to guarantee stability and maintain an acceptable performance level of the

vehicle even when various faults occur. This task is commonly known as fault-tolerant control (FTC) which is extensively researched in both theoretical and practical aspects of modern control [156, 157]. For example, in [73], a proportional integral observer (PIO)-based FTC is adapted to stabilize vehicle lateral dynamics in the presence of faults. An extension to a novel adaptive fault-tolerant lateral tracking control scheme is proposed in [158] for autonomous vehicles subject to intermittent actuator faults. An alternative controller that utilized a spatial learning-based FTC design was proposed in [159] for accurate lateral tracking of uncertain autonomous vehicles subject to exogenous disturbances and multiplicative actuator failures. In [160], an FTC based on a fuzzy neural network is investigated for autonomous vehicles in the event of faults in both sensors and actuators. Several researchers have proposed integrated designs of fault estimation (FE) and FTC for uncertain linear systems with additive or multiplicative faults and disturbances using reduced or full-order unknown input observers to estimate both the state and the fault vectors [161].

3.1.2 Chapter contributions

The main objective of this chapter is to investigate the problem of simultaneous state and actuator fault estimation and design Fault-Tolerant Tracking Control (FTTC) for uncertain switched linear systems in the context of vehicle dynamics. To the best of the authors' knowledge, works on Switched Unknown Input Interval Observer (SUIIO)-based FTTC for vehicle lateral dynamics with unknown but bounded uncertainties subject to faults have not been fully reported in the literature.

The contributions of this chapter are listed below:

- A novel switched unknown input interval observer is investigated for vehicle lateral dynamics model described under uncertain switched systems affected by unknown but bounded uncertainties. Unlike the approach in [151], this method avoids resorting to the transformation of coordinates to ensure the positivity property of the interval observer.

- A dynamic proportional integral observer (DPIO) is introduced to estimate the actuator faults. Along with the H_∞ index, the observer allows to attenuate the negative effects of the uncertainties on the estimation. Compared with the results in [63, 73, 162, 2], the proposed fault estimation technique can deal with fast time-varying signals.

- An extension to work in [112, 153], a fault-tolerant control is designed to guarantee stability and track the reference vehicle lateral dynamic states in the presence of actuator faults. In contrast to the Separation Principle as discussed in [163, 2], an integrated technique is proposed to design the interval observers and controllers at the same time.

- The existence of such observers and controllers is mainly formulated in terms of one-step LMIs using multiple

Input-to-state-stable (ISS) Lyapunov functions with average dwell time (ADT) which being less conservative than common one in [1].

With the proposed method, an SUIIO is designed to estimate the lower and upper bounds of the vehicle lateral dynamics states without being sensitive to the influence of actuator faults. Simultaneously, a dynamic proportional integral observer (DPIO) is developed to reconstruct the unknown input. Based on these estimated variables, fault-tolerant controllers are synthesized to compensate for the actuator fault's effects and track the reference vehicle model. The chapter provides sufficient conditions for the existence of such observers and controllers, which is applied to the vehicle lateral dynamics model.

This chapter is structured as follows: the used vehicle models are introduced in Section 3.2. The design procedure of SUIIO and DPI observer for uncertain switched vehicle lateral models affected by actuator fault is presented in Section 3.3.1 and 3.3.2. In Section 3.3.3, FTC is then synthesized to stabilize the closed-loop system and to track the reference vehicle lateral dynamics model. The simulation results on the two-degree-of-freedom bicycle model demonstrate the effectiveness of the proposed methodology in Section 3.4 before the conclusions in Section 3.5.

3.2 Problem formulation

3.2.1 General case

Consider the continuous-time uncertain switched systems:

$$\begin{cases} \dot{x}(t) = \left(A_{\sigma(t)} + \Delta A_{\sigma(t)}\right) x(t) + B_{\sigma(t)} u(t) + F_{\sigma} f(t) \\ y(t) = Cx(t) \end{cases} \tag{3.1}$$

where $x(t) \in \mathbb{R}^{n_x}$, $u(t) \in \mathbb{R}^{n_u}$, $f(t) \in \mathbb{R}^{n_f}$, $y(t) \in \mathbb{R}^{n_y}$ represent the state vector, the control input, the fault vector and measurement output vector respectively. Switching signal $\sigma(t) : \mathbb{R}^+ \to \mathcal{N} = \{1, 2, \ldots, N\}$ depends on time t and N is the number of subsystems.

The matrices $A_{\sigma(t)} \in \{A_1, A_2, \ldots, A_N\}$, $B_{\sigma(t)} \in \{B_1, B_2, \ldots, B_N\}$, and $F_{\sigma(t)} \in \{F_1, F_2, \ldots, F_N\}$ are known constant matrices with appropriate dimensions corresponding to nominal systems. Without loss of generality, we assume that the output matrix C is constant $\forall \sigma(t)$.

The term $\Delta A_{\sigma(t)} \in \{\Delta A_1, \Delta A_2, \ldots, \Delta A_N\}$ is an unknown time-varying matrix, representing system parameter uncertainties and is assumed to be bounded with a priori known bound. This uncertain state matrix can be structured under the form:

$$\Delta A_{\sigma(t)} = M_{a,\sigma(t)} \Delta_a(t) N_{\sigma(t)} \tag{3.2}$$

with $M_{a,\sigma(t)} \in \mathbb{R}^{n_x \times n_m}$ and $N_{\sigma(t)} \in \mathbb{R}^{n_n \times n_x}$ are known matrices with appropriate dimensions where $M_{a,\sigma(t)}$ rep-

resents the maximum percentage of the state matrices variation, and $N_{\sigma(t)}$ are matrices including nominal values while $\Delta_a(t) \in \mathbb{R}^{n_m \times n_n}$ is unknown matrix satisfying property $\Delta_a^T(t)\Delta_a(t) \leq I_{n_n}$.

3.2.2 Case study: switched vehicle lateral dynamics model

This subsection provides a concise overview of the fundamental concepts and methods for modeling the lateral behavior of vehicles. The system is based on a single-track bicycle vehicle model, which describes the lateral and yaw motions [164]. By using Newton's law of motion, the differential equations below can be used to describe the two-dimensional model characterizing the vehicle's lateral model:

$$\begin{cases} mv_x\big(\dot{\beta} + r\big) = F_{yf} + F_{yr} \\ I_z\dot{r} = l_f F_{yf} - l_r F_{yr} + M_z \end{cases} \tag{3.3}$$

where m is vehicle mass, I_z is the yaw moment of inertia, v_x is longitudinal velocity, r is the yaw rate, l_f and l_r are the lengths from the front and rear axles to COG, while F_{yf} and F_{yr} are the lateral forces of front and rear tires and M_z is corrective yaw moment to handle the system performance which can be realized by braking wheels.

For normal driving situation, the lateral forces F_{yf} and F_{yr} is assumed to be linear function with slip angle:

$$\begin{cases} F_{yf} = c_f\alpha_f \\ F_{yr} = c_r\alpha_r \end{cases} \tag{3.4}$$

where c_f, c_r are the cornering stiffness of front and rear tires and α_f, α_r are the front and rear wheel slip angles defined as:

$$\begin{cases} \alpha_f = \delta_f - \beta - \dfrac{l_f}{v_x}r \\ \alpha_r = -\beta + \dfrac{l_r}{v_x}r \end{cases} \tag{3.5}$$

Note that the validity of this assumption restricts analysis to maneuver low lateral acceleration.

In the proposed model, the longitudinal velocity $v_x(t)$ and front steering angle $\delta_f(t)$ are assumed to be available for measurement while the measurements of the sideslip angle and yaw rate are assumed to be unavailable due to cost reasons of the corresponding sensors.

Substituting equations (3.4) and (3.5) into system (3.3) and selecting $\beta(t)$ and $r(t)$ as state variables with $x(t) = \begin{bmatrix} \beta(t) \\ r(t) \end{bmatrix}$, leads to the following LPV vehicle lateral dynamics:

$$\begin{cases} \dot{x}(t) = A\big(\rho(t), \xi(t)\big)x(t) + Bu(t) + D\big(\rho(t), \xi(t)\big)\delta_f(t) \\ y(t) = Cx(t) \end{cases} \tag{3.6}$$

where $A\big(\rho(t),\xi(t)\big) = \begin{bmatrix} -\frac{c_f+c_r}{mv_x} & \frac{c_r l_r - c_f l_f}{mv_x^2} - 1 \\ \frac{c_r l_r - c_f l_f}{I_z} & -\frac{c_r l_r^2 + c_f l_f^2}{I_z v_x} \end{bmatrix}$, $B = \begin{bmatrix} 0 \\ \frac{1}{I_z} \end{bmatrix}$, $D\big(\rho(t),\xi(t)\big) = \begin{bmatrix} \frac{c_f}{mv_x} \\ \frac{c_f l_f}{I_z} \end{bmatrix}$, $C = \begin{bmatrix} 0 & 1 \end{bmatrix}$ and the time-varying parameters $\rho(t) = \begin{bmatrix} \frac{1}{v_x}, & \frac{1}{v_x^2} \end{bmatrix}$ and $\xi = \begin{bmatrix} c_f, & c_r \end{bmatrix}$ represent measurable and uncertain parameters.

A single observation or controller, however, may not be sufficient to achieve optimal performance when the longitudinal velocity $v_x(t)$ significantly varies over a wide range.

As a result, it is necessary to consider multiple observations or controllers that can adapt to different values of $v_x(t)$. One effective strategy to handle the challenges posed by a large variation range of parameter $v_x(t)$ is to use the switched system technique which involve dividing the parameter v_x range into smaller sub-regions.

Note that, when lateral acceleration becomes high, the tire forces are no longer linear with respect to the wheel slip angles due to the tire saturation property. Accordingly, the cornering stiffness parameters c_f and c_r used in the linear tire model (3.4) will vary when the road friction changes or when the nonlinear tire domain is reached. To deal with these variations, the following linear adaptive tire model is used to correct the cornering stiffness values via the uncertain variables Δc_f and Δc_r as:

$$\begin{cases} F_{yf} = (c_{f0} + \Delta c_f)\,\alpha_f \\ F_{yr} = (c_{r0} + \Delta c_r)\,\alpha_r \end{cases} \tag{3.7}$$

The cornering stiffness:

$$\begin{cases} c_f = c_{f_0} + \Delta c_f \\ c_r = c_{r_0} + \Delta c_r \end{cases} \tag{3.8}$$

where the linear part denoted by $\xi_0 = \begin{bmatrix} c_{f_0}, & c_{r_0} \end{bmatrix}$ presents a known nominal value and the uncertainty term denoted by $\Delta\xi = \begin{bmatrix} \Delta c_f, & \Delta c_r \end{bmatrix}$ is assumed to be unknown but bounded with priori known bounds. Consequently, the uncertain parameters are expressed $\xi = \xi_0 + \Delta\xi$.

Therefore, the vehicle lateral dynamics can be represented by an uncertain switched model with actuator faults as follows:

$$\begin{cases} \dot{x}(t) = \big(A_{\sigma(t)} + \Delta A_{\sigma(t)}\big)x(t) + Bu(t) + \big(D_{\sigma(t)} + \Delta D_{\sigma(t)}\big)\delta_f(t) + Ff(t) \\ y(t) = Cx(t) \end{cases} \tag{3.9}$$

The system is switched according to forward speed variations $v_x(t)$ which vary in a large range. The switching signal is $\sigma(t) \in \mathcal{N} = \{1, 2, \ldots, N\}$ with N is the number of subsystems.
The system matrices

$$A\big(\rho(t),\xi_0\big) = \begin{bmatrix} -\frac{c_{f_0}+c_{r_0}}{mv_x} & \frac{c_{r_0} l_r - c_{f_0} l_f}{mv_x^2} - 1 \\ \frac{c_{r_0} l_r - c_{f_0} l_f}{I_z} & -\frac{c_{r_0} l_r^2 + c_{f_0} l_f^2}{I_z v_x} \end{bmatrix}, \quad D\big(\rho(t),\xi_0\big) = \begin{bmatrix} \frac{c_{f_0}}{mv_x} \\ \frac{c_{f_0} l_f}{I_z} \end{bmatrix} \tag{3.10}$$

The uncertain term $\Delta A_{\sigma(t)} = \begin{bmatrix} -\frac{\Delta c_f + \Delta c_r}{m v_x} & \frac{\Delta c_r l_r - \Delta c_f \Delta l_f}{m v_x^2} \\ \frac{\Delta c_r l_r - \Delta c_f l_f}{I_z} & -\frac{\Delta c_r l_r^2 + \Delta c_f l_f^2}{I_z v_x} \end{bmatrix}$, $\Delta D_{\sigma(t)} = \begin{bmatrix} \frac{\Delta c_f}{m v_x} \\ \frac{\Delta c_f l_f}{I_z} \end{bmatrix}$ and $\Delta A_{\sigma(t)}$ is assumed to be expressed as:

$$\Delta A_{\sigma(t)} = M_{a,\sigma(t)} \Delta(t) N_a \tag{3.11}$$

with $M_{a,\sigma(t)}$ and N_a are known constant matrices with compatible dimension which characterise the structure of the uncertainties while $\Delta(t)$ satisfies the inequality $\Delta^T(t)\Delta(t) \leq I$.

Note that in the model, the yaw moment is chosen as the control input, as is typical in the yaw moment control problem, where the steering angle input set by the driver is not controlled. However, the presented method can be applied to any other configurations, including active steering and steer-by-wire vehicles.

The following assumptions are introduced for system (3.9).

Assumption 3.1 *The initial condition and the front steering angle of the system* (3.9) *are assumed bounded by known vectors:*

$$\begin{aligned} \underline{x}(t_0) \leq x(t_0) \leq \overline{x}(t_0) \\ \underline{\delta}_f \leq \delta_f \leq \overline{\delta}_f \end{aligned} \tag{3.12}$$

Assumption 3.2 *There exist known constant matrices* $\underline{\Delta A}_{\sigma(t)}$, $\overline{\Delta A}_{\sigma(t)}$ *and* $\underline{\Delta D}_{\sigma(t)}$, $\overline{\Delta D}_{\sigma(t)}$ *for all* $\sigma(t) \in \mathcal{N}$ *such that:*

$$\begin{aligned} \underline{\Delta A}_{\sigma(t)} \leq \Delta A_{\sigma(t)} \leq \overline{\Delta A}_{\sigma(t)} \\ \underline{\Delta D}_{\sigma(t)} \leq \Delta D_{\sigma(t)} \leq \overline{\Delta D}_{\sigma(t)} \end{aligned} \tag{3.13}$$

Assumption 3.3 *The following rank condition holds considering* $B = F$

$$rank(CF) = rank(B), \quad \forall \sigma(t) \in \mathcal{N} \tag{3.14}$$

Assumption 3.4 *It is assumed that the fault and its first-time derivative are bounded by known limits.*

These assumptions are not limiting. Assumption 3.1 is widely employed within the framework of interval observer synthesis. Similarly, Assumption 3.2 is frequently invoked when dealing with uncertain LPV systems. The presence of Assumption 3.3 is essential to ensure the existence of the observer. Finally, assumption 3.4 is also common and is necessary for DPI Observer synthesis.

3.3 Main results

In this section, we choose an interval observer in order to estimate the lower bound $\underline{x}(t)$ and the upper bound $\overline{x}(t)$ of the real state $x(t)$. Besides, a DPIO is also designed to reconstruct the actuator faults for the system (3.9).

3.3.1 Switched Unknown Input Interval Observer

In this subsection, an SUIIO is proposed to estimate the boundaries of the real state vector without being affected by unknown input for vehicle model (3.9). The positivity properties of the interval observer used for the estimation error ensure that the real state is always within the two estimated limits.

The following structure is SUIIO for system (3.9)

$$\begin{cases} \overline{\xi}(t) = N_{\sigma(t)}\overline{\xi}(t) + J_{\sigma(t)}y(t) + H_{\sigma(t)}u(t) + T_{\sigma(t)}\delta_f(t) + \overline{\Omega}_{\sigma(t)}(t) \\ \overline{x}(t) = \overline{\xi}(t) + E_{\sigma(t)}y(t) \\ \underline{\xi}(t) = N_{\sigma(t)}\underline{\xi}(t) + J_{\sigma(t)}y(t) + H_{\sigma(t)}u(t) + T_{\sigma(t)}\delta_f(t) + \underline{\Omega}_{\sigma(t)}(t) \\ \underline{x}(t) = \underline{\xi}(t) + E_{\sigma(t)}y(t) \end{cases} \tag{3.15}$$

where $\left(\underline{\xi}(t), \overline{\xi}(t)\right)$ is the lower and upper of the observer state vectors and $\left(\underline{x}(t), \overline{x}(t)\right)$ is the lower and upper estimates of system states $x(t)$. Matrices $N_{\sigma(t)}$, $J_{\sigma(t)}$, $H_{\sigma(t)}$, $E_{\sigma(t)}$ are constant switching matrices of proper dimensions which must be designed in order to ensure stability of the interval observer and to reject the unknown input effects.

The terms $\overline{\Omega}_{\sigma(t)}(t)$ and $\underline{\Omega}_{\sigma(t)}(t)$ are chosen as:

$$\begin{cases} \overline{\Omega}_{\sigma(t)}(t) = Q^{+}_{\sigma(t)}\overline{\nabla}_{\sigma(t)}(t) - Q^{-}_{\sigma(t)}\underline{\nabla}_{\sigma(t)}(t) \\ \underline{\Omega}_{\sigma(t)}(t) = Q^{+}_{\sigma(t)}\underline{\nabla}_{\sigma(t)}(t) - Q^{-}_{\sigma(t)}\overline{\nabla}_{\sigma(t)}(t) \end{cases} \tag{3.16}$$

with $\underline{\nabla}_{\sigma(t)}(t)$ and $\overline{\nabla}_{\sigma(t)}(t)$ are the lower and upper bounds of $\nabla_{\sigma(t)}(t) = \Delta A_{\sigma(t)}x(t) + \Delta D_{\sigma(t)}\delta_f(t)$.

According to assumption 3.2 with $\underline{\Delta A}_{\sigma(t)} \leq \Delta A_{\sigma(t)} \leq \overline{\Delta A}_{\sigma(t)}$, and the state system $x(t)$ is bounded by the lower $\underline{x}(t)$ and upper $\overline{x}(t)$ bounds, i.e $\underline{x}(t) \leq x(t) \leq \overline{x}(t)$. Then applying lemma 2.8, the item $\Delta A_{\sigma(t)}x(t)$ is bounded by $\underline{\nabla}^{A}_{\sigma(t)}(t)$ and $\overline{\nabla}^{A}_{\sigma(t)}(t)$, i.e. $\underline{\nabla}^{A}_{\sigma(t)}(t) \leq \Delta A_{\sigma}x(t) \leq \overline{\nabla}^{A}_{\sigma(t)}(t)$ with

$$\begin{cases} \overline{\nabla}^{A}_{\sigma(t)}(t) = \overline{\Delta A}^{+}_{\sigma(t)}\overline{x}^{+}(t) - \underline{\Delta A}^{+}_{\sigma(t)}\overline{x}^{-}(t) - \overline{\Delta A}^{-}_{\sigma(t)}\underline{x}^{+}(t) + \underline{\Delta A}^{-}_{\sigma(t)}\underline{x}^{-}(t) \\ \underline{\nabla}^{A}_{\sigma(t)}(t) = \underline{\Delta A}^{+}_{\sigma(t)}\underline{x}^{+}(t) - \overline{\Delta A}^{+}_{\sigma(t)}\underline{x}^{-}(t) - \underline{\Delta A}^{-}_{\sigma(t)}\overline{x}^{+}(t) + \overline{\Delta A}^{-}_{\sigma(t)}\overline{x}^{-}(t) \end{cases} \tag{3.17}$$

In the same manner, according to assunptions 3.1, 3.2 with $\underline{\Delta D}_{\sigma(t)} \leq \Delta D_{\sigma(t)} \leq \overline{\Delta D}_{\sigma(t)}$ and $\underline{\delta}_f \leq \delta_f \leq \overline{\delta}_f$. Then applying lemma 2.8, the item $\Delta D_{\sigma(t)}\delta_f$ is bounded by $\underline{\nabla}^{D}_{\sigma(t)}(t)$ and $\overline{\nabla}^{D}_{\sigma(t)}(t)$, i.e. $\underline{\nabla}^{D}_{\sigma(t)}(t) \leq \Delta D_{\sigma(t)}\delta_f \leq \overline{\nabla}^{D}_{\sigma(t)}(t)$ with

$$\begin{cases} \overline{\nabla}^{D}_{\sigma(t)}(t) = \overline{\Delta D}^{+}_{\sigma(t)}\overline{\delta}^{+}_{f} - \underline{\Delta D}^{+}_{\sigma(t)}\overline{\delta}^{-}_{f} - \overline{\Delta D}^{-}_{\sigma(t)}\underline{\delta}^{+}_{f} + \underline{\Delta D}^{-}_{\sigma(t)}\underline{\delta}^{-}_{f} \\ \underline{\nabla}^{D}_{\sigma(t)}(t) = \underline{\Delta D}^{+}_{\sigma(t)}\underline{\delta}^{+}_{f} - \overline{\Delta D}^{+}_{\sigma(t)}\underline{\delta}^{-}_{f} - \underline{\Delta D}^{-}_{\sigma(t)}\overline{\delta}^{+}_{f} + \overline{\Delta D}^{-}_{\sigma(t)}\overline{\delta}^{-}_{f} \end{cases} \tag{3.18}$$

Therefore, the uncertain item $\nabla_{\sigma(t)}(t) = \Delta A_{\sigma(t)}x(t) + \Delta D_{\sigma(t)}\delta_f(t)$ is bounded by $\underline{\nabla}_{\sigma(t)}(t)$ and $\overline{\nabla}_{\sigma(t)}(t)$ as follows:

$$\underline{\nabla}_{\sigma(t)}(t) \leq \nabla_{\sigma(t)}(t) = \Delta A_{\sigma(t)}x(t) + \Delta D_{\sigma(t)}\delta_f(t) \leq \overline{\nabla}_{\sigma(t)}(t) \tag{3.19}$$

where

$$\begin{cases} \overline{\nabla}_{\sigma(t)}(t) = \overline{\nabla}^{A}_{\sigma(t)}(t) + \overline{\nabla}^{D}_{\sigma(t)}(t) \\ \qquad = \overline{\Delta A}^{+}_{\sigma(t)}\overline{x}^{+}(t) - \underline{\Delta A}^{+}_{\sigma(t)}\overline{x}^{-}(t) - \overline{\Delta A}^{-}_{\sigma(t)}\underline{x}^{+}(t) + \underline{\Delta A}^{-}_{\sigma(t)}\underline{x}^{-}(t) \\ \qquad + \overline{\Delta D}^{+}_{\sigma(t)}\overline{\delta}^{+}_{f} - \underline{\Delta D}^{+}_{\sigma(t)}\overline{\delta}^{-}_{f} - \overline{\Delta D}^{-}_{\sigma(t)}\overline{\delta}^{+}_{f} + \underline{\Delta D}^{-}_{\sigma(t)}\underline{\delta}^{-}_{f} \\ \underline{\nabla}_{\sigma(t)}(t) = \underline{\nabla}^{A}_{\sigma(t)}(t) + \underline{\nabla}^{D}_{\sigma(t)}(t) \\ \qquad = \underline{\Delta A}^{+}_{\sigma(t)}\underline{x}^{+}(t) - \overline{\Delta A}^{+}_{\sigma(t)}\underline{x}^{-}(t) - \underline{\Delta A}^{-}_{\sigma(t)}\overline{x}^{+}(t) + \overline{\Delta A}^{-}_{\sigma(t)}\overline{x}^{-}(t) \\ \qquad + \underline{\Delta D}^{+}_{\sigma(t)}\underline{\delta}^{+}_{f} - \overline{\Delta D}^{+}_{\sigma(t)}\underline{\delta}^{-}_{f} - \underline{\Delta D}^{-}_{\sigma(t)}\overline{\delta}^{+}_{f} + \overline{\Delta D}^{-}_{\sigma(t)}\overline{\delta}^{-}_{f} \end{cases} \tag{3.20}$$

The upper and lower estimation errors are defined as:

$$\begin{cases} \overline{e}(t) = \overline{x}(t) - x(t) \\ \underline{e}(t) = x(t) - \underline{x}(t) \end{cases} \tag{3.21}$$

By substituting $\underline{x}(t) = \underline{\xi}(t) + E_{\sigma(t)}y(t)$ and $\overline{x}(t) = \overline{\xi}(t) + E_{\sigma(t)}y(t)$ from the observer (3.15) into equation (3.21), the estimation errors are expressed as:

$$\begin{cases} \overline{e}(t) = \overline{\xi}(t) - \Big(I - E_{\sigma(t)}C\Big)x(t) \\ \underline{e}(t) = \Big(I - E_{\sigma(t)}C\Big)x(t) - \underline{\xi}(t) \end{cases} \tag{3.22}$$

By setting $Q_{\sigma(t)} = I - E_{\sigma(t)}C$, the estimation errors are then governed by:

$$\begin{cases} \overline{e}(t) = \overline{\xi}(t) - Q_{\sigma(t)}x(t) \\ \underline{e}(t) = Q_{\sigma(t)}x(t) - \underline{\xi}(t) \end{cases} \tag{3.23}$$

Combining equations (3.15) and (3.23), the dynamics of the lower and upper observer errors are then determined as:

$$\begin{cases} \dot{\overline{e}}(t) = N_{\sigma(t)}\overline{e}(t) + \Big(N_{\sigma(t)}Q_{\sigma(t)} + J_{\sigma(t)}C - Q_{\sigma(t)}A_{\sigma(t)}\Big)x(t) \\ \qquad + \Big(H_{\sigma(t)} - Q_{\sigma(t)}B\Big)u(t) + \Big(T_{\sigma(t)} - Q_{\sigma(t)}D_{\sigma(t)}\Big)\delta_f(t) \\ \qquad - Q_{\sigma(t)}Ff(t) + \overline{\Omega}_{\sigma(t)}(t) - Q_{\sigma(t)}\nabla_{\sigma(t)}(t) \\ \dot{\underline{e}}(t) = N_{\sigma(t)}\underline{e}(t) + \Big(Q_{\sigma(t)}A_{\sigma(t)} - N_{\sigma(t)}Q_{\sigma(t)} - J_{\sigma(t)}C\Big)x(t) \\ \qquad + \Big(Q_{\sigma(t)}B - H_{\sigma(t)}\Big)u(t) + \Big(Q_{\sigma(t)}D_{\sigma(t)} - T_{\sigma(t)}\Big)\delta_f(t) \\ \qquad + Q_{\sigma(t)}Ff(t) + Q_{\sigma(t)}\nabla_{\sigma(t)}(t) - \underline{\Omega}_{\sigma(t)}(t) \end{cases} \tag{3.24}$$

In order $\underline{e}(t)$ and $\overline{e}(t)$ converge to zero, $N_{\sigma(t)}$ should be Hurwitz and make the following relations hold:

$$N_{\sigma(t)}Q_{\sigma(t)} + J_{\sigma(t)}C - Q_{\sigma(t)}A_{\sigma(t)} = 0 \tag{3.25}$$

$$Q_{\sigma(t)}B = H_{\sigma(t)} \tag{3.26}$$

$$Q_{\sigma(t)}D_{\sigma(t)} = T_{\sigma(t)} \tag{3.27}$$

$$Q_{\sigma(t)}F = 0 \tag{3.28}$$

The estimation errors (3.24) are then simplified to:

$$\begin{cases} \dot{\overline{e}}(t) = N_{\sigma(t)}\overline{e}(t) + \overline{\Omega}_{\sigma(t)}(t) - Q_{\sigma(t)}\nabla_{\sigma(t)}(t) \\ \dot{\underline{e}}(t) = N_{\sigma(t)}\underline{e}(t) + Q_{\sigma(t)}\nabla_{\sigma(t)}(t) - \underline{\Omega}_{\sigma(t)}(t) \end{cases} \tag{3.29}$$

Now, the positivity of the estimation errors (3.29) is considered.

According to (3.19), the item $\nabla_{\sigma(t)}(t)$ is bounded by $\nabla_{\sigma(t)}(t)$ and $\nabla_{\sigma(t)}(t)$, then applying the lemma 2.8 for $Q_{\sigma(t)}\nabla_{\sigma(t)}(t)$ the following condition is obtained:

$$Q^{+}_{\sigma(t)}\underline{\nabla}_{\sigma(t)}(t) - Q^{-}_{\sigma(t)}\overline{\nabla}_{\sigma(t)}(t) \leq Q_{\sigma(t)}\nabla_{\sigma(t)}(t) \leq Q^{+}_{\sigma(t)}\overline{\nabla}_{\sigma(t)}(t) - Q^{-}_{\sigma(t)}\underline{\nabla}_{\sigma(t)}(t) \tag{3.30}$$

From (3.16) and (3.30), it is obvious that the following terms are positive:

$$\begin{cases} \overline{\Omega}_{\sigma(t)}(t) - Q_{\sigma(t)}\nabla_{\sigma(t)}(t) \geq 0 \\ Q_{\sigma(t)}\nabla_{\sigma(t)}(t) - \underline{\Omega}_{\sigma(t)}(t) \geq 0 \end{cases} \tag{3.31}$$

With assumptions 3.1 , it is easy to confirm that the lower and upper initial error conditions $\overline{e}(t_0) = \overline{x}(t_0) - x(t_0)$ and $\underline{e}(t_0) = x(t_0) - \underline{x}(t_0)$ are positive. Then based on lemma 2.6, this means that $\overline{e}(t) \geq 0$ and $\underline{e}(t) \geq 0$ if $N_{\sigma(t)}$ is a Metzler matrix $\forall\sigma(t) \in \mathcal{N}$. Hence, it ensures that the state $x(t)$ is bounded by $\underline{x}(t)$ and $\overline{x}(t)$.

We will now present a procedure for determining the parameters of the SUIIO.

From the relation (3.28) and matrix $Q_{\sigma(t)}$, one can have:

$$E_{\sigma(t)}CF = F \tag{3.32}$$

The solution of matrix $E_{\sigma(t)}$ for (3.32) is given by [112]:

$$E_{\sigma(t)} = F(CF)^{\dagger} + Z_{\sigma(t)}\Big(I - \big(CF\big)\big(CF\big)^{\dagger}\Big) \tag{3.33}$$

where $Z_{\sigma(t)}$ is an arbitrary matrix of appropriate dimension.

For simplification convenience, let's $\Theta = F(CF)^{\dagger}$ and $\Psi = I - (CF)(CF)^{\dagger}$, matrix $E_{\sigma(t)}$ in (3.33) is parameterized as:

$$E_{\sigma(t)} = \Theta + Z_{\sigma(t)}\Psi \tag{3.34}$$

After the matrix $E_{\sigma(t)}$ is determined, the matrix $Q_{\sigma(t)}$ is obtained:

$$Q_{\sigma(t)} = I - \Theta C - Z_{\sigma(t)}\Psi C \tag{3.35}$$

With setting $Q_{\sigma(t)} = I - E_{\sigma(t)}C$, the condition (3.25) is rewritten as:

$$N_{\sigma(t)}\big(I - E_{\sigma(t)}C\big) + J_{\sigma(t)}C - Q_{\sigma(t)}A_{\sigma(t)} = 0 \tag{3.36}$$

$$\rightarrow N_{\sigma(t)} = Q_{\sigma(t)}A_{\sigma(t)} - J_{\sigma(t)}C + N_{\sigma(t)}E_{\sigma(t)}C \tag{3.37}$$

$$\rightarrow N_{\sigma(t)} = Q_{\sigma(t)}A_{\sigma(t)} - \big(J_{\sigma(t)} - N_{\sigma(t)}E_{\sigma(t)}\big)C \tag{3.38}$$

$$\rightarrow N_{\sigma(t)} = Q_{\sigma(t)}A_{\sigma(t)} - Y_{\sigma(t)}C \tag{3.39}$$

where

$$Y_{\sigma(t)} = J_{\sigma(t)} - N_{\sigma(t)}E_{\sigma(t)} \tag{3.40}$$

Substituting (3.39) into (3.40), one can have

$$J_{\sigma(t)} = Y_{\sigma(t)}\big(I - CE_{\sigma(t)}\big) + Q_{\sigma(t)}A_{\sigma(t)}E_{\sigma(t)} \tag{3.41}$$

Remark 3.1 *It is obvious that the design of the observer gain matrices in* (3.15) *is reduced to determine the matrices* $Y_{\sigma(t)}$ *in* (3.39) *and* $Z_{\sigma(t)}$ *in* (3.34) *such that the lower and upper estimation errors in* (3.29) *are ISS as well as positive systems to ensure the properties of interval observer.*

3.3.2 Dynamic Proportional Integral Observer

In this subsection, the estimation of fast time-varying fault signal using a Dynamic Proportional Integral Observer (DPIO) is considered. The main objective of DPIO is to reconstruct the fault signal with robust performance quantified with H_{∞} index. The reconstructed fault is used to design FTTC to compensate for the fault effects in the next section.

The structure below is DPIO for system (3.9).

$$\begin{cases} \dot{\hat{x}}(t) = A_{\sigma(t)}\hat{x}(t) + Bu(t) + L^P_{\sigma(t)}\big(y(t) - \hat{y}(t)\big) + F\hat{f}(t) + D_{\sigma(t)}\delta_f(t) \\ \dot{v}(t) = L^I_{\sigma(t)}\big(y(t) - \hat{y}(t)\big) \\ \hat{f}(t) = v(t) + \lambda_{\sigma(t)}F^T C^T\big(y(t) - \hat{y}(t)\big) \\ \hat{y}(t) = C\hat{x}(t) \end{cases} \tag{3.42}$$

where $\hat{x}(t)$ is the state estimation and $\hat{f}(t)$ is estimated fault vector. $L^P_{\sigma(t)}$ and $L^I_{\sigma(t)}$ are proportional and integral observer gains, respectively, that are designed to ensure stability and performance. A constant parameter $\lambda_{\sigma(t)}$ is an auxiliary variable.

By defining $e_x(t) = x(t) - \hat{x}(t)$ and $e_f(t) = f(t) - \hat{f}(t)$ are the state and fault estimation errors respectively. From (3.9) and (3.42), one can get the dynamics of the estimation errors as:

$$\begin{cases} \dot{e}_x(t) = \big(A_{\sigma(t)} - L^P_{\sigma(t)}C\big)e_x(t) + Fe_f(t) + \Delta A_{\sigma(t)}x(t) + D_{\sigma(t)}\delta_f(t) \\ \dot{e}_f(t) = \dot{f}(t) - L^I_{\sigma(t)}Ce_x(t) - \lambda_{\sigma(t)}F^T C^T C\dot{e}_x(t) \end{cases} \tag{3.43}$$

The estimation error system (3.43) is then expressed under augmented form as follows:

$$\dot{e}(t) = \bar{J}_{\sigma(t)}\big(\bar{A}_{\sigma(t)} - \bar{L}_{\sigma(t)}\bar{C}\big)e(t) + \bar{w}_{\sigma(t)}(t) \tag{3.44}$$

where the augmented error vector $e(t) = \begin{bmatrix} e_x(t) \\ e_f(t) \end{bmatrix}$ and

$$\bar{J}_{\sigma(t)} = \begin{bmatrix} I_{n_x} & 0 \\ \lambda_{\sigma(t)}F^T_{\sigma(t)}C^T C & I_{n_f} \end{bmatrix}^{-1}, \bar{A}_{\sigma(t)} = \begin{bmatrix} A_{\sigma(t)} & F_{\sigma(t)} \\ 0 & 0 \end{bmatrix}, \bar{L}_{\sigma(t)} = \begin{bmatrix} L^P_{\sigma(t)} \\ L^I_{\sigma(t)} \end{bmatrix}, \bar{C} = \begin{bmatrix} C & 0 \end{bmatrix}, \bar{w}_{\sigma(t)}(t) = \bar{J}_{\sigma(t)} \begin{bmatrix} \nabla_{\sigma(t)}(t) \\ \dot{f}(t) \end{bmatrix}$$

Theorem 3.1 *If there exists symmetric positive definite matrix $\bar{P}_i$ and matrix $\bar{Q}_i$, $\forall i \in \mathcal{N}$ such that the following LMI are satisfied*

$$\Upsilon = \begin{bmatrix} He\Big\{\big(\bar{P}_i\bar{J}_i\bar{A}_i - \bar{Q}_i\bar{C}\big)\Big\} + I_{n_a} & \bar{P}_i \\ (*) & -\gamma^2 \end{bmatrix} \prec 0 \tag{3.45}$$

then the DPI observer (3.42) robustly estimate the fault vector and $\|e(t)\|_2 < \bar{\gamma}\|\bar{w}_{\sigma(t)}(t)\|_2$ with $\bar{L}_i = \bar{J}_i^{-1}\bar{P}_i^{-1}\bar{Q}_i$, $n_a = n_x + n_f$

Proof 3.1 *Theorem 3.1. Consider the following Lyapunov function candidate:*

$$V_{f_i}(e(t)) = e^T(t)\bar{P}_i e(t) \tag{3.46}$$

and the first-time derivative along trajectory (3.44) *is given by:*

$$\dot{V}_{f_i}(e(t)) = He\Big\{e^T(t)\bar{P}_i\bar{J}_i\left(\bar{A}_i - \bar{L}_i\bar{C}\right)e(t)\Big\} + He\Big\{e^T(t)\bar{P}_i\bar{w}_i(t)\Big\} \tag{3.47}$$

The $\mathcal{H}_\infty$ performance index is introduced as:

$$\begin{gathered}\lim_{t\to\infty} e(t) = 0, \quad \bar{w}_i(t) = 0, \forall t \geq 0 \\ \int_0^t e^T(s)e(s)ds \leq \bar{\gamma}^2 \int_0^t \bar{w}_i^T(s)\bar{w}_i(s)ds, \quad \bar{w}_i \neq 0\end{gathered} \tag{3.48}$$

Combining (3.47) *and* (3.48) *yields:*

$$\dot{V}_{f_i}(e(t)) + e^T(t)e(t) - \bar{\gamma}^2\bar{w}_i^T(t)\bar{w}_i(t) \prec 0 \tag{3.49}$$

The inequality (3.49) *is then rewritten as:*

$$\begin{bmatrix} e^T(t) & \bar{w}_i^T(t) \end{bmatrix} \Upsilon \begin{bmatrix} e(t) \\ \bar{w}_i(t) \end{bmatrix} \prec 0 \tag{3.50}$$

This implies that $\Upsilon \prec 0$ which completes the proof.

3.3.3 Fault-tolerant controller

In this subsection, the aim is to design a fault-tolerant tracking controller to stabilize the closed-loop system in the case of fault occurrence and track the reference model considered as the perfect behaviors of lateral dynamics. The idea is to force the vehicle to track the desired trajectories $x_r(t) = \begin{bmatrix} \beta_r(t) \\ r_r(t) \end{bmatrix}$ given by the reference model which represents the ideal response of the vehicle according to driver maneuvers.

For the controller synthesis, let's consider the following fault-free lateral dynamics system without uncertainties as reference model:

$$\begin{cases} \dot{x}_r(t) = A_{\sigma(t)}x_r(t) + Bu_r(t) + D_{\sigma(t)}\delta_f(t) \\ y_r(t) = Cx_r(t) \end{cases} \tag{3.51}$$

where $u_r(t) \in \mathbb{R}^{n_u}$ is the nominal reference yaw moment control input vector set to be equal to zero, $x_r(t) \in \mathbb{R}^{n_x}$ is the reference state vector and $y_r(t) \in \mathbb{R}^{n_y}$ is the output vector of reference model.

The interaction of among the uncertain switched LPV systems (3.9), switched unknown input interval observers (3.15) and fault-tolerant tracking control is outlined in Figure 3.1. In this diagram, the interval observer inputs consist of the system input $u(t)$ and the system output $y(t)$ whereas the fault $f(t)$ is treated as unknown input.

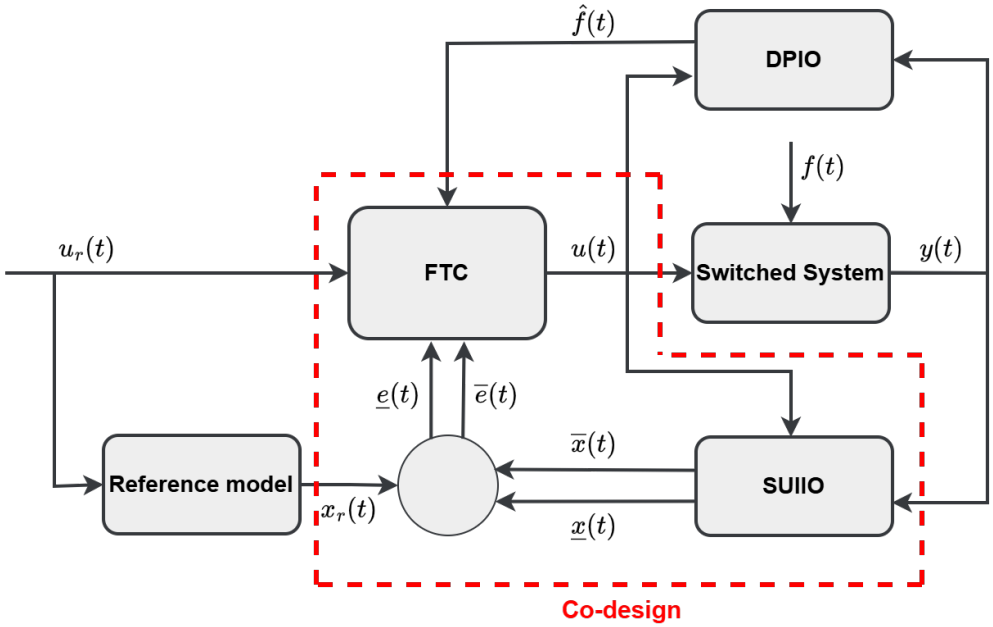

Figure 3.1: Robust co-design of the interval observers and controllers.

The obtained state and fault estimates are combined to design state feedback to track the desired yaw rate. The control law is given as follows:

$$u(t) = -\overline{K}_{\sigma(t)}\big(\overline{x}(t) - x_r(t)\big) - \underline{K}_{\sigma(t)}\big(\underline{x}(t) - x_r(t)\big) - K_f\hat{f}(t) + u_r(t) \tag{3.52}$$

where $\overline{K}_{\sigma(t)}$, $\underline{K}_{\sigma(t)}$ are the lower and upper switching state feedback gain matrices and K_f is the accommodation gain matrix to be designed to mitigate the effects of faults. It is determined as $K_f = B^{\dagger}F$

For the purpose of tracking reference state $x_r(t)$, let's define tracking error $e_r(t) = x(t) - x_r(t)$, its dynamics is then determined as:

$$\begin{aligned}\dot{e}_r(t) = &\Big(A_{\sigma(t)} - B\overline{K}_{\sigma(t)} - B\underline{K}_{\sigma(t)}\Big)e_r(t) - B\overline{K}_{\sigma(t)}\overline{e}(t) + B\underline{K}_{\sigma(t)}\underline{e}(t)\\ &+ \Delta A_{\sigma(t)}e_r(t) + Fe_f(t) + \Delta A_{\sigma(t)}x_r(t) + \Delta D_{\sigma(t)}\delta_f(t)\end{aligned} \tag{3.53}$$

The error system consists of (3.29) and (3.53) is expressed as:

$$\begin{cases}\dot{e}_r(t) = \Big(A_{\sigma(t)} - B\overline{K}_{\sigma(t)} - B\underline{K}_{\sigma(t)}\Big)e_r(t) - B\overline{K}_{\sigma(t)}\overline{e}(t)\\ \qquad\qquad + B\underline{K}_{\sigma(t)}\underline{e}(t) + \Delta A_{\sigma(t)}e_r(t) + w_{1,\sigma(t)}(t)\\ \dot{\overline{e}}(t) = N_{\sigma(t)}\overline{e}(t) - Q_{\sigma(t)}\Delta A_{\sigma(t)}e_r(t) + w_{2,\sigma(t)}(t)\\ \dot{\underline{e}}(t) = N_{\sigma(t)}\underline{e}(t) + Q_{\sigma(t)}\Delta A_{\sigma(t)}e_r(t) + w_{3,\sigma(t)}(t)\end{cases} \tag{3.54}$$

where

$$\begin{cases} w_{1,\sigma(t)}(t) = F_{\sigma(t)}e_f(t) + \Delta A_{\sigma(t)}x_r(t) + \Delta D_{\sigma(t)}\delta_f(t) \\ w_{2,\sigma(t)}(t) = \overline{\Omega}_{\sigma(t)}(t) - Q_{\sigma(t)}\big(\Delta A_{\sigma(t)}x_r(t) + \Delta D_{\sigma(t)}\delta_f(t)\big) \\ w_{3,\sigma(t)}(t) = Q_{\sigma(t)}\big(\Delta A_{\sigma(t)}x_r(t) + \Delta D_{\sigma(t)}\delta_f(t)\big) - \underline{\Omega}_{\sigma(t)}(t) \end{cases}$$

The design procedure is conducted under LMI framework using MATLAB-based optimization solvers.

Remark 3.2 *It is clear that there is an interconnection between estimation errors and tracking error in the augmented error system* (3.54)*. On the one hand, the performance of the lower and upper estimation errors, i.e.* $\underline{e}(t)$, $\overline{e}(t)$ *is affected by the tracking error* $e_r(t)$ *through terms* $Q_{\sigma(t)}\Delta A_{\sigma(t)}e_r(t)$*. On the other hand, the performance of the tracking error is also influenced by the lower and upper bounds of the state and fault estimation errors via terms* $B\overline{K}_{\sigma(t)}\overline{e}(t)$ *and* $B\underline{K}_{\sigma(t)}\underline{e}(t)$*. The bi-directional effects break down the Separation Principle as discussed in work [163].*

Remark 3.3 *The fault estimation error* $e_f(t)$ *is regarded as a disturbance in the augmented system* (3.54)*.*

Let us define the augmented vectors $\chi(t) = \begin{bmatrix} e_r(t) \\ \overline{e}(t) \\ \underline{e}(t) \end{bmatrix}$ and $w_i(t) = \begin{bmatrix} w_{1,i}(t) \\ w_{2,i}(t) \\ w_{3,i}(t) \end{bmatrix}$ before Theorem 3.2 is stated for the augmented system (3.54).

Theorem 3.2 *Suppose assumptions 3.1-3.4 of system* (3.9) *are satisfied and if there exists positive diagonal matrices* $P_{1,i}$, $P_{2,i}$, $P_i = diag(P_{1,i}, P_{2,i}, P_{2,i})$*, a quadratic ISS-Lyapunov function* $V_{\sigma(t)}(\chi(t))$ *switching among* $V_i(\chi(t)) = \chi^T(t)P_i\chi(t)$*, matrices* X_i, W_i, $\underline{G}_i$, $\overline{G}_i$ *given positive scalars* $\eta_{1,i}$, $\eta_{2,i}$, $\eta_{3,i}$ *for all* $i \in \mathcal{N}$ *and constant scalars* $\alpha_2 > \alpha_1 > 0$, $\gamma_i > 0$, $\varepsilon > 0$ *and* $\rho > 0$ *such that the following LMIs hold:*

$$\begin{aligned} &\min_{P_i, X_i, W_i, \underline{G}_i, \overline{G}_i} \gamma_i \\ &\gamma_i \leq \gamma \end{aligned} \tag{3.55}$$

$$\alpha_1 I_{3\times n_x} \leq P_i \leq \alpha_2 I_{3\times n_x} \tag{3.56}$$

$$O = \begin{bmatrix} O_{11} & O_{12} & O_{13} \\ (*) & O_{22} & O_{23} \\ (*) & (*) & O_{33} \end{bmatrix} \prec 0 \tag{3.57}$$

$$P_{2,i}A_i - P_{2,i}\Theta CA_i - X_i\Psi CA_i - W_iC + \rho P_{2,i} \geq 0 \tag{3.58}$$

then the augmented system (3.54) *is stable with* $Z_i = P_{2,i}^{-1}X_i$ *and* $Y_i = P_{2,i}^{-1}W_i$, $\overline{K}_i = \overline{G}_iP_{1,i}^{-1}$ *and* $\underline{K}_i = \underline{G}_iP_{1,i}^{-1}$.

$$O_{11} = \begin{bmatrix} \Gamma^{'''} & P_i^{'} \\ P_i^{'} & -\gamma_i \end{bmatrix} \tag{3.59}$$

$$O_{12} = \begin{bmatrix} P_{1,i}N_{a,i}^T & 0 & 0 \\ 0 & \mathcal{T}_2 M_{a',i} & 0 \\ 0 & 0 & \mathcal{T}_2 M_{a,i} \\ 0 & 0 & 0 \end{bmatrix} \tag{3.60}$$

$$O_{13} = \begin{bmatrix} -B\overline{G}_i & B\underline{G}_i & 0 & 0 \\ 0 & 0 & I_{n_x} & 0 \\ 0 & 0 & 0 & I_{n_x} \\ 0 & 0 & 0 & 0 \end{bmatrix} \tag{3.61}$$

$$O_{22} = -\begin{bmatrix} \left(\eta_{1,i}^{-1} + \eta_{2,i}^{-1} + \eta_{3,i}^{-1}\right) & 0 & 0 \\ (*) & \eta_{2,i} & 0 \\ (*) & (*) & \eta_{3,i} \end{bmatrix}^{-1} \tag{3.62}$$

$$O_{23} = 0 \tag{3.63}$$

$$O_{33} = -\begin{bmatrix} \mu^{-1}P_{1,i} & 0 & 0 & 0 \\ (*) & \mu^{-1}P_{1,i} & 0 & 0 \\ (*) & (*) & \mu P_{1,i} & 0 \\ (*) & (*) & (*) & \mu P_{1,i} \end{bmatrix} \tag{3.64}$$

$$\Gamma^{'''} = \begin{bmatrix} \Gamma_{11}^{''} & 0 & 0 \\ (*) & \Gamma_{22}^{'} & 0 \\ (*) & (*) & \Gamma_{33}^{'} \end{bmatrix} \tag{3.65}$$

$$P_i^{'} = \begin{bmatrix} I_{n_x} & 0 & 0 \\ (*) & P_{2,i} & 0 \\ (*) & (*) & P_{2,i} \end{bmatrix} \tag{3.66}$$

$$\Gamma_{11}^{''} = He\Big\{A_i P_{1,i} - B\overline{G}_i - B\underline{G}_i\Big\} + \eta_{1,i} M_{a,i} M_{a,i}^T + \varepsilon P_{1,i} \tag{3.67}$$

$$\Gamma_{22}^{'} = He\Big\{P_{2,i}A_i - P_{2,i}\Theta C A_i - X_i \Psi C A_i - W_i C\Big\} + \varepsilon P_{2,i} \tag{3.68}$$

$$\Gamma_{33}^{'} = He\Big\{P_{2,i}A_i - P_{2,i}\Theta C A_i - X_i \Psi C A_i - W_i C\Big\} + \varepsilon P_{2,i} \tag{3.69}$$

$$\mathcal{T}_2 = P_{2,i} - P_{2,i}\Theta C - X_i \Psi C \tag{3.70}$$

In addition, the system (3.54) *is ISS with respective to* w_i *under any switching signal with average dwell time satisfying condition* (2.36)*, and*

$$\lim_{t\to\infty} \|\chi(t)\|_2 \leq \sqrt{\frac{\gamma}{\alpha_1 \varepsilon}} \max \|w_i(t)\|_\infty \quad \forall i \in \mathcal{N} \tag{3.71}$$

Proof 3.2 *(Theorem 3.2) Let's consider the following multiple ISS-Lyapunov functions:*

$$\begin{aligned} V_i\big(\chi(t)\big) &= V_{1,i}\big(e_r(t)\big) + V_{2,i}\big(\overline{e}(t)\big) + V_{3,i}\big(\underline{e}(t)\big) \\ &= e_r^T(t) P_{1,i}^{-1} e_r(t) + \overline{e}^T(t) P_{2,i} \overline{e}(t) + \underline{e}^T(t) P_{2,i} \underline{e}(t) \end{aligned} \tag{3.72}$$

Taking the first-order derivative of (3.72) *along trajectory of* (3.54) *as:*

$$\dot{V}_i\big(\chi(t)\big) = \dot{V}_{1,i}\big(e_r(t)\big) + \dot{V}_{2,i}\big(\overline{e}(t)\big) + \dot{V}_{3,i}\big(\underline{e}(t)\big) \tag{3.73}$$

The derivative Lyapunov functions $\dot{V}_{1,i}\big(e_r(t)\big)$*,* $\dot{V}_{2,i}\big(\overline{e}(t)\big)$ *and* $\dot{V}_{3,i}\big(\underline{e}(t)\big)$ *are expressed as:*

$$\begin{aligned} \dot{V}_{1,i}(e_r(t)) &= e_r^T(t) P_{1,i}^{-1} \dot{e}_r(t) + \dot{e}_r^T(t) P_{1,i}^{-1} e_r(t) \\ &= He\Big\{ e_r^T(t) P_{1,i}^{-1} \big(A_i - B\overline{K}_i - B\underline{K}_i\big) e_r(t) \Big\} \\ &- He\Big\{ e_r^T(t) P_{1,i}^{-1} B\overline{K}_i \overline{e}(t) \Big\} + He\Big\{ e_r^T(t) P_{1,i}^{-1} B\underline{K}_i \underline{e}(t) \Big\} \\ &+ He\Big\{ e_r^T(t) P_{1,i}^{-1} w_{1,i}(t) \Big\} + He\Big\{ e_r^T(t) \Big(P_{1,i}^{-1} M_{a,i} \Delta N_{a,i} \Big) e_r(t) \Big\} \end{aligned} \tag{3.74}$$

$$\begin{aligned} \dot{V}_{2,i}(\overline{e}(t)) &= \overline{e}^T(t) P_{2,i} \dot{\overline{e}}(t) + \dot{\overline{e}}^T(t) P_{2,i} \overline{e}(t) \\ &= He\Big\{ \overline{e}^T(t) \big(P_{2,i} N_i \big) \overline{e}(t) \Big\} \\ &- He\Big\{ \overline{e}^T(t) \big(P_{2,i} Q_i \Delta A_i \big) e_r(t) \Big\} \\ &+ He\Big\{ \overline{e}^T(t) P_{2,i} w_{2,i}(t) \Big\} \end{aligned} \tag{3.75}$$

By substituting matrices N_i *in* (3.39) *and* ΔA_i *in* (3.11) *into* (3.75) *and setting* $M_{a',i} = -M_{a,i}$*,, the derivative of* $\dot{V}_2, i(\overline{e}(t))$ *is expressed as:*

$$\begin{aligned} \dot{V}_{2,i}(\overline{e}(t)) &= He\Big\{ \overline{e}^T(t) P_{2,i} \big(Q_i A_i - Y_i C \big) \overline{e}(t) \Big\} \\ &+ He\Big\{ \overline{e}^T(t) \left(P_{2,i} Q_i M_{a',i} \Delta(t) N_{a,i} \right) e_r(t) \Big\} \\ &+ He\Big\{ \overline{e}^T(t) P_{2,i} w_{2,i}(t) \Big\} \end{aligned} \tag{3.76}$$

$$\begin{aligned}\dot{V}_{3,i}(\underline{e}(t)) &= \underline{e}^T(t)P_{2,i}\dot{\underline{e}}(t) + \dot{\underline{e}}^T(t)P_{2,i}\underline{e}(t)\\ &= He\Big\{\underline{e}^T(t)\big(P_{2,i}N_i\big)\underline{e}(t)\Big\}\\ &+ He\Big\{\underline{e}^T(t)\Big(P_{2,i}Q_i\Delta A_i\Big)e_r(t)\Big\}\\ &+ He\Big\{\underline{e}^T(t)P_{2,i}w_{3,i}(t)\Big\}\end{aligned} \tag{3.77}$$

By substituting matrices N_i *in* (3.39) *and* ΔA_i *in* (3.11) *into* (3.77)*, the derivative of* $\dot{V}_3, i(\overline{e}(t))$ *is expressed as:*

$$\begin{aligned}\dot{V}_{3,i}(\underline{e}(t)) &= \underline{e}^T P_{2,i}\dot{\underline{e}}(t) + \dot{\underline{e}}^T P_{2,i}\underline{e}(t)\\ &= He\Big\{\underline{e}^T(t)P_{2,i}\big(Q_iA_i - Y_iC\big)\underline{e}(t)\Big\}\\ &+ He\Big\{\underline{e}^T(t)\Big(P_{2,i}Q_iM_{a,i}\Delta(t)N_{a,i}\Big)e_r(t)\Big\}\\ &+ He\Big\{\underline{e}^T(t)P_{2,i}w_{3,i}(t)\Big\}\end{aligned} \tag{3.78}$$

Consider Majorization lemma 2.10 for derivative of Lyapunov of (3.73) *with any positive scalars* $\eta_{1,i}$*,* $\eta_{2,i}$ *and* $\eta_{3,i}$ *, one can obtain:*

$$\begin{aligned}\dot{V}_{1,i}(e_r(t)) &\le He\Big\{e_r^T(t)P_{1,i}^{-1}\big(A_i - B\overline{K}_i - B\underline{K}_i\big)e_r(t)\Big\}\\ &- He\Big\{e_r^T(t)P_{1,i}^{-1}B\overline{K}_i\overline{e}\Big\}\\ &+ He\Big\{e_r^T(t)P_{1,i}^{-1}w_{1,i}\Big\} + He\Big\{e_r^T(t)P_{1,i}^{-1}B\underline{K}_i\underline{e}(t)\Big\}\\ &+ \eta_{1,i}^{-1}e_r^T(t)N_{a,i}^TN_{a,i}e_r(t) + \eta_{1,i}e_r^T(t)P_{1,i}^{-1}M_{a,i}M_{a,i}^TP_{1,i}^{-1}e_r(t)\end{aligned} \tag{3.79}$$

$$\begin{aligned}\dot{V}_{2,i}(\overline{e}(t)) &\le He\Big\{\overline{e}^T(t)P_{2,i}\big(Q_iA_i - Y_iC\big)\overline{e}(t)\Big\}\\ &+ \eta_{2,i}\overline{e}^T(t)P_{2,i}Q_iM_{a',i}M_{a',i}^TQ_iP_{2,i}^T\overline{e}(t) + \eta_{2,i}^{-1}e_r^T(t)N_{a,i}^TN_{a,i}e_r(t)\\ &+ He\Big\{\overline{e}^T(t)P_{2,i}w_{2,i}(t)\Big\}\end{aligned} \tag{3.80}$$

$$\begin{aligned}\dot{V}_{3,i}(\underline{e}(t)) &\le He\Big\{\underline{e}^T(t)P_{2,i}\big(Q_iA_i - Y_iC\big)\underline{e}(t)\Big\}\\ &+ \eta_{3,i}\underline{e}^T(t)P_{2,i}Q_iM_{a,i}M_{a,i}^TQ_i^TP_{2,i}^T\underline{e}(t) + \eta_{3,i}^{-1}e_r^T(t)N_{a,i}^TN_{a,i}e_r(t)\\ &+ He\Big\{\underline{e}^T(t)P_{2,i}w_{3,i}(t)\Big\}\end{aligned} \tag{3.81}$$

With any scalars $\varepsilon > 0$*,* $\gamma_i > 0$ *for all* $i \in \mathcal{N}$*, equations* (3.79)*,* (3.80) *and* (3.81) *are rewritten as:*

$$\dot{V}_i(\chi) \le \begin{bmatrix}\chi^T(t) & w_i^T(t)\end{bmatrix}\Xi\begin{bmatrix}\chi(t)\\ w_i(t)\end{bmatrix} - \varepsilon V_i(\chi(t)) + \gamma_i w_i^T(t)w_i(t) \tag{3.82}$$

where

$$\Xi = \begin{bmatrix} \Gamma & P \\ P & -\gamma_i \end{bmatrix} \tag{3.83}$$

$$\Gamma = \begin{bmatrix} \Gamma_{11} & \Gamma_{12} & \Gamma_{13} \\ (*) & \Gamma_{22} & \Gamma_{23} \\ (*) & (*) & \Gamma_{33} \end{bmatrix} \tag{3.84}$$

$$P = \begin{bmatrix} P_{1,i}^{-1} & 0 & 0 \\ (*) & P_{2,i} & 0 \\ (*) & (*) & P_{2,i} \end{bmatrix} \tag{3.85}$$

$$\begin{aligned} \Gamma_{11} = & He\Big\{P_{1,i}^{-1}A_i - P_{1,i}^{-1}B\overline{K}_i - P_{1,i}^{-1}B\underline{K}_i\Big\} \\ & + \eta_{1,i}P_{1,i}^{-1}M_{a,i}M_{a,i}^T P_{1,i}^{-1} \\ & + \left(\eta_{1,i}^{-1} + \eta_{2,i}^{-1} + \eta_{3,i}^{-1}\right) N_{a,i}^T N_{a,i} + \varepsilon P_{1,i}^{-1} \end{aligned} \tag{3.86}$$

$$\begin{aligned} \Gamma_{22} = & He\Big\{P_{2,i}A_i - P_{2,i}\Theta CA_i - X_i\Psi CA_i - W_iC\Big\} \\ & + \eta_{2,i}\mathcal{T}_2 M_{a',i}M_{a',i}^T\mathcal{T}_2^T + \varepsilon P_{2,i} \end{aligned} \tag{3.87}$$

$$\begin{aligned} \Gamma_{33} = & He\Big\{P_{2,i}A_i - P_{2,i}\Theta CA_i - X_i\Psi CA_i - W_iC\Big\} \\ & + \eta_{3,i}\mathcal{T}_2 M_{a,i}M_{a,i}^T\mathcal{T}_2^T + \varepsilon P_{2,i} \end{aligned} \tag{3.88}$$

$$\Gamma_{12} = -P_{1,i}^{-1}B\overline{K}_i \tag{3.89}$$

$$\Gamma_{13} = P_{1,i}^{-1}B\underline{K}_i \tag{3.90}$$

$$\Gamma_{23} = 0 \tag{3.91}$$

with $X_i = P_{2,i}Z_i$ *and* $W_i = P_{2,i}Y_i$.

The following is a sufficient condition for system (3.54) *to be Input-to-State-Stable:*

$$\Xi \prec 0 \tag{3.92}$$

Using pre-and post-multiplication Ξ *by* $\begin{bmatrix} P_p & 0 \\ 0 & I \end{bmatrix}$ *with* $P_p = \begin{bmatrix} P_{1,i} & 0 & 0 \\ 0 & I_{n_x} & 0 \\ 0 & 0 & I_{n_x} \end{bmatrix}$*, one can get:*

$$\Xi^{'} = \begin{bmatrix} \Gamma^{'} & P^{'} \\ P^{'} & -\gamma_i \end{bmatrix} \prec 0 \tag{3.93}$$

with

$$\Gamma^{'} = \begin{bmatrix} \Gamma^{'}_{11} & \Gamma^{'}_{12} & \Gamma^{'}_{13} \\ (*) & \Gamma_{22} & \Gamma_{23} \\ (*) & (*) & \Gamma_{33} \end{bmatrix} \tag{3.94}$$

$$P^{'} = \begin{bmatrix} I_{n_x} & 0 & 0 \\ (*) & P_{2,i} & 0 \\ (*) & (*) & P_{2,i} \end{bmatrix} \tag{3.95}$$

$$\begin{aligned} \Gamma^{'}_{11} = He\Big\{A_i P_{1,i} - B\overline{G}_i - B\underline{G}_i\Big\} + \eta_{1,i} M_{a,i} M_{a,i}^T \\ + \left(\eta_{1,i}^{-1} + \eta_{2,i}^{-1} + \eta_{3,i}^{-1}\right) P_{1,i} N_{a,i}^T N_{a,i} P_{1,i} + \varepsilon P_{1,i} \end{aligned} \tag{3.96}$$

$$\Gamma^{'}_{12} = -B\overline{K}_i \tag{3.97}$$

$$\Gamma^{'}_{13} = B\underline{K}_i \tag{3.98}$$

where $\overline{G}_i = \overline{K}_i P_{1,i}$ *and* $\underline{G}_i = \underline{K}_i P_{1,i}$

The term $\Xi^{'}$ *can be written as:*

$$\Xi^{'} = \Xi^{''} + \mathcal{X}^T \mathcal{Y} + \mathcal{Y}^T \mathcal{X} \tag{3.99}$$

By considering Young relation lemma 2.11 for $\Xi^{'}$*, one can obtain the following inequality:*

$$\Xi^{'} \preceq \Xi^{''} + \mu \mathcal{X}^T \mathcal{F} \mathcal{X} + \mu^{-1} \mathcal{Y}^T \mathcal{F}^{-1} \mathcal{Y} \tag{3.100}$$

where

$$\Xi^{''} = \begin{bmatrix} \Gamma^{''} & P^{'} \\ P^{'} & -\gamma_i \end{bmatrix} \tag{3.101}$$

$$\Gamma^{''} = \begin{bmatrix} \Gamma_{11}^{'} & 0 & 0 \\ (*) & \Gamma_{22} & 0 \\ (*) & (*) & \Gamma_{33} \end{bmatrix} \tag{3.102}$$

$$\mathcal{F} = \begin{bmatrix} P_{1,i} & 0 \\ 0 & P_{1,i} \end{bmatrix} \tag{3.103}$$

$$\mathcal{X} = \begin{bmatrix} -\left(B\overline{K}_i\right)^T & 0 & 0 & 0 \\ \left(B\underline{K}_i\right)^T & 0 & 0 & 0 \end{bmatrix} \tag{3.104}$$

$$\mathcal{Y} = \begin{bmatrix} 0 & I_{n_x} & 0 & 0 \\ 0 & 0 & I_{n_x} & 0 \end{bmatrix} \tag{3.105}$$

Then apply the Schur complement lemma 2.9 to (3.100)*, we get:*

$$\Xi^{'} \preceq \begin{bmatrix} \Xi^{''} & O_{13} \\ (*) & O_{33} \end{bmatrix} \tag{3.106}$$

Therefore, the sufficient condition (3.92) *is satisfied if*

$$\begin{bmatrix} \Xi^{''} & O_{13} \\ (*) & O_{33} \end{bmatrix} \prec 0 \tag{3.107}$$

In the same manner, one can get the LMI (3.57)*. This ensures that* $\dot{V}_i(\chi(t)) \leq -\varepsilon V_i(\chi(t)) + \gamma_i w_i^T(t) w_i(t)$*. Hence, according to lemma 2.2, the augmented error system* (3.54) *is ISS with respect to additive disturbance* $w_i(t)$*.*
Then integrating this inequality from t_k *to* t*, we can get:*

$$V_i(\chi(t)) \leq \varepsilon e^{-\varepsilon(t-t_k)} V_i(\chi(t_k)) + \gamma_i \|w_i(t)\|_\infty^2 \tag{3.108}$$

Recall the condition (3.56)*, it follows that*

$$\alpha_1 \|\chi(t)\|^2 \leq V_i(\chi(t)) \leq \alpha_2 \|\chi(t)\|^2 \tag{3.109}$$

From (3.108) *and* (3.109)*, one obtains*

$$\|\chi(t)\|_2 \leq \sqrt{\frac{e^{-\varepsilon(t-t_k)} V_i(\chi(t_k))}{\alpha_1} + \frac{\gamma_i}{\varepsilon \alpha_1} \|w_i(t)\|_\infty^2} \tag{3.110}$$

Hence, when $t \to \infty$ the exponential term goes to zero and $\gamma_i \leq \gamma$ for all $i \in \mathcal{N}$, the inequality (3.110) *becomes LMI* (3.71).

Furthermore, N_i is a Metzler matrix, if $N_i + \rho I_{n_x} \geq 0$ with any $\rho > 0, \forall i \in \mathcal{N}$. LMI in (3.58) *can be obtained by multiplying $P_{2,i}$ on the left side along with change of variables $X_i = P_{2,i}Z_i$ and $W_i = P_{2,i}Y_i$. This completes the proof.*

Remark 3.4 *It should be noted that the augmented state vector $\chi(t)$ has an upper bound defined by $\sqrt{\frac{\gamma}{\alpha_1 \varepsilon}} \max \|w_i(t)\|_\infty$. This upper bound should be minimized as much as possible to improve the robustness of the proposed observer-based controller against perturbations. It is evident that this bound is tighter with smaller γ value for priori known α_1 and ε. Therefore, the minimization of the scalar γ plays a crucial role in minimizing the upper bound of the augmented state χ.*

Overall, the design procedure of the switched unknown input interval observer, the dynamics proportional integral observer and FTTC is determined based on the following algorithms:

3.4 Simulation

The proposed approach is deployed to control yaw dynamics of the vehicle lateral dynamics model. The FTC strategy aims to ensure that yaw moment at center of gravity of the vehicle remains stable, even if actuator faults occur. For the simulation, the front steering angle $\delta_f(t)$ is influenced by the driver through the steering wheel and based on the difference between the actual and reference signals, yaw moment $M_z(t)$ is generated by differential braking on the rear wheels e.g., the rear-left or rear-right brake. During the maneuver, a fault is injected into one of the brake actuators responsible for generating the yaw moment. Cornering stiffness variations are reflected in terms Δc_f and Δc_r which are assumed to be 20% lower than the nominal values.

The design procedure is conducted under LMI framework using MATLAB optimization routines such as SEDUMI [165]. The obtained observers and the fault-tolerant controller are tested in simulation using the Simulink vehicle dynamics blocksets models.

According to assumption 3.4, the actual actuator fault $f(t)$ is depicted in Figure 3.5 and Figure 3.17, which combines constant and sinusoidal forms.

In the simulation, the initial state conditions are set as $\underline{x}_0 = \begin{bmatrix} -0.1 \\ -0.25 \end{bmatrix}, x_0 = \begin{bmatrix} 0.05 \\ 0.1 \end{bmatrix}, \overline{x}_0 = \begin{bmatrix} 0.1 \\ 0.25 \end{bmatrix}$ and $\underline{x}_0 = \begin{bmatrix} -0.4 \\ -1.0 \end{bmatrix}, \overline{x}_0 = \begin{bmatrix} 0.4 \\ 1.0 \end{bmatrix}$

Algorithm 1: Design procedure

for $\sigma(t) = 1 : N$ **do**

if $(rank(CF) == rank(B))$ **then**

- Solve LMI of (3.45) in Theorem 3.1 to find the matrices $\bar{P}_{\sigma(t)}$ and $\bar{Q}_{\sigma(t)}$. The observer gains of DPIO are then determined as:

$$\begin{cases} \bar{L}_{\sigma(t)} = \bar{J}^{-1}_{\sigma(t)} \bar{P}^{-1}_{\sigma(t)} \bar{Q}_{\sigma(t)} \\ L^{P}_{\sigma(t)} = \bar{L}_{\sigma(t)} \begin{bmatrix} I & 0 \end{bmatrix} \\ L^{I}_{\sigma(t)} = \bar{L}_{\sigma(t)} \begin{bmatrix} 0 & I \end{bmatrix} \end{cases}$$

- Solve the optimization problem in Theorem 3.2 and obtain $X_{\sigma(t)}$, $P_{1,\sigma(t)}$, $P_{2,\sigma(t)}$, $W_{\sigma(t)}$, $\underline{G}_{\sigma(t)}$,$\overline{G}_{\sigma(t)}$.

$$\begin{cases} Z_{\sigma(t)} = P^{-1}_{2,\sigma(t)} X_{\sigma(t)} \\ Y_{\sigma(t)} = P^{-1}_{2,\sigma(t)} W_{\sigma(t)} \\ \underline{K}_{\sigma(t)} = \underline{G}_{\sigma(t)} P^{-1}_{1,\sigma(t)} \\ \overline{K}_{\sigma(t)} = \overline{G}_{\sigma(t)} P^{-1}_{1,\sigma(t)} \end{cases}$$

- Determine matrices $E_{\sigma(t)}$, $Q_{\sigma(t)}$, $H_{\sigma(t)}$, $T_{\sigma(t)}$, $N_{\sigma(t)}$ and $J_{\sigma(t)}$ by equations (3.34), (3.35), (3.26), (3.27), (3.39) and (3.41), respectively.

$$\begin{cases} E_{\sigma(t)} = \Theta + Z_{\sigma(t)} \Psi \\ Q_{\sigma(t)} = I - E_{\sigma(t)} C \\ H_{\sigma(t)} = Q_{\sigma(t)} B \\ T_{\sigma(t)} = Q_{\sigma(t)} D_{\sigma(t)} \\ N_{\sigma(t)} = Q_{\sigma(t)} A_{\sigma(t)} - Y_{\sigma(t)} C \\ J_{\sigma(t)} = Y_{\sigma(t)} \big(I - C E_{\sigma(t)} \big) + Q_{\sigma(t)} A_{\sigma(t)} E_{\sigma(t)} \end{cases}$$

else

There is no solution for the set of LMIs.
The SUIIO does not exist

end

end

3.4.1 General profile

For this scenario, three subsystems corresponding to three different longitudinal velocities $v_x^1 = 10(m/s)$, $v_x^2 = 20(m/s)$, and $v_x^3 = 25(m/s)$ are considered with switching signal $\sigma(t)$ given as follows:

$$\sigma(t) = \begin{cases} 1, & v_x(t) \in \begin{bmatrix} 2.5 & 17.5 \end{bmatrix} (m/s) \\ 2, & v_x(t) \in \begin{bmatrix} 17.5 & 22.5 \end{bmatrix} (m/s) \\ 3, & v_x(t) \in \begin{bmatrix} 22.5 & 28.5 \end{bmatrix} (m/s) \end{cases} \tag{3.111}$$

The switching signal $\sigma(t)$ is given in Figure 4.1.

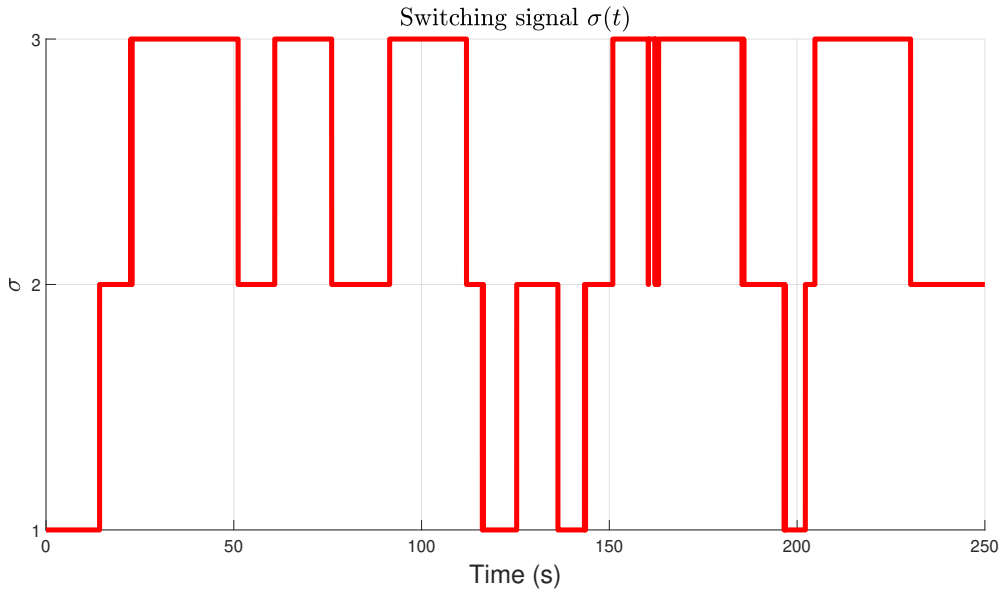

Figure 3.2: Switching signal $\sigma(t)$.

The observer and controller gain matrices solved by a set of LMIs in Theorem 3.2 are obtained as follows:

$$N_1 = \begin{bmatrix} -2.4550 & 0.0666 \\ 0 & -2.6996 \end{bmatrix}, Y_1 = \begin{bmatrix} -1.0022 \\ 2.6996 \end{bmatrix} \tag{3.112}$$

$$\underline{K}_1 = \begin{bmatrix} 3.5572 & 3.8237 \end{bmatrix}, \overline{K}_1 = \begin{bmatrix} 3.5573 & 3.8237 \end{bmatrix} \tag{3.113}$$

$$N_2 = \begin{bmatrix} -1.8413 & 0.1538 \\ 0 & -1.7372 \end{bmatrix}, Y_2 = \begin{bmatrix} -1.1176 \\ 1.7372 \end{bmatrix} \tag{3.114}$$

$$\underline{K}_2 = \begin{bmatrix} 3.9536 & 3.5589 \end{bmatrix}, \overline{K}_2 = \begin{bmatrix} 3.9537 & 3.5589 \end{bmatrix} \tag{3.115}$$

$$N_3 = \begin{bmatrix} -1.4730 & 0.0849 \\ 0 & -1.7866 \end{bmatrix}, Y_3 = \begin{bmatrix} -1.0618 \\ 1.7866 \end{bmatrix} \tag{3.116}$$

$$\underline{K}_3 = \begin{bmatrix} 3.3659 & 3.8126 \end{bmatrix}, \overline{K}_3 = \begin{bmatrix} 3.3660 & 3.8126 \end{bmatrix} \tag{3.117}$$

The front steering angle $\delta_f(t)$ and time-varying longitudinal velocity $v_x(t)$ profiles are shown in Figure 3.3 and 3.4. It also shows the correlation between front steering angle and longitudinal velocity. Especially during turning maneuvers, when $\delta_f(t)$ changes from its baseline value, $v_x(t)$ decreases to allow the vehicle to navigate the turn safely. Simulation results are presented from Figure 3.5 to 3.14.

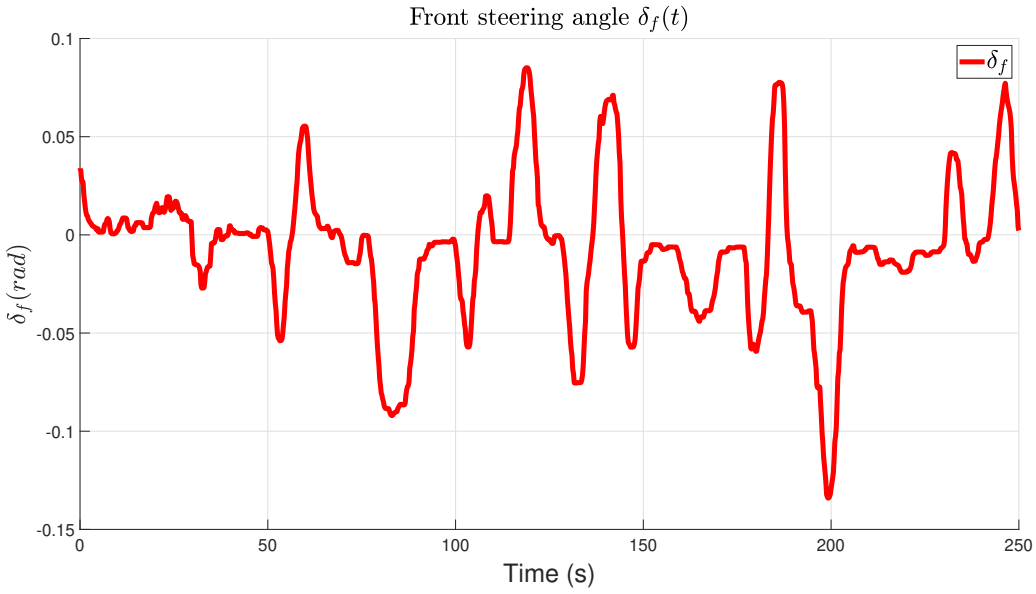

Figure 3.3: Front steering angle $\delta_f(t)$ profile.

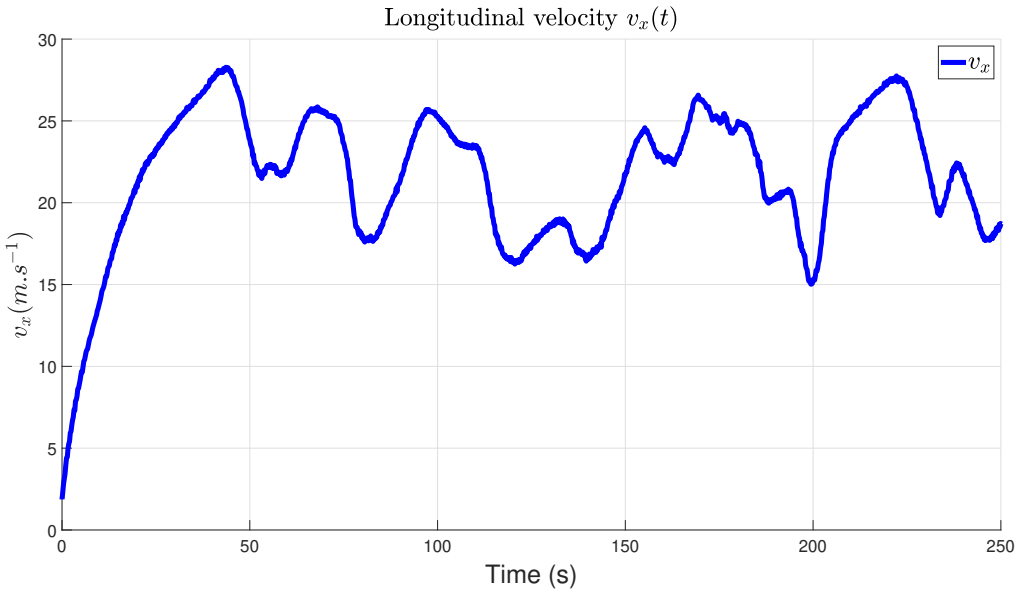

Figure 3.4: Longitudinal velocity $v_x(t)$ profile.

The actual actuator fault $f(t)$ and its estimation $\hat{f}(t)$ are depicted in Figure 3.5. The fault signal is a sinusoidal form at a frequency of $0.2387Hz$ and $0.0796Hz$ from $20s$ to $140s$ and from $160s$ to $230s$, respectively. It combines constant and sinusoidal forms. The fault signal is chosen to vary in order to prove the ability of the DPIO to accurately estimate both constants and fast time-varying scenarios. Figure 3.5 shows a good estimation of the time-varying actuator fault. The estimated fault signal rapidly reaches the actual actuator fault due to coefficient parameter λ_σ of the DPIO (3.42).

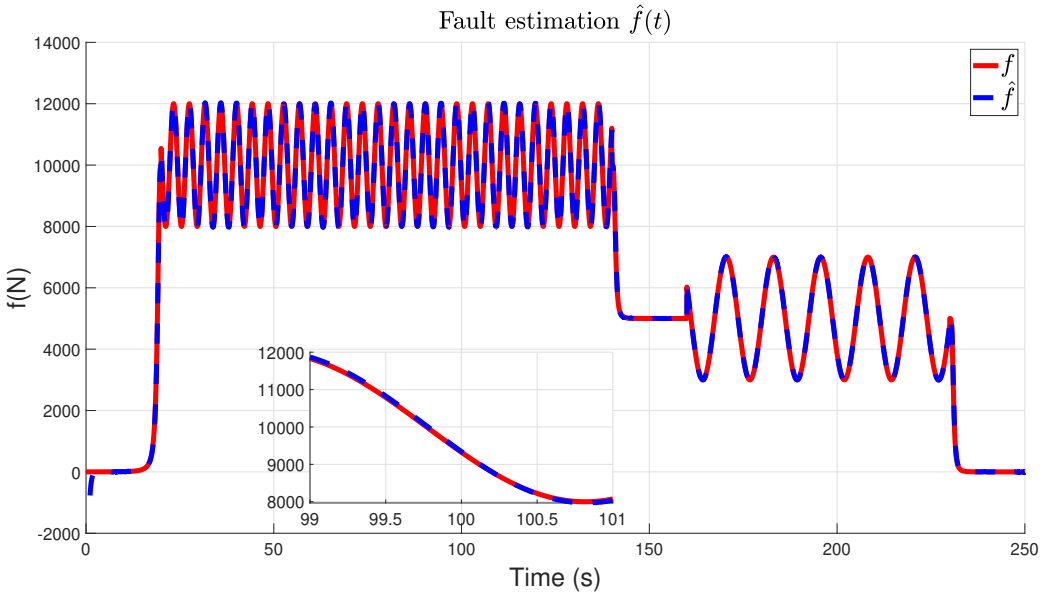

Figure 3.5: Actuator fault estimation $\hat{f}(t)$.

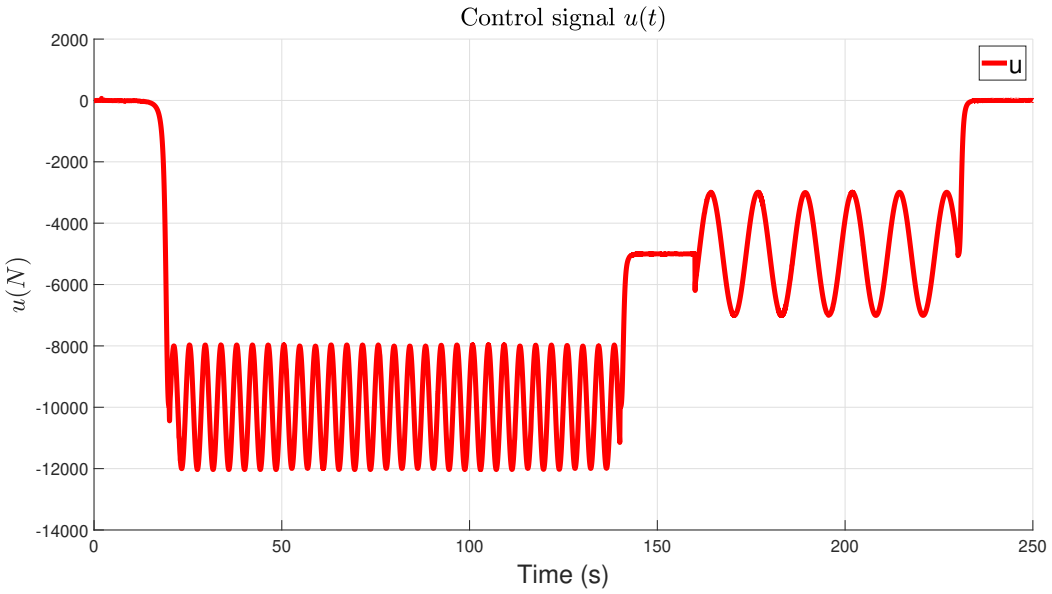

Figure 3.6: Yaw moment control input $u(t)$.

Figure 3.7 and 3.8 show the lower and upper estimations of sideslip angle $\beta(t)$ and yaw rate $r(t)$ of the vehicle dynamics model. The lower and upper bounds estimation always bound the real vehicle states at all times, even when actuator fault occurs. Additionally, the decoupling approach eliminates the effect of faults from the state estimation errors.

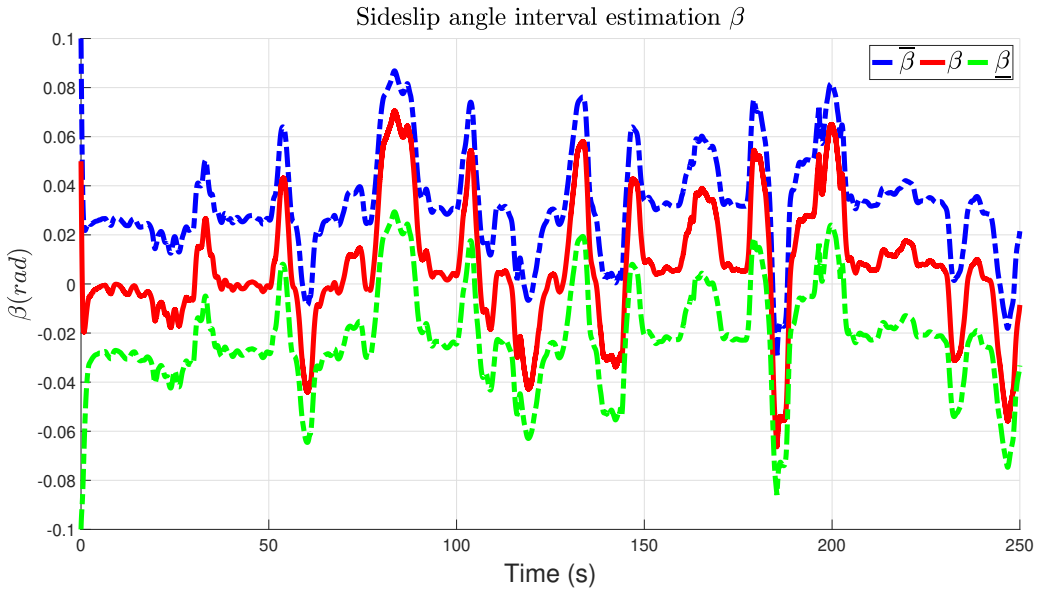

Figure 3.7: Sideslip angle $\beta(t)$ interval estimation.

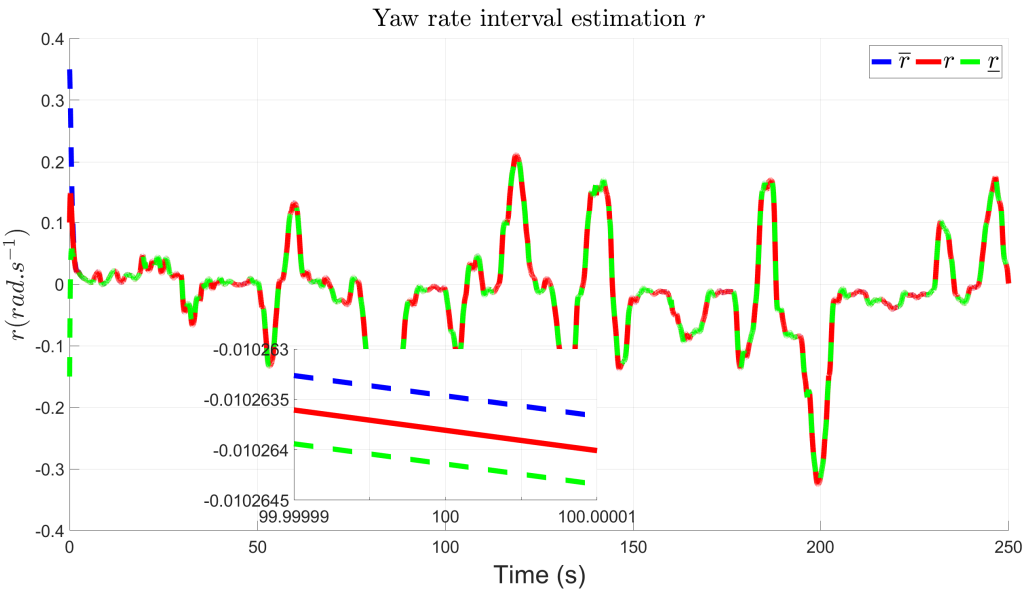

Figure 3.8: Yaw rate $r(t)$ interval estimation.

The results demonstrated in Figure 3.9 and 3.10 show that the vehicle lateral dynamics estimation accuracy achieved by the proposed multiple ISS Lyapunov function-based stability analysis approach surpasses than that of the common one discussed in [1].

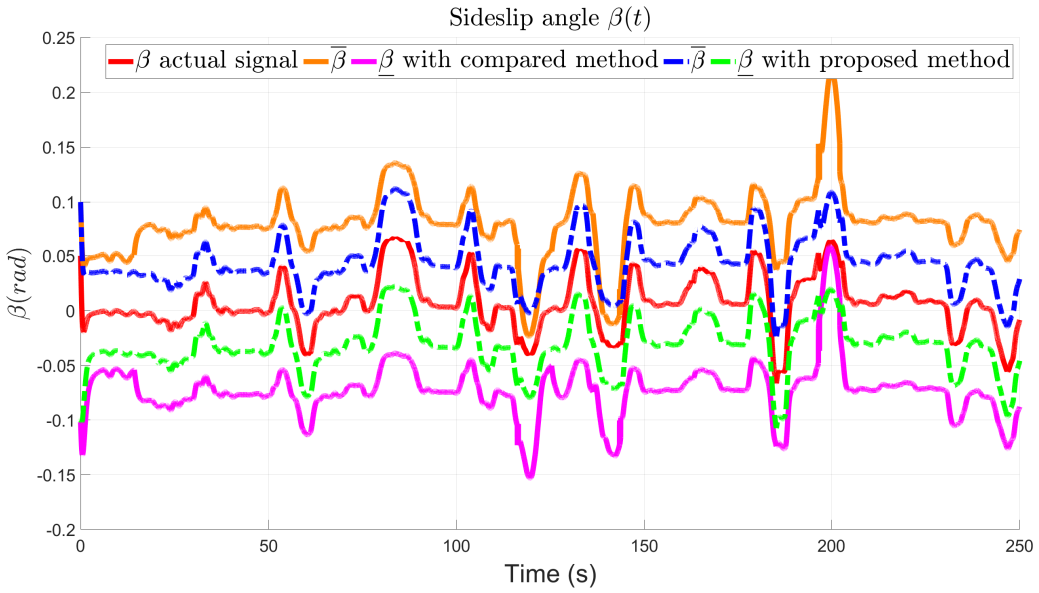

Figure 3.9: Comparison of sideslip angle $\beta(t)$ interval estimations between the proposed approach and compared method in [1].

Unlike the traditional stability analysis using the common ISS Lyapunov function for switched systems [1], the proposed multiple ISS Lyapunov function shows better stability and performance characteristics for vehicle lateral dynamics.

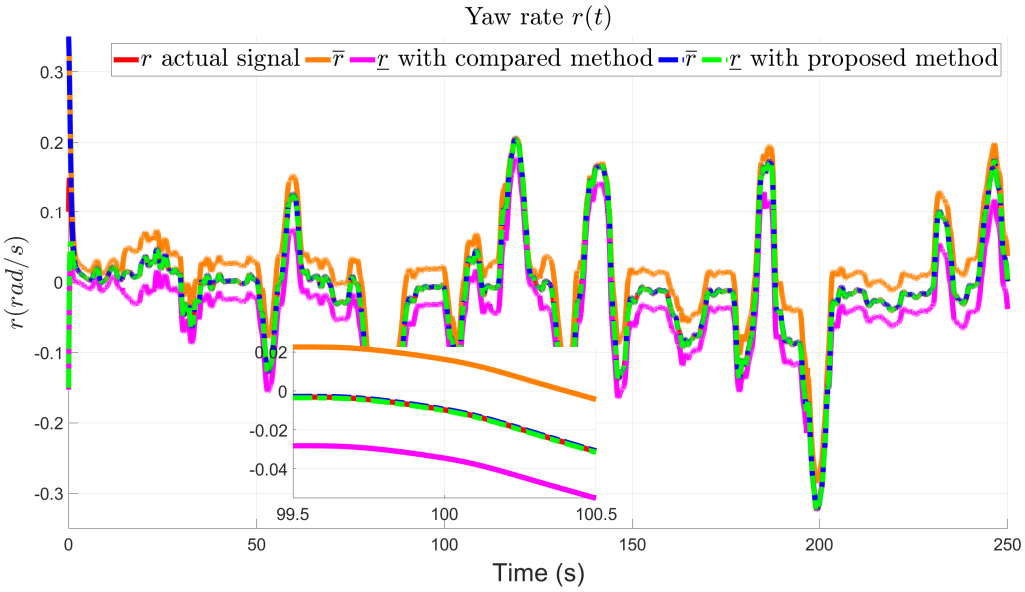

Figure 3.10: Comparison of yaw rate $r(t)$ interval estimations between the proposed approach and compared method in [1].

Notably, the system states obtained through the proposed framework exhibit tighter intervals and closer alignments to the actual system states, highlighting its effectiveness over the conventional common Lyapunov function. This improvement is reasonable since each subsystem can have its own Lyapunov function, allowing for local stability analysis for each subsystem while the common ISS Lyapunov function ensures global stability.

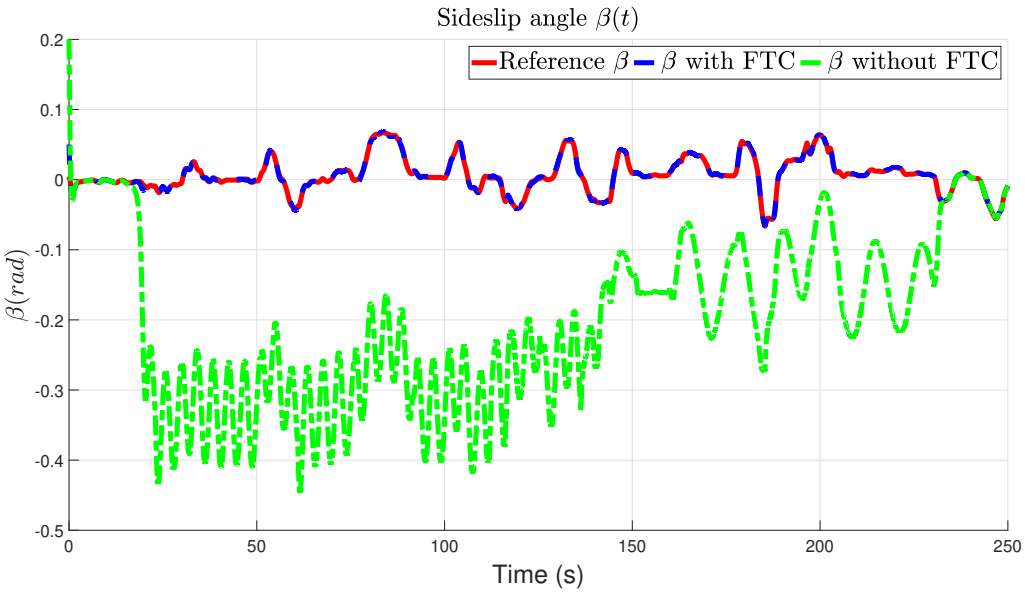

Figure 3.11: Comparison of sideslip angle $\beta(t)$ between with and without FTC.

The fault-tolerant controller stabilizes the closed-loop system and preserves the performance in the presence of faults. The actual state well tracks the reference state as depicted in Figure 3.11 and 3.12. The action of the

FTC controller demonstrates significant improvement in tracking performance compared to an uncontrolled system exhibiting a large tracking error. In fact, tracking errors are close to zero. However, when fast time-varying actuator fault occurs at a frequency of $0.2387Hz$, the tracking error oscillates around zero as illustrated in Figure 3.13 and 3.14.

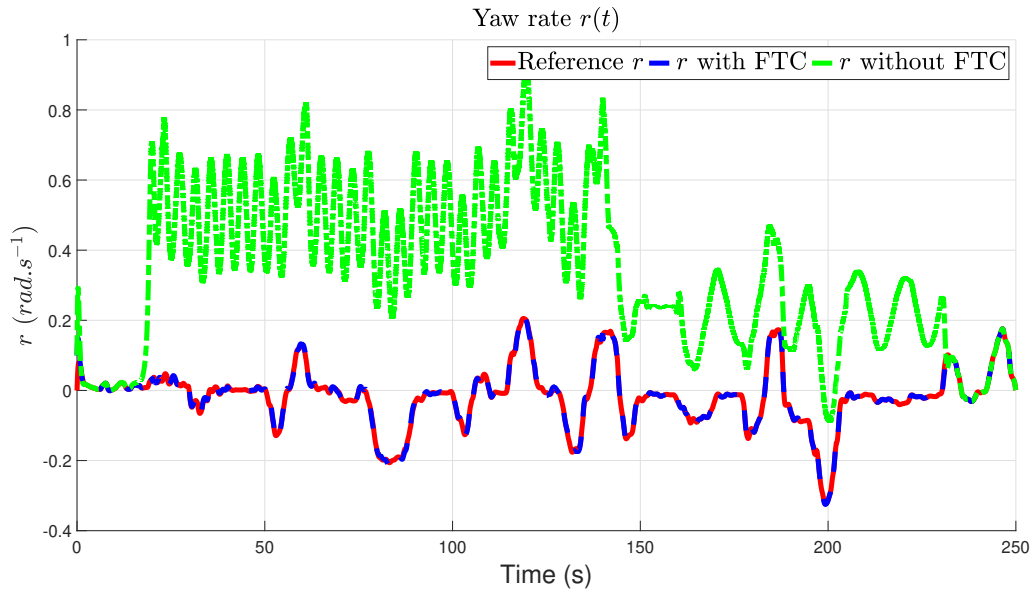

Figure 3.12: Comparison of yaw rate $r(t)$ between with and without FTC.

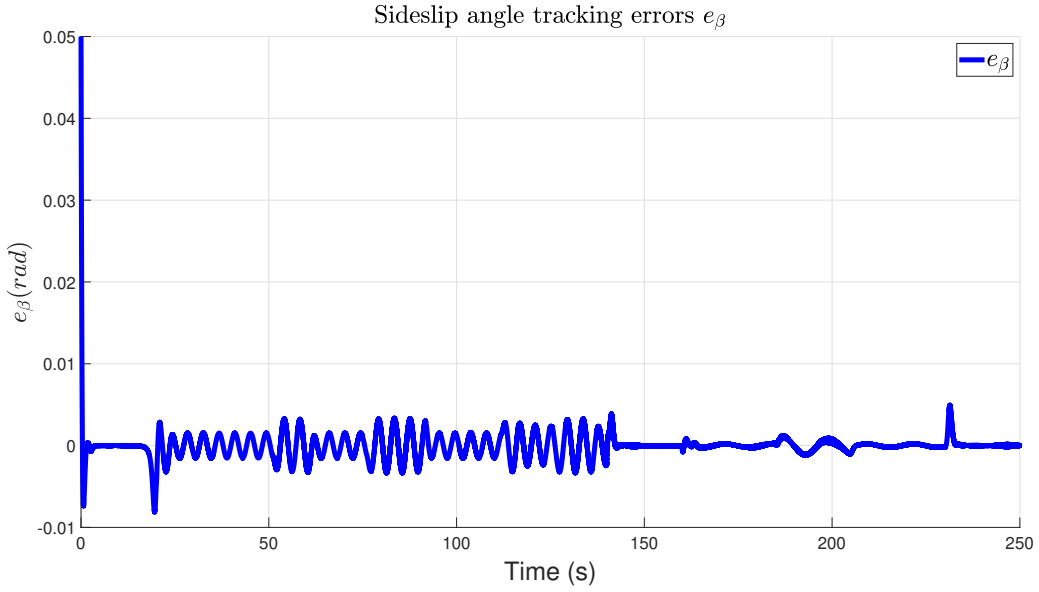

Figure 3.13: Sideslip angle tracking errors $e_\beta(t)$

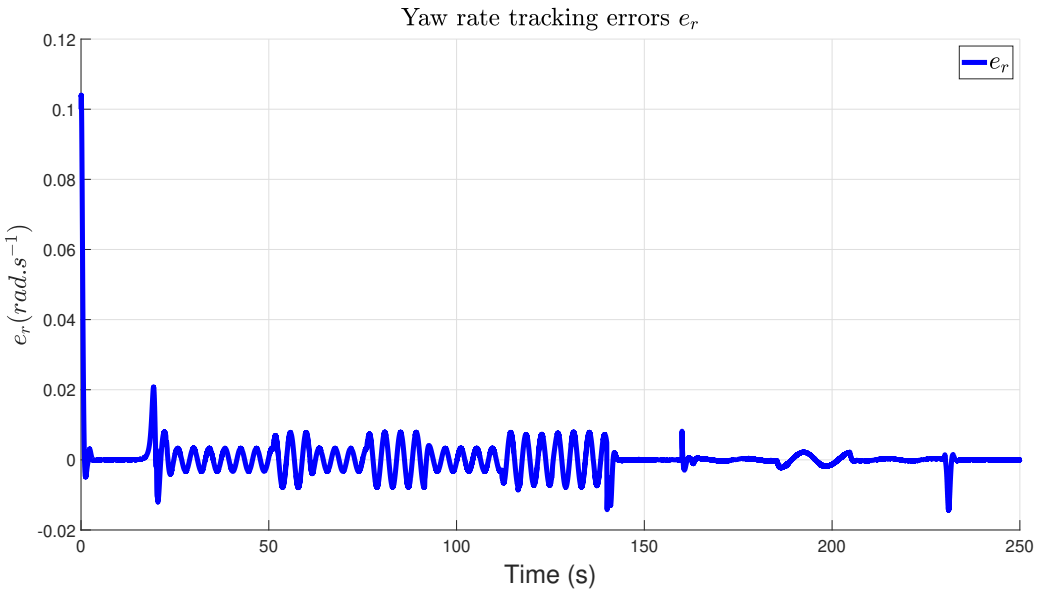

Figure 3.14: Yaw rate tracking errors $e_r(t)$

3.4.2 Double Lane Change Maneuver

A typical maneuver when considering vehicle handling improvement is the double-lane change maneuver. During a double lane change test, the driver exerts a front-wheel steering angle δ_f in order to react to an emergency situation such as obstacle avoidance. This maneuver excites the transient handling dynamics.

During the double lane change maneuver scenario, three subsystems are considered, each with different longitudinal velocities $v_x^1 = 5m/s$, $v_x^2 = 10m/s$, and $v_x^3 = 15m/s$. The switching signal $\sigma(t)$ is defined as follows:

$$\sigma(t) = \begin{cases} 1, & v_x \in [\ 2.5 \quad 7.5\ ](m/s) \\ 2, & v_x \in [\ 7.5 \quad 12.5\ ](m/s) \\ 3, & v_x \in [\ 12.5 \quad 17.5\ ](m/s) \end{cases} \tag{3.118}$$

The observer and controller gain matrices solved by a set of LMIs in Theorem 3.2 are obtained as follows:

$$\begin{aligned} N_1 &= \begin{bmatrix} -7.3651 & 2.7791 \\ 0 & -4.8009 \end{bmatrix}, Y_1 = \begin{bmatrix} -5.4104 \\ 2.9654 \end{bmatrix} \\ \underline{K}_1 &= \begin{bmatrix} 5436.2 & 2873.2 \end{bmatrix}, \overline{K}_1 = \begin{bmatrix} 5445.5 & 2876.8 \end{bmatrix} \end{aligned} \tag{3.119}$$

$$N_2 = \begin{bmatrix} -3.6825 & 1.2150 \\ 0 & -1.7132 \end{bmatrix}, Y_2 = \begin{bmatrix} -2.0707 \\ 1.7136 \end{bmatrix} \tag{3.120}$$
$$\underline{K}_2 = \begin{bmatrix} 3278.5 & 3316.9 \end{bmatrix}, \overline{K}_2 = \begin{bmatrix} 3278.6 & 3317 \end{bmatrix}$$

$$N_3 = \begin{bmatrix} -2.4550 & 0.1567 \\ 0 & -4.3194 \end{bmatrix}, Y_3 = \begin{bmatrix} -1.3091 \\ 1.7194 \end{bmatrix} \tag{3.121}$$
$$\underline{K}_3 = \begin{bmatrix} -13178 & 4827 \end{bmatrix}, \overline{K}_3 = \begin{bmatrix} -13178 & 4827 \end{bmatrix}$$

In this scenario, it is assumed that there is an obstacle on the road; the vehicle moved to the adjacent lane at $16.5sec$ and then moved back to the previous lane again at $21sec$. The corresponding front steering angle $\delta_f(t)$ and the speed longitudinal $v_x(t)$ profiles are depicted in Figure 3.15 and 3.16. For safety reasons, the driver has to manage the vehicle path in order to accomplish a successful double lane change maneuver so that the vehicle does not break the lane barrier at maximum forward speed while none of the tires lifts off the ground. During the maneuver, the vehicle is under a yaw moment fault signal depicted in Figure 3.17.

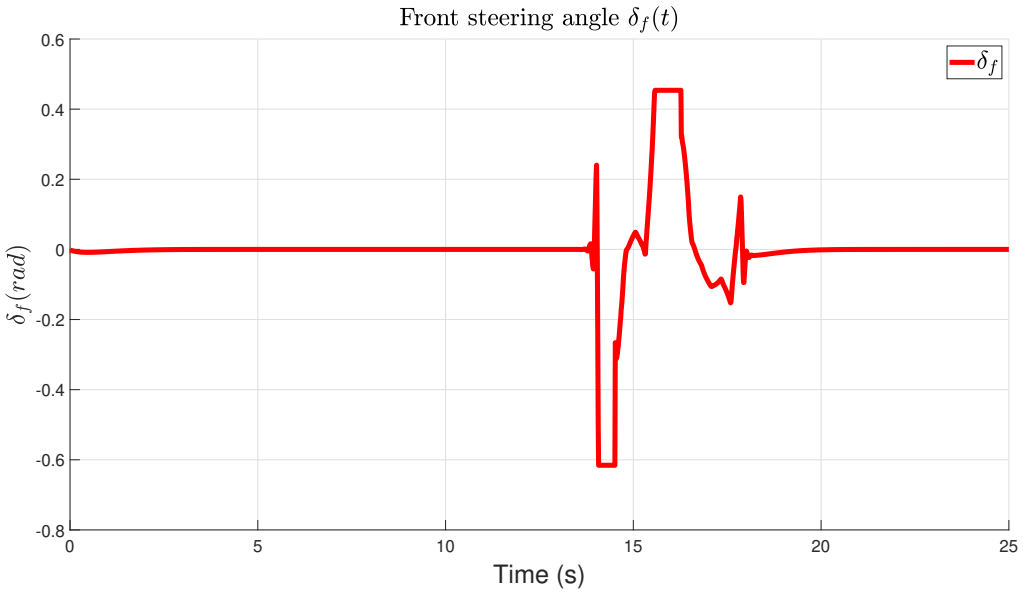

Figure 3.15: Front steering angle $\delta_f(t)$ profile.

As shown in Figure 3.17, it shows a good estimation of time-varying actuator fault. The estimated variable rapidly reaches the actual actuator fault.

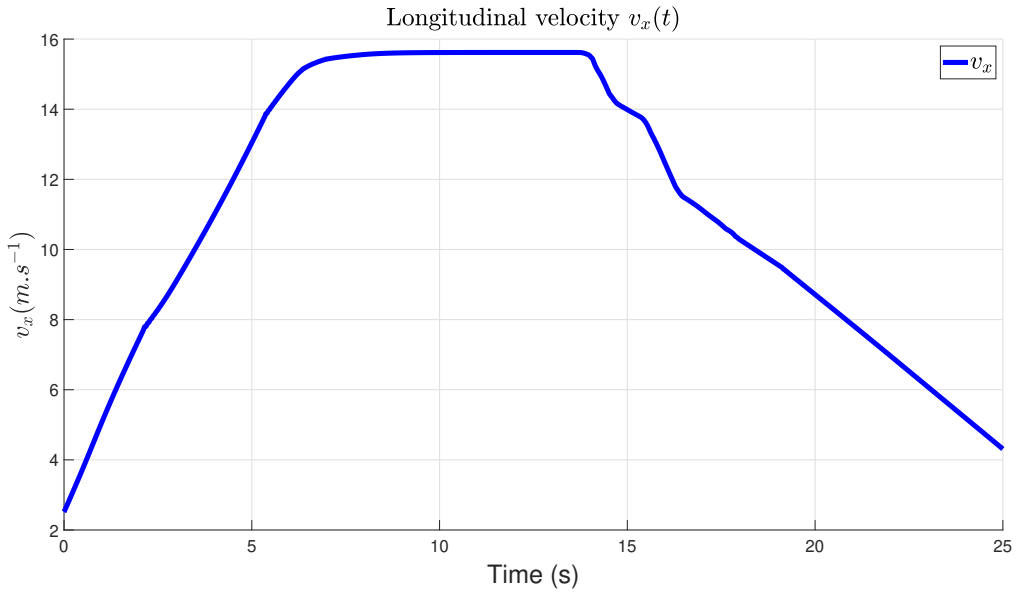

Figure 3.16: Longitudinal velocity $v_x(t)$ profile.

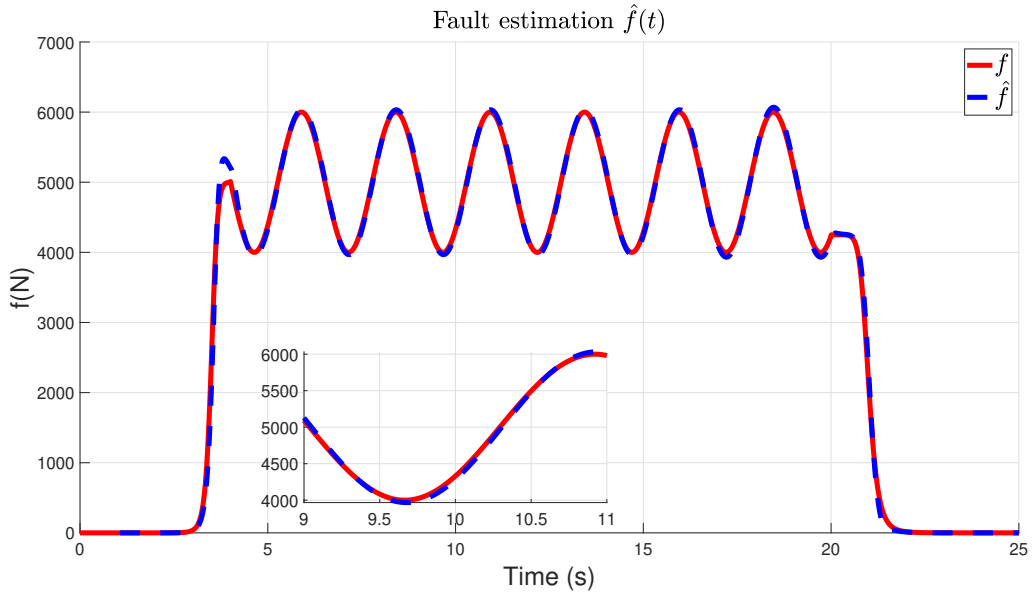

Figure 3.17: Actuator fault estimation $\hat{f}(t)$.

Figure 3.18 and 3.19 show the lower and upper state estimation of sideslip angle $\beta(t)$ and yaw rate $r(t)$. The actual trajectories of sideslip angle and yaw rate are consistently enclosed by these estimates despite the actuator fault occurrence. Moreover, the decoupling approach still eliminates the effect of faults from the state estimation errors.

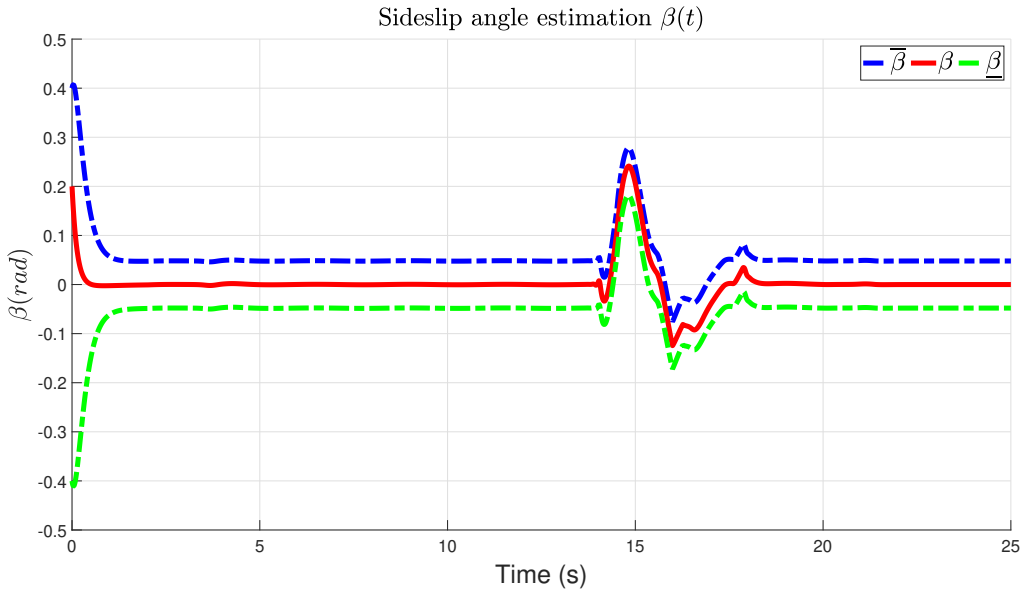

Figure 3.18: Sideslip angle $\beta(t)$ interval estimation.

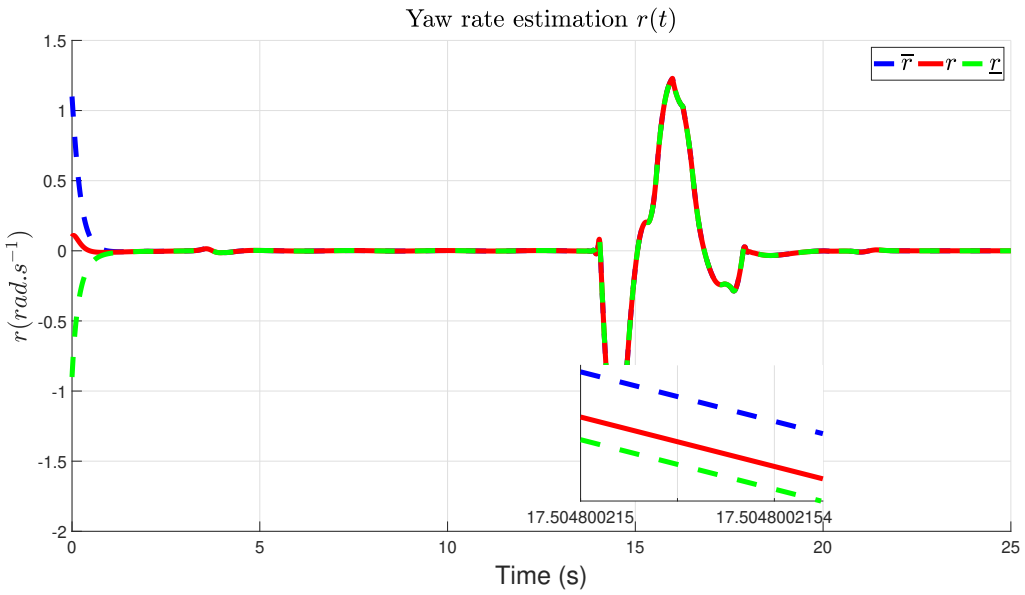

Figure 3.19: Yaw rate $r(t)$ interval estimation.

The fault-tolerant controller stabilizes the closed-loop system and preserves the performance level even when actuator faults occur. The actual sideslip angle $\beta(t)$ and yaw rate $r(t)$ state well track the reference vehicle lateral dynamics system as depicted in Figure 3.20 and 3.21 in which the dashed blue line and dashed green line are state vectors with and without the proposed method, respectively. It is evident that the uncontrolled vehicle is not able to perform the double lane change maneuver. The faulty system without the proposed method significantly deviates from the reference system. In contrast, the vehicle equipped with the proposed controller guarantees the tracking errors that are approximately zero as demonstrated in Figure 3.22 and 3.23.

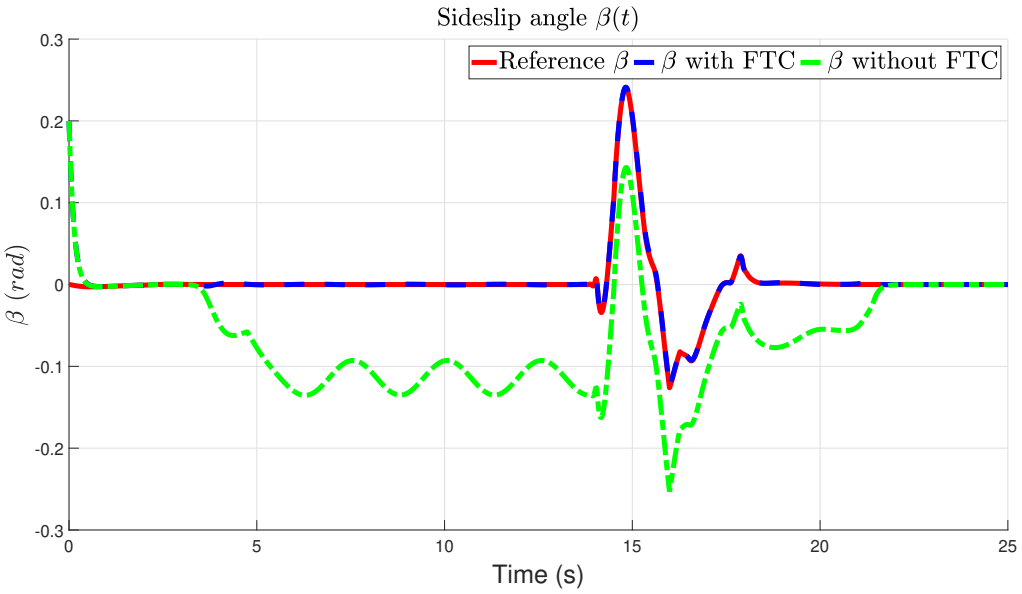

Figure 3.20: Comparison of sideslip angle $\beta(t)$ between with and without FTC.

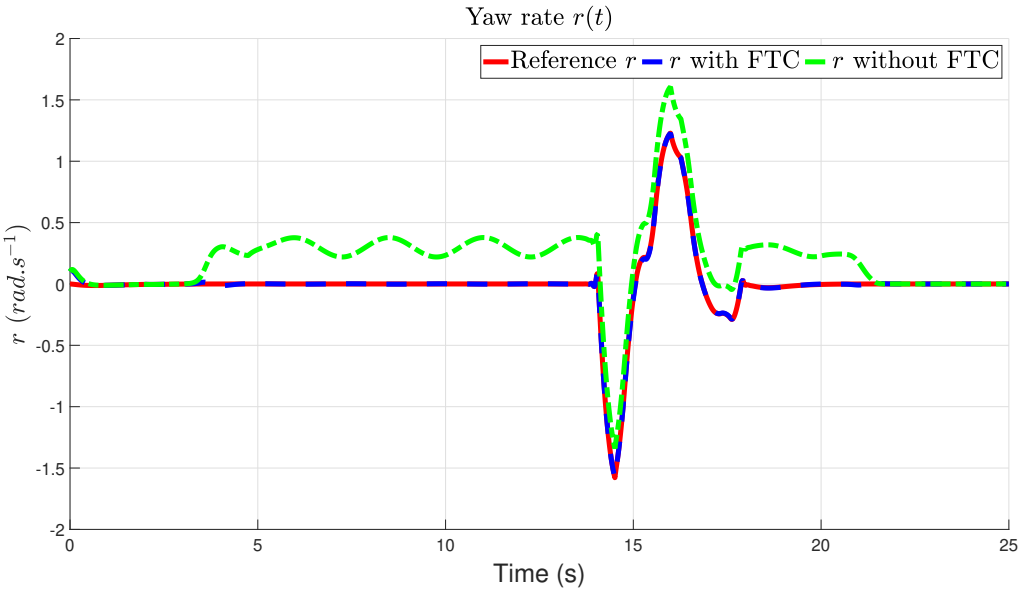

Figure 3.21: Comparison of yaw rate $r(t)$ between with and without FTC.

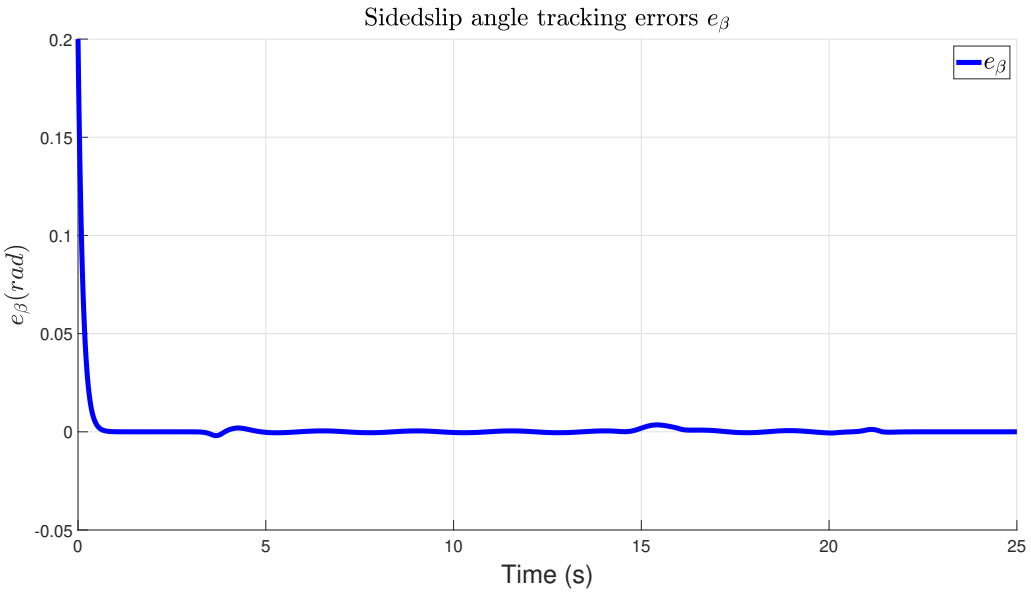

Figure 3.22: Sideslip angle tracking error $e_\beta(t)$.

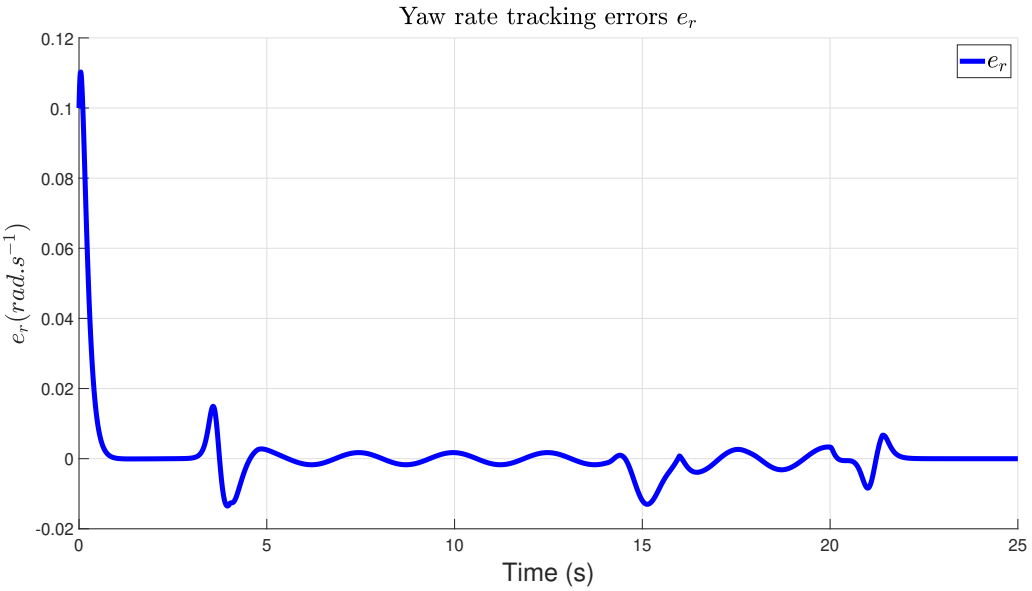

Figure 3.23: Yaw rate tracking error $e_r(t)$.

Furthermore, some comparisons between DPIO and the integrated design given by our approach and PIO and separation principle method in [2] are investigated.

From the analysis of Figure 3.24, Figure 3.25 and 3.26, it is evident that the proposed technique offers superior performance compared to the method investigated in [2]. These figures highlight the effectiveness and robustness of the proposed approach.

In particular, Figure 3.24 illustrates the superior capability of the proposed DPIO in effectively dealing with fast time-varying faults compared to the traditional PIO method discussed in [2]. This advantage is attributed to the

observer's coefficient λ_σ in (3.42) which allows DPIO to dynamically adapt its response to rapid changes in the fault signal. Unlike the conventional PIO approach, which may struggle to keep up with these fast transitions, the DPIO guarantees that it remains robust and effective even under adverse conditions.

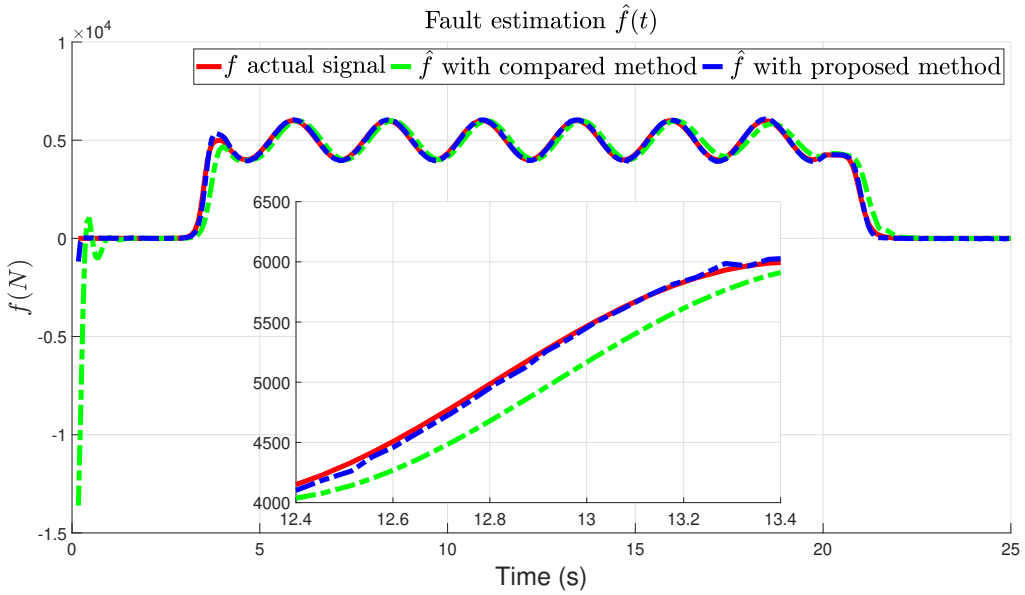

Figure 3.24: Comparison of actuator fault estimation $\hat{f}(t)$ between the proposed approach and method presented in [2].

Furthermore, Figure 3.25 and 3.26 illustrate a comparison of the state tracking performance between the integrated and separated design methods. Although both the proposed technique and the method from [2] deliver satisfactory state tracking results, it is obvious that the proposed methodology consistently outperforms the results in [2].

In other words, the results obtained using the separation principle approach in [2] presented by the dashed green line exhibit a noticeable deviation from the reference vehicle states. This deviation highlights the key limitations of the separation principle approach, where observers and controllers are designed independently. In contrast, the vehicle states generated by the proposed method, represented by the dashed blue line, are closer to the reference states depicted by solid red line. This improvement is due to taking the bi-directional interaction between observers and controllers into account during the design process.

3.5 Conclusions

The proposed approach contributes to vehicle dynamics enhancement under actuator faults. The approach provides a fault-tolerant tracking controller that compensates for the effects of actuator fault and ensures tracking of the reference model, which is critical for safe and efficient operations during cornering, lane keeping and lane change. The

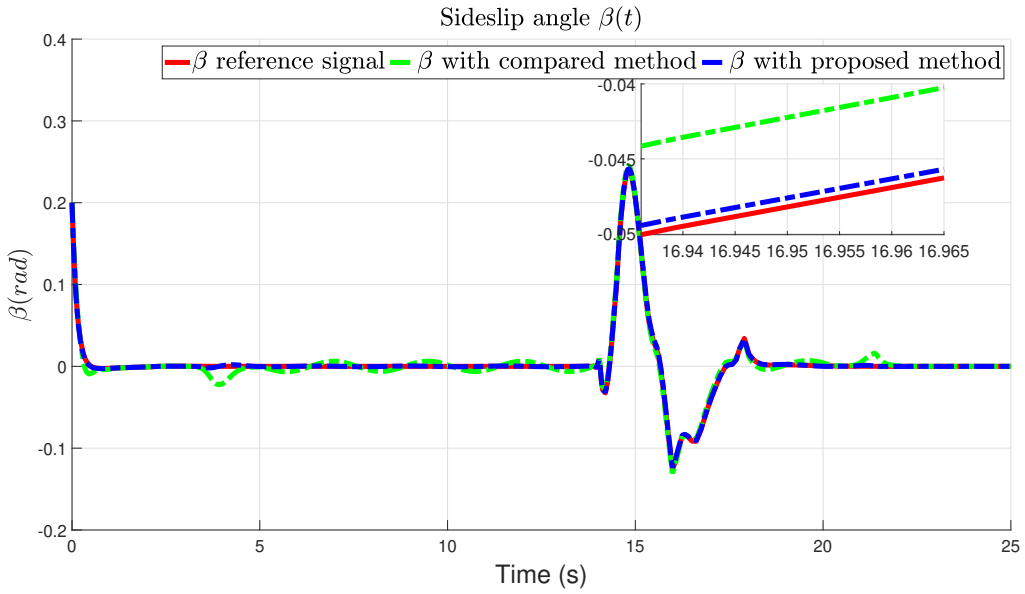

Figure 3.25: Sideslip angle $\beta(t)$ performance between the proposed co-design approach and separation principle design method discussed in [2].

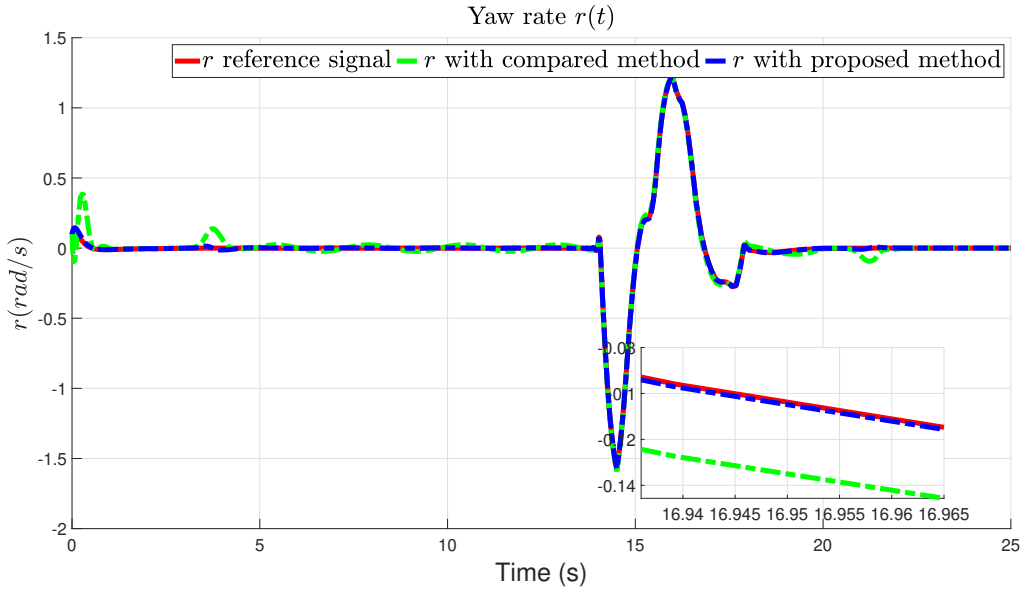

Figure 3.26: Yaw rate $r(t)$ performance between the proposed co-design approach and separation principle design method discussed in [2].

approach uses an SUIIO to estimate the lower and upper bounds of the vehicle's state vector without being affected by the effects of unknown input, which is helpful for accurate tracking. The approach uses multiple ISS Lyapunov functions and LMIs to determine the observer gain matrices, guaranteeing stability and positivity properties. This ensures the vehicle's stability and robustness during operation. Applying the proposed approach for different driving scenarios demonstrates its effectiveness in handling uncertainties and faults that may occur during the vehicle's operation.

Chapter 4

Simultaneous Interval State and Unknown Input Estimation and Fault-Tolerant Tracking Control For Uncertain Switched LPV Systems

Chapter abstract

This chapter investigates the problem of designing a fault-tolerant tracking control procedure for vehicle lateral dynamics. Vehicle dynamics are modeled as an uncertain switched linear parameter varying (LPV) system, subject to actuator faults and characterized by unknown yet bounded uncertainties. First, a switched unknown input interval observer (SUIIO) designed to estimate the lower and upper bounds of system states while remaining unaffected by unknown input disturbances. An algebraic unknown fault interval reconstruction is then established based on the relationship between the unknown input and the lower and upper estimation of the system states. Finally, a fault tolerant controller is developed to guarantee the reference performance in the presence of faults. To establish the viability of such observers and controllers. Sufficient Linear Matrix Inequalities (LMIs) conditions are formulated using Multiple Input-to-State-Stable (ISS) Lyapunov functions integrated with average dwell time (ADT). The efficiency of the proposed methodology is analyzed using Matlab-Simulink, providing a comprehensive assessment of the approach's practicality and applicability in the context of lateral vehicle dynamics estimation and control.

4.1 Introduction

4.1.1 State of the art

In the context of vehicle dynamics, fault estimation and control are important aspects since they can deal with the detection, isolation and correction of possible faults that may affect the performance and safety of the system. For example, unidentified actuator or sensor faults, component malfunctions or external disturbances may cause undesirable behaviors or even catastrophic failures. Therefore, it is essential to design robust and reliable approach that can estimate and compensate for such failures. This task is well known as Fault Tolerant Control (FTC) widely studied in the field of automotive engineering [73], [166].

The synthesis of observers for vehicles has been the subject of numerous studies over the past two decades. More specifically, the estimation of lateral speed or the sideslip angle represents a major challenge. In [167], nonlinear observers based on flatness have been suggested. Observers and controls based on sliding modes have been proposed in [168]. Extensions of Luenberger observers, such as the Proportional Integral observer, have been put forward in [169, 170]. The application of interval observers has been specifically addressed in [3].

Besides, state estimation in the presence of unknown inputs is one of the most crucial aspects of modern control theory and practical control applications. Beyond the case of the nominal model, a system in practice is subject to various uncertainties and exogenous inputs. This problem has been extensively developed over the past decades and motivated by synthesizing robust state estimates that remain insensitive to these uncertainties and disturbances. This leads to the challenge of developing effective unknown input observers (UIO). Several works have been conducted in the framework of UIO for LPV systems to extend linear UIO to LPV systems. The most common method is to transform the LPV system into a polytopic representation with parameter-dependent weighting function satisfying the convex sum property. For example, the work reported in [171] aims at proposing a solution to design functional UIO for nonlinear discrete-time systems under polytopic Takagi-Sugeno (TS) representations which are similar to polytopic LPV systems. Authors in [172], [173] designed UIO for TS fuzzy systems subject to unknown inputs which influence states and outputs simultaneously. In references [174], [175] an interesting approach taking the time derivative of parameter varying into consideration is proposed for the design of modified UIO for a class of LPV systems with parameter varying output matrix. The study in [176] addressed the problem of designing the LPV UIO which its structure can vary along with the change of parameters for polytopic LPV systems.

However, all the aforementioned works on the UIO for polytopic LPV systems are designed with perfect knowledge of parameter information and structure models. This may face some limitations for classical observer design, especially in the cases of LPV systems subject to modeling uncertainties and disturbances. This motivates to study a new robust estimation approach so-called interval observer to deal with a class of systems with uncertainties. A successful framework for interval UIO which can be applied to the problem of fault detection and isolation is proposed for uncertain continuous-time LPV in [157]. The results in [151] have introduced disturbance-decoupling

methods for discrete-time linear switched systems using unknown input interval observers (UIIO) to obtain a subsystem free from disturbance effects. The interval observer stability is guaranteed by Input-to-State-Stability (ISS) property using multiple Lyapunov functions under average dwell time (ADT).

Moreover, the major limitation of the above studies is that the authors only focused on the problem of the disturbance-decoupling approach and did not take the unknown input reconstruction problem into consideration. Therefore, several fruitful results on unknown input interval observers and unknown disturbance reconstruction for LPV systems have been recently studied. The works reported in [63] aim at deploying an interval observer to obtain the lower and upper bounds of system output using the coordinate transformation technique. A novelty algebraic UIO is then designed for linear systems to estimate the system state and reconstruct unknown input simultaneously based on the estimated output variables. Other researchers in [3] have investigated the problem of SUIIO and unknown disturbance interval reconstruction for switched linear systems in the presence of parameter uncertainties and unknown disturbances.

4.1.2 Chapter contributions

The main contribution of this chapter is listed as follows:

- Investigate the problem of the state estimation for uncertain switched LPV lateral vehicle dynamics which are represented by a switched polytopic model with unknown input. The SUIIO can estimate the vehicle states, such as the lateral velocity and the yaw rate while rejecting the unknown input effects. In contrast to the study in [63], the design allows to avoid resorting to the change of coordinates.

- Unlike the results in [63], this work presents a new approach to reconstructing both the lower and upper bounds of unknown disturbances using algebraic equations involving the interval observer estimates and UI.

- As an extension to work of [3, 63], an integrated design of the observers and fault tolerant control is developed, based on the estimated variables, to not only stabilize the closed-loop system but also to ensure the accurate tracking of the reference lateral vehicle dynamics even when the actuator faults occur.

To the best of the authors' knowledge, few works on Switched Unknown Input Interval Observer (SUIIO)-based fault tolerant control and unknown disturbance interval reconstruction for switched LPV systems with disturbances and unknown but bounded uncertainties have been studied in the literature.

With the proposed method, an SUIIO is first designed to estimate the lower and upper boundaries of the system state without being affected by unknown inputs. An unknown disturbance interval reconstruction is then investigated to reconstruct the lower and upper bounds of unknown inputs. Finally, a fault tolerant control is designed for the system in the presence of faults. Sufficient conditions for the stability of the interval observers and the closed-loop

system are expressed in terms of Linear Matrix Inequalities (LMIs) with multiple ISS Lyapunov functions under average dwell time.

This chapter is organized as follows: the vehicle lateral dynamics model is presented in Section 4.2. It takes the form of an LPV switched system which handles vehicle parameters variations and verifying some conditions. Section 4.3.1 and 4.3.2 are dedicated to the presentation of the proposed polytopic switched unknown input interval observers for state and fault estimation. Section 4.3.3 provides the fault-tolerant controller which ensures model reference tracking with fault effect compensation. The application of the proposed theoretical results to the lateral vehicle dynamics estimation is presented in Section 4.4 before the conclusions and recommendations for possible future works in Section 4.5.

4.2 Problem formulation

4.2.1 General case

Consider the following uncertain switched LPV systems:

$$\begin{cases} \dot{x}(t) = \Big(A_{\sigma(t)}\big(\rho(t),\xi(t)\big) + \Delta A_{\sigma(t)}\big(\rho(t),\xi(t)\big)\Big)x(t) + B_{\sigma(t)}\big(\rho(t),\xi(t)\big)u(t) + F_{\sigma(t)}\big(\rho(t),\xi(t)\big)f(t) \\ y(t) = Cx(t) \end{cases} \tag{4.1}$$

where $x(t) \in \mathbb{R}^{n_x}$, $u(t) \in \mathbb{R}^{n_u}$, $f(t) \in \mathbb{R}^{n_d}$, $y(t) \in \mathbb{R}^{n_y}$ are the state vector, control input, fault vector and measurement output respectively. The matrices $A_{\sigma(t)}\big(\rho(t),\xi(t)\big)$, $B_{\sigma(t)}\big(\rho(t),\xi(t)\big)$, $F_{\sigma(t)}\big(\rho(t),\xi(t)\big)$ are switching parameter varying matrices with proper dimension. Without loss of generality, the output matrix C is assumed to be constant. The switching signal is $\sigma(t) \in \mathcal{N} = \big\{1, 2, \ldots, N\big\}$ with N is the number of subsystems. The uncertain term $\Delta A_{\sigma(t)}\big(\rho(t),\xi(t)\big)$ is assumed to be expressed as $\Delta A_{\sigma(t)}\big(\rho(t),\xi(t)\big) = M_{a,\sigma(t)}\Delta(t)N_a$ with $M_{a,\sigma(t)}$ and N_a are known constant matrices with compatible dimension while Δ satisfies the inequality $\Delta^T(t)\Delta(t) \leq I$.

Parameters $\rho(t) \in \mathbb{R}^{n_\rho}$ and $\xi(t) \in \Xi$ represent measured and unmeasured scheduling parameters with known set Ξ. Since the parameter vector $\xi(t)$ is not available to measure in real-time, the nominal value ξ_0 that is assumed to be known a prior is only used. Time-varying parameters $\rho(t) = \big\{\rho_1(t), \rho_2(t), ..., \rho_{n_\rho}(t)\big\}$ represent n_ρ parameter vectors and $\rho_k(t) \in \big[\underline{\rho}_k, \overline{\rho}_k\big]$ for all $k = 1, ..., n_\rho$ with $\underline{\rho}_k$ and $\overline{\rho}_k$ are the lower and upper bounds of $\rho_k(t)$ then it evolves inside a polytope represented by 2^{n_ρ} vertices.

The polytopic representation involves switched weighting functions $\mu_{\sigma(t)}(\rho(t))$ verifying the convex sum property for all $\sigma(t) \in \mathcal{N}$ and $j \in \mathcal{P} = \{1, \cdots, 2^{n_\rho}\}$

$$\begin{cases} 0 \leq \mu^j_{\sigma(t)}(\rho(t)) \leq 1 \\ \displaystyle\sum_{j=1}^{2^{n_\rho}} \mu^j_{\sigma(t)}(\rho(t)) = 1 \end{cases} \tag{4.2}$$

The matrices of the system (4.11) are transformed into polytopic forms with respect to the parameters and are given by:

$$M_{\sigma(t)}\left(\rho(t),\xi_0\right)=\sum_{j=1}^{2^{n_\rho}}\mu^j_{\sigma(t)}(\rho(t))M^j_{\sigma(t)} \tag{4.3}$$

with $M\in\{A,B,\Delta A,F\}$ and $M^j_{\sigma(t)}$ are known constant matrices for all $\sigma(t)\in\mathcal{N}$, $j\in\mathcal{P}$.

Based on (4.2) and (4.3), the uncertain switched LPV system (4.1) can be then expressed exactly in polytopic representation as follows:

$$\begin{cases}\dot{x}(t)=\displaystyle\sum_{j=1}^{2^{n_\rho}}\mu^j_{\sigma(t)}(\rho(t))\Big(\Big(A^j_{\sigma(t)}+\Delta A^j_{\sigma(t)}\Big)x(t)+B^j_{\sigma(t)}u(t)+F^j_{\sigma(t)}f(t)\Big)\\ y(t)=Cx(t)\end{cases} \tag{4.4}$$

4.2.2 Case study: Switched LPV vehicle lateral dynamics model

This subsection provides a concise overview of the fundamental concepts and methods for modeling the lateral behavior of vehicles. The system is based on a bicycle vehicle model, which describes the lateral and yaw motions [164]. The differential equations below can be used to describe the two-dimensional model characterizing the vehicle's lateral model:

$$\begin{cases}m\dot{v}_y+mv_xr=F_{yf}+F_{yr}\\ I_z\dot{r}=l_fF_{yf}-l_rF_{yr}+M_z\end{cases} \tag{4.5}$$

where m, I_z are the mass and the yaw moment, $v_x(t)$ and $v_y(t)$ are lateral and longitudinal velocities, $r(t)$ is the yaw rate, l_f and l_r are distances from the front and rear axles to COG, while F_{yf} and F_{yr} are the lateral forces of front and rear tires and $M_z(t)$ is corrective yaw moment to handle the system performance. For normal driving situation, the lateral forces F_{yf} and F_{yr} can be formed as:

$$\begin{cases}F_{yf}=c_f\alpha_f\\ F_{yr}=c_r\alpha_r\end{cases} \tag{4.6}$$

where c_f, c_r are the cornering stiffness of front and rear tires. And the front and rear wheel slip angles are defined as:

$$\begin{cases}\alpha_f=\delta_f-\dfrac{v_y}{v_x}-\dfrac{l_f}{v_x}r\\ \alpha_r=-\dfrac{v_y}{v_x}+\dfrac{l_r}{v_x}r\end{cases} \tag{4.7}$$

In the proposed model, we assume that the available measurements are longitudinal velocity $v_x(t)$, yaw rate $r(t)$, and front steering angle $\delta_f(t)$. Gathering equations (4.5), (4.6), (4.7) and chosen $v_y(t)$ and $r(t)$ as state variables,

leads to the following LPV system:

$$\begin{cases} \dot{x}(t) = A\big(\rho(t), \xi(t)\big)x(t) + Bu(t) + D(\xi(t))\delta_f(t) \\ y(t) = Cx(t) \end{cases} \tag{4.8}$$

where $x(t) = \begin{bmatrix} v_y(t) \\ r(t) \end{bmatrix}$ is state vector, $u(t) = M_z(t)$ is corrective yaw moment control input, $y(t) = r(t)$ is measurement output, $\delta_f(t)$ is front steering angle and the system matrices $A(\rho(t), \xi(t)) = \begin{bmatrix} -\frac{c_f + c_r}{m v_x} & \frac{c_r L_r - c_f l_f}{m v_x} - v_x \\ \frac{c_r l_r - c_f l_f}{I_z v_x} & -\frac{c_r l_r^2 + c_f l_f^2}{I_z v_x} \end{bmatrix}$, $B = \begin{bmatrix} 0 \\ \frac{1}{I_z} \end{bmatrix}$, $C = \begin{bmatrix} 0 & 1 \end{bmatrix}$, $D(\xi(t)) = \begin{bmatrix} \frac{c_f}{m} \\ \frac{c_f l_f}{I_z} \end{bmatrix}$. The time-varying parameters $\rho(t)$ and $\xi(t)$ represent measurable and unmeasurable scheduling parameters.

Time-varying parameters $\rho(t) = \big\{\rho_1(t), \rho_2(t)\big\} = \Big[v_x, \frac{1}{v_x}\Big]$ represent 2 parameter vectors and $\rho_k(t) \in \big[\underline{\rho}_k, \overline{\rho}_k\big]$ for all $k = 1, ..., 2$ with $\underline{\rho}_k$ and $\overline{\rho}_k$ are the lower and upper bounds of $\rho_k(t)$ then it evolves inside a polytope represented by 2^2 vertices. A single observation or controller, however, may not be sufficient to achieve optimal performance when the time-varying parameter $\rho(t)$ varies over a large range. Therefore, it is necessary to consider multiple observations or controllers that can adapt to different values of $\rho(t)$. One possible way to deal with the infeasibility problem caused by a large variation range of parameter $\rho(t)$ is to apply the switched system approach. This method divides the parameter $\rho(t)$ domain into smaller sub-regions.

Note that, when lateral acceleration becomes high, the tire forces are no longer linear with respect to the wheel slip angles due to the tire saturation property. Accordingly, the cornering stiffness parameters c_f and c_r used in the linear tire model (4.6) will vary when the road friction changes or when the nonlinear tire domain is reached. To deal with these variations, the following linear adaptive tire model is used to correct the cornering stiffness values via the uncertain variables Δc_f and Δc_r as:

$$\begin{cases} F_{yf} = (c_{f_0} + \Delta c_f)\, \alpha_f \\ F_{yr} = (c_{r_0} + \Delta c_r)\, \alpha_r \end{cases} \tag{4.9}$$

The cornering stiffness:

$$\begin{cases} c_f = c_{f_0} + \Delta c_f \\ c_r = c_{r_0} + \Delta c_r \end{cases} \tag{4.10}$$

where the linear part denoted by $\xi_0 = \Big[c_{f_0}, \quad c_{r_0}\Big]$ presents a known nominal value and the uncertainty term denoted by $\Delta\xi(t) = \begin{bmatrix} \Delta c_f, & \Delta c_r \end{bmatrix}$ is assumed to be unknown but bounded with priori known bounds.

Consequently, the lateral vehicle dynamics can be represented by an uncertain switched LPV model with actuator

faults as follows:

$$\begin{cases} \dot{x}(t) = A_{\sigma(t)}\big(\rho(t),\xi_0\big)x(t) + B_{\sigma(t)}u(t) + D_{\sigma(t)}\big(\xi_0\big)\delta_f(t) + F_{\sigma(t)}f(t) \\ \qquad\quad + \Delta A_{\sigma(t)}\big(\rho(t),\Delta\xi(t)\big)x(t) + \Delta D_{\sigma(t)}\big(\Delta\xi(t)\big)\delta_f(t) \\ y(t) = Cx(t) \end{cases} \tag{4.11}$$

where $f(t)$ is fault vector and the switching signal is $\sigma(t) \in \mathcal{N} = \{1, 2, \ldots, N\}$ with N is the number of subsystems. The uncertain terms $\Delta A_{\sigma(t)}\big(\rho(t),\Delta\xi(t)\big)$ and $\Delta D_{\sigma(t)}(\Delta\xi(t))$ are assumed to be bounded with priori known bound $\underline{\Delta A}_{\sigma(t)}, \overline{\Delta A}_{\sigma(t)}$ and $\underline{\Delta D}_{\sigma(t)}, \overline{\Delta D}_{\sigma(t)}$ respectively.

$$\begin{aligned} \underline{\Delta A}_{\sigma(t)} \leq \Delta A_{\sigma(t)}\big(\rho(t),\Delta\xi(t)\big) \leq \overline{\Delta A}_{\sigma(t)} \\ \underline{\Delta D}_{\sigma(t)} \leq \Delta D_{\sigma(t)}(\Delta\xi(t)) \leq \overline{\Delta D}_{\sigma(t)} \end{aligned} \tag{4.12}$$

The term $\Delta A_{\sigma(t)}\big(\rho(t),\Delta\xi(t)\big)$ can be expressed by following structure:

$$\Delta A_{\sigma(t)}\big(\rho(t),\Delta\xi(t)\big) = M_{\sigma(t)}\Delta(t)N_a \tag{4.13}$$

with $M_{\sigma(t)}$ and N_a are known constant matrices with compatible dimensions where $M_{\sigma(t)}$ denotes the maximum percentage of the state matrices variation and N_a represents the nominal values while $\Delta(t)$ satisfies the inequality $\Delta^T(t)\Delta(t) \leq I$.

The front steering control input $\delta_f(t)$ and initial conditions of lateral velocity $v_y(t_0)$ and yaw rate $r(t_0)$ are also assumed to be bounded by priori known bounds.

$$\begin{aligned} \underline{x}(t_0) \leq x(t_0) \leq \overline{x}(t_0) \\ \underline{\delta}_f \leq \delta_f(t) \leq \overline{\delta}_f \end{aligned} \tag{4.14}$$

Moreover, the following rank condition holds for all $\sigma(t) \in \mathcal{N}$.

$$rank\left(CF_{\sigma(t)}\right) = rank\left(F_{\sigma(t)}\right) \tag{4.15}$$

4.3 Main results

In this section, the objective is to design interval observers in order to estimate the lower trajectory $\underline{x}(t)$ and the upper one $\overline{x}(t)$ of the real state $x(t)$ and reconstruct the lower and upper bounds of the unknown disturbances.

4.3.1 Switched unknown input interval observer

In this subsection, a polytopic switched unknown input interval observer is proposed to estimate the boundaries of the real state vector without being affected by the unknown disturbance input.

The following SUIIO structure is proposed for system (4.11).

$$\begin{cases} \dot{\overline{\xi}}(t) = \overline{N}_{\sigma(t)}(\rho(t))\overline{\xi}(t) + \overline{J}_{\sigma(t)}(\rho(t))y(t) + \overline{H}_{\sigma(t)}u(t) + \overline{Q}_{\sigma(t)}\delta_f(t) + \overline{\Omega}_{\sigma(t)}(t) \\ \overline{x}(t) = \overline{\xi}(t) + \overline{E}_{\sigma(t)}y(t) \\ \dot{\underline{\xi}}(t) = \underline{N}_{\sigma(t)}(\rho(t))\underline{\xi}(t) + \underline{J}_{\sigma(t)}(\rho(t)(t))y(t) + \underline{H}_{\sigma(t)}u(t) + \underline{Q}_{\sigma(t)}\delta_f(t) + \underline{\Omega}_{\sigma(t)}(t) \\ \underline{x}(t) = \underline{\xi}(t) + \underline{E}_{\sigma(t)}y(t) \end{cases} \tag{4.16}$$

where $\underline{\xi}(t), \overline{\xi}(t)$ are the lower and upper of the observer state vectors and $\underline{x}(t), \overline{x}(t)$ are the lower and upper estimates of system states x. Matrices $\underline{N}_{\sigma(t)}(\rho(t)), \overline{N}_{\sigma(t)}(\rho(t)) \in \mathbb{R}^{n_x \times n_x}$, $\underline{J}_{\sigma(t)}(\rho(t)), \overline{J}_{\sigma(t)}(\rho(t)) \in \mathbb{R}^{n_x \times n_y}$ are switching parameter varying matrices of proper dimensions which must be designed in order to ensure the stability of the interval observer and to decouple the unknown input effects. Matrices $\underline{H}_{\sigma(t)}, \overline{H}_{\sigma(t)} \in \mathbb{R}^{n_x \times n_u}$, $\underline{E}_{\sigma(t)}, \overline{E}_{\sigma(t)} \in \mathbb{R}^{n_x \times n_y}$ and $\underline{Q}_{\sigma(t)}, \overline{Q}_{\sigma(t)} \in \mathbb{R}^{n_x \times n_{u_\delta}}$ are constant switching matrices.
By setting $\underline{T}_{\sigma(t)} = I_{n_x} - \underline{E}_{\sigma(t)}C$ and $\overline{T}_{\sigma(t)} = I_{n_x} - \overline{E}_{\sigma(t)}C$, the terms $\overline{\Omega}_{\sigma(t)}(t)$ and $\underline{\Omega}_{\sigma(t)}(t)$ are chosen as:

$$\begin{cases} \overline{\Omega}_{\sigma(t)}(t) = \overline{T}^{+}_{\sigma(t)}\overline{\nabla}_{\sigma(t)}(t) - \overline{T}^{-}_{\sigma(t)}\underline{\nabla}_{\sigma(t)}(t) \\ \underline{\Omega}_{\sigma(t)}(t) = \underline{T}^{+}_{\sigma(t)}\underline{\nabla}_{\sigma(t)}(t) - \underline{T}^{-}_{\sigma(t)}\overline{\nabla}_{\sigma(t)}(t) \end{cases} \tag{4.17}$$

with the lower and upper bounds $\underline{\nabla}_{\sigma(t)}(t)$ and $\overline{\nabla}_{\sigma(t)}(t)$ defined using lemma 2.8 such that $\underline{\nabla}_{\sigma(t)}(t) \leq \nabla_{\sigma(t)}(t) = \Delta A_{\sigma(t)}\big(\rho(t), \Delta\xi(t)\big)x(t) + \Delta D_{\sigma(t)}\big(\Delta\xi(t)\big)\delta_f(t) \leq \overline{\nabla}_{\sigma(t)}(t)$ are expressed as:

$$\begin{cases} \overline{\nabla}_{\sigma(t)}(t) = \overline{\Delta A}^{+}_{\sigma(t)}\overline{x}^{+}(t) - \underline{\Delta A}^{+}_{\sigma(t)}\overline{x}^{-}(t) - \overline{\Delta A}^{-}_{\sigma(t)}\underline{x}^{+}(t) + \underline{\Delta A}^{-}_{\sigma(t)}\underline{x}^{-}(t) \\ \qquad\qquad + \overline{\Delta D}^{+}_{\sigma(t)}\overline{\delta}^{+}_{f} - \underline{\Delta D}^{+}_{\sigma(t)}\overline{\delta}^{-}_{f} - \overline{\Delta D}^{-}_{\sigma(t)}\underline{\delta}^{+}_{f} + \underline{\Delta D}^{-}_{\sigma(t)}\underline{\delta}^{-}_{f} \\ \underline{\nabla}_{\sigma(t)}(t) = \underline{\Delta A}^{+}_{\sigma(t)}\underline{x}^{+}(t) - \overline{\Delta A}^{+}_{\sigma(t)}\underline{x}^{-}(t) - \underline{\Delta A}^{-}_{\sigma(t)}\overline{x}^{+}(t) + \overline{\Delta A}^{-}_{\sigma(t)}\overline{x}^{-}(t) \\ \qquad\qquad + \underline{\Delta D}^{+}_{\sigma(t)}\underline{\delta}^{+}_{f} - \overline{\Delta D}^{+}_{\sigma(t)}\underline{\delta}^{-}_{f} - \underline{\Delta D}^{-}_{\sigma(t)}\overline{\delta}^{+}_{f} + \overline{\Delta D}^{-}_{\sigma(t)}\overline{\delta}^{-}_{f} \end{cases} \tag{4.18}$$

Let's define the lower and upper state estimation errors as follows:

$$\begin{cases} \underline{e}(t) = x(t) - \underline{x}(t) \\ \overline{e}(t) = \overline{x}(t) - x(t) \end{cases} \tag{4.19}$$

With the system (4.11) and the interval observer (4.16), the state estimation errors are then governed by:

$$\begin{cases} \overline{e}(t) = \overline{\xi}(t) - \overline{T}_{\sigma(t)}x(t) \\ \underline{e}(t) = \underline{T}_{\sigma(t)}x(t) - \underline{\xi}(t) \end{cases} \tag{4.20}$$

After computations with equations (4.11), (4.16) and (4.20), their dynamics are given by:

$$\begin{cases} \dot{\overline{e}}(t) = \overline{N}_{\sigma(t)}(\rho(t))\overline{e}(t) + \Big(\overline{N}_{\sigma(t)}(\rho(t))\overline{T}_{\sigma(t)} + \overline{J}_{\sigma(t)}(\rho(t))C - \overline{T}_{\sigma(t)}A_{\sigma(t)}(\rho(t))\Big)x(t) - \overline{T}_{\sigma(t)}F_{\sigma(t)}f(t) \\ \qquad + \Big(\overline{H}_{\sigma(t)} - \overline{T}_{\sigma(t)}B_{\sigma(t)}\Big)u(t) + \Big(\overline{Q}_{\sigma(t)} - \overline{T}_{\sigma(t)}D_{\sigma(t)}\Big)\delta_f(t) + \overline{\Omega}_{\sigma(t)}(t) - \overline{T}_{\sigma(t)}\nabla_{\sigma(t)}(t) \\ \dot{\underline{e}}(t) = \underline{N}_{\sigma(t)}(\rho(t))\underline{e}(t) + \Big(\underline{T}_{\sigma(t)}A_{\sigma(t)}(\rho(t)) - \underline{N}_{\sigma(t)}(\rho(t))\underline{T}_{\sigma(t)} - \underline{J}_{\sigma(t)}(\rho(t))C\Big)x(t) + \underline{T}_{\sigma(t)}F_{\sigma(t)}f(t) \\ \qquad + \Big(\underline{T}_{\sigma(t)}B_{\sigma(t)} - \underline{H}_{\sigma(t)}\Big)u(t) + \Big(\underline{T}_{\sigma(t)}D_{\sigma(t)} - \underline{Q}_{\sigma(t)}\Big)\delta_f(t) + \underline{T}_{\sigma(t)}\nabla_{\sigma(t)}(t) - \underline{\Omega}_{\sigma(t)}(t) \end{cases} \tag{4.21}$$

Based on the convex sum property of weighting function (4.2) and (4.3), the estimation error dynamics (4.21) can be then expressed exactly in polytopic representation as follows:

$$\begin{cases} \dot{\overline{e}}(t) = \sum_{j=1}^{4}\mu^j_{\sigma(t)}(\rho(t))\Big(\overline{N}^j_{\sigma(t)}\overline{e}(t) + \Big(\overline{N}^j_{\sigma(t)}\overline{T}_{\sigma(t)} + \overline{J}^j_{\sigma(t)}C - \overline{T}_{\sigma(t)}A^j_{\sigma(t)}\Big)x(t) - \overline{T}_{\sigma(t)}F_{\sigma(t)}f(t) \\ \qquad + \Big(\overline{H}_{\sigma(t)} - \overline{T}_{\sigma(t)}B_{\sigma(t)}\Big)u(t) + \Big(\overline{Q}_{\sigma(t)} - \overline{T}_{\sigma(t)}D_{\sigma(t)}\Big)\delta_f(t) + \overline{\Omega}^j_{\sigma(t)}(t) - \overline{T}_{\sigma(t)}\nabla^j_{\sigma(t)}(t)\Big) \\ \dot{\underline{e}}(t) = \sum_{j=1}^{4}\mu^j_{\sigma(t)}(\rho(t))\Big(\underline{N}^j_{\sigma(t)}\underline{e}(t) + \Big(\underline{T}_{\sigma(t)}A^j_{\sigma(t)} - \underline{N}^j_{\sigma(t)}\underline{T}_{\sigma(t)} - \underline{J}^j_{\sigma(t)}C\Big)x(t) + \underline{T}_{\sigma(t)}F_{\sigma(t)}f(t) \\ \qquad + \Big(\underline{T}_{\sigma(t)}B_{\sigma(t)} - \underline{H}_{\sigma(t)}\Big)u(t) + \Big(\underline{T}_{\sigma(t)}D_{\sigma(t)} - \underline{Q}_{\sigma(t)}\Big)\delta_f(t) + \underline{T}_{\sigma(t)}\nabla^j_{\sigma(t)}(t) - \underline{\Omega}^j_{\sigma(t)}(t)\Big) \end{cases} \tag{4.22}$$

In order $\underline{e}(t)$ and $\overline{e}(t)$ converge to zero, $\underline{N}^j_{\sigma(t)}$ and $\overline{N}^j_{\sigma(t)}$ should be Hurwitz and make the following formulas hold for all $\sigma(t) \in \mathcal{N}$, $j \in \mathcal{P}$:

$$\overline{N}^j_{\sigma(t)}\overline{T}_{\sigma(t)} + \overline{J}^j_{\sigma(t)}C = \overline{T}_{\sigma(t)}A^j_{\sigma(t)}, \quad \underline{N}^j_{\sigma(t)}\underline{T}_{\sigma(t)} + \underline{J}^j_{\sigma(t)}C = \underline{T}_{\sigma(t)}A^j_{\sigma(t)} \tag{4.23}$$

$$\overline{H}_{\sigma(t)} - \overline{T}_{\sigma(t)}B_{\sigma(t)} = 0, \quad \underline{H}_{\sigma(t)} - \underline{T}_{\sigma(t)}B_{\sigma(t)} = 0 \tag{4.24}$$

$$\overline{Q}_{\sigma(t)} - \overline{T}_{\sigma(t)}D_{\sigma(t)} = 0, \quad \underline{Q}_{\sigma(t)} - \underline{T}_{\sigma(t)}D_{\sigma(t)} = 0 \tag{4.25}$$

$$\overline{T}_{\sigma(t)}F_{\sigma(t)} = 0, \quad \underline{T}_{\sigma(t)}F_{\sigma(t)} = 0 \tag{4.26}$$

The estimation errors (4.21) are then simplified to:

$$\begin{cases} \dot{\overline{e}}(t) = \sum_{j=1}^{4} \mu^j_{\sigma(t)}(\rho(t)) \Big(\overline{N}^j_{\sigma(t)} \overline{e}(t) + \overline{\Omega}^j_{\sigma(t)}(t) - \overline{T}_{\sigma(t)} \nabla^j_{\sigma(t)}(t) \Big) \\ \dot{\underline{e}}(t) = \sum_{j=1}^{4} \mu^j_{\sigma(t)}(\rho(t)) \Big(\underline{N}^j_{\sigma(t)} \underline{e}(t) + \underline{T}_{\sigma(t)} \nabla^j_{\sigma(t)}(t) - \underline{\Omega}^j_{\sigma(t)}(t) \Big) \end{cases} \tag{4.27}$$

With the estimation errors in (4.27), the following theorem is presented.

Theorem 4.1 *For system* (4.11)*, the estimations* $\underline{x}(t)$ *and* $\overline{x}(t)$ *of the SUIIO* (4.16) *satisfy* $\underline{x}(t) \leq x(t) \leq \overline{x}(t)$ *provided that* $\overline{N}^j_{\sigma(t)}$ *and* $\underline{N}^j_{\sigma(t)}$ *are Metzler matrices* $\forall \sigma(t) \in \mathcal{N}, j \in \mathcal{P}$ *and the initial state conditions are chosen such that* $x(t_0)$ *is bounded by two known vectors, i.e.* $\underline{x}(t_0) \leq x(t_0) \leq \overline{x}(t_0)$.

Proof 4.1 *(Theorem 4.1)*

From equation (4.17) *and lemma 2.8, it is obvious that the following terms are positive:*

$$\begin{cases} \overline{\Omega}^j_{\sigma(t)} - \overline{T}_{\sigma(t)} \nabla^j_{\sigma(t)} \geq 0 \\ \underline{T}_{\sigma(t)} \nabla^j_{\sigma(t)} - \underline{\Omega}^j_{\sigma(t)} \geq 0 \end{cases} \tag{4.28}$$

By selection the bounds of $x(t_0)$*, the lower and upper initial estimation error conditions* $\overline{e}(t_0) = \overline{x}(t_0) - x(t_0)$ *and* $\underline{e}(t_0) = x(t_0) - \underline{x}(t_0)$ *are positive. Then based on lemma 2.6, this means that* $\overline{e}(t) \geq 0$ *and* $\underline{e}(t) \geq 0$ *if* $\overline{N}^j_{\sigma(t)}$ *and* $\underline{N}^j_{\sigma(t)}$ *are Metzler matrix* $\forall \sigma(t) \in \mathcal{N}$*,* $\forall j \in \mathcal{P}$*. Hence, it ensures that the state* $x(t)$ *is bounded by* $\underline{x}(t)$ *and* $\overline{x}(t)$ *for all* $t \geq t_0$*, i.e.* $\underline{x}(t) \leq x(t) \leq \overline{x}(t)$

We will now present a procedure for determining the parameters of the SUIIO before analyzing the stability of the interval observer.

From the relations (4.26) and matrices $\overline{T}_{\sigma(t)}$, $\underline{T}_{\sigma(t)}$, one can have:

$$\begin{cases} \overline{E}_{\sigma(t)} C F_{\sigma(t)} = F_{\sigma(t)} \\ \underline{E}_{\sigma(t)} C F_{\sigma(t)} = F_{\sigma(t)} \end{cases} \tag{4.29}$$

By seting $\Upsilon_{\sigma(t)} = F_{\sigma(t)}(CF_{\sigma(t)})^\dagger$ and $\Lambda_{\sigma(t)} = I_{n_y} - (CF_{\sigma(t)})(CF_{\sigma(t)})^\dagger$, the general solution of (4.29) $\forall \sigma(t) \in \mathcal{N}$ is given by [112] :

$$\begin{cases} \overline{E}_{\sigma(t)} = \Upsilon_{\sigma(t)} + \overline{Z}_{\sigma(t)} \Lambda_{\sigma(t)} \\ \underline{E}_{\sigma(t)} = \Upsilon_{\sigma(t)} + \underline{Z}_{\sigma(t)} \Lambda_{\sigma(t)} \end{cases} \tag{4.30}$$

where $\overline{Z}_{\sigma(t)}$, $\underline{Z}_{\sigma(t)}$ are arbitrary matrices of appropriate dimension.

From (4.30), the matrices $\overline{T}_{\sigma(t)}$ and $\underline{T}_{\sigma(t)}$ are expressed as:

$$\begin{cases} \overline{T}_{\sigma(t)} = I_{n_x} - \Upsilon_{\sigma(t)}C - \overline{Z}_{\sigma(t)}\Lambda_{\sigma(t)}C \\ \underline{T}_{\sigma(t)} = I_{n_x} - \Upsilon_{\sigma(t)}C - \underline{Z}_{\sigma(t)}\Lambda_{\sigma(t)}C \end{cases} \tag{4.31}$$

The relations (4.23) are then equivalent to:

$$\begin{cases} \overline{N}^j_{\sigma(t)} = \overline{T}_{\sigma(t)}A^j_{\sigma(t)} - \overline{Y}^j_{\sigma(t)}C \\ \underline{N}^j_{\sigma(t)} = \underline{T}_{\sigma(t)}A^j_{\sigma(t)} - \underline{Y}^j_{\sigma(t)}C \end{cases} \tag{4.32}$$

with $\overline{Y}^j_{\sigma(t)} = \overline{J}^j_{\sigma(t)} - \overline{N}^j_{\sigma(t)}\overline{E}_{\sigma(t)}$ and $\underline{Y}^j_{\sigma(t)} = \underline{J}^j_{\sigma(t)} - \underline{N}^j_{\sigma(t)}\underline{E}_{\sigma(t)}$

At this stage, the task of designing the interval observer (4.16) is now turned to determine the matrices $\overline{Y}^j_{\sigma(t)}$ and $\underline{Y}^j_{\sigma(t)}$ such that matrices $\overline{N}^j_{\sigma(t)}$ and $\underline{N}^j_{\sigma(t)}$ are Metzler and Hurwitz to ensure the stability and cooperativity properties for all $\sigma(t) \in \mathcal{N}$, $j \in \mathcal{P}$.

4.3.2 Unknown input interval reconstruction

This subsection aims at investigating an algebraic relationship between the previously designed interval observer and unknown input to reconstruct the lower and upper trajectories of disturbance inputs $f(t)$. The following unknown disturbance interval reconstruction is proposed for system (4.11).

$$\begin{cases} \overline{f}(t) = \Phi^+_{\sigma(t)}\Big(\dot{y}(t) - CB_{\sigma(t)}u(t) - CD_{\sigma(t)}\delta_f(t) - C\underline{\nabla}_{\sigma(t)}(t) - \Big(\Psi^+_{\sigma(t)}(\rho(t))\underline{x}(t) - \Psi^-_{\sigma(t)}(\rho(t))\overline{x}(t)\Big)\Big) \\ \qquad - \Phi^-_{\sigma(t)}\Big(\dot{y}(t) - CB_{\sigma(t)}u(t) - CD_{\sigma(t)}\delta_f(t) - C\overline{\nabla}_{\sigma(t)}(t) - \Big(\Psi^+_{\sigma(t)}(\rho(t))\overline{x}(t) - \Psi^-_{\sigma(t)}(\rho(t))\underline{x}(t)\Big)\Big) \\ \underline{f}(t) = \Phi^+_{\sigma(t)}\Big(\dot{y}(t) - CB_{\sigma(t)}u(t) - CD_{\sigma(t)}\delta_f(t) - C\overline{\nabla}_{\sigma(t)}(t) - \Big(\Psi^+_{\sigma(t)}(\rho(t))\overline{x}(t) - \Psi^-_{\sigma(t)}(\rho(t))\underline{x}(t)\Big)\Big) \\ \qquad - \Phi^-_{\sigma(t)}\Big(\dot{y}(t) - CB_{\sigma(t)}u(t) - CD_{\sigma(t)}\delta_f(t) - C\underline{\nabla}_{\sigma(t)}(t) - \Big(\Psi^+_{\sigma(t)}(\rho(t))\underline{x}(t) - \Psi^-_{\sigma(t)}(\rho(t))\overline{x}(t)\Big)\Big) \end{cases} \tag{4.33}$$

with $\Phi_{\sigma(t)} = \big(CF_{\sigma(t)}\big)^\dagger$ and $\Psi_{\sigma(t)}(\rho(t)) = CA_{\sigma(t)}(\rho(t))$.
Note that, $\dot{y}(t)$ can be obtained by applying various approaches such as sliding mode or algebraic differentiators.

The algebraic observer (4.33) is interval reconstruction of unknown disturbance input $f(t)$, i.e.

$$\underline{f}(t) \leq f(t) \leq \overline{f}(t) \tag{4.34}$$

if the interval observer (4.16) exists the rank condition 4.15 holds. From the output measurement of system (4.11),

its derivative can obtain as:

$$\dot{y}(t) = C\Big(A_{\sigma(t)}(\rho(t))x(t) + B_{\sigma(t)}u(t) + D_{\sigma(t)}\delta_f(t) + F_{\sigma(t)}f(t) + \nabla_{\sigma(t)}(t)\Big) \tag{4.35}$$

Due to the assumption (4.15) satisfied, the unknown input $f(t)$ can be expressed as follows:

$$f(t) = \Phi_{\sigma(t)}\Big(\dot{y}(t) - \Psi_{\sigma(t)}(\rho(t))x(t) - CB_{\sigma(t)}u(t) - CD_{\sigma(t)}\delta_f(t) - C\nabla_{\sigma(t)}(t)\Big) \tag{4.36}$$

Let's introduce the lower and upper estimation error of disturbance

$$\begin{cases} \overline{e}_f(t) = \overline{f}(t) - f(t) \\ \underline{e}_f(t) = f(t) - \underline{f}(t) \end{cases} \tag{4.37}$$

From (4.33) and (4.36), these estimation errors are expressed as follows:

$$\begin{cases} \overline{e}_f(t) = \Phi^+_{\sigma(t)}\Big(\Psi^+_{\sigma(t)}(\rho(t))\underline{e}(t) + \Psi^-_{\sigma(t)}(\rho(t))\overline{e}(t) + C\Big(\nabla_{\sigma(t)}(t) - \underline{\nabla}_{\sigma(t)}(t)\Big)\Big) \\ \qquad + \Phi^-_{\sigma(t)}\Big(\Psi^+_{\sigma(t)}(\rho(t))\overline{e}(t) + \Psi^-_{\sigma(t)}(\rho(t))\underline{e}(t) + C\Big(\overline{\nabla}_{\sigma(t)}(t) - \nabla_{\sigma(t)}(t)\Big)\Big) \\ \underline{e}_f(t) = \Phi^+_{\sigma(t)}\Big(\Psi^+_{\sigma(t)}(\rho(t))\overline{e}(t) + \Psi^-_{\sigma(t)}(\rho(t))\underline{e}(t) + C\Big(\overline{\nabla}_{\sigma(t)}(t) - \nabla_{\sigma(t)}(t)\Big)\Big) \\ \qquad + \Phi^-_{\sigma(t)}\Big(\Psi^+_{\sigma(t)}(\rho(t))\underline{e}(t) + \Psi^-_{\sigma(t)}(\rho(t))\overline{e}(t) + C\Big(\nabla_{\sigma(t)}(t) - \underline{\nabla}_{\sigma(t)}(t)\Big)\Big) \end{cases} \tag{4.38}$$

According to lemma 2.8, the following terms are positive

$$\begin{cases} C\big(\overline{\nabla}_{\sigma(t)} - \nabla_{\sigma(t)}\big) \geq 0 \\ C\big(\nabla_{\sigma(t)} - \underline{\nabla}_{\sigma(t)}\big) \geq 0 \end{cases} \tag{4.39}$$

Moreover, the lower and upper state estimation errors $\underline{e}(t) = x(t) - \underline{x}(t)$ and $\overline{e}(t) = \overline{x}(t) - x(t)$ are also positive by the construction of switched unknown input interval observer (4.16).

The terms $\Psi^+_{\sigma(t)}(\rho(t))$ and $\Psi^-_{\sigma(t)}(\rho(t))$ are positive due to element-wise maximum. Therefore, the following terms hold:

$$\begin{cases} \Psi^+_{\sigma(t)}(\rho(t))\overline{e}(t) + \Psi^-_{\sigma(t)}(\rho(t))\underline{e}(t) \geq 0 \\ \Psi^+_{\sigma(t)}(\rho(t))\underline{e}(t) + \Psi^-_{\sigma(t)}(\rho(t))\overline{e}(t) \geq 0 \end{cases} \tag{4.40}$$

With positive terms in (4.39) and (4.40), one can get:

$$\begin{cases} \Psi^+_{\sigma(t)}(\rho(t))\underline{e}(t) + \Psi^-_{\sigma(t)}(\rho(t))\overline{e}(t) + C\Big(\nabla_{\sigma(t)}(t) - \underline{\nabla}_{\sigma(t)}(t)\Big) \geq 0 \\ \Psi^+_{\sigma(t)}(\rho(t))\overline{e}(t) + \Psi^-_{\sigma(t)}(\rho(t))\underline{e}(t) + C\Big(\overline{\nabla}_{\sigma(t)}(t) - \nabla_{\sigma(t)}(t)\Big) \geq 0 \end{cases} \tag{4.41}$$

In the same manner, the lower and upper unknown input estimation errors are element-wise non-negative for all $t \geq t_0$.

$$\begin{cases} \underline{e}_f(t) = f(t) - \underline{f}(t) \geq 0 \\ \overline{e}_f(t) = \overline{f}(t) - f(t) \geq 0 \end{cases} \tag{4.42}$$

It implies that the unknown input $f(t)$ is bounded by $\underline{f}(t)$ and $\overline{f}(t)$.
Knowing that $\underline{e}(t)$ and $\overline{e}(t)$ converge asymptotically to zero then $\underline{e}_f(t)$ and $\overline{e}_f(t)$ also converge asymptotically to zero in case $\Delta A_{\sigma(t)}\big(\rho(t), \Delta\xi(t)\big) = 0$ and they are bounded in other cases.

4.3.3 Observer-based fault tolerant control

The objective here is to co-design the interval observer and fault-tolerant control to stabilize the closed-loop system and track the reference model considered as a perfect behavior of the lateral dynamics. The idea is to force the vehicle to track desired trajectories $x_r(t) = \begin{bmatrix} v_{y_r}(t) \\ r_r(t) \end{bmatrix}$ given by a reference model which represents the ideal response of the vehicle according to the driver manoeuvres.

Let us consider the fault-free system without uncertainties as the reference. Its LPV-switched form copies that of the system:

$$\begin{cases} \dot{x}_r(t) = A_{\sigma(t)}(\rho(t))x_r(t) + B_{\sigma(t)}u_r(t) + D_{\sigma(t)}(\xi_0)\delta_f(t) \\ y_r(t) = Cx_r(t) \end{cases} \tag{4.43}$$

where $x_r(t)$ and $u_r(t)$ are states and control input of the reference system.

In combination with SUIIO and unknown input interval reconstruction to track the reference model and compensate the influence of faults, the following structure of fault tolerant control law is synthesized to stabilize the closed-loop system:

$$u(t) = -\overline{K}_{\sigma(t)}\big(\overline{x}(t) - x_r(t)\big) - \underline{K}_{\sigma(t)}\big(\underline{x}(t) - x_r(t)\big) - \overline{K}_{\sigma(t),f}\overline{f}(t) - \underline{K}_{\sigma(t),f}\underline{f}(t) + u_r(t) \tag{4.44}$$

where $\underline{K}_{\sigma(t)}$ and $\overline{K}_{\sigma(t)}$ are the lower and upper state feedback gain matrices which need to be designed. The accommodation gain is chosen in order to cancel the effect of the fault. Its value is $\overline{K}_{\sigma(t),f} = \underline{K}_{\sigma(t),f} = \frac{1}{2}B^{\dagger}_{\sigma(t)}F_{\sigma(t)}$. By introducing the tracking error as $e_r(t) = x(t) - x_r(t)$, its dynamics is then expressed by:

$$\begin{aligned} \dot{e}_r(t) = \sum_{j=1}^{4} \mu^j_{\sigma(t)}(\rho(t))\Big(& \big(A^j_{\sigma(t)} - B_{\sigma(t)}\overline{K}_{\sigma(t)} - B_{\sigma(t)}\underline{K}_{\sigma(t)}\big)e_r(t) + \Delta A^j_{\sigma(t)}e_r(t) + \Delta A^j_{\sigma(t)}x_r \\ & - B_{\sigma(t)}\overline{K}_{\sigma(t)}\overline{e}(t) + B_{\sigma(t)}\underline{K}_{\sigma(t)}\underline{e}(t) + B_{\sigma(t)}\overline{K}_{\sigma(t),f}\overline{e}_f(t) + B_{\sigma(t)}\underline{K}_{\sigma(t),f}\underline{e}_f(t)\Big) \end{aligned} \tag{4.45}$$

One now need to define the error dynamics for the whole closed-loop system including the observer and the con-

troller. The following augmented system is obtained:

$$\begin{cases} \dot{e}_r(t) = \sum_{j=1}^{4} \mu^j_{\sigma(t)}(\rho(t))\Big(\big(A^j_{\sigma(t)} - B_{\sigma(t)}\overline{K}_{\sigma(t)} - B_{\sigma(t)}\underline{K}_{\sigma(t)}\big)e_r(t) \\ \qquad\qquad + \Delta A^j_{\sigma(t)} e_r(t) - B_{\sigma(t)}\overline{K}_{\sigma(t)}\overline{e}(t) + B_{\sigma(t)}\underline{K}_{\sigma(t)}\underline{e}(t) + w^j_{\sigma(t),1}\Big) \\ \dot{\overline{e}}(t) = \sum_{j=1}^{4} \mu^j_{\sigma(t)}(\rho(t))\Big(\overline{N}^j_{\sigma(t)}\overline{e}(t) - \overline{T}_{\sigma(t)}\Delta A^j_{\sigma(t)} e_r(t) + \overline{w}^j_{\sigma(t)}\Big) \\ \dot{\underline{e}}(t) = \sum_{j=1}^{4} \mu^j_{\sigma(t)}(\rho(t))\Big(\underline{N}^j_{\sigma(t)}\underline{e}(t) + \underline{T}_{\sigma(t)}\Delta A^j_{\sigma(t)} e_r(t) + \underline{w}^j_{\sigma(t)}\Big) \end{cases} \tag{4.46}$$

where

$$\begin{cases} w^j_{\sigma(t),1} = B_{\sigma(t)}\overline{K}_{\sigma(t),f}\overline{e}_f(t) + B_{\sigma(t)}\underline{K}_{\sigma(t),f}\underline{e}_f(t) + \Delta A^j_{\sigma(t)} x_r(t) \\ \overline{w}^j_{\sigma(t)} = \overline{\nabla}^j_{\sigma(t)} - \overline{T}_{\sigma(t)}\Delta A^j_{\sigma(t)} x_r(t) - \overline{T}_{\sigma(t)}\Delta D_{\sigma(t)}\delta_f(t) \\ \underline{w}^j_{\sigma(t)} = \underline{T}_{\sigma(t)}\Delta A^j_{\sigma(t)} x_r(t) + \underline{T}_{\sigma(t)}\Delta D_{\sigma(t)}\delta_f(t) - \underline{\nabla}^j_{\sigma(t)} \end{cases} \tag{4.47}$$

The following two vectors are defined for the sake of clarity: $\chi(t) = \begin{bmatrix} e_r(t) \\ \overline{e}(t) \\ \underline{e}(t) \end{bmatrix}$ and $w^j_i(t) = \begin{bmatrix} w^j_{1,i}(t) \\ \overline{w}^j_i(t) \\ \underline{w}^j_i(t) \end{bmatrix}$.

The following theorem provides sufficient conditions for the existence of the switched unknown input interval observer given in (4.16) and stabilization of tracking error given in (4.45). It is the primary contribution of this chapter.

Theorem 4.2 *If there exists positive diagonal matrices $\underline{P}_i$, $\overline{P}_i$ and symmetric positive definite matrix P_i with $P_{s,i} = diag\big(P_i, \overline{P}_i, \underline{P}_i\big)$ and multiple ISS-Lyapunov function $V_{\sigma(t)}(\chi(t))$ switching among $V_i(\chi(t)) = \chi^T(t)P_{s,i}\chi(t)$, matrices $\overline{X}_i$, $\overline{W}^j_i$, $\overline{G}_i$, $\underline{X}_i$, $\underline{W}^j_i$, $\underline{G}_i$ for all $i \in \mathcal{N}$, $j \in \mathcal{P}$ and constant scalars $\alpha_2 > \alpha_1 > 0$, $\gamma_i > 0$, $\varepsilon > 0$, $\kappa > 0$ and positive scalars $\eta_{1,i}$, $\eta_{2,i}$, $\eta_{3,i}$ such that the following LMIs hold:*

$$\begin{aligned} \min_{P_{s,i},\overline{W}^j_i,\overline{X}_i,\overline{G}_i,\underline{W}^j_i,\underline{X}_i,\underline{G}_i} \quad & \gamma_i \\ \gamma_i \leq & \gamma \end{aligned} \tag{4.48}$$

$$\alpha_1 I_{3\times n_x} \leq P_{s,i} \leq \alpha_2 I_{3\times n_x} \tag{4.49}$$

$$O = \begin{bmatrix} O_{11} & O_{12} & O_{13} \\ (*) & O_{22} & O_{23} \\ (*) & (*) & O_{33} \end{bmatrix} \prec 0 \tag{4.50}$$

$$\begin{aligned} \overline{P}_i A^j_i - \overline{P}_i \Upsilon_i C A^j_i - \overline{X}_i \Lambda_i C A_i - \overline{W}^j_i C + \kappa \overline{P}_i \geq 0 \\ \underline{P}_i A^j_i - \underline{P}_i \Upsilon_i C A^j_i - \underline{X}_i \Lambda_i C A_i - \underline{W}^j_i C + \kappa \underline{P}_i \geq 0 \end{aligned} \tag{4.51}$$

then the interval observer (4.16) *can estimate the lower and upper bounds of system states and the closed-loop*

system (4.45) *is stable with* $\overline{Z}_i = \overline{P}_i^{-1}\overline{X}_i$, $\overline{Y}_i^j = \overline{P}_i^{-1}\overline{W}_i^j$, $\overline{K}_i = \overline{G}_i P_i^{-1}$ *and* $\underline{Z}_i = \underline{P}_i^{-1}\underline{X}_i$, $\underline{Y}_i^j = \underline{P}_i^{-1}\underline{W}_i^j$, $\underline{K}_i = \underline{G}_i P_i^{-1}$. *where*

$$O_{11} = \begin{bmatrix} \Gamma^{'''} & P^{'} \\ P^{'} & -\gamma_i \end{bmatrix} \tag{4.52}$$

$$O_{13} = \begin{bmatrix} -B_i\overline{G}_i & B_i\underline{G}_i & 0 & 0 \\ 0 & 0 & I_{n_x} & 0 \\ 0 & 0 & 0 & I_{n_x} \\ 0 & 0 & 0 & 0 \end{bmatrix} \tag{4.53}$$

$$O_{12} = \begin{bmatrix} P_i N_{a,i}^T & 0 & 0 \\ (*) & \overline{P}_i\overline{T}_i M_i^{'j} & 0 \\ (*) & (*) & \underline{P}_i\underline{T}_i M_i^j) \end{bmatrix} \tag{4.54}$$

$$O_{22} = -\begin{bmatrix} (\eta_{1,i}^{-1} + \eta_{2,i}^{-1} + \eta_{3,i}^{-1}) & 0 & 0 \\ (*) & \eta_{2,i} & 0 \\ (*) & (*) & \eta_{3,i} \end{bmatrix}^{-1} \tag{4.55}$$

$$O_{33} = -\begin{bmatrix} \mu^{-1}P_i & 0 & 0 & 0 \\ (*) & \mu^{-1}P_i & 0 & 0 \\ (*) & (*) & \mu P_i & 0 \\ (*) & (*) & (*) & \mu P_i \end{bmatrix} \tag{4.56}$$

$$\Gamma^{'''} = \begin{bmatrix} \Gamma_{11}^{''} & 0 & 0 \\ (*) & \Gamma_{22}^{'} & 0 \\ (*) & (*) & \Gamma_{33}^{'} \end{bmatrix} \tag{4.57}$$

$$P^{'} = \begin{bmatrix} I_{n_x} & 0 & 0 \\ (*) & \overline{P}_i & 0 \\ (*) & (*) & \underline{P}_i \end{bmatrix} \tag{4.58}$$

$$\Gamma_{11}^{''} = He\Big\{A_i^j P_i - B_i\overline{G}_i - B_i\underline{G}_i\Big\} + \eta_{1,i}M_i^j {M_i^j}^T + \varepsilon P_i \tag{4.59}$$

$$\Gamma_{22}^{'} = He\Big\{\overline{P}_i A_i^j - \overline{P}_i\Upsilon_i C A_i^j - \overline{X}_i\Lambda_i C A_i - \overline{W}_i^j C\Big\} + \varepsilon\overline{P}_i \tag{4.60}$$

$$\Gamma_{33}^{'} = He\Big\{\underline{P}_i A_i^j - \underline{P}_i\Upsilon_i C A_i^j - \underline{X}_i\Lambda_i C A_i - \underline{W}_i^j C\Big\} + \varepsilon\underline{P}_i \tag{4.61}$$

In addition, the system (4.46) *is ISS with respective to* $w_i(t)$ *under any switching signal with average dwell time*

satisfying condition (2.36) *according to Lemma 2.1, and*

$$\lim_{t\to\infty}\|\chi(t)\|_2 \le \sqrt{\frac{\gamma}{\alpha_1\varepsilon}}\max\|w_i(t)\|_\infty \quad \forall i\in\mathcal{N} \tag{4.62}$$

Proof 4.2 *(Theorem 4.2)*

Let's consider the following multiple ISS-Lyapunov functions:

$$\begin{aligned} V_i(\chi(t)) &= V_{1,i}(e_r(t)) + V_{2,i}(\overline{e}(t)) + V_{3,i}(\underline{e}(t)) \\ &= e_r^T(t)P_i^{-1}e_r(t) + \overline{e}^T(t)\overline{P}_i\overline{e}(t) + \underline{e}^T(t)\underline{P}_i\underline{e}(t) \end{aligned} \tag{4.63}$$

Taking the first-order derivative of (4.63) *along trajectory of* (4.46)*, one can get:*

$$\dot{V}_i(\chi(t)) = \dot{V}_{1,i}(e_r(t)) + \dot{V}_{2,i}(\overline{e}(t)) + \dot{V}_{3,i}(\underline{e}(t)) \tag{4.64}$$

where

$$\begin{aligned} \dot{V}_{1,i}(e_r(t)) &= \overline{e}_r^T(t)\overline{P}_i\dot{\overline{e}}_r(t) + \dot{\overline{e}}_r^T(t)\overline{P}_i\overline{e}_r(t) \\ &= \sum_{j=1}^{4}\mu_i^j(\rho(t))\Big\{He\left\{e_r^T(t)P_i^{-1}\big(A_i^j - B_i\overline{K}_i - B_i^j\underline{K}_i\big)e_r(t)\right\} \\ &\quad - He\Big\{e_r^T(t)P_i^{-1}B_i\overline{K}_i\overline{e}(t)\Big\} + He\Big\{e_r^T(t)P_i^{-1}w_{1,i}^j\Big\} \\ &\quad + He\Big\{e_r^T(t)P_i^{-1}B_i^j\underline{K}_i\underline{e}(t)\Big\} + \eta_{1,i}^{-1}e_r^T(t)N_{a,i}^TN_{a,i}e_r(t) \\ &\quad + \eta_{1,i}e_r^T(t)P_i^{-1}M_i^j{M_i^j}^TP_i^{-1}e_r(t)\Big\} \end{aligned} \tag{4.65}$$

$$\begin{aligned} \dot{V}_{2,i}(\overline{e}(t)) &= \overline{e}^T(t)\overline{P}_i\dot{\overline{e}}(t) + \dot{\overline{e}}^T(t)\overline{P}_i\overline{e}(t) \\ &= \sum_{j=1}^{4}\mu_i^j(\rho(t))\Big\{He\Big\{\overline{e}^T(t)\overline{P}_i\big(T_iA_i^j - Y_i^jC\big)\overline{e}(t)\Big\} \\ &\quad - He\Big\{\overline{e}^T(t)\overline{P}_iT_i\Delta A_i^je_r(t)\Big\} + He\Big\{\overline{e}^T(t)\overline{P}_i\overline{w}_i^j\Big\}\Big\} \end{aligned} \tag{4.66}$$

$$\begin{aligned} \dot{V}_{3,i}(\underline{e}(t)) &= \underline{e}^T(t)\underline{P}_i\dot{\underline{e}}(t) + \dot{\underline{e}}^T(t)\underline{P}_i\underline{e}(t) \\ &= \sum_{j=1}^{4}\mu_i^j(\rho(t))\Big\{He\Big\{\underline{e}^T(t)\underline{P}_i\big(T_iA_i^j - Y_i^jC\big)\underline{e}(t)\Big\} \\ &\quad - He\Big\{\underline{e}^T(t)\underline{P}_iT_i\Delta A_i^je_r(t)\Big\} + He\Big\{\underline{e}^T(t)\underline{P}_iw_{3,i}^j\Big\}\Big\} \end{aligned} \tag{4.67}$$

By applying the Majorization lemma 2.10 , the following inequalities are obtained:

$$\begin{aligned}\dot{V}_{1,i}(e_r) \leq \sum_{j=1}^{4} \mu_i^j(\rho(t))\Big\{ & He\left\{e_r^T(t)P_i^{-1}\big(A_i^j - B_i\overline{K}_i - B_i\underline{K}_i\big)e_r(t)\right\} \\ & - He\Big\{e_r^T(t)P_i^{-1}B_i^j\overline{K}_i\overline{e}(t)\Big\} + He\Big\{e_r^T(t)P_i^{-1}w_{1,i}^j\Big\} \\ & + He\Big\{e_r^T(t)P_i^{-1}B_i^j\underline{K}_i\underline{e}(t)\Big\} + \eta_{1,i}^{-1}e_r^T(t)N_{a,i}^T N_{a,i}e_r(t) \\ & + \eta_{1,i}e_r^T(t)P_i^{-1}M_i^j {M_i^j}^T P_i^{-1}e_r(t)\Big\}\end{aligned} \tag{4.68}$$

$$\begin{aligned}\dot{V}_{2,i}(\overline{e}) \leq \sum_{j=1}^{4} \mu_i^j(\rho(t))\Big\{ & He\Big\{\overline{e}^T(t)\left(\overline{P}_i\big(\overline{T}_iA_i^j - \overline{Y}_i^jC\big)\right)\overline{e}(t)\Big\} \\ & + He\Big\{\overline{e}^T(t)\overline{P}_i\overline{w}_i^j\Big\} + \eta_{2,i}^{-1}e_r^T(t)N_{a,i}^T N_{a,i}e_r(t) \\ & + \eta_{2,i}\overline{e}^T(t)\overline{P}_i\overline{T}_i{M_i^{'}}^j{M_i^{'}}^{jT}\overline{T}_i\overline{P}_i^T\overline{e}(t)\Big\}\end{aligned} \tag{4.69}$$

$$\begin{aligned}\dot{V}_{3,i}(\underline{e}) \leq \sum_{j=1}^{4} \mu_i^j(\rho(t))\Big\{ & He\Big\{\underline{e}^T(t)\left(\underline{P}_i\big(\underline{T}_iA_i^j - \underline{Y}_i^jC\big)\right)\underline{e}(t)\Big\} \\ & + He\Big\{\underline{e}^T(t)\underline{P}_i\underline{w}_i^j\Big\} + \eta_{3,i}^{-1}e_r^T(t)N_{a,i}^T N_{a,i}e_r(t) \\ & + \eta_{3,i}\underline{e}^T(t)\underline{P}_i\underline{T}_iM_i^j{M_i^j}^T\underline{T}_i\underline{P}_i^T\underline{e}(t)\Big\}\end{aligned} \tag{4.70}$$

For any positive scalar ε, γ_i, one can obtain:

$$\dot{V}_i(\chi(t)) \leq \sum_{j=1}^{4}\mu_i^j(\rho(t))\left(\begin{bmatrix}\chi^T(t) & {w_i^j}^T\end{bmatrix}\Xi\begin{bmatrix}\chi(t)\\ w_i^j\end{bmatrix}\right) - \varepsilon V_i(\chi(t)) + \gamma_i w_i^T(t)w_i(t) \tag{4.71}$$

where

$$\Xi = \begin{bmatrix}\Gamma & P\\ P & -\gamma_i\end{bmatrix} \tag{4.72}$$

$$\Gamma = \begin{bmatrix}\Gamma_{11} & \Gamma_{12} & \Gamma_{13}\\ (*) & \Gamma_{22} & \Gamma_{23}\\ (*) & (*) & \Gamma_{33}\end{bmatrix} \tag{4.73}$$

$$P = \begin{bmatrix}P_i^{-1} & 0 & 0\\ (*) & \overline{P}_i & 0\\ (*) & (*) & \underline{P}_i\end{bmatrix} \tag{4.74}$$

$$\begin{aligned}\Gamma_{11} = He\left\{P_i^{-1}A_i^j - P_i^{-1}B_i\overline{K}_i - P_i^{-1}B_i\underline{K}_i\right\} \\ + \eta_{1,i}P_i^{-1}M_i^j{M_i^j}^T P_i^{-1} + \varepsilon P_i^{-1} \\ + \left(\eta_{1,i}^{-1} + \eta_{2,i}^{-1} + \eta_{3,i}^{-1}\right)N_{a,i}^T N_{a,i}\end{aligned} \tag{4.75}$$

$$\begin{aligned}\Gamma_{22} = He\left\{\overline{P}_i A_i^j - \overline{P}_i\Upsilon_i CA_i^j - \overline{X}_i\Lambda_i CA_i - \overline{W}_i^j C\right\} \\ + \eta_{2,i}\overline{P}_i\overline{T}_i{M_i^{'}}^j{M_i^{'}}^{jT}\overline{T}_i^T\overline{P}_i + \varepsilon\overline{P}_i\end{aligned} \tag{4.76}$$

$$\begin{aligned}\Gamma_{33} = He\left\{\underline{P}_i A_i^j - \underline{P}_i\Upsilon_i CA_i^j - \underline{X}_i\Lambda_i CA_i - \underline{W}_i^j C\right\} \\ + \eta_{3,i}\underline{P}_i\underline{T}_i M_i^j{M_i^j}^T\underline{T}_i^T\underline{P}_i + \varepsilon\underline{P}_i\end{aligned} \tag{4.77}$$

$$\Gamma_{12} = -P_i^{-1}B_i\overline{K}_i \tag{4.78}$$

$$\Gamma_{13} = P_i^{-1}B_i\underline{K}_i \tag{4.79}$$

$$\Gamma_{23} = 0 \tag{4.80}$$

with $\overline{X}_i = \overline{P}_i\overline{Z}_i$, $\overline{W}_i^j = \overline{P}_i\overline{Y}_i^j$ *and* $\underline{X}_i = \underline{P}_i\underline{Z}_i$, $\underline{W}_i^j = \underline{P}_i\underline{Y}_i^j$.

The following is a sufficient condition for system (4.46) *to be input-to-state-stable:*

$$\Xi \prec 0 \tag{4.81}$$

Pre-multiplying and post-multiplying Ξ *by* $\begin{bmatrix} P_p & 0 \\ (*) & I \end{bmatrix}$ *with* $P_p = \begin{bmatrix} P_i & 0 & 0 \\ (*) & I_{n_x} & 0 \\ (*) & (*) & I_{n_x} \end{bmatrix}$*, one can get:*

$$\Xi^{'} = \begin{bmatrix} \Gamma^{'} & P^{'} \\ P^{'} & -\gamma_i \end{bmatrix} \prec 0 \tag{4.82}$$

with

$$P^{'} = \begin{bmatrix} I_{n_x} & 0 & 0 \\ 0 & \overline{P}_i & 0 \\ 0 & 0 & \underline{P}_i \end{bmatrix} \tag{4.83}$$

$$\Gamma^{'} = \begin{bmatrix} \Gamma_{11}^{'} & \Gamma_{12}^{'} & \Gamma_{13}^{'} \\ (*) & \Gamma_{22} & \Gamma_{23} \\ (*) & (*) & \Gamma_{33} \end{bmatrix} \tag{4.84}$$

$$\begin{aligned}\Gamma_{11}^{'} &= He\left\{A_i^j P_i - B_i\overline{G}_i - B_i\underline{G}_i\right\} + \eta_{1,i}M_i^j M_i^{jT} \\ &\quad + \left(\eta_{1,i}^{-1} + \eta_{2,i}^{-1} + \eta_{3,i}^{-1}\right)P_i N_{a,i}^T N_{a,i} P_i + \varepsilon P_i \\ \Gamma_{12}^{'} &= -B_i\overline{K}_i, \quad \Gamma_{13}^{'} = B_i\underline{K}_i\end{aligned} \tag{4.85}$$

where $\overline{G}_i = \overline{K}_i P_i$ *and* $\underline{G}_i = \underline{K}_i P_i$

The term $\Xi^{'}$ *can be expressed as:*

$$\Xi^{'} = \Xi^{''} + X_1^T Y_1 + Y_1^T X_1 \tag{4.86}$$

By applying Young relation lemma 2.11 for $\Xi^{'}$ *with*

$$\begin{cases} X_1 = \begin{bmatrix} -\left(B_i\overline{K}_i\right)^T & 0 & 0 & 0 \\ \left(B_i\underline{K}_i\right)^T & 0 & 0 & 0 \end{bmatrix} \\ F_1 = \begin{bmatrix} P_i & 0 \\ 0 & P_i \end{bmatrix} \\ Y_1 = \begin{bmatrix} 0 & I_{n_x} & 0 & 0 \\ 0 & 0 & I_{n_x} & 0 \end{bmatrix} \end{cases} \tag{4.87}$$

one can obtain:

$$\Xi^{'} \prec \Xi^{''} + \mu X_1^T F_1 X_1 + \mu^{-1} Y_1^T F_1^{-1} Y_1 \tag{4.88}$$

with $\Xi^{''} = \begin{bmatrix} \Gamma^{''} & P^{'} \\ P^{'} & -\gamma_i \end{bmatrix}$, $\Gamma^{''} = \begin{bmatrix} \Gamma_{11}^{'} & 0 & 0 \\ (*) & \Gamma_{22} & 0 \\ (*) & (*) & \Gamma_{33} \end{bmatrix}$.

Applying the Schur complement lemma 2.9 to the right side of inequality (4.88) *lead to:*

$$\Xi^{'} \prec \begin{bmatrix} \Xi^{''} & O_{13} \\ (*) & O_{33} \end{bmatrix} \tag{4.89}$$

Therefore, the sufficient condition (4.81) *is satisfied if*

$$\begin{bmatrix} \Xi^{''} & O_{13} \\ (*) & O_{33} \end{bmatrix} \prec 0 \tag{4.90}$$

In the same manner, one can get the LMI (4.50)*.*

This ensures that $\dot{V}_i(\chi(t)) \leq -\varepsilon V_i(\chi(t)) + \gamma_i w_i^T(t) w_i(t)$*. Due to lemma 2.2, the augmented error system* (4.46) *is ISS with respect to additive disturbance* $w_i(t)$*.*

Then integrating this inequality from t_k to t, we can get:

$$\|\chi(t)\|_2 < \sqrt{\frac{e^{-\varepsilon(t-t_k)}V_i(\chi(t_k))}{\alpha_1} + \frac{\gamma_i}{\varepsilon\alpha_1}\|w_i(t)\|_\infty^2} \tag{4.91}$$

Hence, when $t \to \infty$ the exponential term goes to zero and $\gamma_i \leq \gamma$ for all $i \in \mathcal{N}$, the inequality (4.91) *becomes* (4.62).

Furthermore, $\overline{N}_i^j$ and $\underline{N}_i^j$ are Metzler matrices, if $\overline{N}_i^j + \kappa I_{n_x} \geq 0$ and $\underline{N}_i^j + \kappa I_{n_x} \geq 0$ with any $\kappa > 0, \forall i \in \mathcal{N}$, $\forall j \in \mathcal{P}$. LMI in (4.51) *can be obtained by multiplying $\overline{P}_i$ and $\underline{P}_i$ on the left side and performing the change of variables $\overline{W}_i^j = \overline{P}_i\overline{Y}_i^j$ and $\underline{W}_i^j = \underline{P}_i\underline{Y}_i^j$. This completes the proof.*

Overall, the design procedure of the switched unknown input interval observer, the dynamics proportional integral observer and FTTC is determined based on the following algorithms:

Algorithm 2: Design procedure

for $\sigma(t) = 1 : N$ **do**
  if $\left(rank(CF_{\sigma(t)}) == rank(B_{\sigma(t)})\right)$ **then**
    - Solve the optimization problem in Theorem 4.2 and obtain $P_{s,i}, \overline{W}_{\sigma(t)}^j, \overline{X}_{\sigma(t)}, \overline{G}_{\sigma(t)}, \underline{W}_{\sigma(t)}^j, \underline{X}_{\sigma(t)}, \underline{G}_{\sigma(t)}$.

$$\begin{cases} \overline{Z}_{\sigma(t)} = \overline{P}_{\sigma(t)}^{-1}\overline{X}_{\sigma(t)} \\ \overline{Y}_{\sigma(t)}^j = \overline{P}_{\sigma(t)}^{-1}\overline{W}_{\sigma(t)}^j \\ \overline{K}_{\sigma(t)} = \overline{G}_{\sigma(t)}P_{\sigma(t)}^{-1} \\ \underline{Z}_{\sigma(t)} = \underline{P}_{\sigma(t)}^{-1}\underline{X}_{\sigma(t)} \\ \underline{Y}_{\sigma(t)}^j = \underline{P}_{\sigma(t)}^{-1}\underline{W}_{\sigma(t)}^j \\ \underline{K}_{\sigma(t)} = \underline{G}_{\sigma(t)}P_{\sigma(t)}^{-1} \end{cases}$$

    - Determine matrices $\overline{E}_{\sigma(t)}, \underline{E}_{\sigma(t)}, \overline{T}_{\sigma(t)}, \underline{T}_{\sigma(t)}, \overline{N}_{\sigma(t)}^j, \underline{N}_{\sigma(t)}^j$ by equations (4.30), (4.31) and (4.32) respectively. Then matrices $\overline{J}_{\sigma(t)}^j, \underline{J}_{\sigma(t)}^j$ and $\overline{H}_{\sigma(t)}, \underline{H}_{\sigma(t)}, \overline{Q}_{\sigma(t)}, \underline{Q}_{\sigma(t)}$ are obtained by construction.
  else
    There is no solution for set of LMIs.
    The SUIIO and controller do not exist
  end
end

4.4 Simulation results

The proposed approach is deployed to estimate and control the dynamics model (4.11). The objective of FTC strategy is to maintain the stability of the vehicle's yaw motion at the center of gravity, regardless of the actuator faults.

For the simulation, the driver controls the steering angle $\delta_f(t)$ of the vehicle with the steering wheel and the cornering stiffness variations are reflected in terms $\Delta\xi = [\Delta c_f, \Delta c_r]$ which assumed to be unknown but bounded, satisfying $|\Delta\xi| \leq 0.2\xi_0$. The design procedure is conducted under LMI framework using MATLAB SEDUMI optimization [165] and Matlab vehicle dynamics blockset.

4.4.1 Yaw rate profile tracking

For this case, the longitudinal velocity being available in real-time can be divided into three sub-regions given as follows:

$$\sigma(t) = \begin{cases} 1, & v_x \in [\ 12.5 \quad 17.5\ ](m/s) \\ 2, & v_x \in [\ 17.5 \quad 22.5\ ](m/s) \\ 3, & v_x \in [\ 22.5 \quad 28.5\ ](m/s) \end{cases} \tag{4.92}$$

The switching signal $\sigma(t)$ is depicted in Figure 4.1.

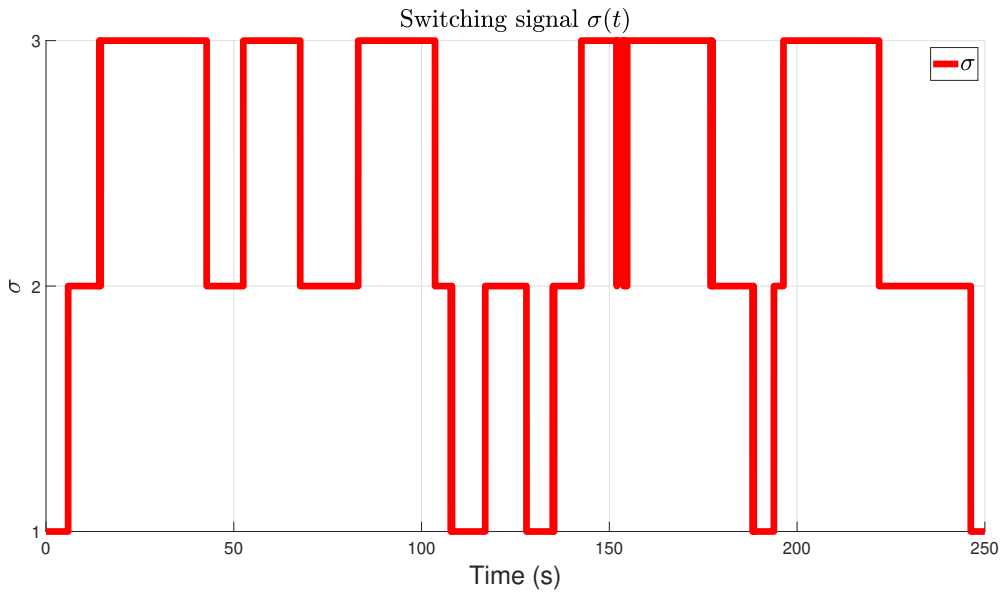

Figure 4.1: Front steering angle and longitudinal velocity profile.

The observer and controller gain matrices are obtained as follows:

$$\overline{N}_1^1 = \begin{bmatrix} -2.1043 & 4.3966 \\ 0 & -4.3973 \end{bmatrix}, \overline{N}_1^2 = \begin{bmatrix} -2.1043 & 4.3963 \\ 0 & -4.3973 \end{bmatrix} \tag{4.93}$$

$$\overline{N}_1^3 = \begin{bmatrix} -2.9460 & 4.4535 \\ 0 & -4.3998 \end{bmatrix}, \overline{N}_1^4 = \begin{bmatrix} -2.9460 & 4.4541 \\ 0 & -4.3997 \end{bmatrix} \tag{4.94}$$

$$\overline{N}_2^1 = \begin{bmatrix} -1.6367 & 4.2226 \\ 0 & -4.3997 \end{bmatrix}, \overline{N}_2^2 = \begin{bmatrix} -1.6367 & 4.2226 \\ 0 & -4.3997 \end{bmatrix} \tag{4.95}$$

$$\overline{N}_2^3 = \begin{bmatrix} -2.1043 & 4.5487 \\ 0 & -4.4006 \end{bmatrix}, \overline{N}_2^4 = \begin{bmatrix} -2.1043 & 4.5491 \\ 0 & -4.4005 \end{bmatrix} \tag{4.96}$$

$$\overline{N}_3^1 = \begin{bmatrix} -1.2921 & 2.4866 \\ 0 & -4.4076 \end{bmatrix}, \overline{N}_3^2 = \begin{bmatrix} -1.2921 & 2.4866 \\ 0 & -4.4075 \end{bmatrix} \tag{4.97}$$

$$\overline{N}_3^3 = \begin{bmatrix} -1.6367 & 3.1486 \\ 0 & -4.4072 \end{bmatrix}, \overline{N}_3^4 = \begin{bmatrix} -1.6367 & 3.1500 \\ 0 & -4.4070 \end{bmatrix} \tag{4.98}$$

$$\underline{N}_1^1 = \begin{bmatrix} -2.1043 & 3.9276 \\ 0 & -4.0527 \end{bmatrix}, \underline{N}_1^2 = \begin{bmatrix} -2.1043 & 3.7814 \\ 0 & -4.0527 \end{bmatrix} \tag{4.99}$$

$$\underline{N}_1^3 = \begin{bmatrix} -2.9460 & 3.9925 \\ 0 & -4.0550 \end{bmatrix}, \underline{N}_1^4 = \begin{bmatrix} -2.9460 & 3.8472 \\ 0 & -4.0549 \end{bmatrix} \tag{4.100}$$

$$\underline{N}_2^1 = \begin{bmatrix} -1.6367 & 3.8320 \\ 0 & -4.0600 \end{bmatrix}, \underline{N}_2^2 = \begin{bmatrix} -1.6367 & 3.7393 \\ 0 & -4.0600 \end{bmatrix} \tag{4.101}$$

$$\underline{N}_2^3 = \begin{bmatrix} -2.1043 & 4.1555 \\ 0 & -4.0608 \end{bmatrix}, \underline{N}_2^4 = \begin{bmatrix} -2.1043 & 4.0632 \\ 0 & -4.0608 \end{bmatrix} \tag{4.102}$$

$$\underline{N}_3^1 = \begin{bmatrix} -1.2921 & 2.5087 \\ 0 & -4.0826 \end{bmatrix}, \underline{N}_3^2 = \begin{bmatrix} -1.2921 & 2.5141 \\ 0 & -4.0825 \end{bmatrix} \tag{4.103}$$

$$\underline{N}_3^3 = \begin{bmatrix} -1.6367 & 3.1712 \\ 0 & -4.0822 \end{bmatrix}, \underline{N}_3^4 = \begin{bmatrix} -1.6367 & 3.1780 \\ 0 & -4.0820 \end{bmatrix} \tag{4.104}$$

$$\overline{K}_1 = 10^3 \begin{bmatrix} -0.6036 & 5.3442 \end{bmatrix}, \underline{K}_1 = 10^3 \begin{bmatrix} -0.6061 & 5.3025 \end{bmatrix} \tag{4.105}$$

$$\overline{K}_2 = 10^4 \begin{bmatrix} -0.0407 & 1.0064 \end{bmatrix}, \underline{K}_2 = 10^3 \begin{bmatrix} -0.4123 & 9.8996 \end{bmatrix} \tag{4.106}$$

$$\overline{K}_3 = 10^4 \begin{bmatrix} -0.0268 & 2.0591 \end{bmatrix}, \underline{K}_3 = 10^4 \begin{bmatrix} -0.0278 & 2.0011 \end{bmatrix} \tag{4.107}$$

The longitudinal velocity $v_x(t)$ varies in a range $[12.5m/s, \quad 28.5m/s]$. The variation of the front steering angle $\delta_f(t)$ and the longitudinal velocity $v_x(t)$ are illustrated in Figure 4.2 and 4.3. The figure shows that the front steering angle

$\delta_f(t)$ is inversely proportional to the longitudinal velocity $v_x(t)$, meaning that the vehicle steers more sharply when it is moving slower and less sharply when it is moving faster. The simulation results are depicted from Figure 4.4 to 4.11. A comparison between the proposed approach and the method discussed in [3] is demonstrated from Figure 4.12 to 4.17.

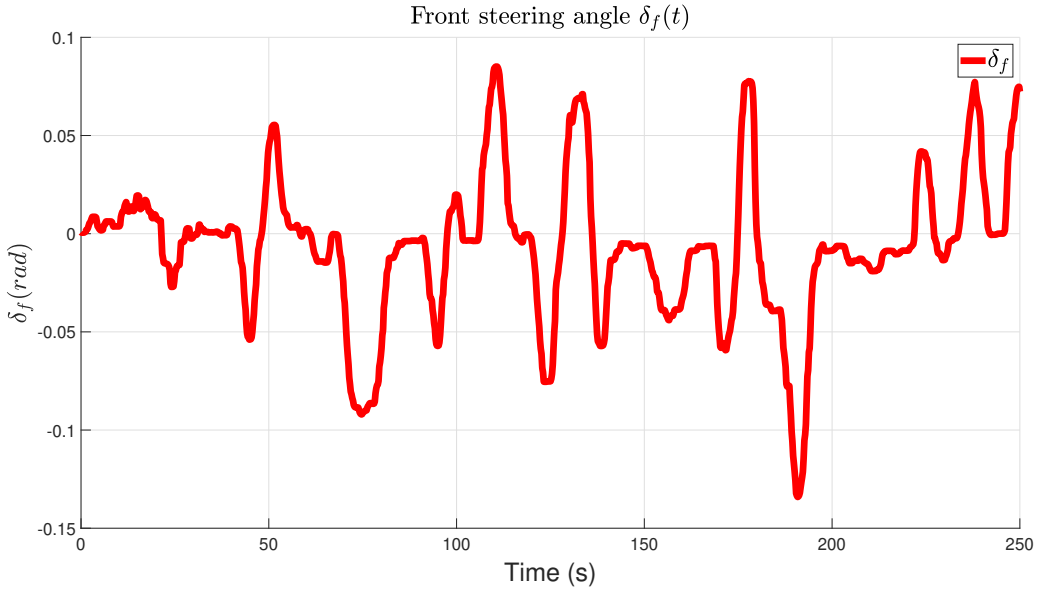

Figure 4.2: Front steering angle $\delta_f(t)$ profile.

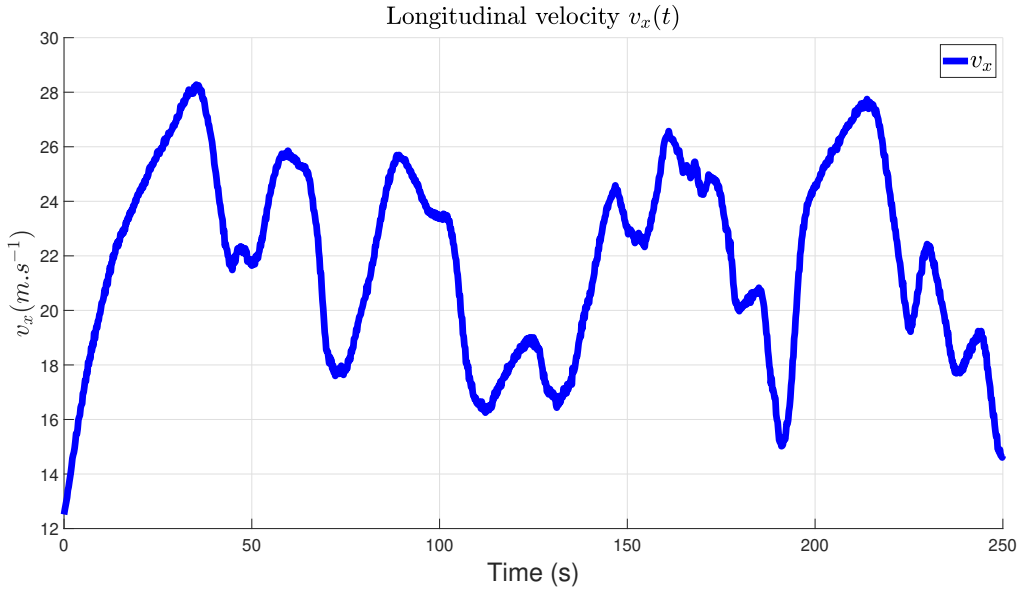

Figure 4.3: Longitudinal velocity $v_x(t)$ profile.

The actuator fault profile is shown in Figure 4.4, it combines constant value and sinusoidal form of frequency at $0.35Hz$ from $20sec$ to $145sec$ and at $0.5Hz$ from $160sec$ to $225sec$ applied as a differential yaw moment in lateral vehicle dynamics.

Figure 4.4 shows the fault interval reconstructions and the control input signal. They show a good estimation of time-varying actuator fault. It is noted that the length of interval reconstruction of the unknown inputs depends on the estimation accuracy of the system states.

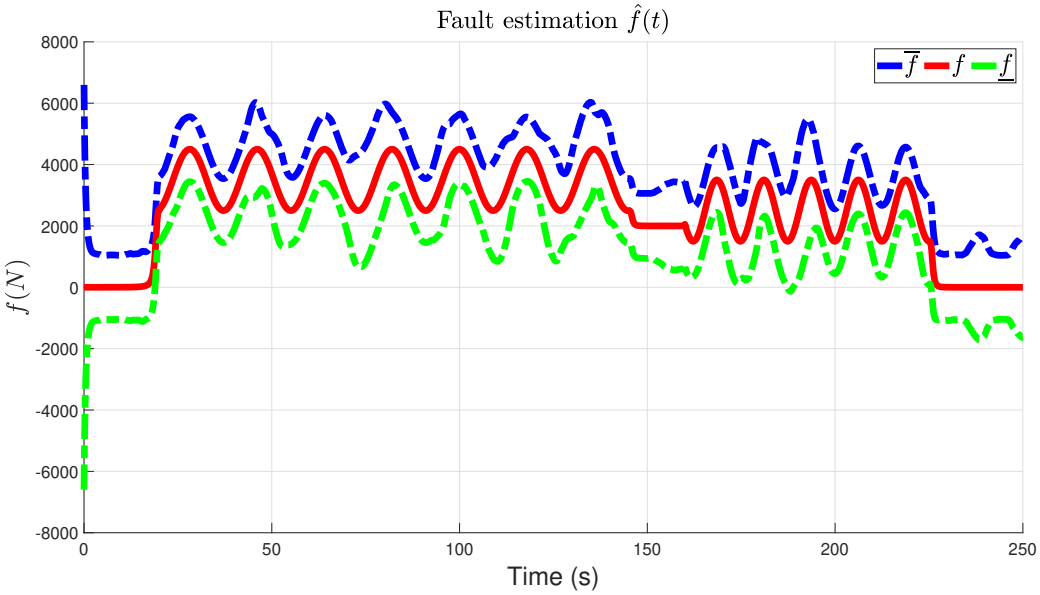

Figure 4.4: The actuator fault profile $f(t)$ and its lower and upper bounds.

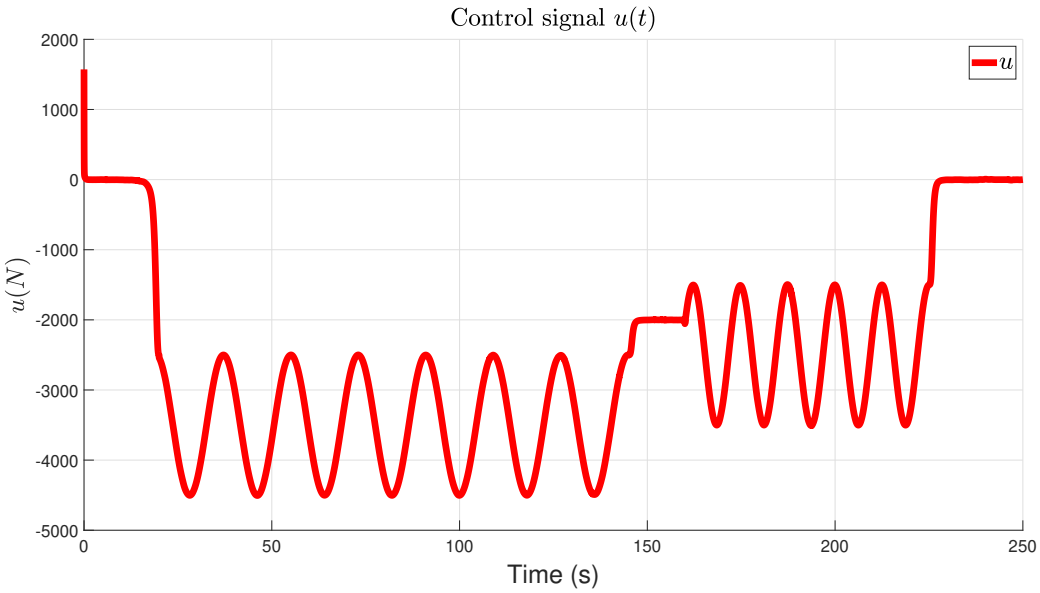

Figure 4.5: Yaw rate control input $u(t)$.

Figure 4.6 and 4.7 depicts the lower and upper bounds of lateral velocity $v_y(t)$ and yaw rate $r(t)$ where the dashed green and blue lines are the lower and upper estimations, respectively, while the red line is the actual state vectors. The lower and upper estimations still bound the real state at all times even when actuator faults occur. Furthermore, the decoupling approach still effectively removes the influence of faults on the state estimation errors.

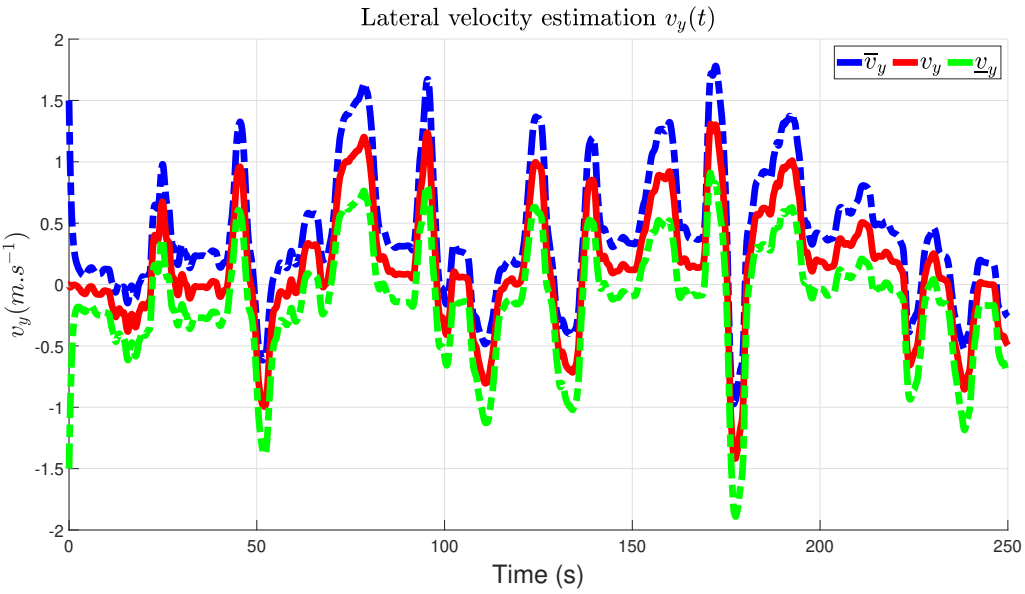

Figure 4.6: Lateral velocity interval estimation $v_y(t)$.

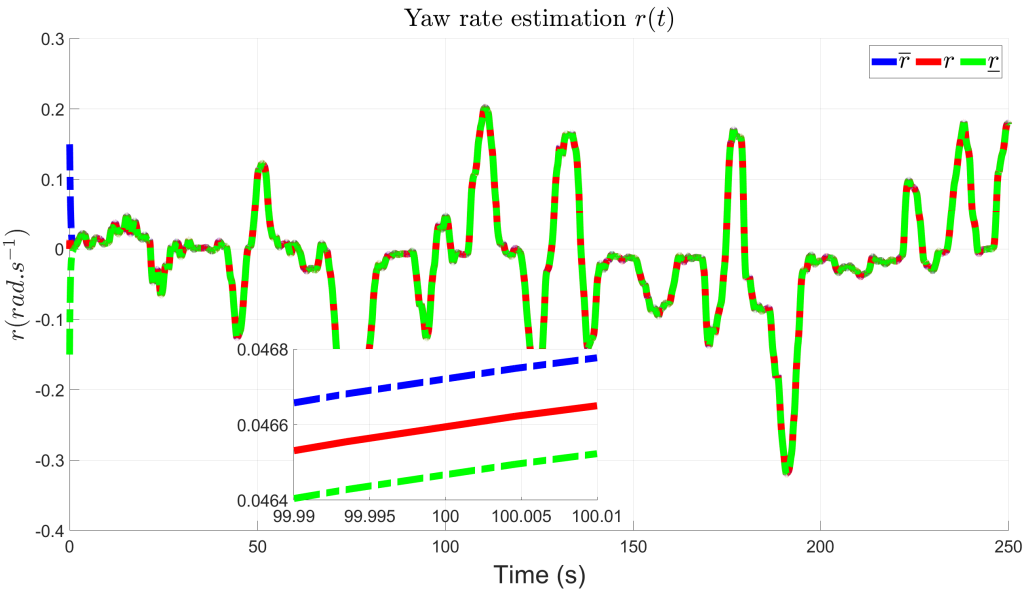

Figure 4.7: Yaw rate interval estimation $r(t)$.

The fault-tolerant controller stabilizes the closed-loop system and preserves the performance in the presence of faults. The actual state well tracks the reference state as demonstrated in Figure 4.8 and 4.9 in which the dashed blue line and dashed green line are state vectors with and without fault-tolerant control strategy, respectively. The faulty system without the proposed method clearly deviates from the reference system. Concerning the controller vehicle, the tracking errors are approximately zero, as illustrated in Figure 4.10 and 4.11.

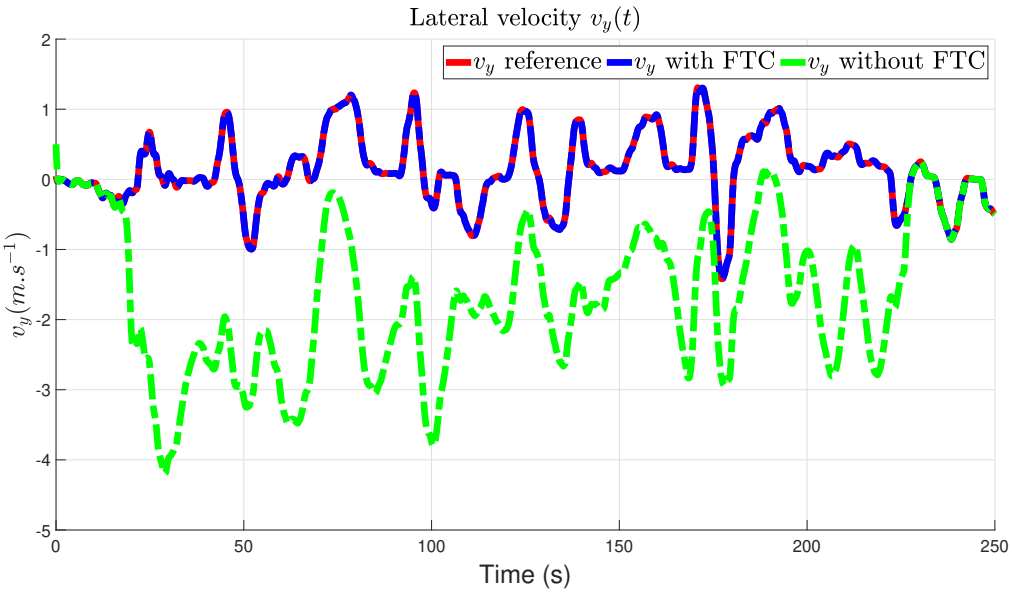

Figure 4.8: State tracking lateral velocity $v_y(t)$ with and without FTC.

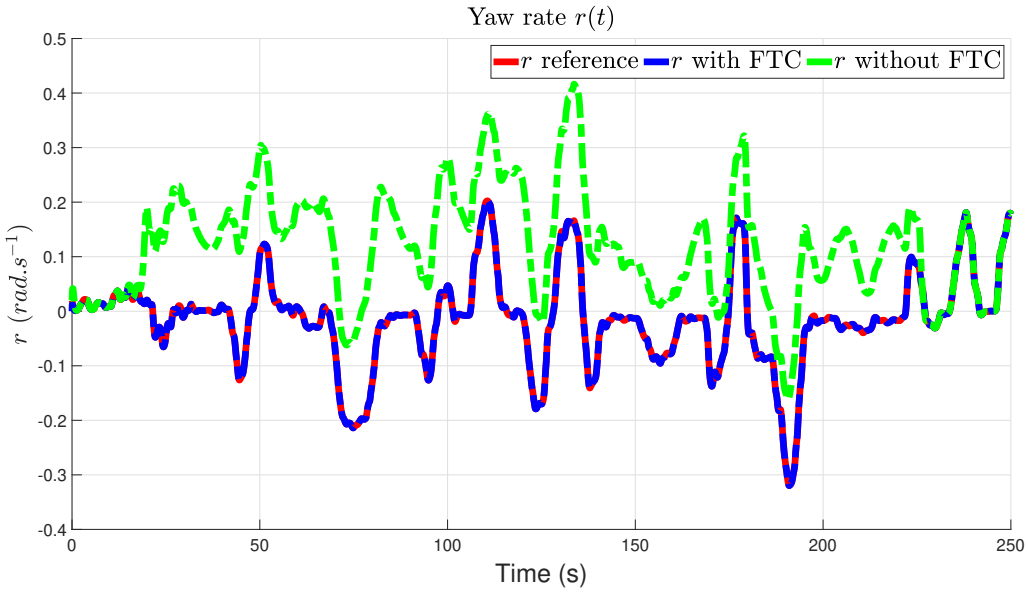

Figure 4.9: State tracking yaw rate $r(t)$ with and without FTC.

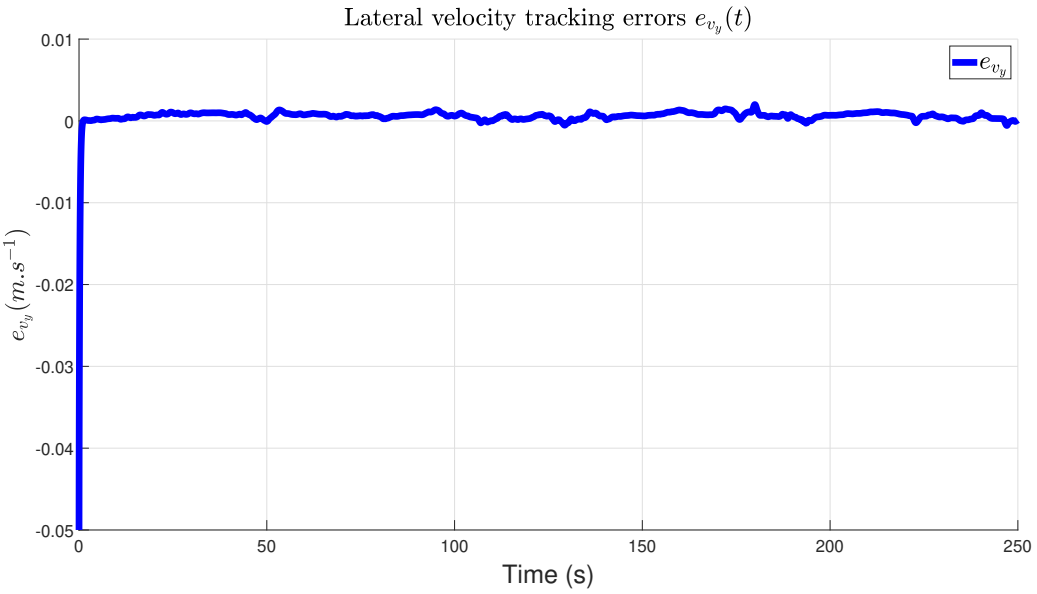

Figure 4.10: Lateral velocity tracking errors e_{v_y}.

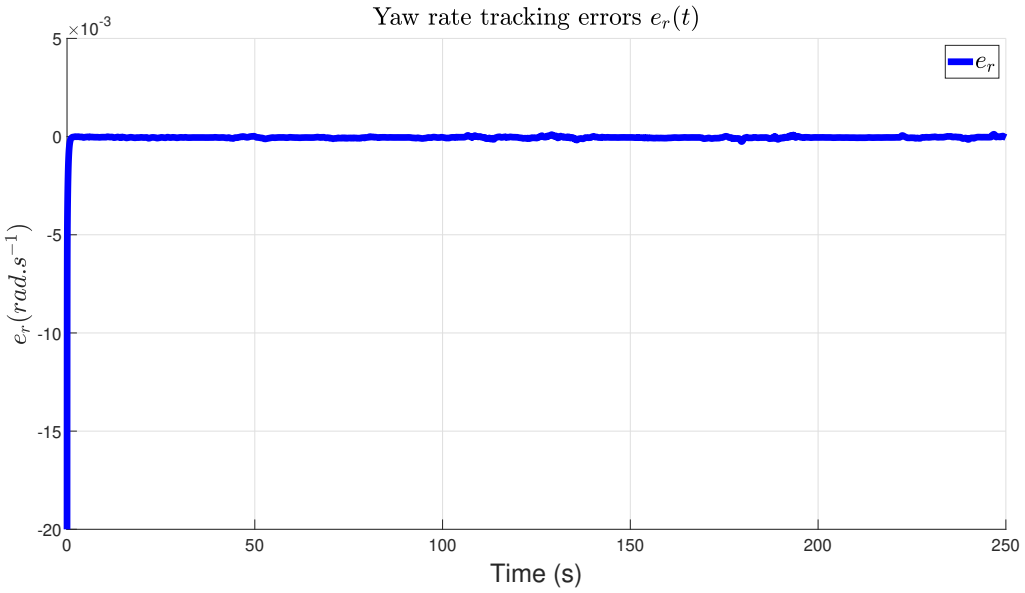

Figure 4.11: Yaw rate tracking errors e_r.

A comparison between the proposed polytopic switched unknown input interval observer design approach and method outlined in [3] is investigated to demonstrate its effectiveness.

As demonstrated in Figure 4.12, 4.13 and 4.14, the proposed approach outperforms the compared method discussed in [3] in term of estimating the lower and upper of vehicle lateral dynamics model. The proposed approach consistently exhibits better precision, as reflected by the interval width of the estimates. In Figure 4.13 and 4.14, the red line presenting the interval width of the proposed technique remains consistently lower than the blue line, which represents the compared approach. This tighter interval indicates that the proposed method achieves a

more confident and accurate estimation of the vehicle lateral dynamics. This achievement plays a crucial role in applications requiring precision vehicle state estimation and control where minimizing the uncertainty is key to enhancing overall system performance and safety.

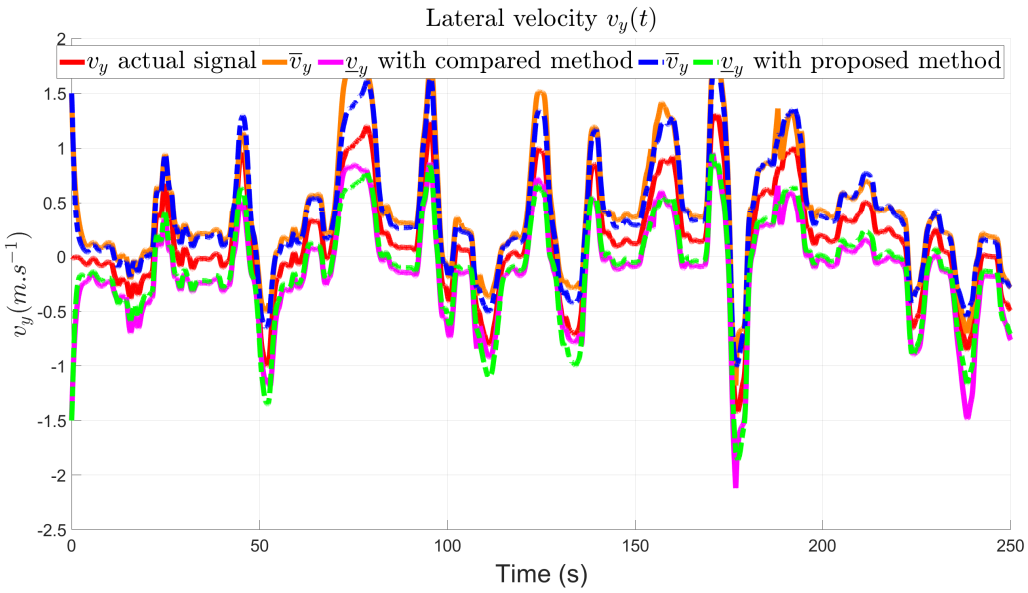

Figure 4.12: Comparison of lateral velocity $v_y(t)$ between the proposed approach with the method in [3]

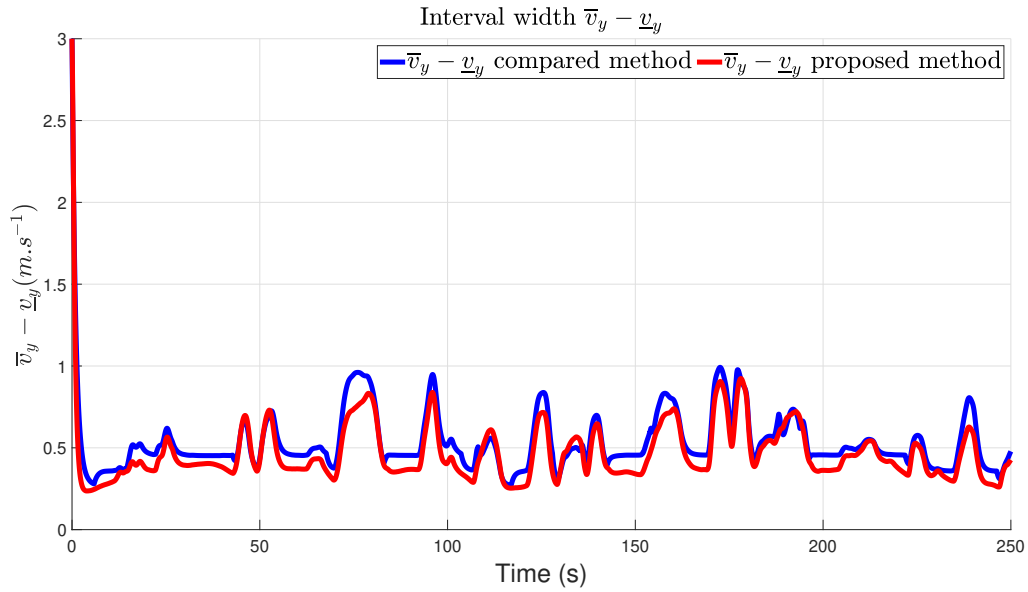

Figure 4.13: Comparison of lateral velocity interval width between the proposed approach with the method in [3]

As depicted in Figure 4.15, the proposed approach represented by the dashed blue and green lines is the most accurate in estimating the lower and upper bounds of the actuator faults. The compared method presented by the dashed orange and sienna lines also shows a good estimation of actuator fault but still exhibits significant deviation in fault estimation. Hence, the proposed approach offers superior fault estimation performance.

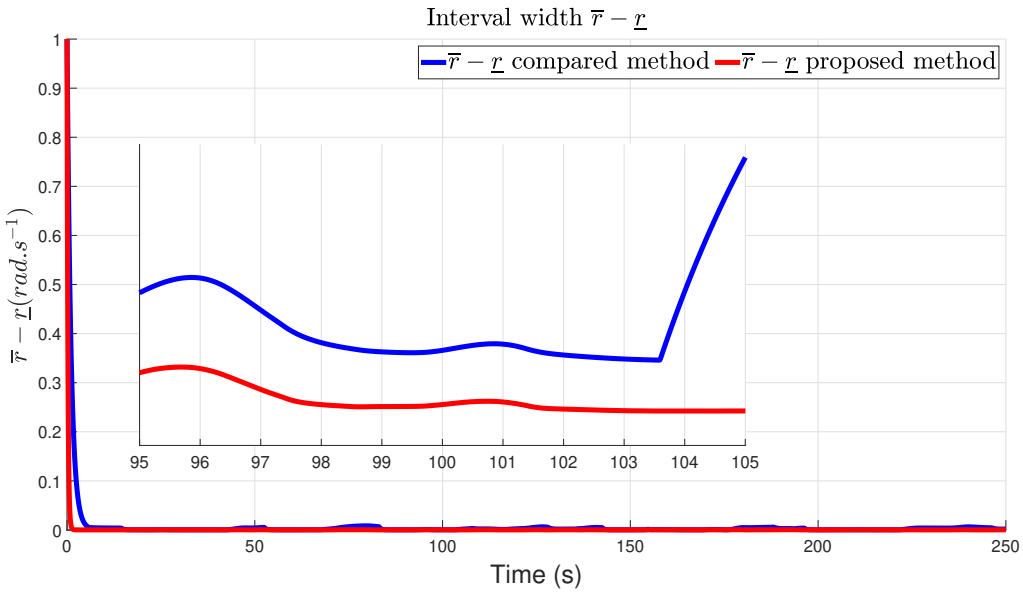

Figure 4.14: Comparison of yaw rate interval width between the proposed approach with the method in [3]

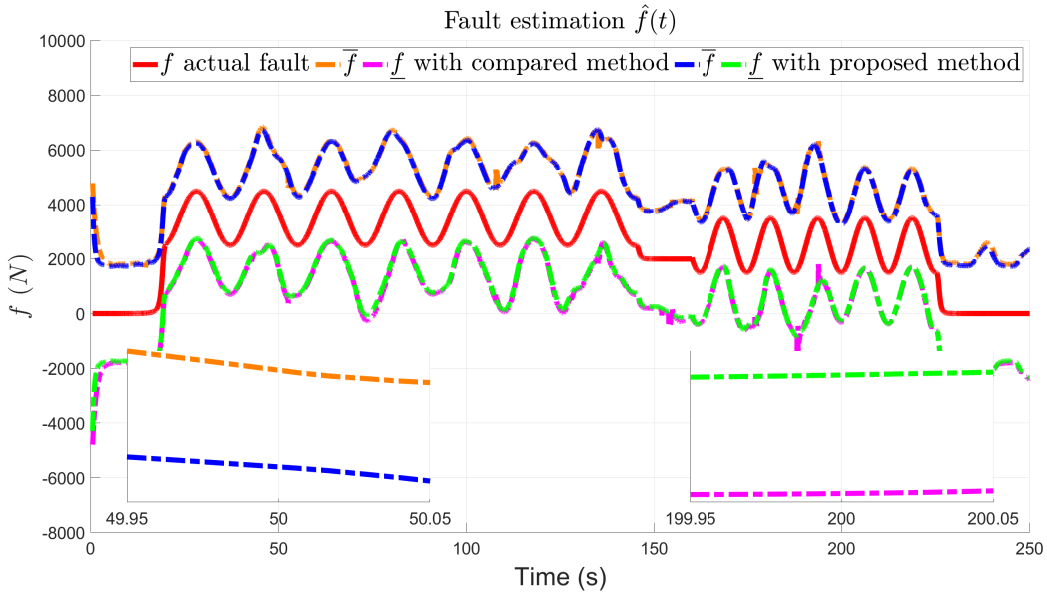

Figure 4.15: Comparison of unknown input interval reconstruction between the proposed approach with the method in [3].

Figure 4.16 and 4.17 show a similar performance of both technique over time. It indicates that the proposed and compared methods closely track the reference model. However, the co-design approach demonstrates outstanding performance than that of the separated method. The dashed green line deviates slightly from the reference model, while the dashed blue line stays close to the red line, indicating better tracking performance in the zoomed-in region.

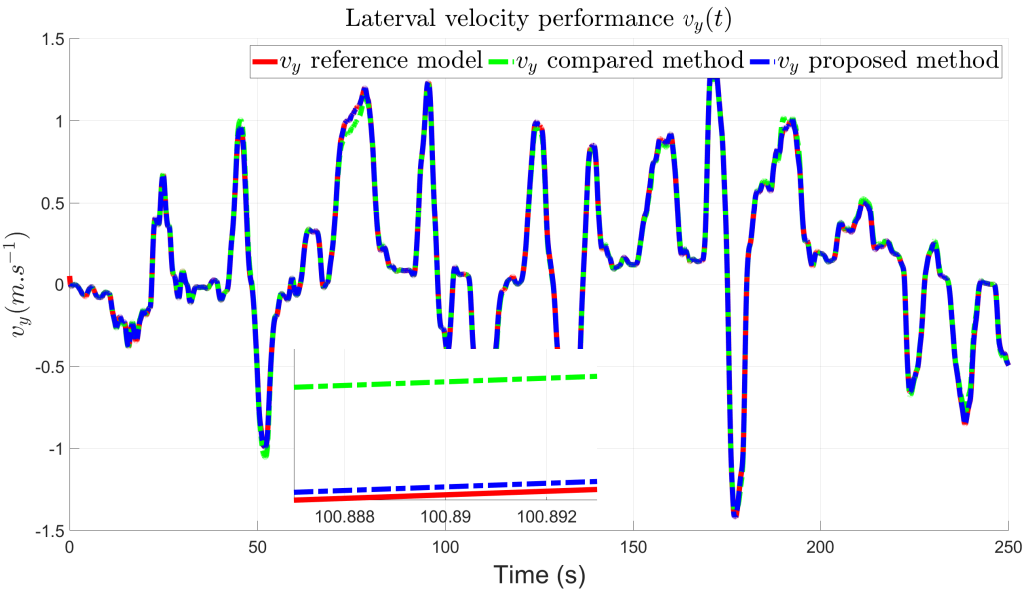

Figure 4.16: Comparison of lateral velocity $v_y(t)$ performance between the co-design approach with the separated method.

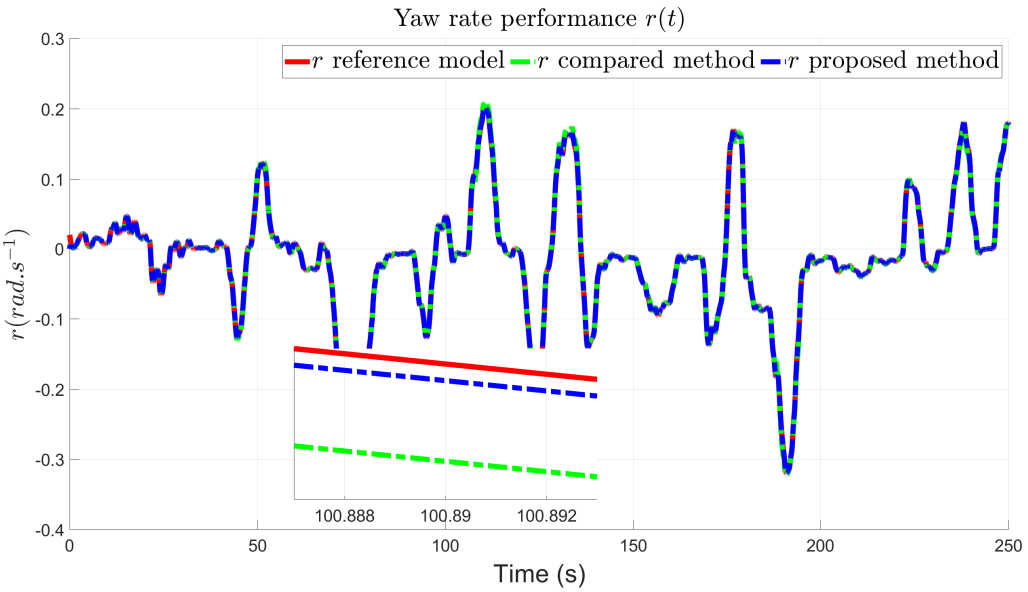

Figure 4.17: Comparison of yaw rate $r(t)$ performance between the co-design approach with the separated method.

These advancements are reasonable since the polytopic switched interval observers utilize the polytope to represent the range of possible system dynamics. This technique allows for more precise modeling of uncertainties and typically results in less conservative interval estimation, offering tighter and more accurate bounds.

4.4.2 Double Lane Change Maneuver

A typical maneuver when considering vehicle handling improvement is the double-lane change maneuver. During a double lane change test, the driver exerts a front-wheel steering angle $\delta_f(t)$ in order to react to an emergency situation such as an obstacle avoidance. This maneuver excites the transient handling dynamics.

In this case, three subsystems corresponding to three different longitudinal velocity subregions are also considered with switching signal $\sigma(t)$ given as follows:

$$\sigma(t) = \begin{cases} 1, & v_x \in [\ 2.5 \quad 7.5\ ](m/s) \\ 2, & v_x \in [\ 7.5 \quad 12.5\ ](m/s) \\ 3, & v_x \in [\ 12.5 \quad 17.5\ ](m/s) \end{cases} \tag{4.108}$$

The switching signal is shown in Figure 4.18.

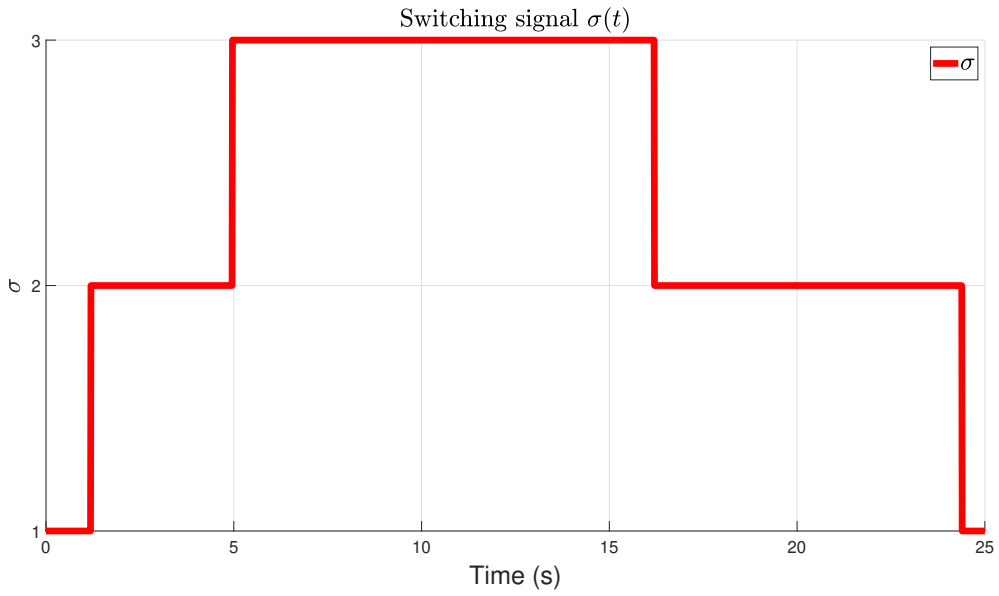

Figure 4.18: Front steering angle profile $\delta_f(t)$.

The following scenario simulates a situation where the vehicle encounters an obstacle on the road and has to change lane to avoid it. The vehicle starts to steer left at $14sec$ with a steering angle of $0.616(rad)$, which moves it to the adjacent lane. After that, the vehicle steers right with a positive steering angle, which returns it to the previous lane. During this maneuver, the longitudinal velocity of the vehicle decreases to reduce the risk of collision as a result of braking. The steering angle and the longitudinal velocity profiles for this scenario are shown in Figure 4.19 and 4.20. For safety reasons, the driver has to manage the vehicle path in order to accomplish a successful double lane change maneuver so that the vehicle does not break the lane barrier at maximum forward speed while none of the tires lifts off the ground. During this maneuver, the vehicle is under a yaw moment fault signal depicted by the

solid red line in Figure 4.26.

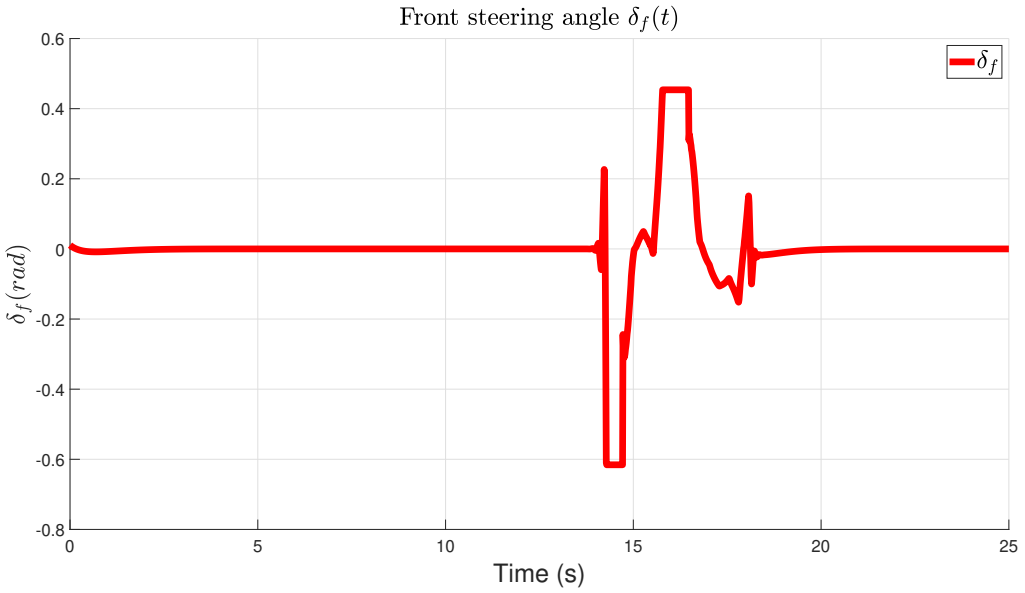

Figure 4.19: Front steering angle profile $\delta_f(t)$.

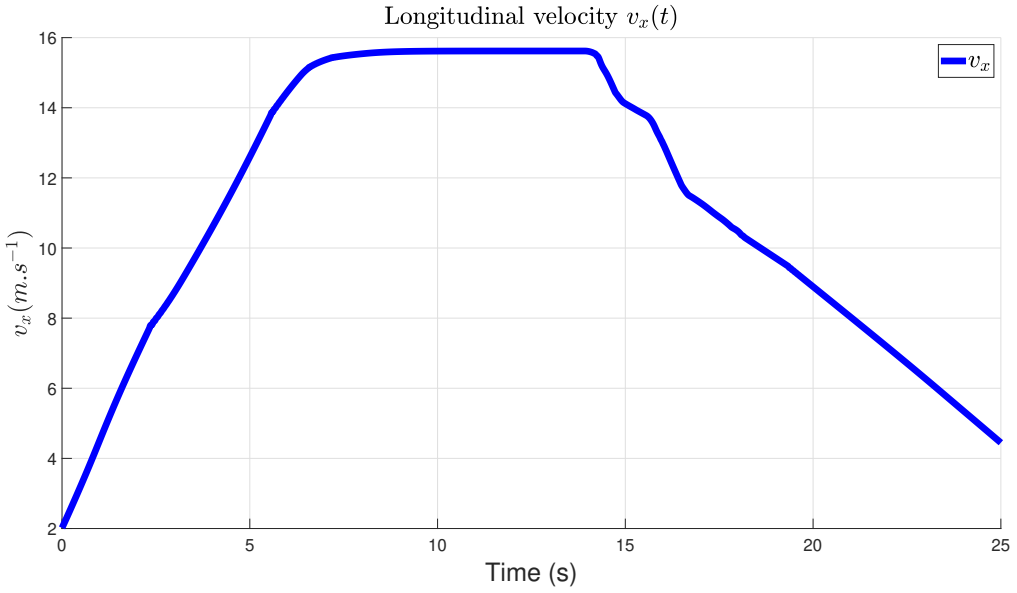

Figure 4.20: Longitudinal velocity profile $v_x(t)$.

The observer and controller gain matrices solved by a set of LMIs in Theorem 4.2 are obtained as follows:

$$\overline{N}_1^1 = \begin{bmatrix} -7.3651 & 3.4925 \\ 0 & -2.8930 \end{bmatrix}, \overline{N}_1^2 = \begin{bmatrix} -7.3651 & 3.4925 \\ 0 & -2.8930 \end{bmatrix} \tag{4.109}$$

$$\overline{N}_1^3 = \begin{bmatrix} -14.7302 & 7.2460 \\ 0 & -2.9456 \end{bmatrix}, \overline{N}_1^4 = \begin{bmatrix} -14.7302 & 7.2460 \\ 0 & -2.9456 \end{bmatrix} \tag{4.110}$$

$$\overline{N}_2^1 = \begin{bmatrix} -2.9460 & 4.5450 \\ 0 & -17.3889 \end{bmatrix}, \overline{N}_2^2 = \begin{bmatrix} -2.9460 & 4.5450 \\ 0 & -17.3889 \end{bmatrix} \tag{4.111}$$

$$\overline{N}_2^3 = \begin{bmatrix} -7.3651 & 7.5719 \\ 0 & -17.5414 \end{bmatrix}, \overline{N}_2^4 = \begin{bmatrix} -7.3651 & 7.5719 \\ 0 & -17.5414 \end{bmatrix} \tag{4.112}$$

$$\overline{N}_3^1 = \begin{bmatrix} -2.1043 & 3.4144 \\ 0 & -10.1027 \end{bmatrix}, \overline{N}_3^2 = \begin{bmatrix} -2.1043 & 3.4144 \\ 0 & -10.1027 \end{bmatrix} \tag{4.113}$$

$$\overline{N}_3^3 = \begin{bmatrix} -2.9460 & 4.0365 \\ 0 & -10.1081 \end{bmatrix}, \overline{N}_3^4 = \begin{bmatrix} -2.9460 & 4.0365 \\ 0 & -10.1081 \end{bmatrix} \tag{4.114}$$

$$\underline{N}_1^1 = \begin{bmatrix} -7.3651 & 3.5012 \\ 0 & -1.6607 \end{bmatrix}, \underline{N}_1^2 = \begin{bmatrix} -7.3651 & 3.5081 \\ 0 & -1.6607 \end{bmatrix} \tag{4.115}$$

$$\underline{N}_1^3 = \begin{bmatrix} -14.7302 & 7.2570 \\ 0 & -1.6909 \end{bmatrix}, \underline{N}_1^4 = \begin{bmatrix} -14.7302 & 7.2640 \\ 0 & -1.6909 \end{bmatrix} \tag{4.116}$$

$$\underline{N}_2^1 = \begin{bmatrix} -2.9460 & 3.5499 \\ 0 & -12.3795 \end{bmatrix}, \underline{N}_2^2 = \begin{bmatrix} -2.9460 & 2.6600 \\ 0 & -12.3795 \end{bmatrix} \tag{4.117}$$

$$\underline{N}_2^3 = \begin{bmatrix} -7.3651 & 6.4238 \\ 0 & -12.4881 \end{bmatrix}, \underline{N}_2^4 = \begin{bmatrix} -7.3651 & 5.5339 \\ 0 & -12.4881 \end{bmatrix} \tag{4.118}$$

$$\underline{N}_3^1 = \begin{bmatrix} -2.1043 & 2.7329 \\ 0 & -4.7564 \end{bmatrix}, \underline{N}_3^2 = \begin{bmatrix} -2.1043 & 2.5070 \\ 0 & -4.7564 \end{bmatrix} \tag{4.119}$$

$$\underline{N}_3^3 = \begin{bmatrix} -2.9460 & 3.3419 \\ 0 & -4.7589 \end{bmatrix}, \underline{N}_3^4 = \begin{bmatrix} -2.9460 & 3.1160 \\ 0 & -4.7589 \end{bmatrix} \tag{4.120}$$

$$\overline{K}_1 = 10^3 \begin{bmatrix} 0.6861 & 3.2374 \end{bmatrix}, \underline{K}_1 = 10^3 \begin{bmatrix} 0.6861 & 3.2061 \end{bmatrix} \tag{4.121}$$

$$\overline{K}_2 = 10^4 \begin{bmatrix} -6.5851 & 2.4203 \end{bmatrix}, \underline{K}_2 = 10^3 \begin{bmatrix} -6.5851 & 2.4203 \end{bmatrix} \tag{4.122}$$

$$\overline{K}_3 = 10^5 \begin{bmatrix} -1.4957 & 0.5771 \end{bmatrix}, \underline{K}_3 = 10^5 \begin{bmatrix} -1.4957 & 0.5771 \end{bmatrix} \tag{4.123}$$

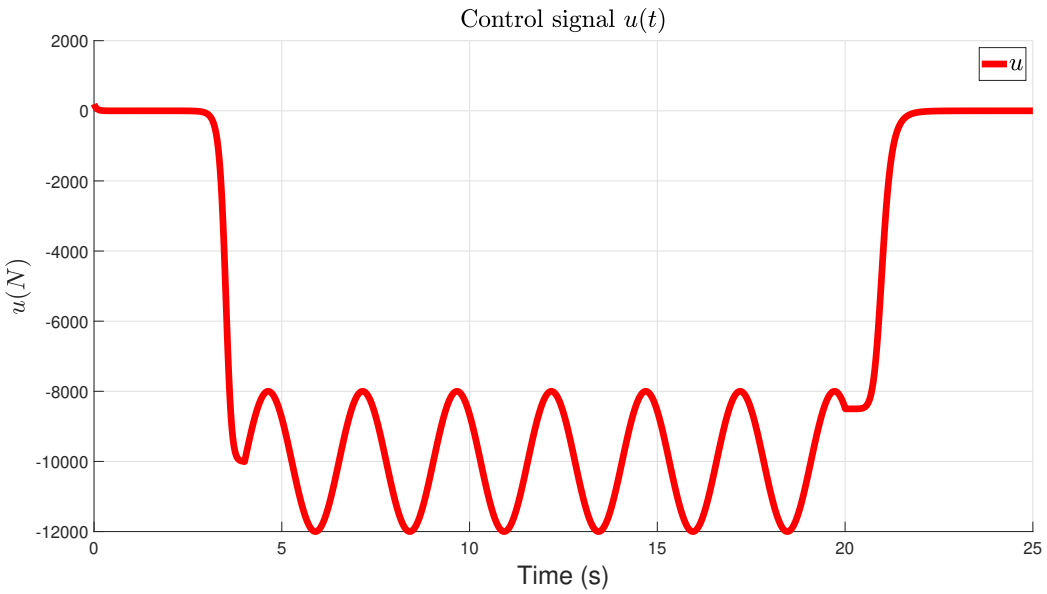

Figure 4.21: Yaw moment control input $u(t)$.

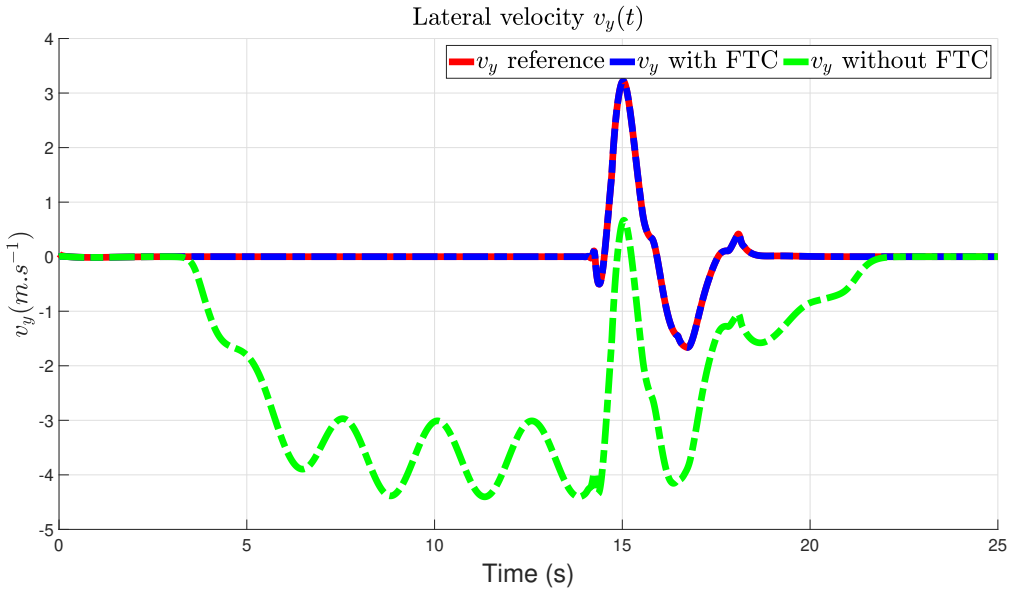

Figure 4.22: Comparison of lateral velocity $v_y(t)$ performance with and without FTC.

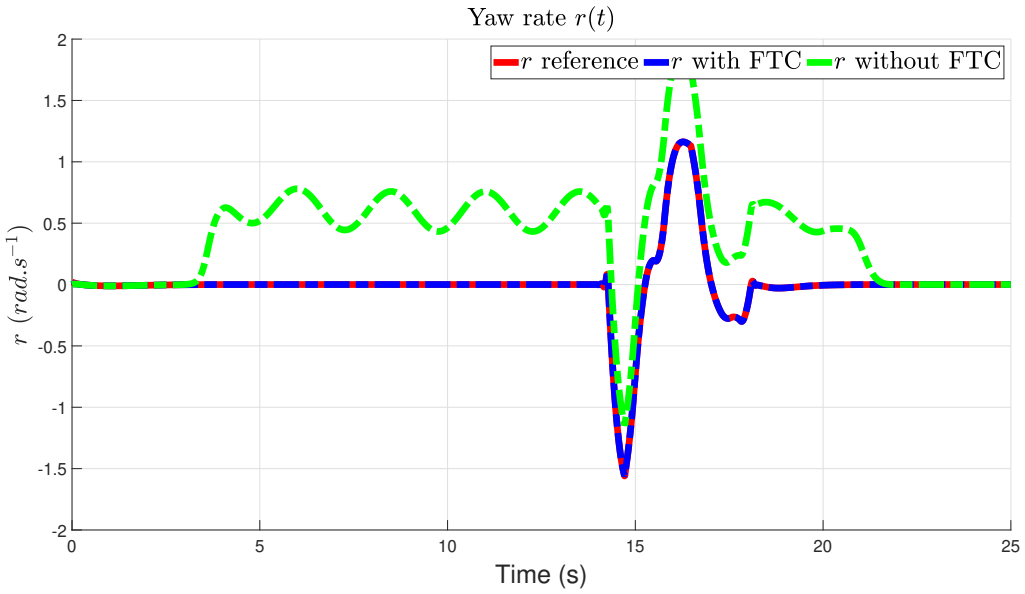

Figure 4.23: Comparison of yaw rate $r(t)$ performance with and without FTC.

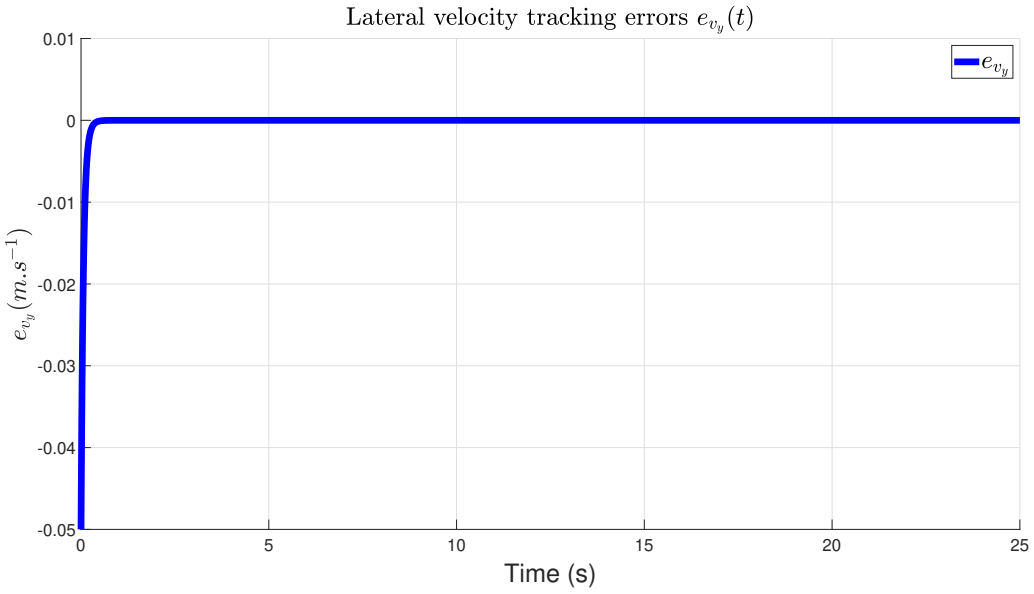

Figure 4.24: Lateral velocity tracking error $e_{v_y}(t)$.

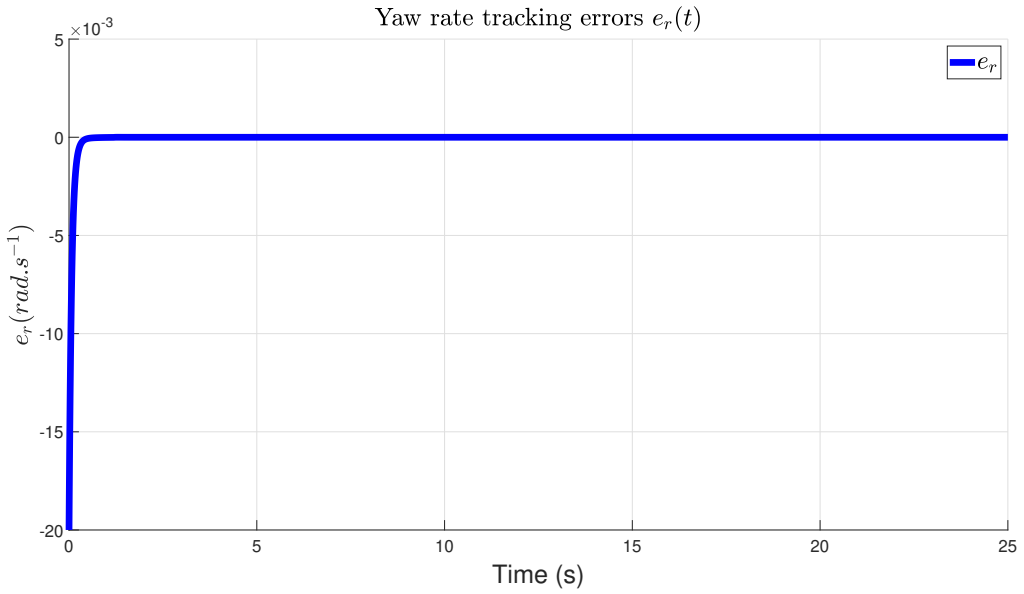

Figure 4.25: Yaw rate tracking error $e_r(t)$.

The fault interval reconstructions are illustrated in Figure 4.26. They show a good estimation of time-varying actuator fault. It is noted that the length of interval reconstruction of the unknown inputs depends on the estimation accuracy of the system states. When the driver performs the double lane change maneuver, the length of the interval of state increases. As a result, the fault interval length also increases from $14sec$ to $18sec$.

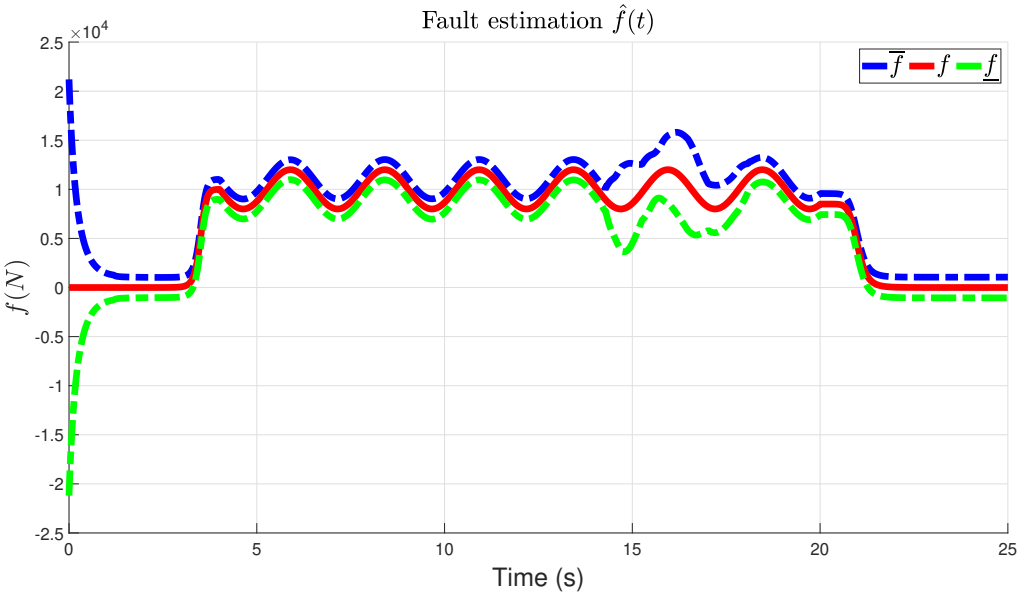

Figure 4.26: Actuator fault interval estimation.

Figure 4.27 and 4.28 show the lower and upper bounds of lateral velocity $v_y(t)$ and yaw rate $r(t)$. The dashed green and blue lines represent the lower and upper estimations, respectively, while the red line shows the actual state vectors. The lower and upper estimations still enclose the real state even when there is an actuator fault. In

addition, the decoupling approach can still successfully eliminate the impact of faults on the state estimation errors.

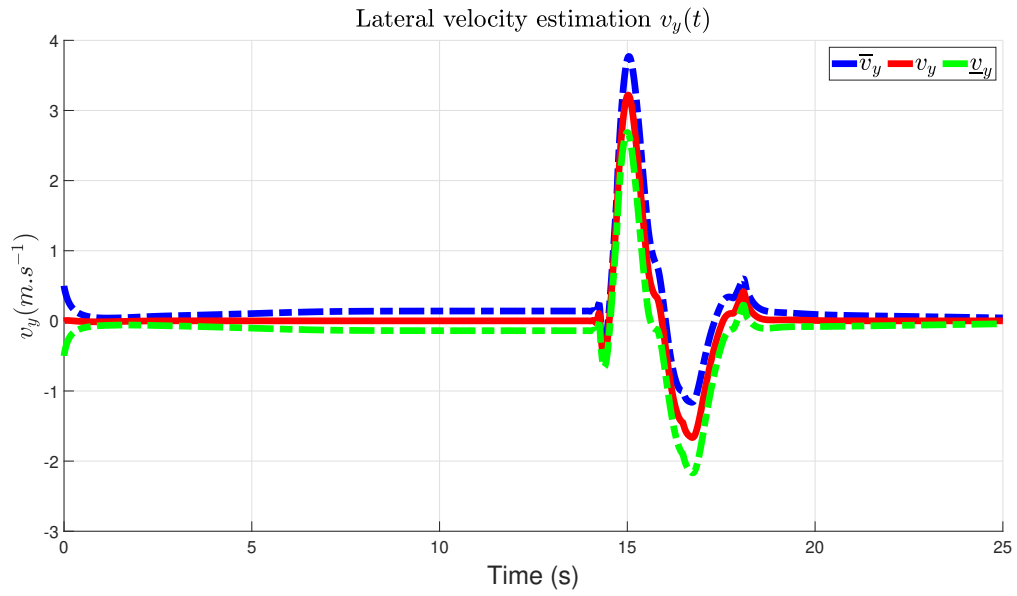

Figure 4.27: Lower and upper bounds of lateral velocity $v_y(t)$.

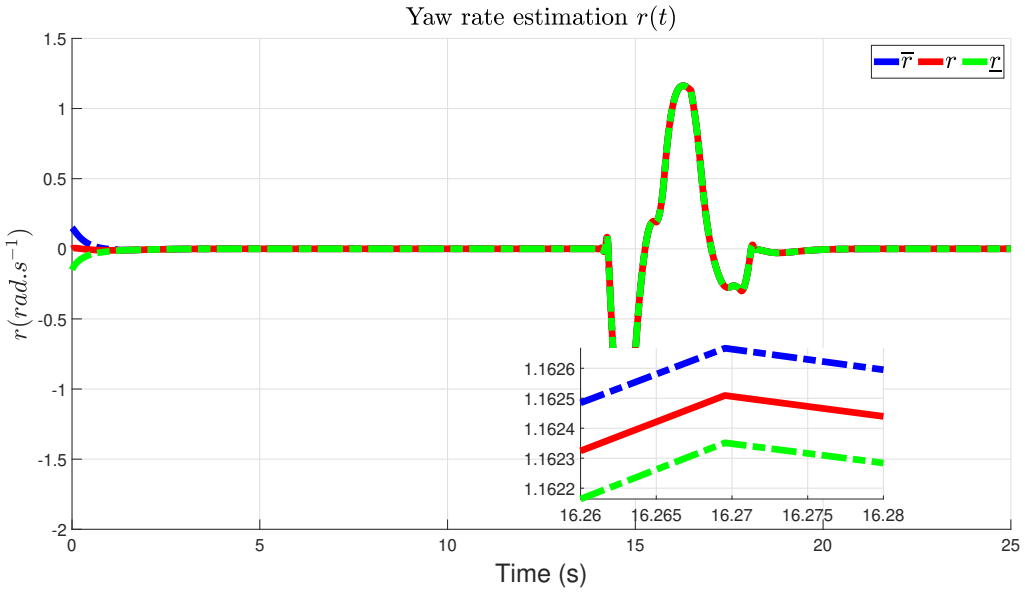

Figure 4.28: Lower and upper bounds of yaw rate $r(t)$.

The closed-loop system remains stable thanks to the fault-tolerant controller, and the FTC enables the vehicle to perform a double lane change maneuver to avoid obstacles safely even when actuator faults occur. The actual state well tracks the reference state as depicted in Figure 4.22 and 4.23 in which the dashed blue line and dashed green line are state vectors with and without the proposed method, respectively. One can see that the uncontrolled vehicle is not able to perform the double lane change maneuver. The faulty system without the proposed method fails to track the reference system and deviates significantly from the desired state. Concerning the controller vehicle, the

tracking errors are approximately zero as illustrated in Figure 4.24 and 4.25.

4.5 Conclusions

The presented approach makes a contribution to vehicle lateral dynamics fault-tolerant control using UI interval observers synthesis. First, the methodology proposed a polytopic Switched model of the vehicle dynamics for which an SUIIO is synthesized to robustly estimate the lower and upper bounds of the state vector in the face of unknown inputs and faults. Thereafter, an algebraic relationship is established to reconstruct the unknown input interval estimation. Finally, a fault-tolerant control law is synthesized to compensate for the effects of actuator faults and ensure the system performance. The approach uses multiple ISS-Lyapunov functions in conjunction with average dwell time, which yields less conservative conditions. This integration, coupled with Linear Matrix Inequalities (LMIs), is instrumental in determining observer gain matrices to guarantee the stability and positivity properties of the interval observer. The effectiveness of the proposed approach is demonstrated through different simulation scenarios. The consideration of parameter-dependence Lyapunov function within the proposed approach is an appealing direction for further research.

Chapter 5

Interval Observer-based Active Fault-Tolerant Control For Discrete-Time Uncertain Switched LPV Systems

Chapter abstract

This chapter presents a novel method for co-designing TNL interval observer and fault tolerant control for discrete-time switched linear parameter varying (LPV) systems with faults and unknown but bounded uncertainties, state disturbances and measurement noise. Introducing the weighting matrices T and N provides further degree of freedom for the calculation of the observer gain matrices to guarantee the cooperative condition of the estimation errors. By considering the fault in an augmented state vector, the TNL interval observer jointly estimates the lower and upper bounds of system state and faults. The fault-tolerant controller (FTC) is designed to compensate the estimated fault and stabilize the closed-loop system in the presence of faults. The sufficient conditions for the stability of the proposed methodology are formulated in terms of Linear Matrix Inequalities (LMIs) obtained using Input-to-State-Stability (ISS) property with multiple Lyapunov functions and Average Dwell Time (ADT). The proposed approach is successfully applied to the problem of estimating and controlling vehicle lateral dynamics. The results demonstrate its efficiency for estimating the lateral speed with a tight interval between the lower and the upper bounds while achieving the control of the yaw rate.

5.1 Introduction

5.1.1 State of the art

Observer-based controller is an important topic in theory of modern control. It has been widely applied in various fields such as aerospace, robotics, and automotive. In real-world scenarios, it is inevitable for the system to encounter faults that may have impacts on its stability and performance. These faults can include unidentified actuator or sensor faults, component malfunctions or external perturbations from the environment that may lead to undesirable behaviors or even catastrophic failures for the system. Therefore, it is essential to design a robust and reliable approach to estimate and compensate for such failures. To deal with this challenging task, a common approach is to synthesize an observer-based fault-tolerant controller which employs observers to simultaneously estimate both the states and faults of the system and then design feedback FTC to compensate for the fault effects and achieve the desired performance [177].

Moreover, systems are subject to process disturbances, measurement noise and modeling uncertainties which introduce significant errors in unmeasured state estimation. Therefore, conventional observers may struggle to cope well with the challenges of state estimation issues effectively [178]. This motivated the development of robust estimation methods such as interval observer for different classes of systems.

The concept of interval observer has been an active area of research in the last decades as they have numerous applications in control and estimation theory [179, 38, 180]. Unlike traditional observers, the interval observer is a pair of estimators that provide the estimates of the lower and upper bounds of state at any instant of time. Interval observer synthesis requires both stability and inclusion properties. When using classical design methods, it is not straightforward to find the observer gain matrices to satisfy both Hurwitz and Metzler conditions. To deal with this difficulty, recent research, as reported in [181], [33], [182] have investigated the utilization of coordinate transformation to relax the cooperative property of the interval observer. Although the obtained results can provide more flexibility for design conditions and reduce the conservatism, the interval observer performance is heavily affected by selecting the non-singular transfer matrix [183].

To overcome this limitation, a novel methodology called TNL is proposed to deal with the challenge of ensuring the cooperative property of the interval observer. The key idea, in addition to the traditional observer gain, is to introduce a weighting matrix, which gives more flexibility to make the lower and upper estimation errors positive without resorting to the change of coordinates.

Numerous achievements for TNL observers have been researched. For example, the study in [184], [185] designed a new interval observer structure to estimate the lower and upper bounds of system state for discrete-time linear systems with process disturbance and measurement noise. However, the limitation of these works is that they did not take into consideration uncertainties in parameters which may affect the performance of the observers in some realistic scenarios. The work in [122], [186] extended the TNL interval observer for continuous-time LPV

system with parametric uncertainties while minimizing their influence and obtained a tight state interval. Authors in [187] considered TNL interval observer for joint estimation of the state and unknown input by considering the unknown input as an auxiliary state for discrete-time LPV system and for continuous-time switched system [188]. However, all the aforementioned approaches are only dedicated to the problem of state and fault estimation and did not address the issue of FTC for systems with state disturbances and measurement noise. To fill this gap, the study in [135] investigated the design problem of an active FTC for discrete-time LPV system subject to disturbance and measurement noise. The state and fault are simultaneously estimated by an augmented system. The interval observer synthesis and FTC are however separately designed by two sets of LMIs. It may lead to instability when put together [138].

5.1.2 Chapter contribution

This chapter proposes a constructive methodology to design a TNL interval observer and fault-tolerant controller for uncertain discrete-time linear parameter varying (LPV) switched systems represented under polytopic form with unknown but bounded state disturbances and measurement noise. The main contributions of this chapter are listed as follows:

- An extension of the results from [186, 187] on interval observer for uncertain discrete-time switched LPV system subject to faults and unknown but bounded disturbances and measurement noise.
- Based on the estimated variables, an integrated design of the interval observer and fault tolerant control law is developed synthesized to stabilize the closed-loop system and to compensate the fault effects. As previously outlined, in [135] the design of the observer and controller are treated as separate tasks. Instead, in this chapter, the observer and FTC are co-designed.
- Less conservative conditions compared to change of coordinates approach as discussed in [189]. In other words, the TNL interval observer synthesis procedure provides more degrees of freedom in computing the observer gains is designed to simultaneously estimate the lower and upper bounds of the system state and faults through an augmented system.
- The sufficient conditions for the stability and co-operativity of the proposed interval observer and associated FTC are formulated using switched ISS-Lyapunov functions under Average Dwell-Time (ADT). They are expressed in terms of Linear Matrix Inequalities (LMIs).

Finally, an application to the lateral vehicle dynamics is considered in order to evaluate the relevance and efficiency of the proposed approach.

The chapter is organized as follows: preliminaries and problem formulation are given in Section 5.2. Section 5.3 provides the main contribution with the design procedure of a TNL interval observer-based controller for uncertain

discrete-time switched LPV systems subject to faults and unknown but bounded state disturbances and measurement noises. Simulation results of the proposed technique are described in Section 5.4. Finally, the conclusion and future works are detailed in Section 5.5.

5.2 Problem formulation

Consider the uncertain discrete-time switched LPV system:

$$\begin{cases} x(k+1) = \mathcal{A}_{\sigma(k)}(\rho(k))x(k) + \mathcal{B}_{\sigma(k)}(\rho(k))u(k) + F_{\sigma(k)}f(k) + \mathcal{D}^{w}_{\sigma(k)}w(k) \\ \qquad y_k = \mathcal{C}x(k) + D^{v}_{\sigma(k)}v(k) \end{cases} \tag{5.1}$$

where $x(k) \in \mathbb{R}^{n_x}$ is the system state, $u(k) \in \mathbb{R}^{n_u}$ is control input, $f(k) \in \mathbb{R}^{n_f}$ is fault vectors, $w(k) \in \mathbb{R}^{n_w}$ is disturbance vector, $v(k) \in \mathbb{R}^{n_v}$ is measurement noise, $y(k) \in \mathbb{R}^{n_y}$ is system output. Switching signal $\sigma(k) \in \mathcal{N} = \{1, \ldots, N\}$ with N is the number of subsystems.

The initial state condition $x(k_0)$ is bounded by two known vectors $\overline{x}(k_0)$ and $\underline{x}(k_0)$, i.e.

$$\underline{x}(k_0) \leq x(k_0) \leq \overline{x}(k_0) \tag{5.2}$$

The state disturbance $w(k)$ and measurement noise $v(k)$ are assumed to be unknown but bounded by $\underline{w}(k)$ and $\overline{w}(k)$, $\underline{v}(k)$ and $\overline{v}(k)$.

$$\begin{aligned} \underline{w}(k) \leq w(k) \leq \overline{w}_(k) \\ \underline{v}(k) \leq v(k) \leq \overline{v}(k) \end{aligned} \tag{5.3}$$

for some known $\underline{w}(k)$ and $\overline{w}(k)$, $\underline{v}(k)$ and $\overline{v}(k)$.

Matrices $\mathcal{A}_{\sigma(k)}(\rho(k)) \in \mathbb{R}^{n_x \times n_x}$, $\mathcal{B}_{\sigma(k)}(\rho(k)) \in \mathbb{R}^{n_x \times n_u}$ are parameter varying matrices of appropriate dimension. Matrices $F_{\sigma(k)} \in \mathbb{R}^{n_x \times n_f}$, $\mathcal{D}^{w}_{\sigma(k)} \in \mathbb{R}^{n_x \times n_w}$, $D^{v}_{\sigma(k)} \in \mathbb{R}^{n_y \times n_v}$ are switching constant matrices and without loss of generality, the output matrix $\mathcal{C}$ is constant matrix for all $\sigma(k) \in \mathcal{N}$.

Time-varying parameters $\rho(k) = [\rho_1(k), \rho_2(k), ..., \rho_P(k)]$ is assumed to be measurable vectors with P is the number of scheduling parameters and $\rho(k) \in [\underline{\rho}(k), \overline{\rho}(k)]$ for all $k = 1 \cdots P$ then it evolves inside a polytope represented by 2^P vertices. The switched weighting function $\mu^{j}_{\sigma(k)}(\rho(k))$ guarantees convex sum property for all $\sigma(k) \in \mathcal{N}$ and $j \in \mathcal{P} = \{1, \cdots, 2^P\}$

$$\begin{cases} 0 \leq \mu^{j}_{\sigma(k)}(\rho(k)) \leq 1 \\ \sum_{j=1}^{2^P} \mu^{j}_{\sigma(k)}(\rho(k)) = 1 \end{cases} \tag{5.4}$$

The system matrices of system (5.1) are exactly represented under polytopic form:

$$\mathcal{M}_{\sigma(k)}(\rho(k)) = \sum_{j=1}^{2^P} \mu^j_{\sigma(k)}(\rho(k))\mathcal{M}^j_{\sigma(k)} \tag{5.5}$$

where $\mathcal{M} \in \{\mathcal{A}, \mathcal{B}\}$.

We introduce now lemmas which are necessary to prove the main results.

Lemma 5.1 *[190] Let $x(k) \in \mathbb{R}^{n_x}$ be a vector such that $\underline{x}(k) \leq x(k) \leq \overline{x}(k)$ for some $\underline{x}(k), \overline{x}(k) \in \mathbb{R}^{n_x}$. If $\mathcal{A} \in \mathbb{R}^{n_m \times n_x}$ is a constant matrix, then:*

$$\mathcal{A}^+\underline{x}(k) - \mathcal{A}^-\overline{x}(k) \leq \mathcal{A}x(k) \leq \mathcal{A}^+\overline{x}(k) - \mathcal{A}^-\underline{x}(k) \tag{5.6}$$

If $\mathcal{A} \in \mathbb{R}^{n_m \times n_x}$ is a variable matrix such that $\underline{\mathcal{A}} \leq \mathcal{A} \leq \overline{\mathcal{A}}$ for some $\underline{\mathcal{A}}, \overline{\mathcal{A}} \in \mathbb{R}^{m \times n_x}$, then:

$$\begin{aligned} &\underline{\mathcal{A}}^+\underline{x}^+(k) - \overline{\mathcal{A}}^+\underline{x}^-(k) - \underline{\mathcal{A}}^-\overline{x}^+(k) + \overline{\mathcal{A}}^-\overline{x}^-(k) \leq \mathcal{A}x(k) \leq \\ &\overline{\mathcal{A}}^+\overline{x}^+(k) - \underline{\mathcal{A}}^+\overline{x}^-(k) - \overline{\mathcal{A}}^-\underline{x}^+(k) + \underline{\mathcal{A}}^-\underline{x}^-(k) \end{aligned} \tag{5.7}$$

Lemma 5.2 *[191] The switched system* (2.43) *is Input-to-State-Stable with respect to disturbance $\delta_i(k)$ if the following inequalities*

$$\begin{aligned} \alpha\|x(k)\|^2 \leq V_i(x(k)) \leq \beta\|x(k)\|^2 \\ \Delta V_i(x(k)) < -\varepsilon V_i(x(k)) + \gamma_i\|\delta_i(k)\| \end{aligned} \tag{5.8}$$

hold for any $\sigma(k) = i \in \mathcal{N}$ with $0 < \alpha < \beta$, $0 < \varepsilon < 1$, $\gamma_i > 0$ and $\sigma(k)$ is switching signal with average dwell time

$$\tau_a \geq \tau_a^* = -\frac{\ln(\mu)}{\ln(1-\varepsilon)} \tag{5.9}$$

where $\mu = \frac{\beta}{\alpha}$.

5.3 TNL Interval Observer-Based Fault Tolerant Control

In this section, a new co-design approach of observer and controller for a class of discrete-time switched LPV systems is presented. The TNL interval observer is proposed to simultaneously estimate the lower and upper bounds of state $x(k)$ and faults $f(k)$, and an FTC is synthesized to stabilize the closed-loop system in the presence of faults.

Before proceeding with the interval observer design, an augmented state $z(k)$ incorporating the original state

$x(k)$ and fault $f(k)$ into a single vector to facilitate simultaneous estimation is introduced.

$$z(k) = \begin{bmatrix} x(k) \\ f(k-1) \end{bmatrix} \tag{5.10}$$

The system (5.1) is then rewritten under the augmented form:

$$\begin{cases} E_{\sigma(k)} z(k+1) = A_{\sigma(k)}(\rho(k)) z(k) + B_{\sigma(k)}(\rho(k)) u(k) + D^w_{\sigma(k)} w(k) \\ y(k) = Cz(k) + D^v_{\sigma(k)} v(k) \end{cases} \tag{5.11}$$

where $E_{\sigma(k)} = \begin{bmatrix} I_{n_x} & -F_{\sigma(k)} \\ 0 & 0 \end{bmatrix}$, $A_{\sigma(k)}(\rho(k)) = \begin{bmatrix} \mathcal{A}_{\sigma(k)}(\rho(k)) & 0 \\ 0 & 0 \end{bmatrix}$, $B_{\sigma(k)}(\rho(k)) = \begin{bmatrix} \mathcal{B}_{\sigma(k)}(\rho(k)) \\ 0 \end{bmatrix}$, $D^w_{\sigma(k)} = \begin{bmatrix} \mathcal{D}^w_{\sigma(k)} \\ 0 \end{bmatrix}$, $C = \begin{bmatrix} \mathcal{C} & 0 \end{bmatrix}$.

Noted that, once the augmented state $z(k)$ is well estimated, the estimation of $x(k)$ and $f(k)$ can be obtained simultaneously from the construction (5.10). Therefore, the interval observer design procedure aimed at estimating both the lower and upper bounds of the state $x(k)$ and fault $f(k)$ for system (5.1) is turned into the problem of interval estimation of state $z(k)$ for the system (5.11).

To proceed, the following TNL interval observer structure for the augmented system (5.11) is proposed:

$$\begin{cases} \overline{\xi}(k+1) = \overline{T}_{\sigma(k)} A_{\sigma(k)}\big(\rho(k)\big)\overline{z}(k) + \overline{T}_{\sigma(k)} B_{\sigma(k)}\big(\rho(k)\big) u(k) + \overline{\nabla}_{\sigma(k)}(k) \\ \qquad\qquad + \overline{L}_{\sigma(k)}\big(\rho(k)\big)\big(y(k) - C\overline{z}(k)\big) \\ \quad \overline{z}(k) = \overline{\xi}(k) + \overline{N}_{\sigma(k)} y(k) \\ \underline{\xi}(k+1) = \underline{T}_{\sigma(k)} A_{\sigma(k)}\big(\rho(k)\big)\underline{z}(k) + \underline{T}_{\sigma(k)} B_{\sigma(k)}\big(\rho(k)\big) u(k) + \underline{\nabla}_{\sigma(k)}(k) \\ \qquad\qquad + \underline{L}_{\sigma(k)}\big(\rho(k)\big)\big(y(k) - C\underline{z}(k)\big) \\ \quad \underline{z}(k) = \underline{\xi}(k) + \underline{N}_{\sigma(k)} y(k) \end{cases} \tag{5.12}$$

where $\underline{\xi}(k)$ and $\overline{\xi}(k)$ are the lower and upper state vectors of the observer, $\underline{z}(k)$ and $\overline{z}(k)$ denote the lower and upper bounds of augmented state $z(k)$. Matrices $\underline{T}_{\sigma(k)} \in \mathbb{R}^{(n_x+n_f)\times(n_x+n_f)}$ and $\overline{T}_{\sigma(k)} \in \mathbb{R}^{(n_x+n_f)\times(n_x+n_f)}$, $\underline{L}_{\sigma(k)}\big(\rho(k)\big) \in \mathbb{R}^{(n_x+n_f)\times n_y}$ and $\overline{L}_{\sigma(k)}\big(\rho(k)\big) \in \mathbb{R}^{(n_x+n_f)\times n_y}$, $\underline{N}_{\sigma(k)} \in \mathbb{R}^{(n_x+n_f)\times n_y}$ and $\overline{N}_{\sigma(k)} \in \mathbb{R}^{(n_x+n_f)\times n_y}$ are unknown matrices of compatible dimension to be designed to satisfy the following relations.

$$\begin{cases} \underline{T}_{\sigma(k)} E_{\sigma(k)} + \underline{N}_{\sigma(k)} C = I_{n_x+n_f} \\ \overline{T}_{\sigma(k)} E_{\sigma(k)} + \overline{N}_{\sigma(k)} C = I_{n_x+n_f} \end{cases} \tag{5.13}$$

The terms $\overline{\nabla}_{\sigma(k)}(k)$ and $\underline{\nabla}_{\sigma(k)}(k)$ appearing (5.12) are chosen as

$$\begin{cases} \overline{\nabla}_{\sigma(k)}(k) = \overline{T}^{+}_{\sigma(k)}\overline{\delta}_{\sigma(k)}(k) - \overline{T}^{-}_{\sigma(k)}\underline{\delta}_{\sigma(k)}(k) \\ \qquad\qquad - \Big(\big(\overline{L}_{\sigma(k)}(\rho(k))D^{v}_{\sigma(k)}\big)^{+}\underline{v}(k) - \big(\overline{L}_{\sigma(k)}(\rho(k))D^{v}_{\sigma(k)}\big)^{-}\overline{v}(k)\Big) \\ \qquad\qquad - \Big(\big(\overline{N}_{\sigma(k)}D^{v}_{\sigma(k)}\big)^{+}\underline{v}(k+1) - \big(\overline{N}_{\sigma(k)}D^{w}_{\sigma(k)}\big)^{-}\overline{v}(k+1)\Big) \\ \underline{\nabla}_{\sigma(k)}(k) = \underline{T}^{+}_{\sigma(k)}\underline{\delta}_{\sigma(k)}(k) - \underline{T}^{-}_{\sigma(k)}\overline{\delta}_{\sigma(k)}(k) \\ \qquad\qquad - \Big(\big(\underline{L}_{\sigma(k)}(\rho(k))D^{v}_{\sigma(k)}\big)^{+}\overline{v}(k) - \big(\underline{L}_{\sigma(k)}(\rho(k))D^{v}_{\sigma(k)}\big)^{-}\underline{v}(k)\Big) \\ \qquad\qquad - \Big(\big(\underline{N}_{\sigma(k)}D^{v}_{\sigma(k)}\big)^{+}\overline{v}(k+1) - \big(\underline{N}_{\sigma(k)}D^{v}_{\sigma(k)}\big)^{-}\underline{v}(k+1)\Big) \end{cases} \tag{5.14}$$

where $\overline{\delta}_{\sigma(k)}(k)$ and $\underline{\delta}_{\sigma(k)}(k)$ are the upper and lower bounds of $\delta_{\sigma(k)}(k) = D^{w}_{\sigma(k)}w(k)$ determined under conditions 5.2, 5.3 and lemma 5.1.

$$\begin{cases} \overline{\delta}_{\sigma(k)}(k) = {D^{w}_{\sigma(k)}}^{+}\overline{w}(k) - {D^{w}_{\sigma(k)}}^{-}\underline{w}(k) \\ \underline{\delta}_{\sigma(k)}(k) = {D^{w}_{\sigma(k)}}^{+}\underline{w}(k) - {D^{w}_{\sigma(k)}}^{-}\overline{w}(k) \end{cases} \tag{5.15}$$

From (5.12), $\overline{z}(k+1)$ and $\underline{z}(k+1)$ are expressed as follows:

$$\begin{cases} \overline{z}(k+1) = \overline{T}_{\sigma(k)}A_{\sigma(k)}\big(\rho(k)\big)\overline{z}(k) + \overline{T}_{\sigma(k)}B_{\sigma(k)}\big(\rho(k)\big)u(k) + \overline{\nabla}_{\sigma(k)}(k) + \overline{L}_{\sigma(k)}\big(\rho(k)\big)\big(y(k) - C\overline{z}(k)\big) \\ \qquad\qquad + \overline{N}_{\sigma(k)}\big(Cz(k+1) + D^{v}_{\sigma(k)}v(k+1)\big) \\ \underline{z}(k+1) = \underline{T}_{\sigma(k)}A_{\sigma(k)}\big(\rho(k)\big)\underline{z}(k) + \underline{T}_{\sigma(k)}B_{\sigma(k)}\big(\rho(k)\big)u(k) + \underline{\nabla}_{\sigma(k)}(k) + \underline{L}_{\sigma(k)}\big(\rho(k)\big)\big(y(k) - C\underline{z}(k)\big) \\ \qquad\qquad + \overline{N}_{\sigma(k)}\big(Cz(k+1) + D^{v}_{\sigma(k)}v(k+1)\big) \end{cases} \tag{5.16}$$

First of all, let's define the upper and lower estimation errors as follows:

$$\begin{cases} \overline{e}(k) = \overline{z}(k) - z(k) \\ \underline{e}(k) = z(k) - \underline{z}(k) \end{cases} \tag{5.17}$$

From (5.11), (5.16) and (5.17), their dynamics are given as:

$$\begin{cases} \overline{e}(k+1) = \Big(\overline{T}_{\sigma(k)}A_{\sigma(k)}\big(\rho(k)\big) - \overline{L}_{\sigma(k)}\big(\rho(k)\big)C\Big)\overline{e}(k) + \overline{\nabla}_{\sigma(k)}(k) + \overline{N}_{\sigma(k)}D^{v}_{\sigma(k)}v(k+1) \\ \qquad\qquad - \overline{T}_{\sigma(k)}D^{w}_{\sigma(k)}w(k) + \overline{L}_{\sigma(k)}\big(\rho(k)\big)D^{v}_{\sigma(k)}v(k) \\ \underline{e}(k+1) = \Big(\underline{T}_{\sigma(k)}A_{\sigma(k)}\big(\rho(k)\big) - \underline{L}_{\sigma(k)}\big(\rho(k)\big)C\Big)\underline{e}(k) - \underline{\nabla}_{\sigma(k)}(k) - \underline{N}_{\sigma(k)}D^{v}_{\sigma(k)}v(k+1) \\ \qquad\qquad + \underline{T}_{\sigma(k)}D^{w}_{\sigma(k)}w(k) - \underline{L}_{\sigma(k)}\big(\rho(k)\big)D^{v}_{\sigma(k)}v(k) \end{cases} \tag{5.18}$$

The aim is to prove that $\underline{e}(k)$ and $\overline{e}(k)$ are non-negative.

Based on lemma 5.1 and the terms $\underline{\nabla}_{\sigma(k)}(k)$ and $\overline{\nabla}_{\sigma(k)}(k)$ in (5.14), the following terms are non-negative.

$$\begin{cases} \overline{\nabla}_{\sigma(k)}(k) + \overline{N}_{\sigma(k)} D^{v}_{\sigma(k)} v(k+1) - \overline{T}_{\sigma(k)} \delta_{\sigma(k)}(k) + \overline{L}_{\sigma(k)}\big(\rho(k)\big) D^{v}_{\sigma(k)} v(k) \geq 0 \\ -\underline{\nabla}_{\sigma(k)}(k) - \underline{N}_{\sigma(k)} D^{v}_{\sigma(k)} v(k+1) + \underline{T}_{\sigma(k)} \delta_{\sigma(k)}(k) - \underline{L}_{\sigma(k)}\big(\rho(k)\big) D^{v}_{\sigma(k)} v(k) \geq 0 \end{cases} \tag{5.19}$$

Moreover, with the initial state condition 5.2, $\underline{x}(k_0) \leq x(k_0) \leq \overline{x}(k_0)$ indicate that $\underline{z}(k_0) \leq z(k_0) \leq \overline{z}(k_0)$ due to the construction. It implies that the initial augmented state conditions are non-negative, i.e. $\underline{e}(k_0) = z(k_0) - z(k_0) \geq 0$ and $\overline{e}(k_0) = \overline{z}(k_0) - z(k_0) \geq 0$. Therefore, the error system (5.18) is a positive system thanks to lemma 2.7 if $\underline{T}_{\sigma(k)} A_{\sigma(k)}\big(\rho(k)\big) - \underline{L}_{\sigma(k)}\big(\rho(k)\big) C$ and $\overline{T}_{\sigma(k)} A_{\sigma(k)}\big(\rho(k)\big) - \overline{L}_{\sigma(k)}\big(\rho(k)\big) C$ are nonnegative matrices for all $\sigma(k) \in \mathcal{N}$.

In addition to the cooperativity property of estimation errors, it is essential for both $\underline{T}_{\sigma(k)} A_{\sigma(k)}\big(\rho(k)\big) - \underline{L}_{\sigma(k)}\big(\rho(k)\big) C$ and $\overline{T}_{\sigma(k)} A_{\sigma(k)}\big(\rho(k)\big) - \overline{L}_{\sigma(k)}\big(\rho(k)\big) C$ to be Schur stable. This condition ensures that the interval error, defined as $e(k) = \overline{e}(k) - \underline{e}(k)$ approaches zero asymptotically in the nominal case and obtains a tight interval error in other cases.

Remark 5.1 *If matrices $\underline{T}_{\sigma(k)}$, $\overline{T}_{\sigma(k)}$ are set to identity matrices and $\underline{N}_{\sigma(k)}$, $\overline{N}_{\sigma(k)}$ are set to zero then the TNL interval observer* (5.12) *becomes the Luenberger interval observer.*

$$\begin{cases} \overline{z}(k+1) = \Big(A_{\sigma(k)}\big(\rho(k)\big) - \overline{L}_{\sigma(k)}\big(\rho(k)\big) C\Big) \overline{z}(k) + B_{\sigma(k)}\big(\rho(k)\big) u(k) + \overline{L}_{\sigma(k)}\big(\rho(k)\big) y(k) + \overline{\nabla}_{\sigma(k)}(k) \\ \underline{z}(k+1) = \Big(A_{\sigma(k)}\big(\rho(k)\big) - \underline{L}_{\sigma(k)}\big(\rho(k)\big) C\Big) \underline{z}(k) + B_{\sigma(k)}\big(\rho(k)\big) u(k) + \underline{L}_{\sigma(k)}\big(\rho(k)\big) y(k) + \underline{\nabla}_{\sigma(k)}(k) \end{cases} \tag{5.20}$$

Obviously, the advantage of the proposed TNL interval observer is that introducing matrices $\underline{T}_{\sigma(k)}$, $\overline{T}_{\sigma(k)}$ and $\underline{N}_{\sigma(k)}$, $\overline{N}_{\sigma(k)}$ gives an alternative solution in the cases when it is impossible to find the observer gains $\underline{L}_{\sigma(k)}\big(\rho(k)\big)$ and $\overline{L}_{\sigma(k)}\big(\rho(k)\big)$ such that $A_{\sigma(k)}\big(\rho(k)\big) - \underline{L}_{\sigma(k)}\big(\rho(k)\big) C$ and $A_{\sigma(k)}\big(\rho(k)\big) - \overline{L}_{\sigma(k)}\big(\rho(k)\big) C$ are Schur stable and nonnegative matrices. Consequently, the proposed methodology, in addition to offering tight intervals, is less conservative.

5.3.1 Observer matrices determination

The equation (5.13) is rewritten as:

$$\begin{cases} \begin{bmatrix} \underline{T}_{\sigma(k)} & \underline{N}_{\sigma(k)} \end{bmatrix} \Omega_{\sigma(k)} = I_{n_x+n_f} \\ \begin{bmatrix} \overline{T}_{\sigma(k)} & \overline{N}_{\sigma(k)} \end{bmatrix} \Omega_{\sigma(k)} = I_{n_x+n_f} \end{cases} \tag{5.21}$$

with $\Omega_{\sigma(k)} = \begin{bmatrix} E_{\sigma(k)} \\ C \end{bmatrix}$.

The generalized solution of (5.21) is given as follows:

$$\begin{cases} \begin{bmatrix} \underline{T}_{\sigma(k)} & \underline{N}_{\sigma(k)} \end{bmatrix} = \Omega^{\dagger}_{\sigma(k)} + \underline{Z}_{\sigma(k)} \big(I - \Omega_{\sigma(k)} \Omega^{\dagger}_{\sigma(k)}\big) \\ \begin{bmatrix} \overline{T}_{\sigma(k)} & \overline{N}_{\sigma(k)} \end{bmatrix} = \Omega^{\dagger}_{\sigma(k)} + \overline{Z}_{\sigma(k)} \big(I - \Omega_{\sigma(k)} \Omega^{\dagger}_{\sigma(k)}\big) \end{cases} \tag{5.22}$$

where $\underline{Z}_{\sigma(k)}$ and $\overline{Z}_{\sigma(k)}$ are arbitrary matrices of proper dimension.

By setting $\alpha = \begin{bmatrix} I_{n_x+n_f} \\ 0 \end{bmatrix}$, $\beta = \begin{bmatrix} 0 \\ I_{n_y} \end{bmatrix}$ and $\Theta_{\sigma(k)} = I - \Omega_{\sigma(k)} \Omega^{\dagger}_{\sigma(k)}$, matrices in (5.22) are then expressed as:

$$\begin{cases} \underline{T}_{\sigma(k)} = \Omega^{\dagger}_{\sigma(k)} \alpha + \underline{Z}_{\sigma(k)} \Theta_{\sigma(k)} \alpha \\ \overline{T}_{\sigma(k)} = \Omega^{\dagger}_{\sigma(k)} \alpha + \overline{Z}_{\sigma(k)} \Theta_{\sigma(k)} \alpha \\ \underline{N}_{\sigma(k)} = \Omega^{\dagger}_{\sigma(k)} \beta + \underline{Z}_{\sigma(k)} \Theta_{\sigma(k)} \beta \\ \overline{N}_{\sigma(k)} = \Omega^{\dagger}_{\sigma(k)} \beta + \overline{Z}_{\sigma(k)} \Theta_{\sigma(k)} \beta \end{cases} \tag{5.23}$$

At this point, the observer design problem can now be solved by designing matrices $\underline{Z}_{\sigma(k)}, \overline{Z}_{\sigma(k)}$ and $\underline{L}_{\sigma(k)}(\rho(k)), \overline{L}_{\sigma(k)}(\rho(k))$ to ensure that matrices $\underline{T}_{\sigma} A_{\sigma}(\rho(k)) - \underline{L}_{\sigma}(\rho(k)) C$ and $\overline{T}_{\sigma(k)} A_{\sigma(k)}(\rho(k)) - \overline{L}_{\sigma(k)}(\rho(k)) C$ are both nonnegative and Schur stable for all $\sigma \in \mathcal{N}$. The matrices $\underline{Z}_{\sigma(k)}, \overline{Z}_{\sigma(k)}$ and $\underline{L}_{\sigma(k)}(\rho(k)), \overline{L}_{\sigma(k)}(\rho(k))$ can be obtained by solving a set of LMIs proposed in the next section.

Remark 5.2 *The existence conditions of the interval observer* (5.12) *are determined by the solution of* (5.21)*. A solution to this equation can only be found if and only if the ranking condition* $rank(\Omega_{\sigma}) = n_x + n_f$ *hold for all* $\sigma \in \mathcal{N}$*.*

5.3.2 Integrated observer and FTC synthesis

Throughout section we propose an integrated design of the TNL structure interval observer and a fault-tolerant state feedback controller in order to ensure the stability of the closed-loop system in the presence of faults.

Before designing the control law, it's essential to determine the interval estimations of the state and fault of the original system (5.1). According to the construction of the augmented state vector $z(k)$ in (5.10), the interval estimation of state is determined by:

$$\begin{cases} \underline{x}(k) = \begin{bmatrix} I_{n_x} & 0 \end{bmatrix} \underline{z}(k) \\ \overline{x}(k) = \begin{bmatrix} I_{n_x} & 0 \end{bmatrix} \overline{z}(k) \end{cases} \tag{5.24}$$

and the interval fault estimation is given as:

$$\begin{cases} \underline{f}(k-1) = \begin{bmatrix} 0 & I_{n_f} \end{bmatrix} \underline{z}(k) \\ \overline{f}(k-1) = \begin{bmatrix} 0 & I_{n_f} \end{bmatrix} \overline{z}(k) \end{cases} \tag{5.25}$$

where $\underline{x}(k)$ and $\overline{x}(k)$ are the lower and upper bounds of the state estimation and $\underline{f}(k-1)$ and $\overline{f}(k-1)$ are the lower and upper bounds of fault estimation.

Based on the estimated variables from the equations (5.24) and (5.25), the following control law is then synthesized to stabilize the closed-loop system and compensate for fault effects:

$$u(k) = -\overline{K}_{\sigma(k)}\overline{x}(k) - \underline{K}_{\sigma(k)}\underline{x}(k) - \overline{K}_{\sigma(k),f}\overline{f}(k) - \underline{K}_{\sigma(k),f}\underline{f}(k) \tag{5.26}$$

where $\underline{K}_{\sigma(k)}$, $\overline{K}_{\sigma(k)}$ are the lower and upper state feedback gain matrices and $\overline{K}_{\sigma(k),f}$, $\underline{K}_{\sigma(k),f}$ are the lower and upper accommodation gain matrices chosen in order to cancel the effect of the faults. Their values are given by $\overline{K}_{\sigma(k),f} = \underline{K}_{\sigma(k),f} = \frac{1}{2}B^{\dagger}_{\sigma(k)}(\rho(k))F_{\sigma(k)}$ with $B^{\dagger}_{\sigma(k)}(\rho(k)) = \sum_{j=1}^{2^P} \mu^j_{\sigma(k)}(\rho(k))B^j_{\sigma(k)}{}^{\dagger}$.

By replacing the control law input $u(k)$ of equation (5.26) into the system (5.1), the closed-loop system is expressed as:

$$\begin{aligned} x(k+1) = &\Big(\mathcal{A}_{\sigma(k)}\big(\rho(k)\big) - \mathcal{B}_{\sigma(k)}\big(\rho(k)\big)\overline{K}_{\sigma(k)} - \mathcal{B}_{\sigma(k)}\big(\rho(k)\big)\underline{K}_{\sigma(k)}\Big)\, x(k) \\ &- \mathcal{B}_{\sigma(k)}\big(\rho(k)\big)\overline{K}_{\sigma(k)}\overline{e}_{x_k} + \mathcal{B}_{\sigma(k)}\big(\rho(k)\big)\underline{K}_{\sigma(k)}\underline{e}_{x_k} \\ &- \mathcal{B}_{\sigma(k)}\big(\rho(k)\big)\overline{K}_{\sigma(k),f}\overline{e}_{f_k} + \mathcal{B}_{\sigma(k)}\big(\rho(k)\big)\underline{K}_{\sigma(k),f}\underline{e}_{f_k} \\ &+ \mathcal{D}^w_{\sigma(k)}w(k) \end{aligned} \tag{5.27}$$

with

$$\begin{cases} \underline{e}_{x_k} = x(k) - \underline{x}(k) \\ \overline{e}_{x_k} = \overline{x}(k) - x(k) \end{cases} \tag{5.28}$$

are the lower and upper state estimation errors while

$$\begin{cases} \underline{e}_{f_k} = f(k) - \underline{f}(k) \\ \overline{e}_{f_k} = \overline{f}(k) - f(k) \end{cases} \tag{5.29}$$

are the lower and upper fault estimation errors.

It is now necessary to define the dynamics for the closed-loop system gathering the observer and the controller.

As a result, the following system is obtained:

$$\begin{cases} x(k+1) = \big(\mathcal{A}_{\sigma(k)}\big(\rho(k)\big) - \mathcal{B}_{\sigma(k)}\big(\rho(k)\big)\overline{K}_{\sigma(k)} - \mathcal{B}_{\sigma(k)}\big(\rho(k)\big)\underline{K}_{\sigma(k)}\big)x(k) + w^1_{\sigma(k)}(k) \\ \overline{e}(k+1) = \Big(\overline{T}_{\sigma(k)}A_{\sigma(k)}\big(\rho(k)\big) - \overline{L}_{\sigma(k)}\big(\rho(k)\big)C\Big)\overline{e}(k) + w^2_{\sigma(k)}(k) \\ \underline{e}(k+1) = \Big(\underline{T}_{\sigma(k)}A_{\sigma(k)}\big(\rho(k)\big) - \underline{L}_{\sigma(k)}\big(\rho(k)\big)C\Big)\underline{e}(k) + w^3_{\sigma(k)}(k) \end{cases} \tag{5.30}$$

where

$$\begin{cases} w^1_{\sigma(k)}(k) = -\mathcal{B}_{\sigma(k)}\big(\rho(k)\big)\overline{K}_{\sigma(k)}\overline{e}_{x,k} + \mathcal{B}_{\sigma(k)}\big(\rho(k)\big)\underline{K}_{\sigma(k)}\underline{e}_{x,k} \\ \qquad\qquad - \mathcal{B}_{\sigma(k)}\big(\rho(k)\big)\overline{K}_{\sigma(k),f}\overline{e}_{f,k} + \mathcal{B}_{\sigma(k)}\big(\rho(k)\big)\underline{K}_{\sigma(k),f}\underline{e}_{f,k} \\ \qquad\qquad + \mathcal{D}^w_{\sigma(k)}w(k) \\ w^2_{\sigma(k)}(k) = \overline{\nabla}_{\sigma(k)}(k) - \overline{T}_{\sigma(k)}D^w_{\sigma(k)}w(k) \\ \qquad\qquad + \overline{L}_{\sigma(k)}\big(\rho(k)\big)D^v_{\sigma(k)}v(k) + \overline{N}_{\sigma(k)}D^v_{\sigma(k)}v(k+1) \\ w^3_{\sigma(k)}(k) = \underline{T}_{\sigma(k)}D^w_{\sigma(k)}w(k) - \underline{\nabla}_{\sigma(k)}(k) \\ \qquad\qquad - \underline{L}_{\sigma(k)}\big(\rho(k)\big)D^v_{\sigma(k)}v(k) - \underline{N}_{\sigma(k)}D^v_{\sigma(k)}v(k+1) \end{cases} \tag{5.31}$$

The following two vectors are defined for the sake of clarity: $\chi(k) = \begin{bmatrix} x(k) \\ \overline{e}(k) \\ \underline{e}(k) \end{bmatrix}$ and $w_\sigma(k) = \begin{bmatrix} w^1_\sigma(k) \\ w^2_\sigma(k) \\ w^3_\sigma(k) \end{bmatrix}$. The following theorem provides sufficient conditions for the existence of the TNL interval observer given in (5.12), the convergence of the closed-loop system described by (5.27) and the minimization of the effects of disturbance w_σ. It is the main contribution of this chapter.

Theorem 5.1 *If there exist a symmetric positive definite matrix $P_{1,i}$ and positive diagonal matrices $\overline{P}_i$, $\underline{P}_i$ with $P_i = diag(P_{1,i}, \overline{P}_i, \underline{P}_i)$ and multiple ISS Lyapunov function $V_\sigma(\chi_k)$ switching among $V_i(\chi(k)) = \chi^T(k)P_i\chi(k)$, matrices $\underline{W}_i$, $\overline{W}_i$ and $\underline{Y}^j_i$, $\overline{Y}^j_i$ and $\underline{Q}_i$, $\overline{Q}_i$ for all $i \in \mathcal{N}, j \in \mathcal{P}$ and constant scalars $\gamma_i > 0$, $\varepsilon > 0$, $0 < \alpha_1 < \alpha_2$, such that the following LMIs hold:*

$$\min_{P_i, \underline{W}_i, \overline{W}_i, \underline{Q}_i, \overline{Q}_i, \underline{Y}^j_i, \overline{Y}^j_i} \gamma \tag{5.32}$$

$$\gamma_i \leq \gamma$$

$$\alpha_1 I_{3n_x+2n_f} \leq P_i \leq \alpha_2 I_{3n_x+2n_f} \tag{5.33}$$

$$O_1 = \begin{bmatrix} -P & X_P & P_{23} \\ (*) & (\varepsilon-1)P & 0 \\ (*) & (*) & -\gamma_i \end{bmatrix} \prec 0 \tag{5.34}$$

$$O_2 = \begin{bmatrix} X_P^{22} & 0 \\ 0 & X_P^{33} \end{bmatrix} \geq 0 \tag{5.35}$$

then the system (5.30) *robustly estimates the lower and upper bounds of the augmented state and stabilizes the closed-loop system with* $\underline{K}_i = \underline{W}_i P_{1,i}^{-1}$, $\overline{K}_i = \overline{W}_i P_{1,i}^{-1}$ *and* $\underline{L}_i^j = \underline{P}^{-1}\underline{Y}_i^j$, $\overline{L}_i^j = \overline{P}^{-1}\overline{Y}_i^j$ *and* $\underline{Z}_i = \underline{P}_i^{-1}\underline{Q}_i$, $\overline{Z}_i = \overline{P}_i^{-1}\overline{Q}_i$.

$$X_P^{11} = \mathcal{A}_i\big(\rho(k)\big)P_{1,i} - \mathcal{B}_i\big(\rho(k)\big)\overline{W}_i - \mathcal{B}_i\big(\rho(k)\big)\underline{W}_i \tag{5.36}$$

$$X_P^{22} = \overline{P}_i\Omega_i^{\dagger}\alpha A_i\big(\rho(k)\big) + \overline{Q}_i\Theta_i\alpha A_i\big(\rho(k)\big) - \overline{Y}_i\big(\rho(k)\big)C \tag{5.37}$$

$$X_P^{33} = \underline{P}_i\Omega_i^{\dagger}\alpha A_i\big(\rho(k)\big) + \underline{Q}_i\Theta_i\alpha A_i\big(\rho(k)\big) - \underline{Y}_i\big(\rho(k)\big)C \tag{5.38}$$

$$X_P = \begin{bmatrix} X_P^{11} & 0 & 0 \\ (*) & X_P^{22} & 0 \\ (*) & (*) & X_P^{33} \end{bmatrix} \tag{5.39}$$

$$P = \begin{bmatrix} P_{1,i} & 0 & 0 \\ 0 & \overline{P}_i & 0 \\ 0 & 0 & \underline{P}_i \end{bmatrix} \tag{5.40}$$

$$P_{23} = \begin{bmatrix} I_{n_x} & 0 & 0 \\ 0 & \overline{P}_i & 0 \\ 0 & 0 & \underline{P}_i \end{bmatrix} \tag{5.41}$$

In addition, the system (5.30) *is Input-to-State-Stable with respect to additive disturbance* $w(k)$ *under any switching signal with ADT* (5.9)*. Moreover,*

$$\lim_{k\to\infty} \|\chi(k)\|_2 \leq \sqrt{\frac{\gamma}{\alpha_1\varepsilon}} \max \|w_i(k)\|_\infty \tag{5.42}$$

Proof 5.1 *To study the ISS property of the interval observer-based FTC, multiple quadratic ISS-Lyapunov functions applied to the augmented vector* χ_k *of the system* (5.30) *is defined by*

$$\begin{aligned} V_i\big(\chi(k)\big) &= V_{1,i}\big(x(k)\big) + V_{2,i}\big(\overline{e}(k)\big) + V_{3,i}\big(\underline{e}(k)\big) \\ &= x^T(k)P_{1,i}^{-1}x(k) + \overline{e}^T(k)\overline{P}_i\overline{e}(k) + \underline{e}^T(k)\underline{P}_i\underline{e}(k) \end{aligned} \tag{5.43}$$

The derivative of the Lyapunov function along trajectory of (5.30) *as follows:*

$$\Delta V_i\big(\chi(k)\big) = \Delta V_{1,i}\big(x(k)\big) + \Delta V_{2,i}\big(\overline{e}(k)\big) + \Delta V_{3,i}\big(\underline{e}(k)\big) \tag{5.44}$$

where

$$\begin{aligned}
\Delta V_1\big(x(k)\big) &= V_1\big(x(k+1)\big) - V_1\big(x(k)\big) \\
&= x^T(k+1)P_1^{-1}x(k+1) - x^T(k)P_1^{-1}x(k) \\
&= x^T(k)\Big(\mathcal{A}_i(\rho(k)) - \mathcal{B}_i(\rho(k))\overline{K}_i - \mathcal{B}_i(\rho(k))\underline{K}_i\Big)^T P_{1,i}^{-1} \\
&\quad \Big(\mathcal{A}_i(\rho(k)) - \mathcal{B}_i(\rho(k))\overline{K}_i - \mathcal{B}_i(\rho(k))\underline{K}_i\Big)x(k) \\
&\quad + x^T(k)\Big(\mathcal{A}_i(\rho(k)) - \mathcal{B}_i(\rho(k))\overline{K}_i - \mathcal{B}_i(\rho(k))\underline{K}_i\Big)^T P_{1,i}^{-1}w_i^1(k) \\
&\quad + {w_i^1}^T(k)P_{1,i}^{-1}\Big(\mathcal{A}_i(\rho(k)) - \mathcal{B}_i(\rho(k))\overline{K}_i - \mathcal{B}_i(\rho(k))\underline{K}_i\Big)x(k) \\
&\quad + {w_i^1}^T(k)P_{1,i}^{-1}w_i^1(k) - x^T(k)P_{1,i}^{-1}x(k)
\end{aligned} \tag{5.45}$$

$$\begin{aligned}
\Delta V_2\big(\overline{e}(k)\big) &= V_2\big(\overline{e}(k+1)\big) - V_2\big(\overline{e}(k)\big) \\
&= \overline{e}(k+1)^T\overline{P}_i\overline{e}(k+1) - \overline{e}^T(k)\overline{P}_i\overline{e}(k) \\
&= \overline{e}^T(k)\Big(T_iA_i(\rho(k)) - L_i(\rho(k))C\Big)^T\overline{P}_i\Big(T_iA_i(\rho(k)) - L_i(\rho(k))C\Big)\overline{e}(k) \\
&\quad + \overline{e}^T(k)\Big(T_iA_i(\rho(k)) - L_i(\rho(k))C\Big)^T\overline{P}_iw_i^2(k) \\
&\quad + {w_i^2}^T(k)\overline{P}_i\Big(T_iA_i(\rho(k)) - L_i(\rho(k))C\Big)\overline{e}(k) \\
&\quad + {w_i^2}^T(k)\overline{P}_iw_i^2(k) - \overline{e}^T(k)\overline{P}_i\overline{e}(k)
\end{aligned} \tag{5.46}$$

$$\begin{aligned}
\Delta V_3\big(\underline{e}(k)\big) &= V_3\big(\underline{e}(k+1)\big) - V_3\big(\underline{e}(k)\big) \\
&= \underline{e}^T(k+1)\underline{P}_i\underline{e}(k+1) - \underline{e}^T(k)\underline{P}_i\underline{e}(k) \\
&= \underline{e}^T(k)\Big(T_iA_i(\rho(k)) - L_i(\rho(k))C\Big)^T\underline{P}_i\Big(T_iA_i(\rho(k)) - L_i(\rho(k))C\Big)\underline{e}(k) \\
&\quad + \underline{e}^T(k)\Big(T_iA_i(\rho(k)) - L_i(\rho(k))C\Big)^T\underline{P}_iw_i^3(k) \\
&\quad + {w_i^3}^T(k)\underline{P}_i\Big(T_iA_i(\rho(k)) - L_i(\rho(k))C\Big)\underline{e}(k) \\
&\quad + {w_i^3}^T(k)\underline{P}_iw_i^3(k) - \underline{e}^T(k)\underline{P}_i\underline{e}(k)
\end{aligned} \tag{5.47}$$

From (5.45), (5.46), (5.47) *and with any* $0 < \varepsilon < 1$, $\gamma_i > 0$ *one can have:*

$$\Delta V_i\big(\chi(k)\big) = \begin{bmatrix} \chi^T(k) & w^T(k) \end{bmatrix}\Xi\begin{bmatrix} \chi(k) \\ w(k) \end{bmatrix} - \varepsilon\chi^T(k)P\chi(k) + \gamma_iw_i^T(k)w_i(k) \tag{5.48}$$

where

$$\Xi = \begin{bmatrix} X^TP'X + (\varepsilon-1)P' & X^TP' \\ (*) & P' - \gamma_i \end{bmatrix} \tag{5.49}$$

$$X = \begin{bmatrix} X_{11} & 0 & 0 \\ (*) & X_{22} & 0 \\ (*) & (*) & X_{33} \end{bmatrix} \tag{5.50}$$

$$P^{'} = \begin{bmatrix} P_1^{-1} & 0 & 0 \\ (*) & \overline{P}_i & 0 \\ (*) & (*) & \underline{P}_i \end{bmatrix} \tag{5.51}$$

$$X_{11} = \mathcal{A}_i(\rho_k) - \mathcal{B}_i(\rho(k))\overline{K}_i - \mathcal{B}_i(\rho(k))\underline{K}_i \tag{5.52}$$

$$X_{22} = \overline{T}_i A_i(\rho(k)) - \overline{L}_i(\rho(k))C \tag{5.53}$$

$$X_{33} = \underline{T}_i A_i(\rho(k)) - \underline{L}_i(\rho(k))C \tag{5.54}$$

The following condition is a sufficient condition for system (5.30) *to be input-to-state-stable:*

$$\Xi \prec 0 \tag{5.55}$$

The term Ξ *can be rewritten as follows:*

$$\Xi = \begin{bmatrix} (\varepsilon - 1)P^{'} & 0 \\ 0 & -\gamma_i \end{bmatrix} + \begin{bmatrix} (P^{'}X)^T \\ P^{'} \end{bmatrix} P^{'-1} \begin{bmatrix} P^{'}X & P^{'} \end{bmatrix} \tag{5.56}$$

Applying Schur complement lemma 2.9 to equation (5.56)*, one can get:*

$$\begin{bmatrix} -P^{'} & P^{'}X & P^{'} \\ (*) & (\varepsilon - 1)P^{'} & 0 \\ (*) & (*) & -\gamma_i \end{bmatrix} \prec 0 \tag{5.57}$$

Pre-and post multiply (5.57) *by* $P_p = \begin{bmatrix} P_I & 0 & 0 \\ (*) & P_I & 0 \\ (*) & (*) & I_{n_x+n_f} \end{bmatrix}$ *with* $P_I = \begin{bmatrix} P_1 & 0 & 0 \\ (*) & I_{n_x+n_f} & 0 \\ (*) & (*) & I_{n_x+n_f} \end{bmatrix}$*, one can obtain:*

$$O_1 = \begin{bmatrix} -P & X_P & P_{23} \\ (*) & (\varepsilon - 1)P & 0 \\ (*) & (*) & -\gamma_i \end{bmatrix} \prec 0 \tag{5.58}$$

If the sufficient condition (5.55) *holds, it follows that*

$$\Delta V_i\big(\chi(k)\big) \leq -\varepsilon \chi^T(k) P_i \chi(k) + \gamma_i w_i^T(k) w_i(k) \tag{5.59}$$

it indicates that

$$V_i\big(\chi(k+1)\big) \leq (1-\varepsilon) V_i(\chi(k)) + \gamma_i \|w_i(k)\|^2 \tag{5.60}$$

Then integrating (5.60) *on the interval* $[k_0, k)$ *one can get the inequality*

$$V\big(\chi(k)\big) \leq (1-\varepsilon)^{k-k_0} V\big(\chi(k_0)\big) + \gamma_i \sum_{m=0}^{k-k_0-1} (1-\varepsilon)^m \|w_i(k)\|^2 \tag{5.61}$$

with LMI condition (5.33)*, it allows that*

$$\|\chi(k)\|_2 \leq \sqrt{\frac{(1-\varepsilon)^{k-k_0} \|\chi(k_0)\|_2^2 + \gamma_i \sum_{m=0}^{k-k_0-1} (1-\varepsilon)^m \|w_i\|_2^2}{\alpha_1}} \tag{5.62}$$

Once $k \to \infty$ *and* $\gamma_i \leq \gamma$*, LMI condition* (5.42) *is obtained.*

It should be noted that the augmented state vector χ_k *has an upper bound defined by* $\sqrt{\frac{\gamma}{\alpha_1 \varepsilon}} \max \|w_i(k)\|_\infty$*. This upper bound should be minimized as much as possible to improve the robustness of the proposed observer-based controller against perturbations. It is evident that this bound is tighter with smaller* γ_i *value for priori known* α_1 *and* ε*. Therefore, the problem of minimizing the upper bounds is equivalent to the minimization of the scalar* γ_i*.*

Moreover, $\underline{T}_i A_i(\rho(k)) - \underline{L}_i(\rho(k))C$ *and* $\overline{T}_i A_i(\rho(k)) - \overline{L}_i(\rho(k))C$ *are nonnegative matrices, by replacing* $\underline{T}_i = \Omega_i^\dagger \alpha + \underline{Z}_i \Theta_i \alpha$*,* $\overline{T}_i = \Omega_i^\dagger \alpha + \overline{Z}_i \Theta_i \alpha$ *and multiplying by* $\underline{P}_i$ *and* $\overline{P}_i$ *on the left side and performing the change of variables* $\underline{Y}_i(\rho(k)) = \underline{P}_i \underline{L}_i(\rho(k))$*,* $\overline{Y}_i(\rho(k)) = \overline{P}_i \overline{L}_i(\rho(k))$*, one can obtain the LMI in* (5.35)*. This completes the proof.*

Remark 5.3 *In addition to ensuring stability, the interval observer design requires to satisfy an additional constraint of positivity. Such a condition leads to more computational complexity and theoretical difficulty involved in identifying the interval observer gains* $\underline{L}_{\sigma(k)}(\rho(k))$ *and* $\overline{L}_{\sigma(k)}(\rho(k))$*. One of the well-known approaches in the literature to address this challenge is to deploy changes of coordinates. Such a technique has limitations since it is impossible to determine the observer gains, simultaneously satisfying the inclusion property and the other performance criteria, such as robust constraints. By introducing additional weighted matrices* $\underline{T}_{\sigma(k)}$ *and* $\overline{T}_{\sigma(k)}$*,* $\underline{N}_{\sigma(k)}$ *and* $\overline{N}_{\sigma(k)}$ *in the interval observer frameworks, it offers a novel solution to handle the complex design challenge associated with coordinates transformation commonly deployed in the literature.*

Overall, the design procedure of the TNL interval observer-based FTC is determined based on the following algorithms:

Algorithm 3: Design procedure

for $\sigma(k) = 1 : N$ **do**

if $\left(rank(\Omega_{\sigma(k)}) == n_x + n_f\right)$ **then**

- Solve the optimization problem in Theorem 5.1 and obtain $P_{\sigma(k)}$, $\underline{W}_{\sigma(k)}$, $\overline{W}_{\sigma(k)}$, $\underline{Y}^j_{\sigma(k)}$, $\overline{Y}^j_{\sigma(k)}$, $\underline{Q}_{\sigma(k)}$, $\overline{Q}_{\sigma(k)}$.

$$\begin{cases} \overline{K}_{\sigma(k)} = \overline{W}_{\sigma(k)} P^{-1}_{1,\sigma(k)} \\ \underline{K}_{\sigma(k)} = \underline{W}_{\sigma(k)} P^{-1}_{1,\sigma(k)} \\ \overline{Z}_{\sigma(k)} = \overline{P}^{-1}_{\sigma(k)} \overline{Q}_{\sigma(k)} \\ \underline{Z}_{\sigma(k)} = \underline{P}^{-1}_{\sigma(k)} \underline{Q}_{\sigma(k)} \\ \overline{L}_{\sigma(k)}(\rho_k) = \overline{P}^{-1}_{\sigma(k)} \sum_{j=1}^{2^P} \mu^j_{\sigma(k)}(\rho(k)) \overline{Y}^j_{\sigma(k)} \\ \underline{L}_{\sigma(k)}(\rho(k)) = \underline{P}^{-1}_{\sigma(k)} \sum_{j=1}^{2^P} \mu^j_{\sigma(k)}(\rho(k)) \underline{Y}^j_{\sigma(k)} \end{cases}$$

- Determine matrices $\overline{T}_{\sigma(k)}, \underline{T}_{\sigma(k)}, \overline{N}_{\sigma(k)}, \underline{N}_{\sigma(k)}$ by equations (5.23)

$$\begin{cases} \underline{T}_{\sigma(k)} = \Omega^{\dagger}_{\sigma(k)} \alpha + \underline{Z}_{\sigma(k)} \Theta_{\sigma(k)} \alpha \\ \overline{T}_{\sigma(k)} = \Omega^{\dagger}_{\sigma(k)} \alpha + \overline{Z}_{\sigma(k)} \Theta_{\sigma(k)} \alpha \\ \underline{N}_{\sigma(k)} = \Omega^{\dagger}_{\sigma(k)} \beta + \underline{Z}_{\sigma(k)} \Theta_{\sigma(k)} \beta \\ \overline{N}_{\sigma(k)} = \Omega^{\dagger}_{\sigma(k)} \beta + \overline{Z}_{\sigma(k)} \Theta_{\sigma(k)} \beta \end{cases}$$

else

There is no solution for a set of LMIs.
The TNL interval observer does not exist

end

end

5.4 Application to lateral vehicle dynamics

This section applies the developed procedure to the lateral vehicle dynamics model. A single-track 2-DOF model is obtained from the nonlinear vehicle dynamics model with the second law of Newton and some simplifying assumptions [192]. The following structure of lateral vehicle dynamics is considered:

$$\begin{bmatrix} \dot{v}_y \\ \dot{r} \end{bmatrix} = \begin{bmatrix} -\frac{c_f+c_r}{mv_x} & \frac{c_r l_r - c_f l_f}{mv_x} - v_x \\ \frac{c_r l_r - c_f l_f}{I_z v_x} & -\frac{c_r l_r^2 + c_f l_f^2}{I_z v_x} \end{bmatrix} \begin{bmatrix} v_y \\ r \end{bmatrix} + \begin{bmatrix} 0 \\ \frac{1}{I_z} \end{bmatrix} u + \begin{bmatrix} \frac{c_f}{m} \\ \frac{c_f l_f}{I_z} \end{bmatrix} \delta_f \tag{5.63}$$

where v_y is lateral velocity, r is yaw rate, δ_f is front steering angle commanded by the driver. The controller outputs is $u = \Delta M_z$ which is a yaw moment obtained from differential wheels braking. This kind of controller is used in vehicle handling improvement by reducing the sideslip angle and yaw rate deviations from the desired values. The distances from the front and rear axles to the center of gravity are represented by l_f and l_r. Moreover, vehicle mass m, longitudinal vehicle velocity v_x, moment of inertia I_z are other important parameters that determine how the vehicle responds to the lateral dynamics. The cornering stiffness parameters c_f and c_r depend on the friction of the road surface and cannot be directly observable.

Then, the system (5.63) is expressed as:

$$\begin{cases} \dot{x}(t) = \mathcal{A}_{\sigma(k)}(\rho)x(t) + \mathcal{B}u(t) + \mathcal{D}\delta_f(t) \\ y(t) = \mathcal{C}x(t) \end{cases} \tag{5.64}$$

By using the Euler's discretization approach along with sampling time $T_s = 0.01s$, one can obtain the following approximation:

$$\dot{x}(t) \approx \frac{x(k+1) - x(k)}{T_s} \tag{5.65}$$

Then, a discrete-time switched LPV system of continuous-time lateral vehicle dynamics model (5.64) with actuator fault, process disturbances and measurement noise can be obtained as follows:

$$\begin{cases} x(k+1) = \mathcal{A}_{\sigma(k)}(\rho(k))x(k) + \mathcal{B}u(k) + \mathcal{D}\delta_f(k) + Ff(k) + \mathcal{D}^w w(k) \\ \quad y(k) = \mathcal{C}x(k) + D^v v(k) \end{cases} \tag{5.66}$$

where the distribution matrices $\mathcal{A}_{\sigma(k)}(\rho(k)) = I_{n_x} + \begin{bmatrix} -\frac{c_f+c_r}{mv_x} & \frac{c_r l_r - c_f l_f}{mv_x} - v_x \\ \frac{c_r l_r - c_f l_f}{I_z v_x} & -\frac{c_r l_r^2 + c_f l_f^2}{I_z v_x} \end{bmatrix} \times T_s$, $\mathcal{B} = F = \begin{bmatrix} 0 \\ \frac{1}{I_z} \end{bmatrix} \times T_s$, $\mathcal{C} = \begin{bmatrix} 0 & 1 \end{bmatrix}$, $\mathcal{D} = \begin{bmatrix} \frac{c_f}{m} \\ \frac{c_f l_f}{I_z} \end{bmatrix} \times T_s$, $\mathcal{D}^w = \begin{bmatrix} \frac{1}{m} \\ \frac{l_w}{I_z} \end{bmatrix} \times T_s$, $D^v = 1$ and $w(k)$ is disturbance wind gust, measurement noise $v(k)$, distance wind fore action l_w.

The vehicle motion is managed by two parameters known as longitudinal velocity and steering angle as depicted in Figure 5.1 and 5.2. The steering angle $\delta_f(k)$ is the known control input which is controlled by the driver or steering system through the steering wheel of the vehicle.

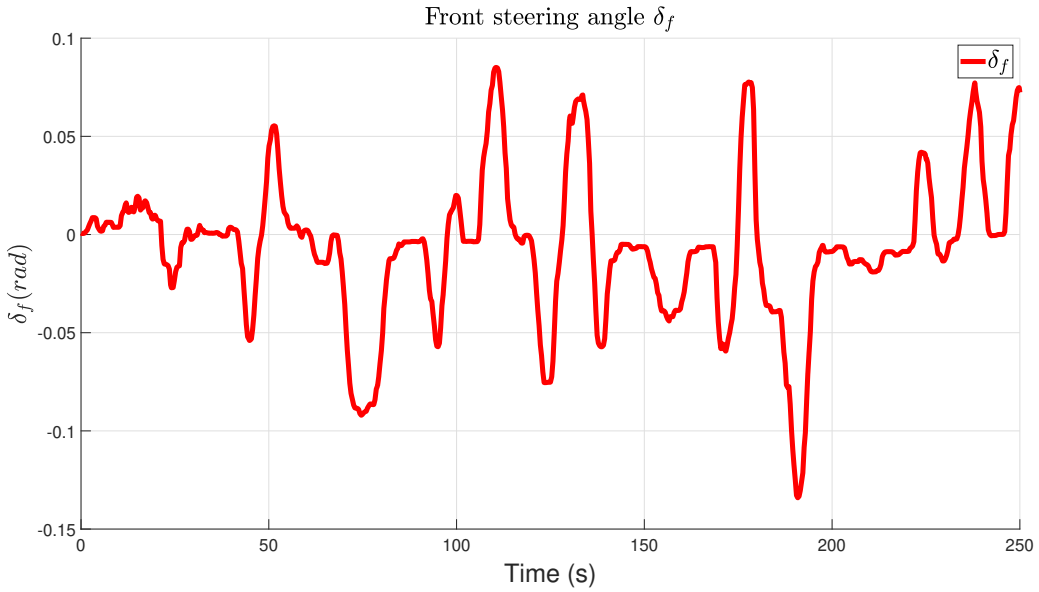

Figure 5.1: Front steering angle $\delta_f(k)$ profiles.

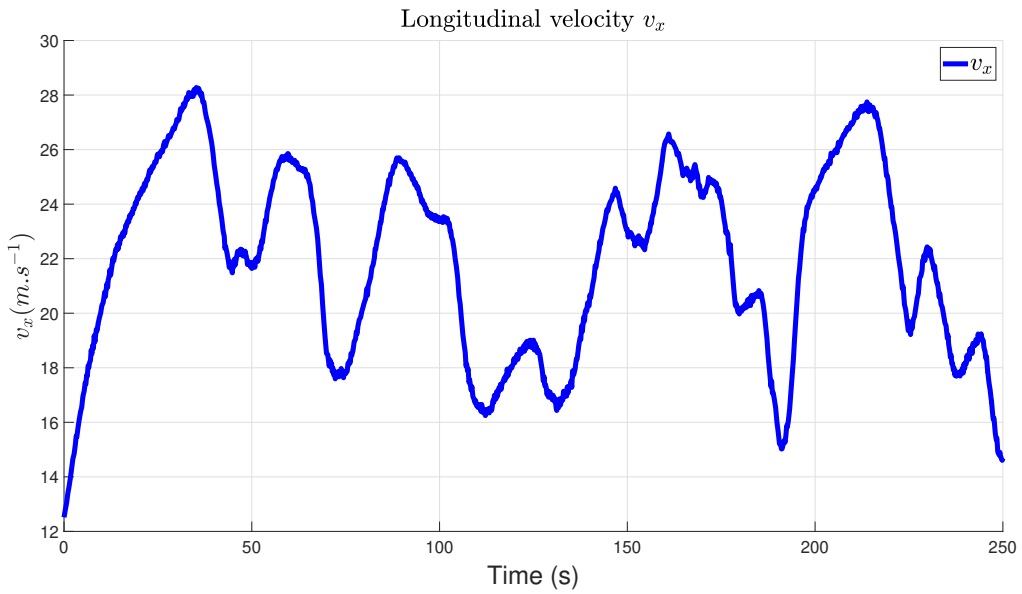

Figure 5.2: Longitudinal velocity $v_x(k)$ profiles.

As shown in Figure 5.2, the longitudinal velocity is considered as a time-varying parameter varying in a range from $12.5(m.s^{-1})$ to $28.5(m.s^{-1})$. The polytopic representation is thus obtained by considering the two-dimensional vector $\rho_\sigma(k) = \left[\rho_\sigma^1(k), \rho_\sigma^2(k)\right] = \left[v_x, \frac{1}{v_x}\right]$. Therefore, there are four submodels for each subsystem.

With the assumption

$$\begin{aligned}\underline{\rho}^1_{\sigma(k)} \leq \rho^1_{\sigma(k)}(k) \leq \overline{\rho}^1_{\sigma(k)} \\ \underline{\rho}^2_{\sigma(k)} \leq \rho^2_{\sigma(k)}(k) \leq \overline{\rho}^2_{\sigma(k)}\end{aligned} \tag{5.67}$$

the weighting function $\mu^j_{\sigma(k)}(\rho(k))$ are determined as follows:

$$\begin{aligned}\mu^1_{\sigma(k)}(\rho(k)) = \mu^{11}_{\sigma(k)}(\rho(k))\mu^{21}_{\sigma(k)}(\rho(k)), \quad \mu^2_{\sigma(k)}(\rho(k)) = \mu^{11}_{\sigma(k)}(\rho(k))\mu^{22}_{\sigma(k)}(\rho(k)) \\ \mu^3_{\sigma(k)}(\rho(k)) = \mu^{12}_{\sigma(k)}(\rho(k))\mu^{21}_{\sigma(k)}(\rho(k)), \quad \mu^4_{\sigma(k)}(\rho(k)) = \mu^{12}_{\sigma(k)}(\rho(k))\mu^{22}_{\sigma(k)}(\rho(k))\end{aligned} \tag{5.68}$$

where the functions $\mu^{ij}_{\sigma(k)}(\rho(k))$ are given as follows:

$$\begin{aligned}\mu^{11}_{\sigma(k)}(\rho(k)) = \frac{\overline{\rho}^1_{\sigma(k)} - \rho^1_{\sigma(k)}(k)}{\overline{\rho}^1_{\sigma(k)} - \underline{\rho}^1_{\sigma(k)}}, \quad \mu^{12}_{\sigma(k)}(\rho(k)) = \frac{\rho^1_{\sigma(k)}(k) - \underline{\rho}^1_{\sigma(k)}}{\overline{\rho}^1_{\sigma(k)} - \underline{\rho}^1_{\sigma(k)}} \\ \mu^{21}_{\sigma(k)}(\rho(k)) = \frac{\overline{\rho}^2_{\sigma(k)} - \rho^2_{\sigma(k)}(k)}{\overline{\rho}^2_{\sigma(k)} - \underline{\rho}^2_{\sigma(k)}}, \quad \mu^{22}_{\sigma(k)}(\rho(k)) = \frac{\rho^2_{\sigma(k)}(k) - \underline{\rho}^2_{\sigma(k)}}{\overline{\rho}^2_{\sigma(k)} - \underline{\rho}^2_{\sigma(k)}}\end{aligned} \tag{5.69}$$

and the submodel matrices are determined at each vertex.

Therefore, the exact polytopic representation of the vehicle lateral dynamics (5.66) is expressed as:

$$\begin{cases} x(k+1) = \sum_{j=1}^{4} \mu^j_\sigma(\rho_k)\mathcal{A}^j_\sigma x(k) + \mathcal{B}u(k) + \mathcal{D}\delta_f + Ff(k) + \mathcal{D}^w w(k) \\ \qquad y(k) = \mathcal{C}x(k) + D^v v(k) \end{cases} \tag{5.70}$$

with A^j_σ are system and uncertain matrices at each vertex of the polytope.

$$\begin{aligned}\mathcal{A}^1_\sigma &= \begin{bmatrix} -\frac{c_f+c_r}{m}\underline{\rho}^1_\sigma & \frac{c_r l_r - c_f l_f}{m}\underline{\rho}^1_\sigma - \underline{\rho}^2_\sigma \\ \frac{c_r l_r - c_f l_f}{I_z}\underline{\rho}^1_\sigma & -\frac{c_r l_r^2 + c_f l_f^2}{I_z}\underline{\rho}^1_\sigma \end{bmatrix} \\ \mathcal{A}^2_\sigma &= \begin{bmatrix} -\frac{c_f+c_r}{m}\overline{\rho}^1_\sigma & \frac{c_r l_r - c_f l_f}{m}\overline{\rho}^1_\sigma - \underline{\rho}^2_\sigma \\ \frac{c_r l_r - c_f l_f}{I_z}\overline{\rho}^1_\sigma & -\frac{c_r l_r^2 + c_f l_f^2}{I_z}\overline{\rho}^1_\sigma \end{bmatrix} \\ \mathcal{A}^3_\sigma &= \begin{bmatrix} -\frac{c_f+c_r}{m}\underline{\rho}^1_\sigma & \frac{c_r l_r - c_f l_f}{m}\underline{\rho}^1_\sigma - \overline{\rho}^2_\sigma \\ \frac{c_r l_r - c_f l_f}{I_z}\underline{\rho}^1_\sigma & -\frac{c_r l_r^2 + c_f l_f^2}{I_z}\underline{\rho}^1_\sigma \end{bmatrix} \\ \mathcal{A}^4_\sigma &= \begin{bmatrix} -\frac{c_f+c_r}{m}\overline{\rho}^1_\sigma & \frac{c_r l_r - c_f l_f}{m}\overline{\rho}^1_\sigma - \overline{\rho}^2_\sigma \\ \frac{c_r l_r - c_f l_f}{I_z}\overline{\rho}^1_\sigma & -\frac{c_r l_r^2 + c_f l_f^2}{I_z}\overline{\rho}^1_\sigma \end{bmatrix}\end{aligned} \tag{5.71}$$

Moreover, three subsystems are considered with switching signal $\sigma(k)$ given as:

$$\sigma(k) = \begin{cases} 1, & 12.5(m.s^{-1}) \leq v_x < 17.5(m.s^{-1}) \\ 2, & 17.5(m.s^{-1}) \leq v_x < 22.5(m.s^{-1}) \\ 3, & 22.5(m.s^{-1}) \leq v_x \leq 28.5(m.s^{-1}) \end{cases} \tag{5.72}$$

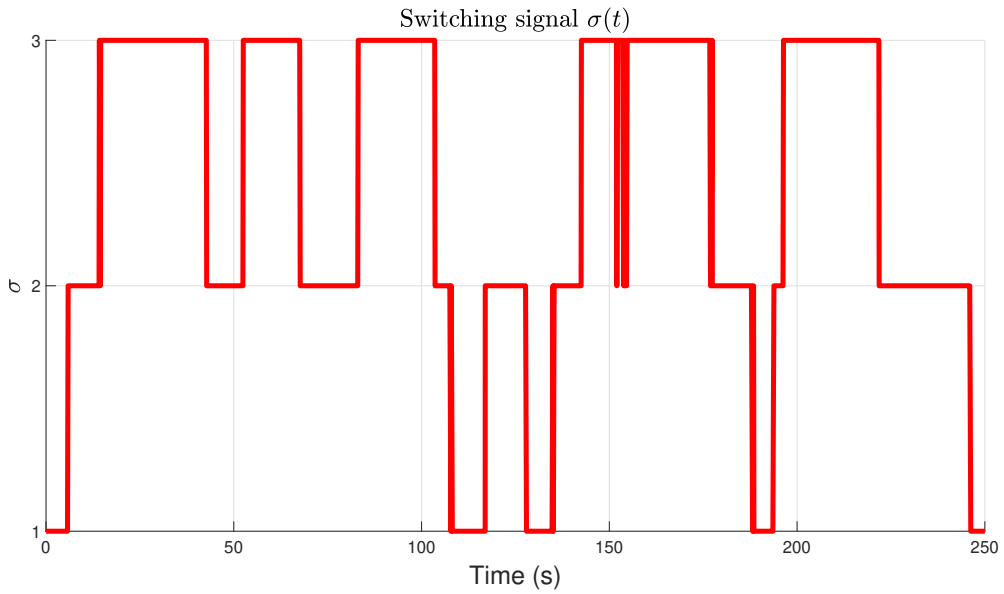

Figure 5.3: Switching signal $\sigma(k)$ profiles.

As shown in Figure 5.8, the actuator fault profile consists of a constant and sinusoidal form of frequency at $0.35Hz$ between $20sec$ and $145sec$ and at $0.5Hz$ from $160sec$ $225sec$. This fault profile is applied as a differential torque in lateral vehicle dynamics.

The disturbance wind gust and measurement noise are shown in Figure 5.4 and 5.5. The wind gust affects the vehicle dynamics from $50sec$ to $200sec$ with the variation between $250N$ and $450N$. The measurement noise is a random signal bounded by $\begin{bmatrix} -0.25, & 0.25 \end{bmatrix}$.

Using the Matlab SEDUMI optimization tools [193], Theorem 5.1 provides a set of LMIs that is solved by minimizing γ. The observer and controller gain matrices are obtained by solving LMIs in Theorem 5.1.

$$\begin{aligned} \overline{L}_1^1 &= \begin{bmatrix} -0.0012 \\ 0.0000 \\ 2.4330 \end{bmatrix}, \overline{L}_1^2 = \begin{bmatrix} -0.0017 \\ 0.0000 \\ 2.4714 \end{bmatrix}, \overline{L}_1^3 = \begin{bmatrix} -0.0012 \\ 0.0000 \\ 1.9081 \end{bmatrix}, \overline{L}_1^4 = \begin{bmatrix} -0.0017 \\ 0.0000 \\ 2.4572 \end{bmatrix} \\ \underline{L}_1^1 &= \begin{bmatrix} -0.0012 \\ 0.0000 \\ 2.9054 \end{bmatrix}, \underline{L}_1^2 = \begin{bmatrix} -0.0018 \\ 0.0000 \\ 1.3566 \end{bmatrix}, \underline{L}_1^3 = \begin{bmatrix} -0.0011 \\ 0.0000 \\ 5.7771 \end{bmatrix}, \underline{L}_1^4 = \begin{bmatrix} -0.0017 \\ 0.0000 \\ 3.1166 \end{bmatrix} \end{aligned} \tag{5.73}$$

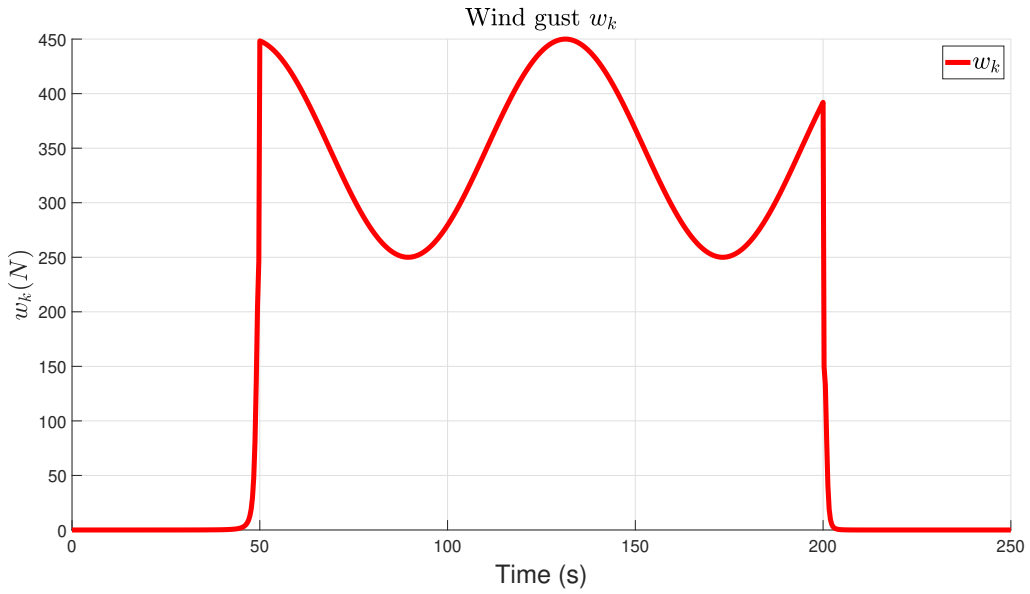

Figure 5.4: Disturbance wind gust $w(k)$.

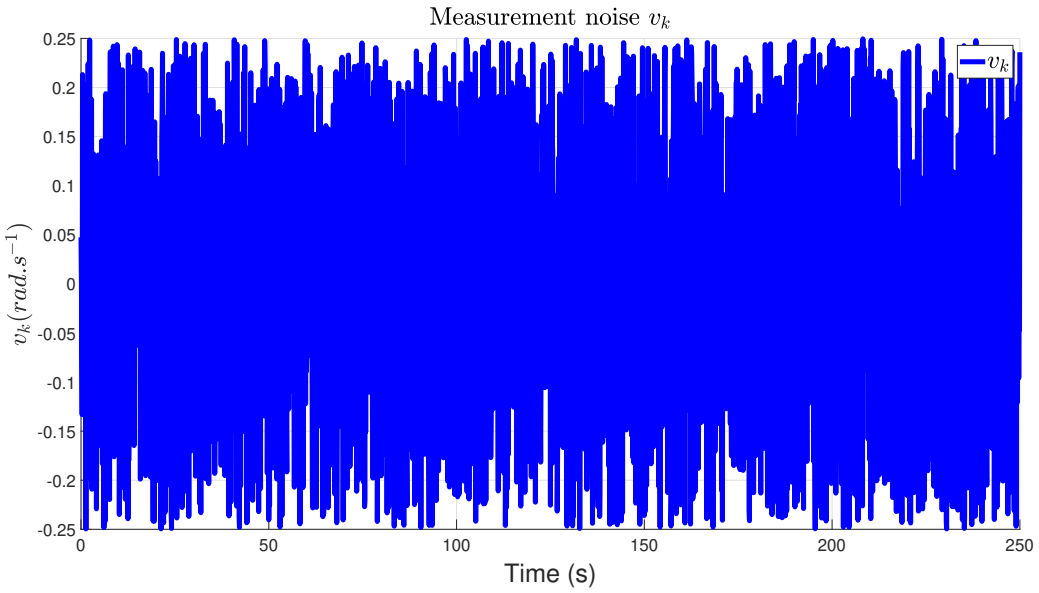

Figure 5.5: Measurement noise $v(k)$.

$$\begin{aligned}
\overline{L}_2^1 &= \begin{bmatrix} -0.0017 \\ 0.0000 \\ 2.1112 \end{bmatrix}, \overline{L}_2^2 = \begin{bmatrix} -0.0022 \\ 0.0000 \\ 3.2915 \end{bmatrix}, \overline{L}_2^3 = \begin{bmatrix} -0.0017 \\ 0.0000 \\ 1.8715 \end{bmatrix}, \overline{L}_2^4 = \begin{bmatrix} -0.0022 \\ 0.0000 \\ 1.9549 \end{bmatrix} \\
\underline{L}_2^1 &= \begin{bmatrix} -0.0017 \\ 0.0000 \\ 2.5265 \end{bmatrix}, \underline{L}_2^2 = \begin{bmatrix} -0.0023 \\ 0.0000 \\ 1.8086 \end{bmatrix}, \underline{L}_2^3 = \begin{bmatrix} -0.0017 \\ 0.0000 \\ 6.1706 \end{bmatrix}, \underline{L}_2^4 = \begin{bmatrix} -0.0022 \\ 0.0000 \\ 2.4894 \end{bmatrix}
\end{aligned} \tag{5.74}$$

$$
\begin{aligned}
\overline{L}_3^1 &= \begin{bmatrix} -0.0223 \\ 0.0000 \\ 0.2961 \end{bmatrix}, \overline{L}_3^2 = \begin{bmatrix} -0.0282 \\ 0.0000 \\ -2.0947 \end{bmatrix}, \overline{L}_3^3 = \begin{bmatrix} -0.0222 \\ 0.0000 \\ 2.1761 \end{bmatrix}, \overline{L}_3^4 = \begin{bmatrix} -0.0282 \\ 0.0000 \\ 2.3728 \end{bmatrix} \\
\underline{L}_3^1 &= \begin{bmatrix} -0.0022 \\ 0.0000 \\ -0.1154 \end{bmatrix}, \underline{L}_3^2 = \begin{bmatrix} -0.0029 \\ 0.0000 \\ 0.3602 \end{bmatrix}, \underline{L}_3^3 = \begin{bmatrix} -0.0022 \\ 0.0000 \\ -1.4110 \end{bmatrix}, \underline{L}_3^4 = \begin{bmatrix} -0.0028 \\ 0.0000 \\ 0.0532 \end{bmatrix}
\end{aligned} \tag{5.75}
$$

$$
\underline{K}_1 = \begin{bmatrix} 0.7837 & 2.6264 \end{bmatrix}, \overline{K}_1 = \begin{bmatrix} 0.2274 & 0.6152 \end{bmatrix}
$$

$$
\underline{K}_2 = \begin{bmatrix} 0.4780 & 3.0614 \end{bmatrix}, \overline{K}_2 = \begin{bmatrix} -0.0288 & -0.1486 \end{bmatrix}
$$

$$
\underline{K}_3 = \begin{bmatrix} 0.2035 & 1.3437 \end{bmatrix}, \overline{K}_3 = \begin{bmatrix} 0.0289 & 0.2038 \end{bmatrix}
$$

The simulation results obtained by the proposed method are depicted in Figure 5.8 to 5.11.

In Figure 5.6 and 5.7, it shows a good estimation of lateral velocity $v_y(k)$ and yaw rate $r(k)$ of the vehicle in which the solid lines represent the actual system states and the dashed blue and green lines represent the lower and upper bounds. The actual state is always bounded by the lower and upper estimation at any instant time.

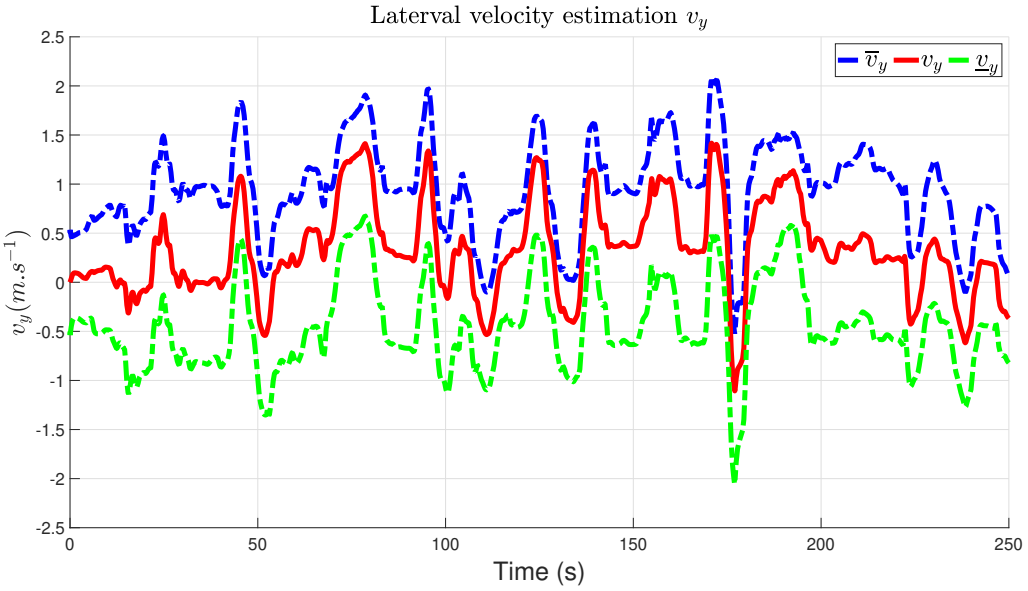

Figure 5.6: Lateral vehicle velocity $v_y(k)$ interval estimation.

Figure 5.8 shows the estimation of the actuator fault signal in which $\underline{f}(k)$ and $\overline{f}(k)$ are denoted by the dashed green and blue lines, respectively. Additionally, the figure also illustrates the control input signal. The designed controller ensures the desired stability and performance of the closed-loop system under actuator fault conditions. The proposed FTC system can also effectively compensate for the actuator fault effects and maintain the vehicle

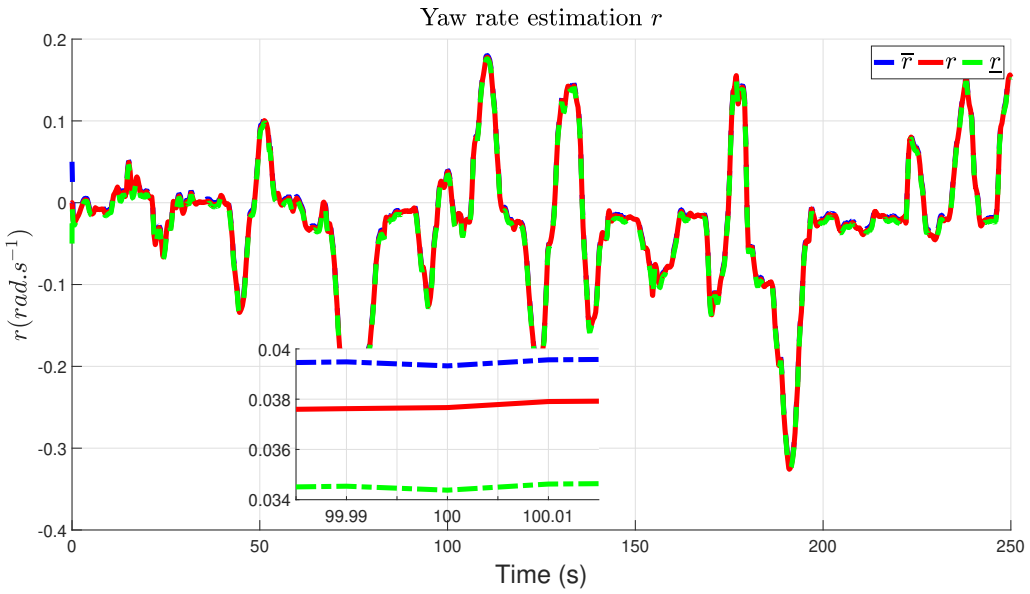

Figure 5.7: Yaw rate $r(k)$ interval estimation.

operation as demonstrated in Figure 5.10 and 5.11. The faulty system without FTC is unable to deal with the fault and exhibits significant deviation from the fault-free system due to the fault effects. This result is achieved by the design of FTC that adapts the gain according to increasing of actuator fault thanks to reconfiguration mechanism as demonstrated in Figure 5.9.

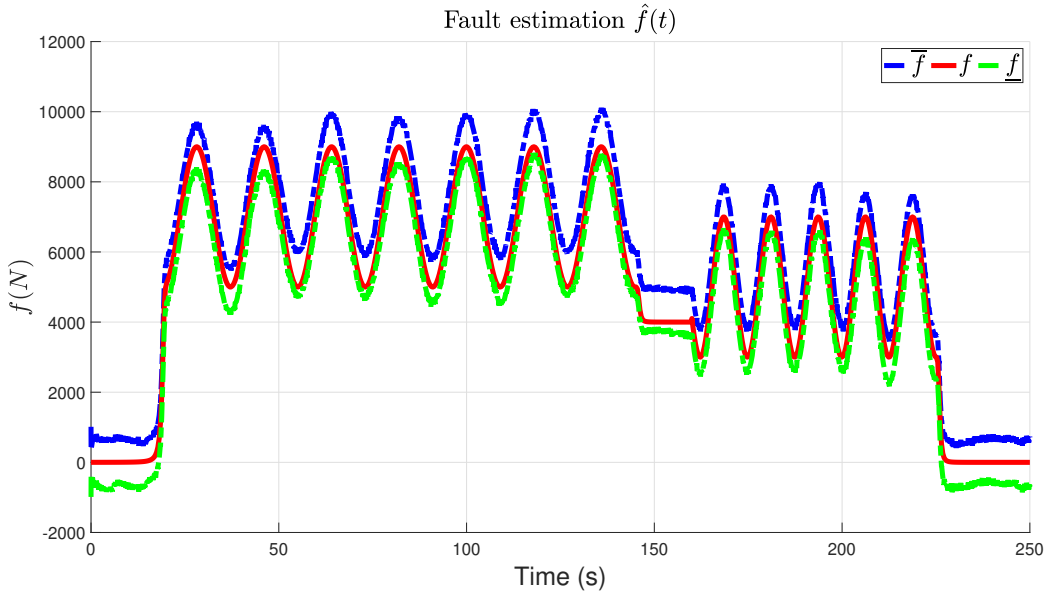

Figure 5.8: Actuator fault $f(k)$ interval estimation.

To demonstrate the efficacy of co-designing the observers and controllers in this chapter, the proposed approach is compared to the conventional separate-design strategy discussed in [135]. The comparative analysis of both methodologies are illustrated in Figure 5.12 and 5.15.

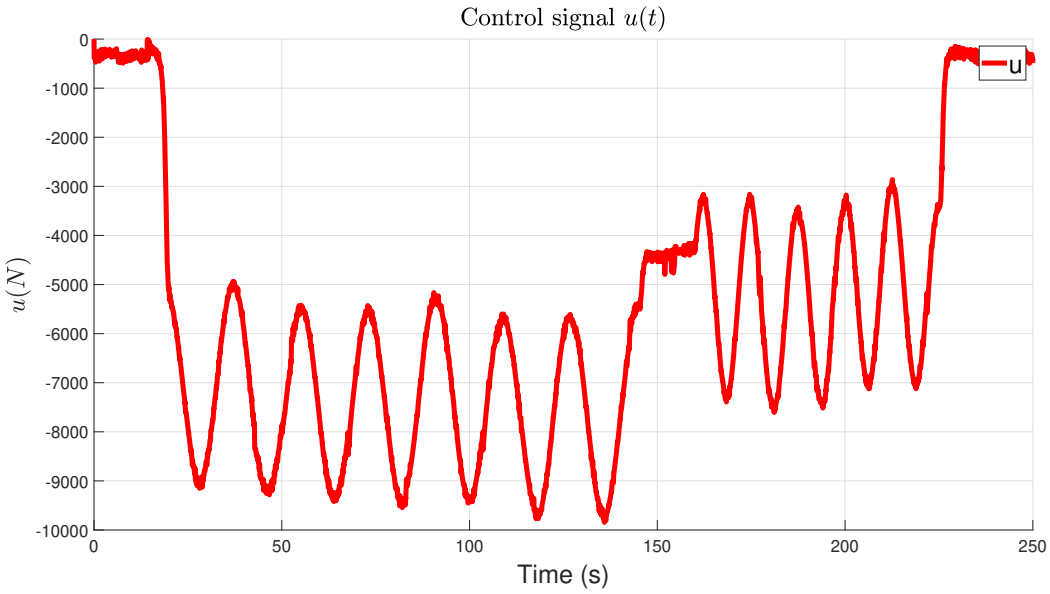

Figure 5.9: Yaw moment control input $u(k)$.

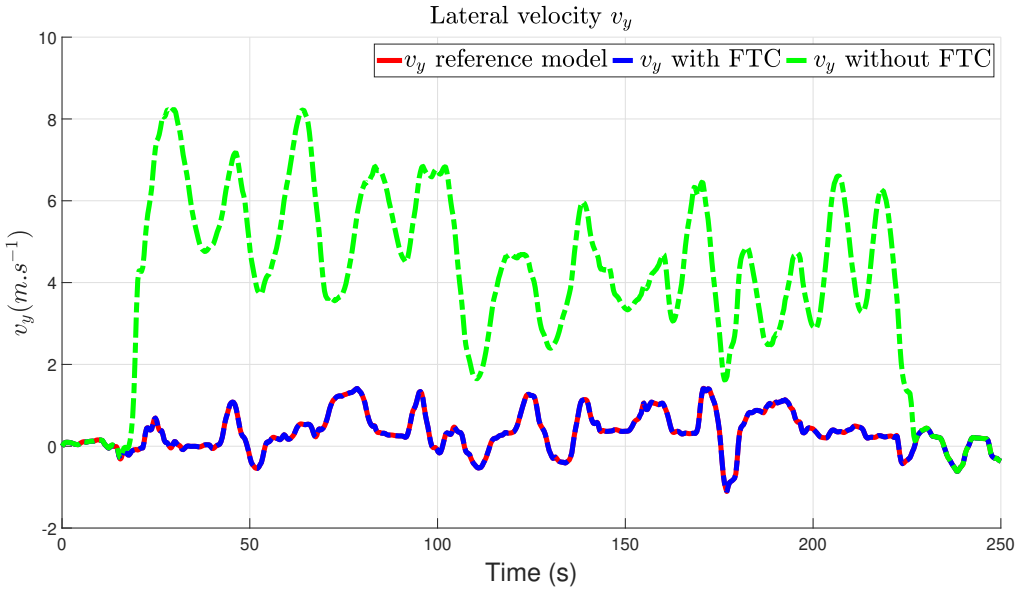

Figure 5.10: Comparison of lateral velocity $v_y(k)$ performance between with and without FTC.

The results depicted in Figure 5.12 and 5.13 show that the augmented state estimation accuracy achieved by the proposed approach surpasses than of the approach investigated in [135].

In contrast to the Separate Principle-based design methodology, the co-design of observer and controller shows better stability and performance characteristics as evidenced in Figure 5.14 and 5.15. The outcomes obtained from both methods are compared to the state of the ideal fault-free system without disturbances and measurement noise.

Notably, the system states obtained through the co-design framework exhibit closer to the reference states highlighting its effectiveness over the conventional separate design approach. It is reasonable since the bi-directional

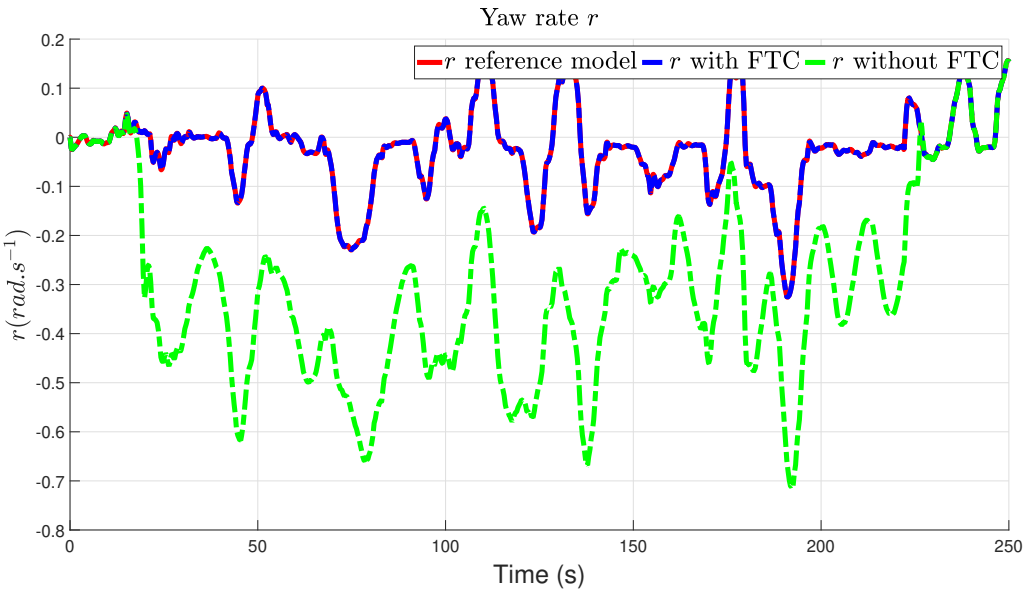

Figure 5.11: Comparison of yaw rate $r(k)$ performance between with and without FTC.

interaction between observer and controller is taken into consideration during control system design process.

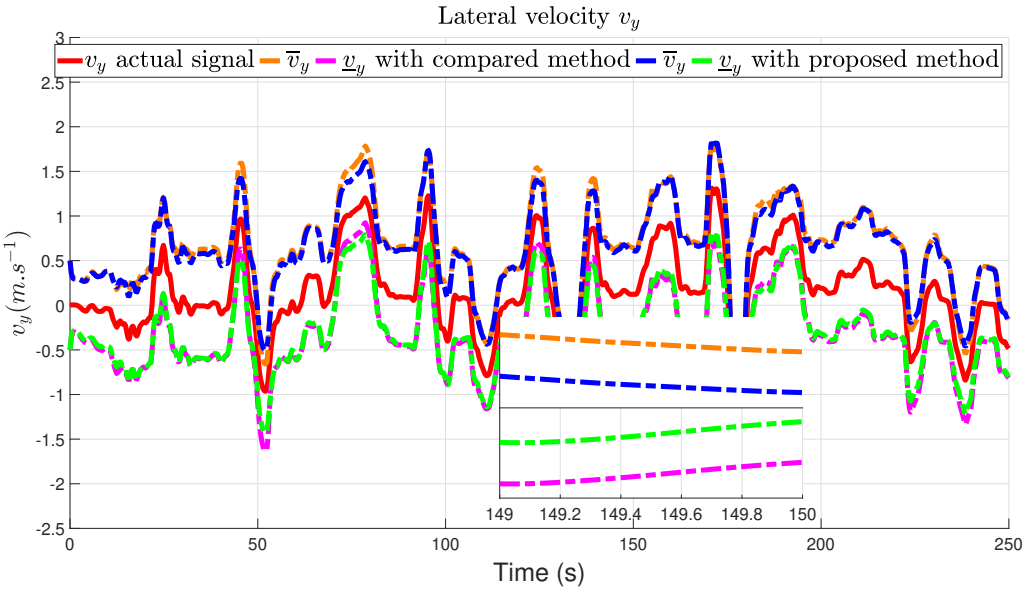

Figure 5.12: Comparison of lateral velocity $v_y(k)$ interval estimation between the proposed and compared method.

5.5 Conclusions

This chapter presented a co-design method of an integrated observer and fault tolerant controller for uncertain switched LPV systems subjected to faults, unknown but bounded disturbances and measurement noise. The co-design approach allows for tighter integration between the observer and controller. A TNL interval observer is

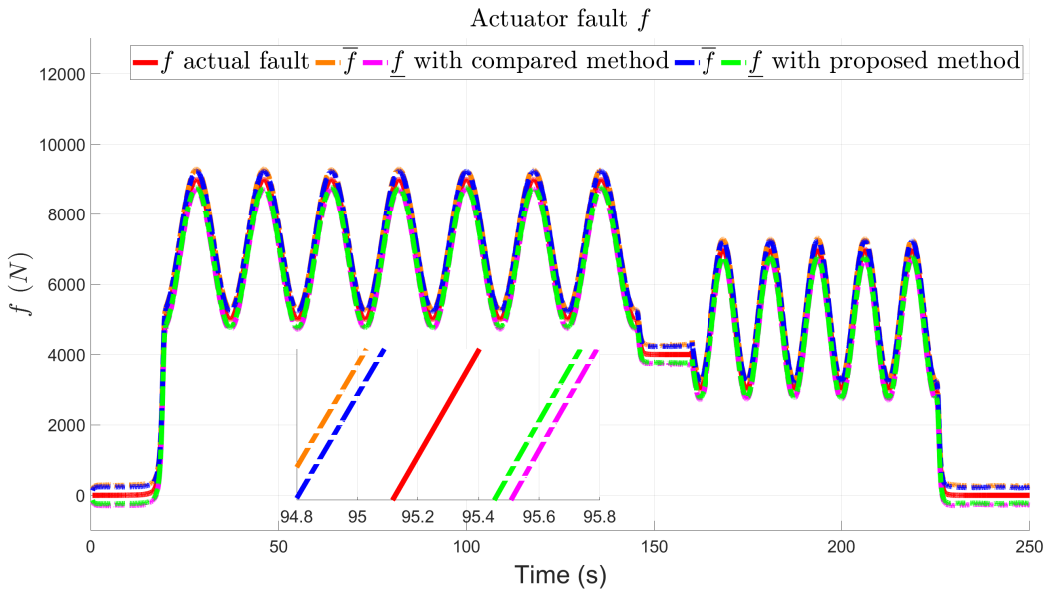

Figure 5.13: Comparison of actuator fault $r(k)$ interval estimation between the proposed and compared method.

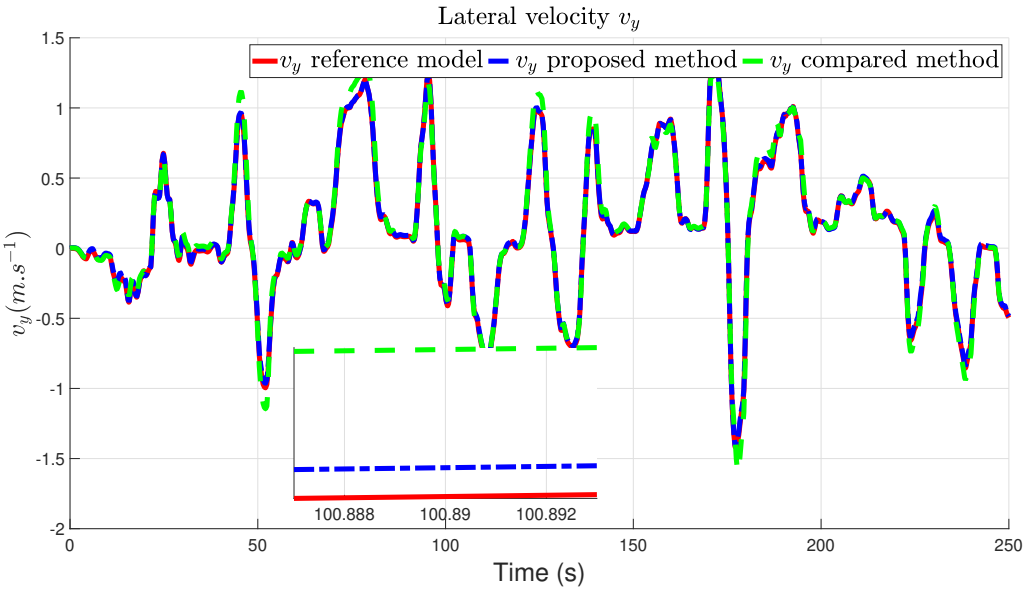

Figure 5.14: The lateral velocity $v_x(k)$ performance between the co-design and separated approach.

designed to jointly estimate the lower and upper bounds of the system states and the actuator faults. Afterward, a fault-tolerant controller is synthesized to stabilize the closed-loop system and compensate for fault effects. The existence conditions are formulated in terms of LMIs with multiple ISS-switched Lyapunov functions under the average dwell time. These conditions ensure stability, positivity and error attenuation. Introducing weighting matrices T and N provides more design degrees of freedom in the determination of the observer gain matrices. The proposed approach proves its efficiency when applied to lateral vehicle dynamics estimation and control as shown by the simulation results conducted on varying longitudinal velocity and steering angle profiles. Future works will consider

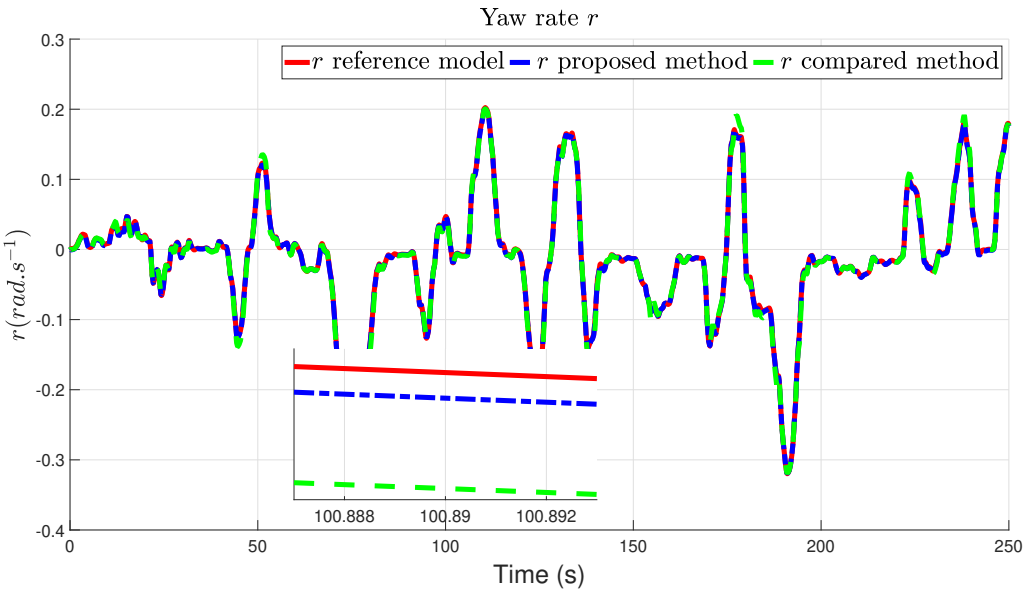

Figure 5.15: The yaw rate $r(k)$ performance between the co-design and separated approach.

the validation on experimental data obtained with a prototype vehicle. The conservativeness of the LMI conditions will be further reduced by exploring the use of the parameter-dependent Lyapunov function.

Chapter 6

General Conclusion and Perspectives

6.1 Conclusions

This thesis is mainly dedicated to the study of state estimation and fault-tolerant control for a class of switched systems. Most of the proposed methodologies are introduced in the presence of unknown but bounded disturbances and measurement noise.

In **Chapter 1**, a general introduction to the switched systems, interval observer, and fault-tolerant control has been presented. After reviewing the state of the art, **Chapter 2** provides fundamental concepts and theoretical frameworks utilized in this thesis, Linear Matrix Inequality (LMI), Convex Optimization, the switched LTI/LPV systems along with stability analysis, state feedback control design methodologies.

In **Chapter 3**, to deal with the additive fast time-varying faults, an active fault-tolerant control framework is proposed to automatically estimate and compensate for actuator faults for uncertain switched systems with average dwell time switching constraints. The AFTC framework integrates an estimation algorithm composed of a dynamics proportional integral observer (DPIO) and a switched interval observer with a state feedback fault-tolerant control (FTC) strategy. The DPIO provides fault estimation by integrated dynamic system behavior while the switched interval observer enhances robustness by accommodating the uncertainties. Thanks to the reconfiguration mechanism, the FTC adaptively generates appropriate corrective control action to ensure the system tracks the reference model with minimal performance degradation, even in the presence of actuator faults.

In **Chapter 4**, a class of continuous-time switched LPV systems with both measurable and unmeasurable parameters has been considered. A decoupling approach is employed to isolate the effects of unknown inputs from estimation errors. This isolation significantly improves state estimation accuracy, a crucial aspect of control synthesis. Furthermore, an algebraic relationship is established between the unknown input and the interval observer allowing to reconstruct the the boundaries of fault signals. To address the complexity of the design process, this chapter introduces an innovative technique based on a polytopic framework leveraging a convex representation of

system dynamics to achieve a finite-dimensional relaxation of the design conditions. Based on multiple Input-to-State-Stability Lyapunov functions, the stability and cooperativity properties have been relaxed and expressed on the vertices of each polytope.

In **Chapter 5**, a novel T-N-L interval observer structure has been proposed for uncertain discrete-time switched LPV systems. It has been shown that this new structure deals with the problem of joint state and fault estimation by reformulating into augmented state estimation using the augmented technique. The assumption made in this context is that both external disturbances and measurement noise are not precisely known but are enclosed within known bounds. Compared to the classical interval observer, the proposed approach demonstrates that the novel T-N-L interval observer structure significantly reduces conservatism in terms of design conditions and provides more design degrees of freedom by introducing additional weighting matrices. By incorporating fault estimation into control law, the proposed fault-tolerant control enables proactive fault compensation and minimizes the effects of the fault on the system behaviors.

Finally, the proposed interval observer-based control design approaches effectively address robust state estimation and control in vehicle lateral dynamics. Future research directions to enhance robustness and optimize performance are discussed in the next section.

6.2 Perspectives

There are still several issues that remain to be addressed. In particular, some future research directions are suggested as follows:

- It is important to emphasize that the results presented in this thesis are mainly based on an ideal scenario. Specifically, the assumption is that the switching between the system modes and observers or controllers is perfectly synchronized. However, this assumption is often impractical in real-world applications. In reality, the available information about the system modes is subject to delays, leading to asynchronous switching between the system modes and the corresponding interval observers and controllers. This asynchronous switching introduces significant challenges, as it invalidates the applicability of conventional techniques, such as Average Dwell Time (ADT) switching methods. Addressing this limitation represents a promising direction for future research. Exploring the impact of asynchronous switching and developing robust methodologies to handle it could pave the way for more realistic and applicable solutions in observer and control design for switched systems.

- In this thesis, fault estimation results are primarily obtained for additive actuator fault scenarios. Similar to actuator faults, sensor faults can significantly degrade the system performance and in extreme cases, lead to catastrophic events. Developing fault estimation and fault-tolerant control algorithms to deal with sensor faults

would provide an additional layer of safety and reliability to systems.

- The presence of a time delay can affect the stability and the performance of dynamical systems and complicate the fault diagnosis design problem. It is worth noting that, the findings in this thesis are focused on switched systems without considering time delays. In the literature, few works deal with robust fault detection for switched systems under a time-varying delay assumption. Thus, in future works, a time delay could be introduced to consider fault diagnosis and fault-tolerant control problems for switched systems. Additionally, the real-time implementation of FTC strategies on a prototype will be necessary to experimentally validate the performance of the proposed method.

Appendices

Appendix A

Vehicle Lateral Dynamics Models

In order to analyze and design the observers and controllers for the yaw stability control system, it is essential to develop vehicle dynamics models where mathematical model of vehicle dynamic motion is derived from Newton's 2^{nd} law that manages the forces and moments acting on the vehicle body and tires. In the following, the linearized vehicle models applied in the scope of this thesis are introduced.

A.1 Bicycle model

Vehicle lateral dynamics may be modeled as a "bicycle model" with two degrees of freedom as shown in Figure A.1. The four wheels are regarded as one front wheel and one rear wheel at the center line of the vehicle in the bicycle model.

This representation, known as the single-track model, has been proven to perfectly represent the vehicle lateral dynamic behavior. The two degrees of freedom are represented by the lateral and yaw motion. The lateral motion is measured along the lateral axis of the vehicle. The vehicle yaw motion is measured with respect to the global X axis.

The differential equations below can be used to describe the two-dimensional model characterizing the vehicle's lateral model as describe in the following equations.

- *Lateral motion*: One can have the following:

$$m\dot{v}_y + mv_x r = F_{yf} + F_{yr} \tag{A.1}$$

- *Yaw motion*: One can have the following:

$$I_z\dot{r} = l_f F_{yf} - l_r F_{yr} \tag{A.2}$$

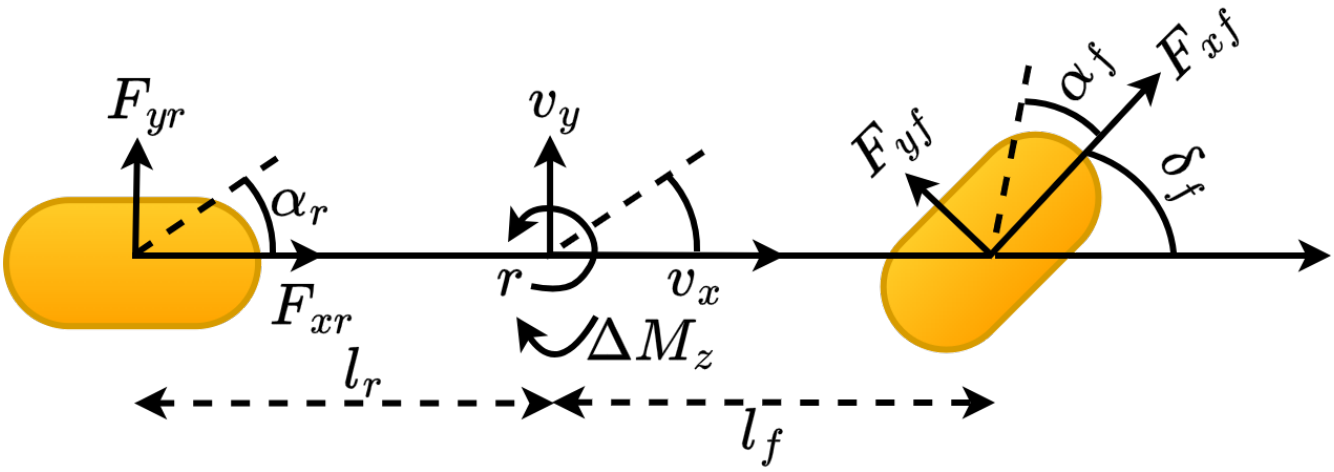

Figure A.1: Classical bicycle model.

where m, I_z are the mass and the yaw moment, v_x and v_y are lateral and longitudinal velocities, r is the yaw rate, l_f and l_r are distance from front and rear axle to COG, while F_{yf} and F_{yr} are the lateral tire force of front and rear tires.

For normal driving situation, the lateral forces F_{yf} and F_{yr} can be formed as:

$$\begin{cases} F_{yf} = c_f \alpha_f \\ F_{yr} = c_r \alpha_r \end{cases} \tag{A.3}$$

where c_f, c_r are the cornering stiffness of front and rear tires.

The front and rear wheel slip angles for linear tire forces are defined in the following equations:

$$\begin{cases} \alpha_f = \delta_f - \dfrac{v_y}{v_x} - \dfrac{l_f}{v_x} r \\ \alpha_r = -\dfrac{v_y}{v_x} + \dfrac{l_r}{v_x} r \end{cases} \tag{A.4}$$

In the proposed model, we assume that the available measurements are longitudinal velocity v_x, yaw rate r, and front steering angle δ_f.

By rearranging and simplifying (A.1), (A.2), (A.3) and (A.4), the differential equations of lateral velocity and yaw rate variables can be simplified as a linear state space model as follows:

$$\begin{bmatrix} \dot{v}_y \\ \dot{r} \end{bmatrix} = \begin{bmatrix} -\frac{c_f + c_r}{m v_x} & \frac{c_r L_r - c_f l_f}{m v_x} - v_x \\ \frac{c_r l_r - c_f l_f}{I_z v_x} & -\frac{c_r l_r^2 + c_f l_f^2}{I_z v_x} \end{bmatrix} \begin{bmatrix} v_y \\ r \end{bmatrix} + \begin{bmatrix} \frac{c_f}{m} \\ \frac{c_f l_f}{I_z} \end{bmatrix} \delta_f \tag{A.5}$$

A.2 Impact of lateral wind gust

Note that vehicles traveling at high speeds may experience lateral motion due to wind gust disturbances. The resulting force, denoted as f_w acts at the aerodynamics center (AC). The distance between the aerodynamics center and the vehicle's center of gravity is represented by l_w. Consequently, the vehicle's lateral motion under the influence of wind force can be expressed as:

- *Lateral motion*: One can have the following:

$$m\dot{v}_y + mv_x r = F_{yf} + F_{yr} + f_w \tag{A.6}$$

- *Yaw motion*: One can have the following:

$$I_z\dot{r} = l_f F_{yf} - l_r F_{yr} + l_w f_w \tag{A.7}$$

The state space model is therefore given by:

$$\begin{bmatrix} \dot{v}_y \\ \dot{r} \end{bmatrix} = \begin{bmatrix} -\frac{c_f+c_r}{mv_x} & \frac{c_r L_r - c_f l_f}{mv_x} - v_x \\ \frac{c_r l_r - c_f l_f}{I_z v_x} & -\frac{c_r l_r^2 + c_f l_f^2}{I_z v_x} \end{bmatrix} \begin{bmatrix} v_y \\ r \end{bmatrix} + \begin{bmatrix} \frac{c_f}{m} \\ \frac{c_f l_f}{I_z} \end{bmatrix} \delta_f + \begin{bmatrix} \frac{1}{m} \\ \frac{l_w}{I_z} \end{bmatrix} f_w \tag{A.8}$$

A.3 Direct yaw moment control

The active control of the yaw stability control system can be realized through active chassis control that is direct yaw moment control or active steering control or integrated active steering and direct yaw moment control. In direct yaw moment control, which can be implemented by active braking or active differential torque distribution, the required yaw moment is generated by the designed controller that controls the desired yaw rate [194]. In this thesis, only direct yaw moment control is considered.

Direct yaw moment control is recognized as an effective method to enhance the vehicle lateral stability during crucial driving manoeuvre by controlling the slip ratio of individual wheel. As illustrated in Figure A.1, the required corrective yaw moment ΔM_zwhich is generated by the transverse distribution of braking forces between the vehicle wheels is calculated by the designed controller based on the error between actual and desired vehicle model.

- *Lateral motion*: One can have the following:

$$m\dot{v}_y + mv_x r = F_{yf} + F_{yr} \tag{A.9}$$

- *Yaw motion*: One can have the following:

$$I_z\dot{r} = l_f F_{yf} - l_r F_{yr} + \Delta M_z \tag{A.10}$$

The state-space representation is expressed as:

$$\begin{bmatrix} \dot{v}_y \\ \dot{r} \end{bmatrix} = \begin{bmatrix} -\frac{c_f+c_r}{mv_x} & \frac{c_r L_r - c_f l_f}{mv_x} - v_x \\ \frac{c_r l_r - c_f l_f}{I_z v_x} & -\frac{c_r l_r^2 + c_f l_f^2}{I_z v_x} \end{bmatrix} \begin{bmatrix} v_y \\ r \end{bmatrix} + \begin{bmatrix} \frac{c_f}{m} \\ \frac{c_f l_f}{I_z} \end{bmatrix} \delta_f + \begin{bmatrix} 0 \\ \frac{1}{I_z} \end{bmatrix} \Delta M_z \tag{A.11}$$

A.4 Vision system dynamics

The vision system model characterizes the evolution of angular and lateral displacements of the vehicle from the center-line at a particular look-ahead distance l_s in (A.2). These measurements are determined using images captured by vision systems which consistently monitor the vehicle's position relative to the road geometry.

The equations describing the vision system model are given by:

$$\begin{cases} \dot{\psi}_L = r - v_x \rho \\ \dot{y}_L = v_y + v_x \psi_L + l_s (r - v_x \rho) \end{cases} \tag{A.12}$$

The system (A.12) can be rewritten in the following state representation form:

$$\begin{bmatrix} \dot{\psi}_L \\ \dot{y}_L \end{bmatrix} = \begin{bmatrix} 0 & 0 \\ v_x & 0 \end{bmatrix} \begin{bmatrix} \psi_L \\ y_L \end{bmatrix} + \begin{bmatrix} 0 & 1 \\ 1 & l_s \end{bmatrix} \begin{bmatrix} v_y \\ r \end{bmatrix} + \begin{bmatrix} -v_x \\ -l_s v_x \end{bmatrix} \rho \tag{A.13}$$

where y_L and Ψ_L are the offset and angular displacement at a look ahead distance l_s, while ρ represents the road curvature.

A.5 Derivation using slip angle as a state variable

In, the vehicle sideslip angle β is defined as the angle between the lateral and longitudinal velocities. This angle is modeled as arctangent of velocities at the vehicle center of gravity:

$$\beta = \arctan \frac{v_y}{v_x} \tag{A.14}$$

For small angle assumption, the sideslip angle equation becomes $\beta \approx \frac{v_y}{v_x}$, the vehicle lateral dynamics is given by:

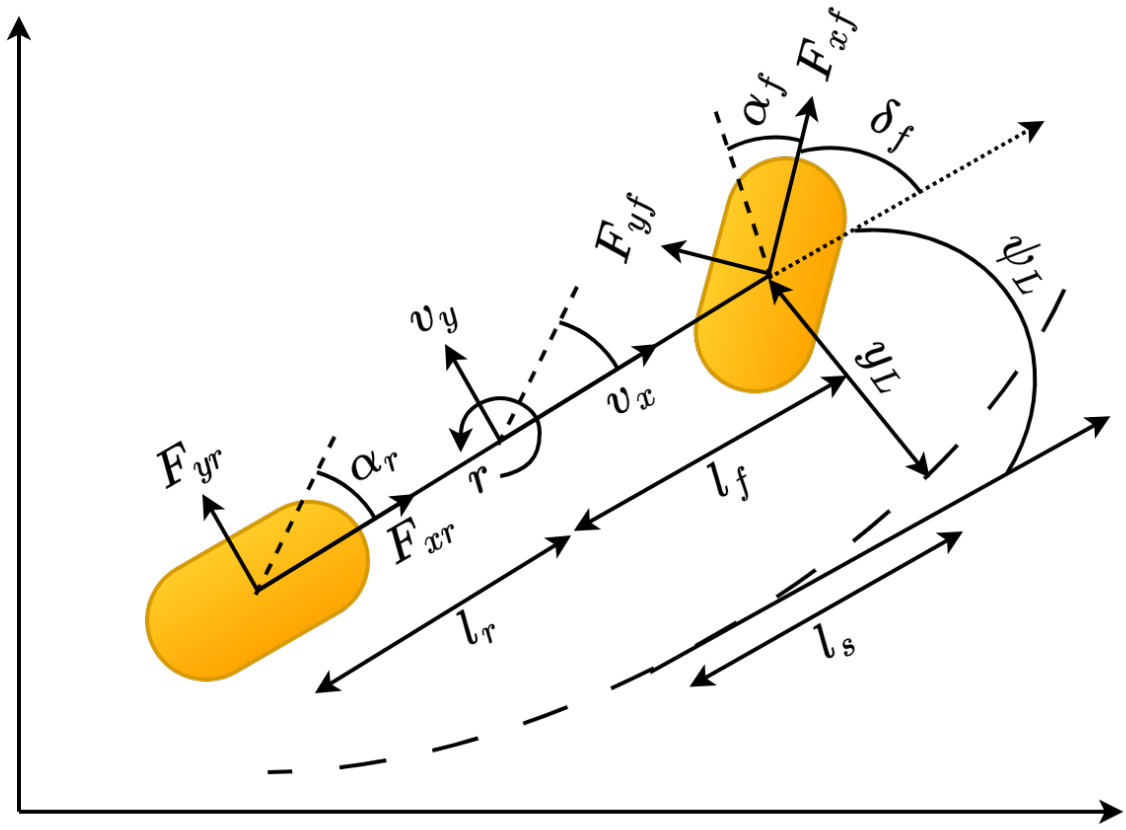

Figure A.2: Vision system dynamics.

- *Lateral motion*: One can have the following:

$$mv_x\dot{\beta} + mv_x r = F_{yf} + F_{yr} \tag{A.15}$$

- *Yaw motion*: One can have the following:

$$I_z\dot{r} = l_f F_{yf} - l_r F_{yr} \tag{A.16}$$

For small sideslip angle β, the lateral tire forces are approximated as follows:

$$\begin{cases} F_{yf} = c_f\Big(\delta_f - \beta - \dfrac{l_f}{v_x} r\Big) \\ F_{yr} = c_r\Big(-\beta + \dfrac{l_r}{v_x} r\Big) \end{cases} \tag{A.17}$$

Simplified (A.15), (A.16) and (A.17), the vehicle lateral dynamics model is given as follows:

$$\begin{bmatrix} \dot{\beta} \\ \dot{r} \end{bmatrix} = \begin{bmatrix} -\frac{c_f + c_r}{m v_x} & \frac{c_r L_r - c_f l_f}{m v_x^2} - 1 \\ \frac{c_r l_r - c_f l_f}{I_z} & -\frac{c_r l_r^2 + c_f l_f^2}{I_z v_x} \end{bmatrix} \begin{bmatrix} \beta \\ r \end{bmatrix} + \begin{bmatrix} \frac{c_f}{m v_x} \\ \frac{c_f l_f}{I_z} \end{bmatrix} \delta_f \tag{A.18}$$

It should be noted that a formulation in terms of the vehicle sideslip angle β and yaw rate r is also used in this thesis as well.

Remark A.1 *It is obvious that the vehicle bicycle model* (A.5) *and the other previously derived formulations depend on the longitudinal velocity v_x, which plays a crucial role in shaping vehicle behavior and introduces significant nonlinearities into the dynamics. Due to these nonlinear effects, the use of linear parameter-varying (LPV) models presents a more flexible and less conservative alternative to stationary models, enabling a more accurate representation of the system's behavior across varying operating conditions. In this framework, the longitudinal velocity is selected as a measurable scheduling parameter, while the cornering stiffness, which varies due to factors such as road surface conditions and tire wear, is treated as an unmeasurable scheduling parameter. However, when the system exhibits a large parameter variation range, a single estimator or controller may lead to conservative performance and the problem of searching for the observer and controller gains may become infeasible. To address this issue, the switched LPV system can be employed. In this method, the longitudinal velocity parameter domain is divided into multiple sub-regions, with a dedicated local observer or controller designed for each subsystem. As a result, the vehicle lateral dynamics are then captured using a switched LPV model with measurable premise variables, enhancing the overall robustness and efficiency of state estimation and control in dynamic driving conditions.*

In this thesis, a switched system is adopted, where each subsystem operates within a specific subregion of longitudinal velocity range (e.g., three subsystems corresponding to low, average, and high longitudinal velocity). A switching signal, based on the measured longitudinal velocity, is then implemented to select the appropriate subsystem in real-time.

Bibliography

[1] Sara Ifqir, Dalil Ichalal, Naima Ait-Oufroukh, and Saïd Mammar. Vehicle lateral velocity and lateral tire-road forces estimation based on switched interval observers. *2020 American Control Conference (ACC)*, pages 3023–3028, 2020.

[2] Dongsheng Du and Vincent Cocquempot. Non-fragile actuator fault estimation and accommodation for switched systems. *IFAC-PapersOnLine*, 51(24):110–116, 2018. 10th IFAC Symposium on Fault Detection, Supervision and Safety for Technical Processes SAFEPROCESS 2018.

[3] Sara Ifqir, Dalil Ichalal, Naima Ait Oufroukh, and Said Mammar. Robust interval observer for switched systems with unknown inputs: Application to vehicle dynamics estimation. *European Journal of Control*, 44:3–14, 2018. Advanced Control and Observer Design for Nonlinear Systems via LMIs.

[4] Houssem Jerbi. An enhanced stabilizing strategy for switched nonlinear systems. *Studies in Informatics and Control*, 28, 12 2019.

[5] D. Liberzon and A.S. Morse. Basic problems in stability and design of switched systems. *IEEE Control Systems Magazine*, 19(5):59–70, 1999.

[6] Dariush Tavakolifar, Hamid Khaloozadeh, and Roya Amjadifard. Stabilization of switched systems with all unstable modes: Application to the aircraft team problem. *Journal of Systems Engineering and Electronics*, 30(4):792–798, 2019.

[7] Shuji Chen, L. Jiang, W. Yao, and Q.H. Wu. Application of switched system theory in power system stability. In *2014 49th International Universities Power Engineering Conference (UPEC)*, pages 1–6, 2014.

[8] F.S. Garcia Deaecto, J.C. Geromel and J.A. Pomilio. Switched affine systems control design with application to dc–dc converters. *IET Control Theory & Applications*, 4:1201–1210(9), July 2010.

[9] Mona Faraji-Niri, Vahid Asadzadeh, and Javad Fard. Stabilization of arbitrary switched nonlinear fractional order dynamical systems: Application to francis hydro-turbine governing system. *Information Technology And Control*, 48:401–414, 09 2019.

[10] Hai Lin and Panos J. Antsaklis. Stability and stabilizability of switched linear systems: A survey of recent results. *IEEE Transactions on Automatic Control*, 54(2):308–322, 2009.

[11] Jin Lu and Lyndon J. Brown. A multiple lyapunov functions approach for stability of switched systems. In *Proceedings of the 2010 American Control Conference*, pages 3253–3256, 2010.

[12] L. Vu, D. Chatterjee, and D. Liberzon. Iss of switched systems and applications to switching adaptive control. In *Proceedings of the 44th IEEE Conference on Decision and Control*, pages 120–125, 2005.

[13] A.S. Morse. Supervisory control of families of linear set-point controllers - part i. exact matching. *IEEE Transactions on Automatic Control*, 41(10):1413–1431, 1996.

[14] Annalisa Zappavigna, Patrizio Colaneri, José C. Geromel, and Robert Shorten. Dwell time analysis for continuous-time switched linear positive systems. In *Proceedings of the 2010 American Control Conference*, pages 6256–6261, 2010.

[15] Masood Dehghan and Marcelo H. Ang. Stability of switched linear systems under dwell time switching with piece wise quadratic functions. In *2014 13th International Conference on Control Automation Robotics & Vision (ICARCV)*, pages 1257–1260, 2014.

[16] Songlin Zhuang, Huijun Gao, and Yang Shi. Model predictive control of switched linear systems with persistent dwell-time constraints: Recursive feasibility and stability. *IEEE Transactions on Automatic Control*, 68(12):7887–7894, 2023.

[17] J.P. Hespanha and A.S. Morse. Stability of switched systems with average dwell-time. *Proceedings of the 38th IEEE Conference on Decision and Control (Cat. No.99CH36304)*, 3:2655–2660 vol.3, 1999.

[18] G. Zhai, B. Hu, K. Yasuda, and A.N. Michel. Stability analysis of switched systems with stable and unstable subsystems: an average dwell time approach. *Proceedings of the 2000 American Control Conference. ACC (IEEE Cat. No.00CH36334)*, (6):200–204 vol.1, 2000.

[19] Ying Jin, Youmin Zhang, Yuanwei Jing, and Jun Fu. An average dwell-time method for fault-tolerant control of switched time-delay systems and its application. *IEEE Transactions on Industrial Electronics*, 66(4):3139–3147, 2019.

[20] Caiyun Wu and Jun Zhao. h_∞ adaptive tracking control for switched systems based on an average dwell-time method. *International Journal of Systems Science*, 46(14):2547–2559, 2015.

[21] Stefan Leutenegger, Amir Melzer, Kostas Alexis, and Roland Siegwart. Robust state estimation for small unmanned airplanes. In *2014 IEEE Conference on Control Applications (CCA)*, pages 1003–1010, 2014.

[22] Alexander Wischnewski, Tim Stahl, Johannes Betz, and Boris Lohmann. Vehicle dynamics state estimation and localization for high performance race cars**research was supported by the basic research fund of the institute of automotive technology of the technical university of munich. *IFAC-PapersOnLine*, 52(8):154–161, 2019. 10th IFAC Symposium on Intelligent Autonomous Vehicles IAV 2019.

[23] A. Rendon, C. Fuerte, and Jorge Calderon. State estimation of electrical power grids incorporating scada and pmu measurements. *IEEE Latin America Transactions*, 13:2245–2251, 07 2015.

[24] A. Alessandri and P. Coletta. Design of observers for switched discrete-time linear systems. *Proceedings of the 2003 American Control Conference, 2003.*, 4:2785–2790 vol.4, 2003.

[25] H. Ríos, D. Efimov, J. Davila, T. Raïssi, L. Fridman, and A. Zolghadri. State estimation for linear switched systems with unknown inputs*. *IFAC Proceedings Volumes*, 45(9):271–276, 2012. 4th IFAC Conference on Analysis and Design of Hybrid Systems.

[26] Shasha Fu, Jianbin Qiu, Liheng Chen, and Shaoshuai Mou. Adaptive fuzzy observer design for a class of switched nonlinear systems with actuator and sensor faults. *IEEE Transactions on Fuzzy Systems*, 26(6):3730–3742, 2018.

[27] Liheng Chen, Shasha Fu, Yuxin Zhao, Ming Liu, and Jianbin Qiu. State and fault observer design for switched systems via an adaptive fuzzy approach. *IEEE Transactions on Fuzzy Systems*, 28(9):2107–2118, 2020.

[28] M. Ait Rami, C. H. Cheng, and C. de Prada. Tight robust interval observers: An lp approach. In *2008 47th IEEE Conference on Decision and Control*, pages 2967–2972, 2008.

[29] Tarek Raïssi, Gaétan Videau, and Ali Zolghadri. Interval observer design for consistency checks of nonlinear continuous-time systems. *Automatica*, 46(3):518–527, 2010.

[30] S. Ifqir, N. Ait-Oufroukh, D. Ichalal, and S. Mammar. Synchronous interval observer design for switched lpv systems using multiple quadratic iss-lyapunov functions. In *2017 25th Mediterranean Conference on Control and Automation (MED)*, pages 388–393, 2017.

[31] Tarek Raissi, Denis Efimov, and Ali Zolghadri. Interval state estimation for a class of nonlinear systems. *IEEE Transactions on Automatic Control*, 57(1):260–265, 2012.

[32] Denis Efimov, Wilfrid Perruquetti, Tarek Raïssi, and Ali Zolghadri. Interval observers for time-varying discrete-time systems. *IEEE Transactions on Automatic Control*, 58(12):3218–3224, 2013.

[33] Ghassen Marouani, Thach Ngoc Dinh, Tarek Rassï, and Hassani Messaoud. Interval observers design for discrete-time linear switched systems. In *2018 European Control Conference (ECC)*, pages 801–806, 2018.

[34] Frédéric Mazenc and Olivier Bernard. Interval observers for linear time-invariant systems with disturbances. *Automatica*, 47(1):140–147, 2011.

[35] Filippo Cacace, Alfredo Germani, and Costanzo Manes. A new approach to design interval observers for linear systems. *IEEE Transactions on Automatic Control*, 60(6):1665–1670, 2015.

[36] Jean-Luc Gouze, Alain Rapaport, and M.Z. Hadj-Sadok. Interval observers for uncertain biological systems. *Ecological Modelling*, 133:45–56, 08 2000.

[37] Andrey Polyakov, Denis Efimov, Wilfrid Perruquetti, and Jean-Pierre Richard. Interval observer approach to output stabilization of time-varying input delay systems. In *2013 European Control Conference (ECC)*, pages 4412–4417, 2013.

[38] Denis Efimov, Tarek Raïssi, Wilfrid Perruquetti, and Ali Zolghadri. Design of interval observers for estimation and stabilization of discrete-time LPV systems. *IMA Journal of Mathematical Control and Information*, 33(4):1051–1066, 06 2015.

[39] Rihab El Houda Thabet, Tarek Raïssi, Christophe Combastel, Denis Efimov, and Ali Zolghadri. An effective method to interval observer design for time-varying systems. *Automatica*, 50(10):2677–2684, 2014.

[40] Da-Ke Gu, Li-Song Sun, and Yin-Dong Liu. Functional interval observer design for linear time-varying systems with additive disturbances. *Transactions of the Institute of Measurement and Control*, 45(4):736–746, 2023.

[41] H. Ethabet, T. Raïssi, M. Amairi, C. Combastel, and M. Aoun. Interval observer design for continuous-time switched systems under known switching and unknown inputs. *International Journal of Control*, 93(5):1088–1101, 2020.

[42] Thach Ngoc Dinh, Ghassen Marouani, Tarek Raïssi, Zhenhua Wang, and Hassani Messaoud. Optimal interval observers for discrete-time linear switched systems. *International Journal of Control*, 93(11):2613–2621, 2020.

[43] Sara Ifqir, Dalil Ichalal, Naima Ait-Oufroukh, and Saïd Mammar. Interval observer design for switched systems with state and output uncertainties: Application to vehicle sideslip angle estimation. In *2019 American Control Conference (ACC)*, pages 4307–4312, 2019.

[44] Yue-E Wang, Yongfeng Gao, Di Wu, and Ben Niu. Interval observer-based event-triggered control for switched linear systems. *Journal of the Franklin Institute*, 357(10):5753–5772, 2020.

[45] Chaima Zammali, Jeremy Van Gorp, and Tarek Raïssi. Interval observers based fault detection for switched systems with l_∞ performances. In *2020 European Control Conference (ECC)*, pages 1053–1056, 2020.

[46] Zhongwei He and Wei Xie. Control of non-linear switched systems with average dwell time: interval observer-based framework. *IET Control Theory & Applications*, 10(1):10–16, 2016.

[47] Daniel Ulises Campos Delgado, D. Espinoza-Trejo, and Elvia Palacios. Fault-tolerant control in variable speed drives: A survey. *Electric Power Applications, IET*, 2:121 – 134, 04 2008.

[48] Xiang Yu and Jin Jiang. A survey of fault-tolerant controllers based on safety-related issues. *Annual Reviews in Control*, 39:46–57, 2015.

[49] Wang Jun, Zhang Xiao-Yan, and LI Wei. Hybrid active-passive α-stability fault-tolerant control research of nonlinear ncs under detcs. In *2018 IEEE 4th International Conference on Control Science and Systems Engineering (ICCSSE)*, pages 40–48, 2018.

[50] Xiaofeng Liu. Hybrid fault-tolerant control system for multiple faults of aeroengines. In *2019 Chinese Control And Decision Conference (CCDC)*, pages 1328–1331, 2019.

[51] Mickael Rodrigues, Didier Theilliol, Samir Aberkane, and Dominique Sauter. Fault tolerant control design for polytopic lpv systems. *International Journal of Applied Mathematics and Computer Science*, 17:27–37, 03 2007.

[52] Marcel Luzar and Marcin Witczak. Fault-tolerant control and diagnosis for lpv system with h-infinity virtual sensor. In *2016 3rd Conference on Control and Fault-Tolerant Systems (SysTol)*, pages 825–830, 2016.

[53] Hemza Mekki, Djamel Boukhetala, and Ahmad Taher Azar. *Sliding Modes for Fault Tolerant Control*, pages 407–433. Springer International Publishing, Cham, 2015.

[54] Ying Yang, Yan-Jun Wang, Ji-Qing Qiu, and Yan-Rong Niu. Robust h_∞ passive fault-tolerant control for uncertain singular systems. *2011 International Conference on Machine Learning and Cybernetics*, 3:1308–1312, 2011.

[55] Abdel-Razzak Merheb, Hassan Noura, and François Bateman. Passive fault tolerant control of quadrotor uav using regular and cascaded sliding mode control. In *2013 Conference on Control and Fault-Tolerant Systems (SysTol)*, pages 330–335, 2013.

[56] Rihab Lamouchi, Tarek Raissi, Messaoud Amairi, and Mohamed Aoun. Interval observer-based methodology for passive fault tolerant control of linear parameter-varying systems. *Transactions of the Institute of Measurement and Control*, 44(5):986–999, 2022.

[57] Himanshukumar R. Patel and Vipul A. Shah. Passive fault tolerant control system using feed-forward neural network for two-tank interacting conical level control system against partial actuator failures and disturbances. *IFAC-PapersOnLine*, 52(14):141–146, 2019. 18th IFAC Symposium on Control, Optimization and Automation in Mining, Mineral and Metal Processing, MMM 2019.

[58] Zichen Yan, Junbo Tan, Bin Liang, Houde Liu, and Jun Yang. Active fault-tolerant control integrated with reinforcement learning application to robotic manipulator. In *2022 American Control Conference (ACC)*, pages 2656–2662, 2022.

[59] Christoffer Sloth, Thomas Esbensen, and Jakob Stoustrup. Active and passive fault-tolerant lpv control of wind turbines. In *Proceedings of the 2010 American Control Conference*, pages 4640–4646, 2010.

[60] G. Bertoni, N. Bertozzi, P. Castaldi, and S. Simani. A nonlinear guidance and active fault tolerant control system for a fixed wing unmanned aerial vehicle. In *Proceedings of the 2010 American Control Conference*, pages 812–817, 2010.

[61] Mickaël Rodrigues, Didier Theilliol, and Dominique Sauter. Fault tolerant control design for switched systems. *IFAC Proceedings Volumes*, 39(5):223–228, 2006. 2nd IFAC Conference on Analysis and Design of Hybrid Systems.

[62] Hao Yang, Hong Li, Bin Jiang, and Vincent Cocquempot. Fault tolerant control of switched systems: A generalized separation principle. *IEEE Transactions on Control Systems Technology*, 27(2):553–565, 2019.

[63] Yanzheng Zhu and Wei Xing Zheng. An integrated design approach for fault-tolerant control of switched lpv systems with actuator faults. *IEEE Transactions on Systems, Man, and Cybernetics: Systems*, 53(2):908–921, 2023.

[64] Ayyoub Ait Ladel, Abdellah Benzaouia, Rachid Outbib, and Mustapha Ouladsine. Integrated state/fault estimation and fault-tolerant control design for switched t–s fuzzy systems with sensor and actuator faults. *IEEE Transactions on Fuzzy Systems*, 30(8):3211–3223, 2022.

[65] Rihab Lamouchi, Tarek Raissi, Messaoud Amairi, and Mohamed Aoun. On interval observer design for active fault tolerant control of linear parameter-varying systems. *Systems & Control Letters*, 164:105218, 2022.

[66] Xue Han, Rim Rammal, Zetao Li, Michel Cabassud, and Boutaib Dahhou. Interval observer-based active fault tolerant control for an intensified heat exchanger/reactor. In *2021 9th International Conference on Systems and Control (ICSC)*, pages 133–138, 2021.

[67] Duc Lich Luu and Ciprian Lupu. Dynamics model and design for adaptive cruise control vehicles. In *2019 22nd International Conference on Control Systems and Computer Science (CSCS)*, pages 12–17, 2019.

[68] J. Shao, L. Zheng, Y. N. Li, J. S. Wei, and M. G. Luo. The integrated control of anti-lock braking system and active suspension in vehicle. In *Fourth International Conference on Fuzzy Systems and Knowledge Discovery (FSKD 2007)*, volume 4, pages 519–523, 2007.

[69] S. Mammar, S. Glaser, and M. Netto. Vehicle lateral dynamics estimation using unknown input proportional-integral observers. *2006 American Control Conference*, pages 6 pp.–, 2006.

[70] Markus Tranninger, Martin Steinberger, Leonid Fridman, Martin Horn, and Sergiy Zhuk. Robust state estimation for linear time varying lateral vehicle dynamics with unknown road curvature. In *2018 15th International Workshop on Variable Structure Systems (VSS)*, pages 384–389, 2018.

[71] Naoufal Elyoussfi, Mohammed Oudghiri, and Rachid El Bachtiri. Observer-based fault tolerant control for vehicle lateral dynamics. In *2017 14th International Multi-Conference on Systems, Signals & Devices (SSD)*, pages 70–75, 2017.

[72] Mohammed Oudghiri, Mohammed Chadli, and Ahmed El Hajjaji. A fuzzy approach for sensor fault-tolerant control of vehicle lateral dynamics. In *2007 IEEE International Conference on Control Applications*, pages 1221–1226, 2007.

[73] Naoufal El Youssfi and Mohammed Oudghiri. Fault estimation and tolerant control for vehicle lateral dynamics. In *2018 7th International Conference on Systems and Control (ICSC)*, pages 213–218, 2018.

[74] Bei Lu and Fen Wu. Switching lpv control designs using multiple parameter-dependent lyapunov functions. *Automatica*, 40(11):1973–1980, 2004.

[75] Michael Branicky. Multiple lyapunov functions and other analysis tools for switched and hybrid systems. *Automatic Control, IEEE Transactions on*, 43:475 – 482, 05 1998.

[76] Bei Lu and Fen Wu. Switching lpv control designs using multiple parameter-dependent lyapunov functions. *Automatica*, 40(11):1973–1980, 2004.

[77] Eduardo D. Sontag and Yuan Wang. On characterizations of the input-to-state stability property. *Systems & Control Letters*, 24(5):351–359, 1995.

[78] Eduardo D. Sontag. *Input to State Stability: Basic Concepts and Results*, pages 163–220. Springer Berlin Heidelberg, Berlin, Heidelberg, 2008.

[79] Matthias A. Müller and Daniel Liberzon. Input/output-to-state stability and state-norm estimators for switched nonlinear systems. *Automatica*, 48(9):2029–2039, 2012.

[80] GuangXue Zhang and Aneel Tanwani. Iss lyapunov functions for cascade switched systems and sampled-data control. *Automatica*, 105:216–227, 2019.

[81] Shivaraj Mohite, Marouane Alma, and Ali Zemouche. Design of a nonlinear observer for a class of locally lipschitz systems by using input-to-state stability: An lmi approach. In *2023 62nd IEEE Conference on Decision and Control (CDC)*, pages 7501–7506, 2023.

[82] Guosong Yang and Daniel Liberzon. Input-to-state stability for switched systems with unstable subsystems: A hybrid lyapunov construction. In *53rd IEEE Conference on Decision and Control*, pages 6240–6245, 2014.

[83] Stefania Andersen, Peter Giesl, and Sigurdur Hafstein. Common lyapunov functions for switched linear systems: Linear programming-based approach. *IEEE Control Systems Letters*, 7:901–906, 2023.

[84] Xu He, Georgi M. Dimirovski, and Jun Zhao. Control of switched lpv systems using common lyapunov function method and an f-16 aircraft application. In *2010 IEEE International Conference on Systems, Man and Cybernetics*, pages 386–392, 2010.

[85] Xu He, Georgi M. Dimirovski, and Jun Zhao. Control of switched lpv systems using common lyapunov function method and an f-16 aircraft application. In *2010 IEEE International Conference on Systems, Man and Cybernetics*, pages 386–392, 2010.

[86] Falk M. Hante and Mario Sigalotti. Existence of common lyapunov functions for infinite-dimensional switched linear systems. In *49th IEEE Conference on Decision and Control (CDC)*, pages 5668–5673, 2010.

[87] Stefania Andersen, Peter Giesl, and Sigurdur Hafstein. Common lyapunov functions for switched linear systems: Linear programming-based approach. *IEEE Control Systems Letters*, 7:901–906, 2023.

[88] Liying Zhu and Gang Feng. Necessary and sufficient conditions for stability of switched nonlinear systems. *Journal of the Franklin Institute*, 352(1):117–137, 2015.

[89] Fanglai Zhu, Wei Zhang, Jiancheng Zhang, and Shenghui Guo. Unknown input reconstruction via interval observer and state and unknown input compensation feedback controller designs. *International Journal of Control, Automation and Systems*, 19, 08 2020.

[90] G Davrazos and NT Koussoulas. A review of stability results for switched and hybrid systems. In *Mediterranean Conference on Control and Automation*. Citeseer, 2001.

[91] Ding Zhai, An-Yang Lu, Jiuxiang Dong, and Qing-Ling Zhang. Stability analysis and state feedback control of continuous-time t–s fuzzy systems via anew switched fuzzy lyapunov function approach. *Applied Mathematics and Computation*, 293:586–599, 2017.

[92] Flavio A. Faria, Vilma A. Oliveira, Leandro J. Elias, Jorge M. V. Capela, and Julia S. Tanaka. Less conservative conditions for stabilization of switched ts fuzzy systems using fuzzy lyapunov functions. In *2018 IEEE International Conference on Fuzzy Systems (FUZZ-IEEE)*, pages 1–7, 2018.

[93] Leonardo A. Mozelli and Ricardo L. S. Adriano. On computational issues for stability analysis of lpv systems using parameter-dependent lyapunov functions and lmis. *International Journal of Robust and Nonlinear Control*, 29(10):3267–3277, 2019.

[94] Leandro J. Elias, Flávio A. Faria, Rayza Araujo, and Vilma A. Oliveira. Stability analysis of takagi–sugeno systems using a switched fuzzy lyapunov function. *Information Sciences*, 543:43–57, 2021.

[95] Sara Ifqir, Ichalal Dalil, Ait-Oufroukh Naïma, and Mammar Saïd. Adaptive threshold generation for vehicle fault detection using switched t–s interval observers. *IEEE Transactions on Industrial Electronics*, 67(6):5030–5040, 2020.

[96] Mohamed R. M. Rizk, Mazhar B. Tayel, and Walied M. Saed. Observer design of discrete time t-s fuzzy systems with measurable premise variables based on common quadratic lyapunov function. In *2017 4th International Conference on Control, Decision and Information Technologies (CoDIT)*, pages 0462–0465, 2017.

[97] D. Luenberger. Observers for multivariable systems. *IEEE Transactions on Automatic Control*, 11(2):190–197, 1966.

[98] Sara Ifqir, Puig Vicenç, Ichalal Dalil, Ait-Oufroukh Naima, and Mammar Saïd. Zonotopic set-membership state estimation for switched systems. *Journal of the Franklin Institute*, 359(16):9241–9270, 2022.

[99] Marco Casini, Andrea Garulli, and Antonio Vicino. Set membership state estimation for discrete-time linear systems with binary sensor measurements. *Automatica*, 159:111396, 2024.

[100] T. Raissi, N. Ramdani, and Y. Candau. Set membership state and parameter estimation for systems described by nonlinear differential equations. *Automatica*, 40(10):1771–1777, 2004.

[101] R. Lamouchi, T. Raïssi, M. Amairi, and M. Aoun. Fault tolerant control in a set-membership framework. In *2016 European Control Conference (ECC)*, pages 1099–1104, 2016.

[102] Fatiha Nejjari, Vicenç Puig, Saúl Montes de Oca, and Atefeh Sadeghzadeh. Robust fault detection for lpv systems using interval observers and zonotopes. In *Proceedings of the 48h IEEE Conference on Decision and Control (CDC) held jointly with 2009 28th Chinese Control Conference*, pages 1002–1007, 2009.

[103] Mohammad Khajenejad, Scott Brown, and Sonia Martínez. Distributed interval observers for bounded-error lti systems. In *2023 American Control Conference (ACC)*, pages 2444–2449, 2023.

[104] Awais Khan, Wei Xie, Bo Zhang, and Long-Wen Liu. A survey of interval observers design methods and implementation for uncertain systems. *Journal of the Franklin Institute*, 358(6):3077–3126, 2021.

[105] Tarek Raissi, Denis Efimov, and Ali Zolghadri. Interval state estimation for a class of nonlinear systems. *IEEE Transactions on Automatic Control*, 57(1):260–265, 2012.

[106] L. Meyer, D. Ichalal, and V. Vigneron. Interval observer for nonlinear lipschitz systems with unknown inputs. *2018 Annual American Control Conference (ACC)*, pages 5962–5967, 2018.

[107] Chaima Zammali, Jeremy Van Gorp, Xubin Ping, and Tarek Raïssi. Interval estimation for discrete-time lpv switched systems. *2019 IEEE 58th Conference on Decision and Control (CDC)*, pages 2479–2484, 2019.

[108] Denis Efimov and Tarek Raissi. Design of interval observers for uncertain dynamical systems. *Automation and Remote Control*, 77:191–225, 02 2016.

[109] Guang-Ren Duan and Hai-Hua Yu. *LMIs in Control Systems*. CRC Press, June 2013.

[110] Liang Qiao and Ying Yang. Nonfragile fault-tolerant observer-based controller design for descriptor systems. *2017 Chinese Automation Congress (CAC)*, pages 3286–3290, 2017.

[111] Jianglin Lan and Ron J. Patton. Integrated fault estimation and fault-tolerant control design for large-scale interconnected systems. *2016 3rd Conference on Control and Fault-Tolerant Systems (SysTol)*, pages 263–268, 2016.

[112] Anh-Tu Nguyen, Truong Quang Dinh, Thierry-Marie Guerra, and Juntao Pan. Takagi–sugeno fuzzy unknown input observers to estimate nonlinear dynamics of autonomous ground vehicles: Theory and real-time verification. *IEEE/ASME Transactions on Mechatronics*, 26(3):1328–1338, 2021.

[113] Duc-Tien Nguyen, David Saussié, and Lahcen Saydy. Universal adaptive fault-tolerant control of a multicopter uav**this work was supported by nserc under grant numbers rgpin-2014-03942 and rgpin-2012-122106. *IFAC-PapersOnLine*, 53(2):9340–9347, 2020. 21st IFAC World Congress.

[114] Xitao Wu, Chao Wei, Hanqing Tian, Weida Wang, and Chaoyang Jiang. Fault-tolerant control for path-following of independently actuated autonomous vehicles using tube-based model predictive control. *IEEE Transactions on Intelligent Transportation Systems*, 23(11):20282–20297, 2022.

[115] A. Freddi, S. Longhi, A. Monteriù, D. Ortenzi, and D. Proietti Pagnotta. Fault tolerant control scheme for robotic manipulators affected by torque faults. *IFAC-PapersOnLine*, 51(24):886–893, 2018. 10th IFAC Symposium on Fault Detection, Supervision and Safety for Technical Processes SAFEPROCESS 2018.

[116] Youmin Zhang and Jin Jiang. Bibliographical review on reconfigurable fault-tolerant control systems. *Annual Reviews in Control*, 32(2):229–252, 2008.

[117] Afef Fekih. Fault diagnosis and fault tolerant control design for aerospace systems: A bibliographical review. In *2014 American Control Conference*, pages 1286–1291, 2014.

[118] Shen Yin, Bing Xiao, Steven X. Ding, and Donghua Zhou. A review on recent development of spacecraft attitude fault tolerant control system. *IEEE Transactions on Industrial Electronics*, 63(5):3311–3320, 2016.

[119] Halim Alwi, Christopher Edwards, and Chee Pin Tan. *Fault Tolerant Control and Fault Detection and Isolation*, pages 7–27. Springer London, London, 2011.

[120] Abdel-Razzak Merheb, Franc¸ois Bateman, and Hassan Noura. Passive and active fault tolerant control of octorotor uav using second order sliding mode control. *2015 IEEE Conference on Control Applications (CCA)*, pages 1907–1912, 2015.

[121] Mehran Mirshams, Mohsen Khosrojerdi, and Mahdi Hassani. Passive fault tolerant sliding mode attitude control for flexible spacecraft with faulty thrusters. *Journal of Aerospace Engineering, Proceedings of the Institution of Mechanical Engineers Part G*, 228, 11 2013.

[122] Ning Li, Haiyi Sun, and Qingling Zhang. Robust passive adaptive fault tolerant control for stochastic wing flutter via delay control. *European Journal of Control*, 48:74–82, 2019. Advanced Control Theory and Applications for Next-Generation Engineered Systems.

[123] Salman Ijaz, Hamdoon Ijaz, Maria Khodaverdian, and Ahmad Nasr. Passive fault tolerant control allocations for nonlinear systems. *2022 34th Chinese Control and Decision Conference (CCDC)*, pages 2948–2953, 2022.

[124] Ryszard Studanski Jerzy Garus and Tomislav Batur. Passive fault tolerant control allocation for small unmanned underwater vehicle. *Journal of Marine Engineering & Technology*, 16(4):420–424, 2017.

[125] Saeedreza Jadidi, Hamed Badihi, and Youmin Zhang. Passive fault-tolerant control strategies for power converter in a hybrid microgrid. *Energies*, 13(21), 2020.

[126] Mouhacine Benosman. *Passive Fault Tolerant Control*. 04 2011.

[127] Alireza Abbaspour, Sohrab Mokhtari, Arman Sargolzaei, and Kang K. Yen. A survey on active fault-tolerant control systems. *Electronics*, 9(9), 2020.

[128] Jin Jiang and Xiang Yu. Fault-tolerant control systems: A comparative study between active and passive approaches. *Annual Reviews in Control*, 36(1):60–72, 2012.

[129] Arslan Ahmed Amin and Khalid Mahmood Hasan. A review of fault tolerant control systems: Advancements and applications. *Measurement*, 143:58–68, 2019.

[130] M. Saied, B. Lussier, I. Fantoni, H. Shraim, and C. Francis. Active versus passive fault-tolerant control of a redundant multirotor uav. *The Aeronautical Journal*, 124(1273):385–408, 2020.

[131] Kristen Severson, Paphonwit Chaiwatanodom, and Richard D. Braatz. Perspectives on process monitoring of industrial systems. *Annual Reviews in Control*, 42:190–200, 2016.

[132] Halim Alwi, Christopher Edwards, and Prathyush P. Menon. Sensor fault tolerant control using a robust lpv based sliding mode observer. *2012 IEEE 51st IEEE Conference on Decision and Control (CDC)*, pages 1828–1833, 2012.

[133] Alberto San Miguel, Vicenç Puig, and Guillem Alenyà. Fault-tolerant control of a service robot using a lpv robust unknown input observer. *2019 4th Conference on Control and Fault Tolerant Systems (SysTol)*, pages 207–212, 2019.

[134] Jing-Jing Yan, Guang-Hong Yang, and Xiao-Jian Li. Adaptive observer-based fault-tolerant tracking control for t–s fuzzy systems with mismatched faults. *IEEE Transactions on Fuzzy Systems*, 28(1):134–147, 2020.

[135] Rihab Lamouchi, Tarek Raissi, Messaoud Amairi, and Mohamed Aoun. On interval observer design for active fault tolerant control of linear parameter-varying systems. *Systems & Control Letters*, 164:105218, 2022.

[136] Jian Han, Xiuhua Liu, Xinjiang Wei, and Shaoxin Sun. A dynamic proportional-integral observer-based nonlinear fault-tolerant controller design for nonlinear system with partially unknown dynamic. *IEEE Transactions on Systems, Man, and Cybernetics: Systems*, 52(8):5092–5104, 2022.

[137] Daoliang Tan and Ron J. Patton. Integrated fault estimation and fault tolerant control: A joint design. *IFAC-PapersOnLine*, 48(21):517–522, 2015. 9th IFAC Symposium on Fault Detection, Supervision andSafety for Technical Processes SAFEPROCESS 2015.

[138] Jianglin Lan and Ron J. Patton. A new strategy for integration of fault estimation within fault-tolerant control. *Automatica*, 69:48–59, 2016.

[139] Jianglin Lan and Ron Patton. An iterative strategy for robust integration of fault estimation and fault-tolerant control. *Automatica*, 145:110556, 2022.

[140] Abdelaziz Abboudi, Sofiane Bououden, Mohammed Chadli, Ilyes Boulkaibet, and Bilel Neji. Observer-based fault-tolerant predictive control for lpv systems with sensor faults: An active car suspension application. *Applied Sciences*, 12(2), 2022.

[141] Saïd Mammar, Duc-To Nguyen, Dalil Ichalal, and Mohand Smaïli. Control and dynamic proportional integral observer co-design for uncertain linear systems. In *2022 IEEE International Conference on Systems, Man, and Cybernetics (SMC)*, pages 2209–2214, 2022.

[142] Jianglin Lan and Ron J. Patton. Integrated design of robust fault estimation and fault-tolerant control for linear systems. *2015 54th IEEE Conference on Decision and Control (CDC)*, pages 5105–5110, 2015.

[143] Yingchun Zhang Qingxian Jia, Wen Chen and Huayi Li. Integrated design of fault reconstruction and fault-tolerant control against actuator faults using learning observers. *International Journal of Systems Science*, 47(16):3749–3761, 2016.

[144] S. Mahdi Fazeli and Mostafa Abedi. An integrated fault estimation and fault tolerant control method using -based adaptive observers. *International Journal of Adaptive Control and Signal Processing*, 34(9):1259–1280, 2020.

[145] Hui Zhang, Xiaoyu Huang, Junmin Wang, and Hamid Reza Karimi. Robust energy-to-peak sideslip angle estimation with applications to ground vehicles. *Mechatronics*, 30:338–347, 2015.

[146] A. Rezaeian, A. Khajepour, W. Melek, S.-Ken Chen, and N. Moshchuk. Simultaneous vehicle real-time longitudinal and lateral velocity estimation. *IEEE Transactions on Vehicular Technology*, 66(3):1950–1962, 2017.

[147] Yongjian Hou, Fanglai Zhu, Xudong Zhao, and Shenghui Guo. Observer design and unknown input reconstruction for a class of switched descriptor systems. *IEEE Transactions on Systems, Man, and Cybernetics: Systems*, 48(8):1411–1419, 2018.

[148] Z. Yacine, D. Ichalal, N. Ait Oufroukh, S. Mammar, and S. Djennoune. Unknown input observer for vehicle lateral dynamics based on a takagi-sugeno model with unmeasurable premise variables. In *2012 IEEE 51st IEEE Conference on Decision and Control (CDC)*, pages 6211–6216, 2012.

[149] Anh-Tu Nguyen, Thierry-Marie Guerra, Chouki Sentouh, and Hui Zhang. Unknown input observers for simultaneous estimation of vehicle dynamics and driver torque: Theoretical design and hardware experiments. *IEEE/ASME Transactions on Mechatronics*, 24(6):2508–2518, 2019.

[150] Zedjiga Yacine, Dalil Ichalal, Naïma Ait-Oufroukh, and Saïd Mammar. Detection of critical situations in vehicle lateral dynamics by lpv unknown input observers with finite time property. *2014 IEEE Conference on Control Applications (CCA)*, pages 334–339, 2014.

[151] Ghassen Marouani, Thach Ngoc Dinh, Tarek Raïssi, Xin Wang, and Hassani Messaoud. Unknown input interval observers for discrete-time linear switched systems. *European Journal of Control*, 59:165–174, 2021.

[152] Nicolas Ellero, David Gucik-Derigny, and David Henry. An unknown input interval observer for lpv systems under l_2-gain and l_∞-gain criteria. *Automatica*, 103:294–301, 2019.

[153] Sara Ifqir, Naima Ait Oufroukh, Dalil Ichalal, and Saïd Mammar. Vehicle lateral dynamics estimation using switched unknown inputs interval observers: Experimental validation. *2018 Annual American Control Conference (ACC)*, pages 1138–1143, 2018.

[154] Naoufal El Youssfi, Rachid El Bachtiri, Taha Zoulagh, and Hicham El Aiss. Unknown input observer design for vehicle lateral dynamics described by takagi–sugeno fuzzy systems. *Optimal Control Applications and Methods*, 43(2):354–368, 2022.

[155] Jian Han, Xiuhua Liu, Xinjiang Wei, and Shaoxin Sun. A dynamic proportional-integral observer-based nonlinear fault-tolerant controller design for nonlinear system with partially unknown dynamic. *IEEE Transactions on Systems, Man, and Cybernetics: Systems*, 52(8):5092–5104, 2022.

[156] Seshan Ramanathan Venkita, Boulaid Boulkroune, Anurodh Mishra, and Ellen van Nunen. A fault tolerant lateral control strategy for an autonomous four wheel driven electric vehicle. *2020 IEEE Intelligent Vehicles Symposium (IV)*, pages 1492–1497, 2020.

[157] Damiano Rotondo. *Background on Fault Tolerant Control*, pages 129–145. Springer International Publishing, Cham, 2018.

[158] Haiyan Liu, Yadong Wang, and Kunfeng Wang. Adaptive fault-tolerate lateral control for autonomous electric vehicles with unknown parameters and actuator faults. *Mathematical Problems in Engineering*, 2023:1–11, 04 2023.

[159] Xuefang Li, Hongbo Li, and Deyuan Meng. A spatial learning-based fault tolerant lateral tracking control for autonomous driving. *IEEE Transactions on Vehicular Technology*, 72(10):12567–12579, 2023.

[160] Turki Alsuwian, Mian Hamza Usman, and Arslan Ahmed Amin. An autonomous vehicle stability control using active fault-tolerant control based on a fuzzy neural network. *Electronics*, 11(19), 2022.

[161] S.M.Savaresi, C.Novara, G.Balazs, and F.Forni. Fault-tolerant control for automotive applications: Trends and challenges. *Annual Reviews in Control*, 2018.

[162] Manh-Hung Do, Damien Koenig, and Didier Theilliol. An integrated design for robust actuator fault accommodation based on $\mathcal{H}_\infty$ proportional-integral observer. *2018 IEEE Conference on Decision and Control (CDC)*, pages 6346–6352, 2018.

[163] Wen-Bo Xie, Yu-Long Wang, Jian Zhang, and Ming-Yu Fu. Novel separation principle based h_∞ observer–controller design for a class of t–s fuzzy systems. *IEEE Transactions on Fuzzy Systems*, 26(6):3206–3221, 2018.

[164] Rajesh Rajamani. *Vehicle dynamics and control*. Mechanical Engineering Series. Springer, New York, NY Heidelberg, 2. ed edition, 2012.

[165] Jos F. Sturm. Using sedumi 1.02, a matlab toolbox for optimization over symmetric cones. *Optimization Methods and Software*, 11(1-4):625–653, 1999.

[166] M. Oudghiri, M. Chadli, and A. El hajjaji. Control and sensor fault-tolerance of vehicle lateral dynamics. *IFAC Proceedings Volumes*, 41(2):123–128, 2008. 17th IFAC World Congress.

[167] Simon Göltz, Daniel L. Ossig, Weixin Fu, and Oliver Sawodny. Nonlinear flatness-based observer for vehicle dynamics control. *IECON 2021 – 47th Annual Conference of the IEEE Ind. Elec. Society*, pages 1–6, 2021.

[168] Jie Zhang, Hai Wang, Jinchuan Zheng, Zhenwei Cao, Zhihong Man, Ming Yu, and Long Chen. Adaptive sliding mode-based lateral stability control of steer-by-wire vehicles with experimental validations. *IEEE Trans. on Vehicular Technology*, 69(9):9589–9600, 2020.

[169] Z. Yacine, D. Ichalal, N. Ait Oufroukh, S. Mammar, and S. Djennoune. Nonlinear vehicle lateral dynamics estimation with unmeasurable premise variable takagi-sugeno approach. *2012 20th Med. Conf. on Control & Automation (MED)*, pages 1117–1122, 2012.

[170] Duc To Nguyen, Said Mammar, Dalil Ichalal, and Mohand Smaili. An integrated design of pi interval observer-based ftc for lti systems. *2022 30th Med. Conf. on Control and Automation (MED)*, pages 878–883, 2022.

[171] Souad Bezzaoucha Rebaï, Holger Voos, Mohamed Darouach, and Khadidja Chaib Draa. Unknown input functional observers design for polytopic discrete time systems. *2017 6th International Conference on Systems and Control (ICSC)*, pages 261–266, 2017.

[172] Mohammed Chadli and Hamid Reza Karimi. Notice of violation of ieee publication principles: Robust observer design for unknown inputs takagi–sugeno models. *IEEE Transactions on Fuzzy Systems*, 21(1):158–164, 2013.

[173] Luc Meyer, Dalil Ichalal, and Vincent Vigneron. State and unknown input h_∞ observers for discrete-time lpv systems. *Asian Journal of Control*, 22(1):49–62, 2020.

[174] D. Ichalal, B. Marx, J. Ragot, and D. Maquin. Unknown input observer for lpv systems with parameter varying output equation. *IFAC-PapersOnLine*, 48(21):1030–1035, 2015. 9th IFAC Symposium on Fault Detection, Supervision andSafety for Technical Processes SAFEPROCESS 2015.

[175] Dalil Ichalal and Thierry-Marie Guerra. Decoupling unknown input observer for nonlinear quasi-lpv systems. *2019 IEEE 58th Conference on Decision and Control (CDC)*, pages 3799–3804, 2019.

[176] Hung Pham, Dalil Ichalal, and Said Mammar. Lpv unknown input observer for attitude of a mass-varying quadcopter. In *2020 16th International Conference on Control, Automation, Robotics and Vision (ICARCV)*, pages 917–924, 2020.

[177] H. L. Trentelman and P. Antsaklis. Observer-based control. *Encyclopedia of Systems and Control*, pages 1–6, 2013.

[178] Rihab Lamouchi, Tarek Raissi, Messaoud Amairi, and Mohamed Aoun. Interval observer framework for fault tolerant control of linear parameter-varying systems. *International Journal of Control*, 91:1–16, 01 2017.

[179] Frédéric Mazenc, Michel Kieffer, and Eric Walter. Interval observers for continuous-time linear systems with discrete-time outputs. *2012 American Control Conference (ACC)*, pages 1889–1894, 2012.

[180] Kwassi H. Degue, Denis Efimov, Jerome Le Ny, and Eric Feron. Interval observers for secure estimation in cyber-physical systems. *2018 IEEE Conference on Decision and Control (CDC)*, pages 4559–4564, 2018.

[181] Haifa Ethabet, Djahid Rabehi, Denis Efimov, and Tarek Raïssi. Interval estimation for continuous-time switched linear systems. *Automatica*, 90:230–238, 2018.

[182] Shenghui Guo and Fanglai Zhu. Interval observer design for discrete-time switched system. *IFAC-PapersOnLine*, 50(1):5073–5078, 2017.

[183] Emmanuel Chambon, Laurent Burlion, and Pierre Apkarian. Overview of lti interval observer design: towards a non-smooth optimisation-based approach. *IET Control Theory & Applications*, 10:1258–1268, 07 2016.

[184] Zhenhua Wang, Cheng chew Lim, and Yi Shen. Interval observer design for uncertain discrete-time linear systems. *Systems & Control Letters*, 116:41–46, 05 2018.

[185] Thomas Chevet, Andreas Rauh, Thach Ngoc Dinh, Julien Marzat, and Tarek Raïssi. Robust interval observer for systems described by the fornasini–marchesini second model. *IEEE Control Systems Letters*, 6:1940–1945, 2022.

[186] Thomas Chevet, Thach Ngoc Dinh, Julien Marzat, and Tarek Raissi. Robust sensor fault detection for linear parameter-varying systems using interval observer. *Proceedings of the 31st European Safety and Reliability Conference (ESREL 2021)*, pages 1486–1493, 01 2021.

[187] Thomas Chevet, Thach Ngoc Dinh, Julien Marzat, and Tarek Raïssi. Interval estimation for discrete-time linear parameter-varying system with unknown inputs. *2021 60th IEEE Conference on Decision and Control (CDC)*, pages 4002–4007, 2021.

[188] C. Zammali, J. Van Gorp, X. Ping, and T. Raïssi. Simultaneous interval state and fault estimation for continuous-time switched systems. *IFAC-PapersOnLine*, 55(25):73–78, 2022. 10th IFAC Symposium on Robust Control Design ROCOND 2022.

[189] Thach Ngoc Dinh, Ghassen Marouani, Tarek Raïssi, Zhenhua Wang, and Hassani Messaoud. Optimal interval observers for discrete-time linear switched systems. *International Journal of Control*, pages 1–9, 2020.

[190] Jitao Li, Zhenhua Wang, Yi Shen, and Yan Wang. Interval observer design for discrete-time uncertain takagi–sugeno fuzzy systems. *IEEE Transactions on Fuzzy Systems*, 27(4):816–823, 2019.

[191] Qiang Yu and Hao Lv. Stability analysis for discrete-time switched systems with stable and unstable modes based on a weighted average dwell time approach. *Nonlinear Analysis: Hybrid Systems*, 38:100949, 2020.

[192] Benoit Lacroix, Zhaoheng Liu, and Patrice Seers. A comparison of two control methods for vehicle stability control by direct yaw moment. *Applied Mechanics and Materials*, 120:203–217, 01 2012.

[193] Jos F. Sturm. Using sedumi 1.02, a matlab toolbox for optimization over symmetric cones. *Optimization Methods and Software*, 11(1-4):625–653, 1999.

[194] M.K Aripin, Yahaya Md Sam, Kumeresan A. Danapalasingam, Kemao Peng, Norhazimi Hamzah, and Muhamad Ismail. A review of active yaw control system for vehicle handling and stability enhancement. *International Journal of Vehicular Technology*, 2014:1–15, 06 2014.

université PARIS-SACLAY
ÉCOLE DOCTORALE
Sciences et technologies de l'information et de la communication (STIC)

Titre: Contrôle Tolérant Aux Défauts Basé Observateurs Par Intervalle Pour Systèmes LPV Commutés

Mots clés: Systèmes à paramètres variants, Systèmes commuté, Observateur par intervalles, Commande tolérante, Robustesse, Entrée inconnue

Résumé: Les systèmes à commutation attirent de plus en plus l'attention dans le domaine scientifique grâce à leur capacité à représenter des phénomènes complexes issus de diverses applications en ingénierie.
L'estimation d'état joue un rôle clé dans ces systèmes, notamment pour le diagnostic de pannes et le contrôle. Toutefois, les méthodes classiques d'observateurs peinent à traiter efficacement les incertitudes, limitant ainsi la précision et la fiabilité des résultats. Dans les applications industrielles, les perturbations externes, le bruit de mesure ou les défaillances d'actionneurs engendrent fréquemment des entrées inconnues ou des défauts.
Ces aléas peuvent dégrader les performances, provoquer une instabilité, voire conduire à des dysfonctionnements critiques. Il devient donc primordial de développer des solutions algorithmiques robustes pour estimer et compenser ces anomalies, améliorant ainsi la sûreté de fonctionnement.
L'un des axes principaux de cette étude concerne l'estimation d'état robuste par intervalles, une approche novatrice permettant de borner les états malgré des perturbations bornées ou un bruit de mesure. Fondée sur la théorie des systèmes coopératifs, la méthodologie proposée garantit des bornes inférieures et supérieures aux estimations, offrant une robustesse accrue face aux incertitudes par rapport aux observateurs conventionnels.
Parallèlement, des stratégies de commande active tolérante aux défauts (AFTC) sont développées pour maintenir la stabilité et les performances du système, même en présence de défauts. Une approche de co-conception intègre observateurs et contrôleurs dans un cadre unifié, tenant compte des interactions entre estimation et commande. Cette synergie optimise la résilience globale et les performances. Les conditions d'existence des observateurs par intervalles et des contrôleurs sont exprimées via des inégalités matricielles linéaires (LMIs), dérivées de la théorie de Lyapunov et de la stabilité entrée-état (ISS) sous contraintes de temps de commutation moyen (ADT).
Enfin, les applications à la dynamique latérale d'un véhicule, simulée sous MATLAB/Simulink, valide l'efficacité des solutions proposées. Les résultats démontrent que les observateurs par intervalles maintiennent des estimations précises malgré les incertitudes, tandis que les lois de commande AFTC préservent la stabilité et les performances, même dans des scénarios dégradés. Ces contributions renforcent la fiabilité des systèmes complexes soumis à des environnements imprévisibles.

Université Paris-Saclay
Espace Technologique / Immeuble Discovery
Route de l'Orme aux Merisiers RD 128 / 91190 Saint-Aubin, France

université PARIS-SACLAY
ÉCOLE DOCTORALE
Sciences et technologies de l'information et de la communication (STIC)

Title: Interval Observers-Based Fault-Tolerant Control Of LPV Switched Systems

Keywords: Linear Parameter Varying Systems, Switched systems, Interval observers, Fault tolerant control, Robustness, Unknown input

Abstract: Switched systems have drawn considerable attention from researchers due to their ability to model a variety of practical systems. The synthesis of observers for this class of systems has gained increasing interest over the past few decades since the estimation plays a fundamental role in determining the current system states, including measured and unmeasured variables, which is crucial for fault diagnosis and control. However, the conventional observer synthesis technique may struggle to cope with the uncertainties, resulting in reduced estimation accuracy and reliability.
Moreover, in practical engineering applications, it is inevitable to encounter unknown inputs and faults due to unpredictable external disturbances, measurement noise, and potential actuator faults. Such factors may cause system performance degradation, instability, or even catastrophic failures. It is, therefore essential to enhance the system safety and reliability by developing well-designed algorithms that can effectively estimate and compensate for faults affecting the performance.
The objective of this thesis is to provide some contributions to the state-of-the-art in the field of robust state estimation and fault-tolerant control (FTC) for a class of switched systems by addressing the aforementioned problems.
The present research mainly focuses on addressing the challenge of robust state bounding estimation using interval observer techniques for uncertain switched systems subject to unknown but bounded exogenous disturbances and/or measurement noise. Based on the cooperativity system theory, the methodology presents novel interval observer structures that provide notable improvement, particularly in enhancing the robustness and accuracy of state estimation under uncertain conditions. In contrast to conventional observers may struggle to deal with uncertainties, the proposed observer can effectively cope with the problems by offering guaranteed lower and upper bounds of state estimations.
In addition to robust state estimation, the thesis also focuses on the synthesis of active fault-tolerant control (AFTC) strategies designed to preserve system stability and ensure desired performance levels, even in the presence of faults. The approach employs a co-design methodology, which integrates the design of observers and controllers into a cohesive framework. This integrated design approach considers the bi-directional interaction between the estimation process and control actions, leading to the optimized overall system performance and enhanced resilience to faults.
Sufficient conditions for proving the existence of the interval observers and controllers are formulated in terms of Linear Matrix Inequalities (LMIs) constraints. These conditions are derived through a combination of Lyapunov theory and Input-to-State-Stability (ISS) under the Average-Dwell Time (ADT) concept.
Finally, to validate the efficacy of the proposed interval observer structures and the synthesized control laws, an application to the vehicle lateral dynamics model is presented, using MATLAB Simulink. The simulations validate the robustness of the interval observer structures and fault-tolerant control strategies, showing that the proposed approach can effectively maintain vehicle stability and control even in challenging and unpredictable environments. The results highlight the ability of the interval observers to accurately bound state estimates despite uncertainties, while the synthesized control laws successfully ensure system stability and performance even in the occurrence of faults.

Université Paris-Saclay
Espace Technologique / Immeuble Discovery
Route de l'Orme aux Merisiers RD 128 / 91190 Saint-Aubin, France